TEXT CUT OFF IN ORIGINAL

THE EARLY HYDRATION OF CEMENT

ALI BEHROOZ AFSHAR
BSc, MSc, AMICE

A THESIS PRESENTED FOR THE DEGREE OF
DOCTOR OF PHILOSOPHY

HERIOT-WATT UNIVERSITY
DEPARTMENT OF CIVIL ENGINEERING
EDINBURGH

SEPTEMBER 1986

CONTENTS

LIST OF FIGURES

LIST OF PLATES

LIST OF TABLES

ACKNOWLEDGEMENTS

The author wishes to thank Professor A Bolton, former Head of the Department of Civil Engineering and Professor A D Edwards, Head of the Department of Civil Engineering for placing the facilities of the department at his disposal.

The author is particularly grateful to Dr W J McCarter for the supervision, generous help, guidance, constructive comments and criticism given to him while carrying out the work described in this thesis.

The author also appreciates the assistance of Dr Dhariwal (Department of Electrical and Electronic Engineering, Heriot-Watt University) in carrying out the SEM work, the constructive discussion with Professor Taylor (Department of Chemistry, Aberdeen University), and the technical input from the department's technical staff.

Blue Circle and Clyde Cement are also thanked for their contribution, by providing quantities of cement.

I am also indebted to my family for their continuous support, encouragement and patience.

Finally, I express my thanks to Mrs Isobel Gordon for expertly typing the thesis and gratefully acknowledge the receipt of research grant Nos GR/C/29430, GR/D/38200 from the Science and Engineering Research Council.

ABSTRACT

This thesis details the development and use of an electrical response technique for monitoring the chemical and physical changes occurring within the cement paste during the initial 24 hours after gauging with water.

Traditional empirical tests and the more sophisticated laboratory examinations such as X-ray diffraction, scanning and transmission electron microscopy are critically reviewed.

The study involves the electrical measurements on realistic sample sizes and constituent proportions. A modified electrical model for the response of cement paste to an applied electrical field is proposed. An automated microcomputer data logging system has been developed to facilitate electrical measurements.

It has been demonstrated that the electrical response measurements of cement paste can be related to the physio-chemical processes that take place during hydration. Extensive microstructural examination of fracture surfaces of cement pastes using Scanning Electron Microscopy revealed that regions of definite crystallization and the prediction as to the hydrate morphology can be linked to the electrical response.

The technique could be offered as an additional tool for investigating the structure building processes and microstructure development within cement paste. The electrical response data can be used to monitor cement hydration and it is shown that

assessment of the effect of varying chemical composition; age of cement; addition of admixtures and environmental conditions have a definite influence on hydration processes.

CHAPTER 1

INTRODUCTION

1. INTRODUCTION

Clays were the first cementitious materials to be used in building construction, this was followed by ordinary lime where its hydration created a cementitious material which was used as mortar for holding brick, stone and other masonary units together. Pozzolanic cements were developed by the Romans from materials of volcanic origin, when mixed with lime they exhibited highly cementitious properties. Hydraulic limes were pioneered in the United Kingdom by John Smeaton towards the end of the 18th century; made from limestones with high clay content, their cementitious properties were due primarily to the presence of silicates.

Portland Cement was developed by Joseph Aspdin in 1824. It is essentially an artificial material produced by burning a blend of limestone and clay. Aspdin called it Portland Cement simply because the cast concrete produced from it resembled in colour the stone quarried on the Isle of Portland, off the English coast.

Today, the world manufacture of hydraulic cements is in excess of one billion tonnes[1] per year, and is, along with steel, the most important construction material. In spite of the amount of research that has been carried out on hydraulic cements, including chemical analysis, X-ray diffraction, and electron microscopy, our understanding of the structure and properties of cements are not as advanced as that of steel.

During the period when oil prices were low, material research throughout the world was dominated by the organic chemist and metallurgist who had little interest in inorganic materials, particularly those having a direct relevance to the ceramic building products and construction industries. More recently, it has been widely realised that inorganic materials are more useful than was believed and, in particular, that hydraulic Portland Cements have considerable potential for development and use in novel ways. The necessary raw materials are in abundant supply and available worldwide. The manufacturing technology is simple, the energy consumed in manufacturing is relatively low and the hardening takes place with water at ordinary temperatures. Therefore, the motivation exists for scientists to research for a better understanding of the microstructure; improving the strength, toughness and durability of cements, not only for conventional use, but also so they may be used in new applications such as replacements for energy intensive plastic, metals and other ceramic materials.

The problems with cement and concrete are normally associated with their long-term durability,[2] and are often caused by adverse chemical reactions that affect the microstructure of the matrix, as is the case with concrete cancer[3,4]. These reactions attack the concrete and cause the expansion of the matrix from within, and results in the degradation of the surface layers and the eventual loss of strength. The Royal Devon and Exeter Hospital completed in 1974 is a perfect example.

The hydration processes and the resulting hydration products are

believed to have major control over almost all the important engineering properties of cement, such as strength, elasticity, shrinkage, creep, permeability, durability and setting time. There are, at present, two approaches used for evaluating the properties of cement and the understanding of its hydration:

a) One group of the tests developed relatively recently include X-ray Diffraction, Scanning Electron Microscopy, Flame Atomic Absorption Spectrophotometry, Energy Dispersive Analysis and Calorimetry. These microscopic and submicroscopic physical and chemical studies have contributed towards our understanding of the microstructural building processes, strength development and the hydration characteristics of cement paste. Attempts have been made by various researchers to use the knowledge gained from the above studies of the microstructure to provide a fundamental approach to the understanding of concrete behaviour.

b) The traditional approaches form the second group of tests (compressive strength test, Vicat Needle test, VB test, etc). These tests are made on much larger sample sizes in order to measure the engineering properties of the sample directly. The results are used to relate parameters such as water/cement ratio and temperature which affect hydration process to the resulting engineering properties.

Both methods have their shortfalls. The former deals with samples that are often difficult, costly and time consuming to prepare, the instrumentation is not readily available and

requires skilled interpretation. Only a very small area of the sample is examined (as little as a few microns) and therefore care must be taken in evaluating macroscale performance for microscale examination.

The latter, lack theoretical backing; hence, for every new circumstance, a new test would have to be devised.

In addition to their individual advantages and disadvantages, the two approaches have two common practical disadvantages[5]:

1. before any measurements can be taken using current engineering methods, one must wait for the samples to harden;

2. most of the tests are destructive in nature, therefore, there is a need for (and great benefits to be derived from) a non-destructive test which could predict the properties of cement and concrete from those of the fresh mix.

1.1 THE ADOPTED APPROACH

In the present study, attempts have been made to monitor the hydration of cement paste using an electrical response technique. Cement hydration results from various chemical reactions that take place when water is added to cement. During the early hydration, cement paste changes from a fluid to a rigid matrix, this change in viscosity will affect its response to an applied electrical field. The present research programme investigates the electrical properties of cement paste during the initial

24-hours after mixing with water. Attention has been directed towards monitoring the changes in capacitance (hence, the dielectric constant) and resistance (hence, resistivity) over this period to establish if there is a correlation between changes in the physical and chemical state of the paste and the changes in the measured electrical parameters.

The electrical model used in previous work was a purely resistive one with the matrix constituents being represented by a parallel combination of resistive elements. The electrical model used in this study represents the matrix as a parallel combination of a capacitive element, C, and a resistive element, R. The capacitance element, C, is to account for the overall reactance, and hence the polarisation of the paste, whereas the resistive element, R, is to reflect the conduction effect caused by the drift of unbound charges, in the form of ions, through the solution and their discharge at the electrodes.

In parallel to the electrical investigation, extensive Scanning Electron Microscopy studies on the cement paste microstructure were undertaken using fracture samples to attempt to correlate the electrical results with crystal formations and morphology changes of the microstructure.

The electrical method presented may be of great practical and theoretical value in studies of cement hydration. It has the following major advantages over other techniques:

a) The samples are of realistic size and require no special preparation techniques, the parameters measured are directly affected by the physio-chemical changes that are taking place.

b) The test is carried out and the results are absorbed within a short time after placement, therefore no time is lost.

c) The test is non-destructive.

d) The test method could easily be adopted for use in the field.

CHAPTER 2

CHEMISTRY OF HYDRATION

2.1 INTRODUCTION

In general terms, the word cement is described as any type of adhesive used for bonding. In Civil Engineering terms, cement is a complex system composed of a mixture of finely powdered minerals, which readily react with water to form insoluble hydrates. Through time, the remaining water within the mix and that absorbed from the atmosphere is for further hydration. The hydration products gradually replace the water-filled pores between cement grains and eventually results in a solid matrix.

The hydration of cement has been the subject of intensive investigation and considerable strides have been taken in our knowledge and understanding of the hydrolysis and hydration processes. The availability of new experimental techniques and analytical methods has been responsible and made this advancement possible.

2.2 DIFFERENT TYPES OF CEMENT

The previous chapter outlined a brief history of the development of cement. In this section, the different types of cements available to the construction industry are briefly mentioned and the more widely used are discussed in detail. Further information on this and other aspects of cement can be found in numerous publications[6-13].

The physical properties of a cement type are dictated by:

i) the physical and chemical characteristics of the constituent minerals,

ii) the percentage of these minerals,

iii) the environmental conditions to which it is subjected.

It should be possible, therefore, to obtain a cement of particular properties by careful selection of its mineralogical composition. Today a variety of cement types are available for use in the construction industry for normal concreting or special use. There are two main categories of cement:

i) Portland Cements,

ii) Non-Portland inorganic cements.

A summary of the different cements falling within these categories are given in Table 2.1.

2.2.1 Portland Cements

Originally called Portland Cement because of the resemblance of the colour of the set cement to that of Portland limestone quarried in Dorset, the name now applies to a family of closely related cements all of which have an overall similarity of properties. They are manufactured by intimately mixing together calcareous and argillaceous materials; burning them at a high temperature (1400-1600^{o}C) and then grinding the resulting clinker.

Ordinary Portland Cement (OPC) is by far the most widely used in the United Kingdom, some 18 million tonnes of OPC are used annually in the construction industry (90% of all cement used). On a world scale, this figure approaches 1 billion tonnes[1].

Portland Cements	Modified Portland Cements	Non-Portland Inorganic Cements
Ordinary Portland Cement	Portland Blast-furnace Cement	High Alumina Cement
Rapid Hardening Portland Cement	Super Sulphate Cement	Gypsum Plaster
Low heat Portland Cement	Portland-Pozzolana Cement	Magnesium Oxychloride
Sulphate Resisting Portland Cement	White Cement (iron free)	Phosphate Bonded Cement
	Oil Well Cement (low C_3A)	
	Masonary Cement	
	Expanding Cement	

Table 2.1: TYPES OF CEMENT IN CURRENT USE

The raw materials used in the manufacture of a typical Ordinary Portland Cement comprises primarily lime, silica, alumina, and iron oxides. The four chemical compounds identified[6-9] as being the active ingredients in cement clinker are; tricalcium silicate, tricalcium aluminate, dicalcium silicate, and tetracalcium aluminoferrite. When hydrated, these materials make a major contribution to the strength development of cement.

a) Tricalcium Silicate (C_3S)

Formed from CaO and SiO_2, with the chemical formula $3CaOSiO_2$. This is the major component in Portland Cement, constituting 40-45% of the total in normally retarded cements and 60-65% for high early strength cements. C_3S contributes greatly to all stages of strength development, but principally the early stages.

b) Tricalcium Aluminate (C_3A)

Formed by combination of CaO and Al_2O_3 with chemical formula of $3CaOAl_2O_3$ and percentage by weight of between 3-15%. Although C_3A does not contribute greatly to the final strength of the set cement, it sets rapidly and plays an important role in the early strength development of cement clinker, C_3S setting time can be controlled by the amount of gypsum added to the clinker.

c) Dicalcium Silicate (C_2S)

Is also formed by the reaction between CaO and SiO_2 with the chemical formula of $2CaOSiO_2$ and percentage by weight of up to 25%. C_2S hydrates slowly, hence it does not influence the initial setting but is very important in the final strength development.

d) Tetracalcium Aluminoferrite (C_4AF)

Is formed by the reaction between CaO, SiO_2 and Fe_2O_3, with chemical formula of $4CaOAl_2O_3Fe_2O_3$ and percentage by weight of up to 8%. C_4AF contributes little to the strength development of cement.

In addition to the above basic compounds, Portland Cement in its final form may contain gypsum, alkali, sulphates, magnesia, free lime and other minor compounds. At normal concentrations, these materials do not significantly affect the properties of set cement, however, they do influence rates of hydration and resistance to chemical attack. The two calcium silicates are the main cementitious compounds and the physical behaviour of cement is largely dictated by these compounds[14], therefore, by careful manipulation of the compound composition, it is possible to modify certain properties of the OPC in order that the new cement will perform more satisfactorily in particular application.

When rapid strength development is desired for practical and economical reasons (i.e. precasting, structural repair), Rapid Hardening Portland Cement (RHPC) is used. The increase in the rate of gain of strength is achieved by increasing the C_3S content and by finer grinding of the cement clinker, the latter will result in an increase in the surface area and hence a faster rate of hydration. The percentage weight of C_3S can be as high as 70%. The strength gained after three days by RHPC is of the same order as the 7-day strength of OPC cement using the same water-cement ratio.

When low heat of hydration is required to prevent, for example, shrinkage and thermal cracking in mass concreting, Low Heat Portland Cement (LHPC) is used. To achieve low heat of hydration, the percentage of C_3S and C_3A within the composition is reduced, the C_3S and C_3A percentage could be reduced to 25% and 5% respectively. This will result in a slower rate of gain of strength, but the ultimate strength is not affected.

When concrete is exposed to an aggressive environment, such as sea water and constant wetting and drying, the calcium aluminate hydrate (a by-product of the reaction between C_3A and gypsum, $CaSO_4 2H_2O$) present within the cement matrix, can react with sulphate salts from the external environment, to form calcium sulphoaluminate, which is insoluble and will remain within the framework of the hydrated cement paste. This results in an increase in the volume and a gradual disintegration of the matrix. Sulphate-resisting Portland Cement (SRPC) with a low C_3A content (below 5%) has proved to provide satisfactory performance even in the most aggressive environments.

Modified Portland Cements are cements formed either by adding other ingredients to the clinker or by varying the manufacturing process to form different compounds during burning. Numerous types of cement developed for special use, all of which fall within this category, are listed in Table 2.1 and their specialised properties are dealt with in detail by Mindess[6] and Neville[8].

2.2.2 Non-Portland Cements

The most important cement type in this category is High-Alumina Cement (HAC) or Ciment Fondu Lafarge. Unlike Portland Cement, where the main phases are calcium silicates, with only minor quantities of C_3A, the major constituent of High-Alumina Cement is 60% CA (calcium aluminate, $CaOAl_2O_3$), with up to 10% C_2S and between 5-20% C_2AS (dicalcium-aluminosilicate, $2CaOAl_2O_3SiO_2$), the minor constituents, which collectively amount to between 10-20%, include $C_{12}A_7FeO$.

The setting time of a HAC cement paste is comparable to that of Portland Cement, but it hardens rapidly and gains considerable strength within the first 24-hours after gauging. HAC was developed to overcome the problem of attack of sulphate-bearing water on Portland Cement, but, because of several roof and floor failures[15] associated with precast concrete beams made with HAC cement, the structural use of HAC is now limited. The problem is associated with the loss in strength caused by a combination of adverse chemical reaction (conversion) and adverse environmental conditions[16]. A number of other notable Non-Portland Cements are listed in Table 2.1, and their properties are dealt with in detail by Kurdowski and Sorrentino[17].

2.3 MANUFACTURE OF PORTLAND CEMENT

The manufacture of cement involves grinding and mixing raw materials, and then subjecting the blend to high temperatures to produce compounded oxides, so that when hydrated they will have cementitious properties. Pollitt[18] and Kerton and Murray[19] have given detailed accounts of the processes involved, and only

a summary of the events is outlined below.

2.3.1 The Raw Materials

The raw materials are calcareous and argillaceous rocks, or other by-products which contain these materials. Because the process of separating the desired ingredients from rock is not an exact one, the composition of the final product depends heavily on that of the raw materials.

Calcareous materials contain calcium carbonate or calcium oxide. The rocks that are commonly used are:

Limestone: A rock that is formed mainly by accumulation of organic remains (marine shells or coral). Its basic component is calcium carbonate.

Cement rock: A rock with similar composition to artificial cement.

Chalk: A soft white/grey buff limestone composed mainly of marine shells.

Marl: A loose or crumbly earthy deposit containing a substantial amount of calcium carbonate.

Alkali waste: The waste from chemical plants which contains calcium oxides or calcium carbonate.

Argillaceous materials contain clay or clay minerals, and the rocks that are commonly used are:

Clay: An earthy material, plastic when moist, but hard when fired, it is composed mainly of hydrous aluminium silicates and other minerals.

Shale: A fossil rock that is formed by the consolidation of clay, mud or silt, composition of which has not been altered since deposition. It has a finely laminated structure.

Slate: A dense, fine-grained rock produced by the compression of clay, shales and other rocks.

Ash: A by-product of coal combustion; it has traces of silicate.

2.3.2 Preparation of the Raw Materials

There are two methods of manufacturing cement - wet and dry processes. The difference between the processes lies in the technique used in seperating the unwanted minerals from the raw materials. Figures 2.1 and 2.2 show the flow chart of manufacturing steps taken in producing Portland Cement, dry and wet respectively.

Dry Process: Clays and limestone materials are fed to separate crushers and the finely crushed products are stored in seperate bins, their chemical compositions are analysed and a desired compositon is blended. The blend is then delivered to a grinder for pulverization.

Wet Process: The limestone is ground and stored in bins. Clay materials are slurried so that pebbles and the larger unwanted particles will settle out. The two minerals are then ground together in a mill and once the desired composition is achieved, the mixture is partially dried and sent to the kiln for firing.

The wet process is more controllable, but requires extra input of energy in wetting and drying processes, this makes the process more expensive.

2.3.3 The Burning Operation

The most important part of the manufacturing process takes place in a long rotary kiln. The blended raw mixture is fed at a uniform rate into the upper end of the kiln and heated, gradually, to a liquid state. The reaction in the kiln and the temperatures at which they take place are:

100°C:	Evaporation of free water.
500°C:	Dehydroxylation of clay minerals.
900°C:	Crystallisation of products of clay mineral dehydroxylation, decomposition of $CaCO_3$.
900-1200°C:	Reaction between $CaCO_3$ or CaO with aluminosilicates.
1250-1280°C:	Beginning of liquid formation.
1280°C+:	Further liquid formation and formation of cementitious compounds.

2.3.4 The Cooling Process

The rate and method of the cooling process has a profound effect on the quality of the clinker compound. Slow cooling, will allow the crystallisation of the clinker components, this ensures better grindability and higher long term strength. Fast cooling, on the other hand, results in the formation of glass which makes the clinker difficult to grind. The cement develops high early strength, but may deteriorate with time.

2.3.5 Final Grinding

The clinker is ground in ball-type grinding mills. During grinding, a certain amount of gypsum is added to the clinker to prevent flash setting of the cement, the amount added varying between 1.5% and 3%.

2.4 THE HYDRATION OF PORTLAND CEMENT

The hydration of Portland Cement varies according to the structure of clinker grains, which, in turn, is influenced by the raw materials; particle size and distribution; and the burning and cooling processes[20]. These variables affect the crystallisation of the various final compounds[21-25] and the porosity of the clinker grains themselves.

In general, C_3S (alite), which is the major component of clinker grains, crystallises as angular particles. C_2S (belite) crystallises as smaller, more rounded particles which are distributed amongst the C_3S particles. C_3A, which forms a small percentage of clinker grains, also crystallises as angular particles. C_4AF forms the internal phase within the clinker grain structure. Figure 2.3 shows a suggested clinker grain structure[26].

Because of the complexities of the hydration of Portland Cement, it is necessary to study the hydration of pure compounds (C_3S, C_3A, C_2S, C_4AF) forming it, and, although it is incorrect to assume independent hydration of phases without interaction between hydrating compounds, the understanding of the hydration

of individual phases can help in giving an insight as to the hydration of Portland Cement.

Conduction calorimetry, a technique in which the rate of heat liberation in the hydration process is monitored with respect to time, has been widely employed by researchers in studying the hydration of cement and its individual compounds[27-30]. A detailed description of the design of calorimeters and of the variation in calorimetry techniques, may be found in the papers of Forrester[29] and Monfore[28]. Amongst other methods employed to study cement hydration is the monitoring of the calcium ion (Ca^{2+}) concentration in the liquid phase as a function of time[31]. Skalny et al[32] and Jawad et al[33] have reviewed previous work by other researchers on the hydration mechanisms of individual clinker compounds and that of Portland Cement using various methods, i.e. conduction calorimetry, scanning electron microscopy, X-ray diffraction, transmission electron microscopy.

2.4.1 Crystal Morphologies and Microstructure of Hydrates

The crystal morphology of hydrates needs specific classification to allow easier recognition of hydration products during observation by scanning electron microscopy.

Hardened cement paste is a composite matrix composed of a mixture of crystalline and amorphous products, with a large percentage of the total volume comprising gel and capillary pores. An approximate composition, by percentage volume, is[33]:

Calcium Silicate Hydrate (C-S-H)	50%
Calcium Hydroxide (CH)	12%
Calcium Sulpho-Aluminate Hydrates (AFm) (AFt)	13%
Pores	25%

C-S-H is the predominant constituent of cement paste and it appears in a variety of morphologies, Jawed[25] sees a need for a universal adoption of single nomenclature for C-S-H types and suggests a classification of C-S-H morphologies with an adopted nomenclature as summarised in Table 2.2.

	Early products	Middle products	Late products	
Designation	II	I	III	IV
Morphology	Reticulated	Needles radiating from grain	Indefinite	Spherical Agglomerates

Table 2.2 CLASSIFICATION OF C-S-H MORPHOLOGIES

Type I C-S-H:

Morphology appears as needle-like crystals. They form in the middle period of hydration (0-16 hours), when pores are filled with water containing high concentration of ions.

Type II C-S-H:

Seen as reticulated crystals (net like) and start to form in the early period of hydration .

Type III C-S-H:

Has an indefinite morphology, but believed to appear as crumpled foils.

Type IV C-S-H:

Morphology resembles a spherical-like product. Both Types III and IV are formed when space becomes restricted for particle growth and ionic mobilities are low, i.e. the late period of hydration.

Calcium Hydroxide (CH):

Displays a well crystallised morphology. The crystals are large in comparison to C-S-H crystals (up to three orders of magnitude larger 0.01 - 0.1mm) and can sometimes be seen by the naked eye. They form within cement voids and are seen as well defined hexagonal prisms.

Calcium Sulpho-Aluminate (AFm, AFt):

Can assume two morphologies depending on sulphate ion (So_4^{2-}) concentration within the capillary water of the matrix. The crystals are also hexagonal prisms, but with much higher aspect ratio (10:1). In Portland Cement, ettringite (AFt) appears as long slender needles radiating from the grain with an aspect ratio of 20:1, the crystals are small in comparison with calcium hydroxide crystals and cannot be viewed with an optical microscope. When there is a lack of SO_4^{2-} ions within the matrix, calcium monosulpho-aluminate (AFm) hydrate is produced with irregular, thin hexagonal plate crystals forming in clusters.

A large percentage of the volume of the paste consists of pores, which comprise both capillary pores and gel pores. The percentage volume of pores within the paste is dependent on the water-cement ratio of the mix, the temperature of hydration and curing conditions, and degree of hydration.

2.4.2 Hydration of Tricalcium Silicate (C_3S)

The hydration of C_3S has been studied extensively by monitoring the rate at which heat is evolved during hydration using conduction calorimetry. Skalny[34] has reviewed the existing knowledge and only a summary of essential aspects will be dealt with here. The general shape of the heat evolution curve with respect to time for hydration of C_3S is given in Figure 2.4, along with a curve showing the Ca^{2+} ion concentration in liquid phase. Five stages have been developed from the heat evolution curve to represent C_3S hydration.

Stage 1: Rapid hydration of C_3S and release of calcium and hydroxyl ions (Ca^{2+},OH^-) into the gauging water (0-80 minutes).

Stage 2: A period of slow chemical activity, during which Ca^{2+} concentration is increased in the solution (0-3 hours).

Stage 3: A period of renewed chemical activity, during which C_3S hydrates with vigour. The rate of heat liberation reaches a maximum during this period (3-10 hours).

Stage 4: The rate of chemical reaction is slowed down during this period and Ca^{2+} ion concentration is reduced.

Stage 5: The reactions take place at a much reduced rate, as hardening commences.

It has been postulated by the majority of researchers, that Stage 2 (the induction or dormant period), is the most important stage of hydration, it is affected by the water to solid ratio, temperature, particle size and admixtures. It is believed that

the ultimate properties of the cement matrix is dictated by the chemical reactions taking place in this period[34]. The complete hydration reaction of tricalcium silicate (C_3S), equation 2.1, produces as hydration products: calcium silicate hydrates ($C_3S_2H_4$) known as C-S-H (of various morphologies) and calcium hydroxide $Ca(OH)_2$ known as CH.

$$2(3CaO.SiO_2) + 7\ H_2 \quad > \quad 3CaO.2SiO_2.4H_2O + 3Ca(OH)_2 \quad ..(2.1)$$

$$(2C_3S) \quad + (7H) \quad > \quad (C_3S_2H_4) \quad + \quad (3CH)$$

Attempts to explain the mechanism of the induction period has produced two main theories, and although not all researchers agree on every point within each theory, they are in agreement on certain principal points.

2.4.2.1 Protective Membrane Theories

It is suggested that as gauging water is added to C_3S clinker, calcium and hydroxyl ions (Ca^{2+},OH^-) are leached into solution with C-S-H forming as a protective layer on the silica rich surface of the clinker grain (start of induction period). The induction period is said to end when this protective layer is disturbed[36-44]. Researchers following this theory are in agreement over the formation of a protective membrane, but cannot agree over its morphology and also the reason for the onset of Stage 3 of hydration.

Lea[7] and Stein[36-38] proposed that on gauging, C_3S reacts vigorously, Ca^{2+} and OH^- ions are released into solution. The early high rate of heat liberation (Stage I, Figure 2.4) is

attributed to this reaction. The relatively sudden decrease in the rate of heat liberation is caused by the initial hydration products (calcium silicate hydrate) coating the C_3S grain as a protective layer. This is taken to be the onset of the induction period. The initial C-S-H hydrate has a high calcium-silicate ratio (≈3:1) and is relatively impervious. This coating retards further hydration of C_3S and the reaction rate decreases. The hydrate is unstable because of high calcium/silica ratio. It is suggested that during the induction period, C-S-H changes it morphology depending on the calcium/silica ratio within the aqueous phase and converts to a more permeable secondary hydrate with a calcium/silica ratio of between 0.8-1.5. The aqueous phase becomes supersaturated with respect to Ca^{2+} and renewed reaction on the unhydrated C_3S will be initiated by disruption or recrystallisation of the protective layer, this is marked by the rapid rate of heat liberation (Figure 2.4, Stage 3). Stages 4 and 5 are controlled by a steady release of ions and further formation of hydrates.

Skalny[32] and Fujii[39] believe that the initial membrane which causes the onset of the induction period consists of a skin of water and the first noted hydration product does not crystallise on C_3S surface for some twenty minutes after gauging. Moreover, the end of the induction period is attributed to supersaturation of solution with Ca^{2+} ions and nucleation growth of C-S-H. Magnan[38] believes in the formation of the protective layer during Stage 1, but could not detect it by electron microscopy. However, assuming the early formation of C-S-H, his scenario for early hydration postulates the liberation of soluble Ca^{2+} ions

from the primary amorphous C-S-H leaving a silicate rich surface layer around the grain. This layer, in time, reacts by pozzolanic effect with Ca^{2+} ion-rich solution to form the final silicate hydrate, equation 2.3 and Figure 2.5.

$$CH + S + H \rightarrow C\text{-}S\text{-}H \quad \ldots(2.3)$$

Double[40-42], using a novel electron microscopy system (developed by him and his co-researchers), studied the early hydration of cement slurries. Previous studies of cement hydration using electron microscopy had its limitation caused by the need for complete dehydration of the samples and hence some disruption of its crystalline micro-structure. The new process enabled the direct observation of the hydration products formed during early hydration. Resulting from their observations, they postulated a new, two-stage, scenario for the hydration of cement clinker on contact with water:

a) the rapid formation of a coating of gelatinous hydration products (C-S-H) around the cement grain which, in turn, inhibits subsequent reactions (the induction period), and

b) the eventual growth of fibrillar C-S-H crystals from the coatings which will form a reticulate network between grains.

The amorphous coating forming during stage (a) above allows the gradual passage of Ca^{2+} ions from the grain to the aqueous phase and water from the solution into the grain. In time the aqueous phase becomes supersaturated in Ca^{2+} ions; moreover, the surface of the grain is depleted with Ca^{2+} ions, and will become negatively charged with a silica-rich surface layer. An osmotic

pressure is built-up within the protective coating and eventually causes it to rupture at weak points. Tubular fibrils of C-S-H will then begin to grow at the point of rupture through the amorphous C-S-H hydrate on the grain surface. It has been implied that this process resembles the silicate garden morphology which has also been proposed by Birchall[43] and Powers[44]. A schematic model for the above hydration scenario is given in Figure 2.6.

It must be pointed out at this stage that there are controversies on the osmotic hypothesis[43,50]. Osmotic mechanisms are not observed in the hydration of pure C_3S, therefore, their occurrence in cement hydration must be the result of the presence of alumina, sulphate and other species[33]. To substantiate this hypothesis, further experimental evidence is required.

2.4.2.2 Delayed-Neucleation Theories

The second group of researchers propose the delay in nucleation of calcium hydroxide and calcium silicate hydrates as the reason for the onset of the induction period. Therefore, it is the nucleation of CH and C-S-H that ends the induction period and initiates renewed hydration of the anhydrous C_3S core.

Young[45] believes that the induction period is controlled by the nucleation and growth of CH from solution. C_3S is dissolved during the induction period, Ca^{2+} and OH^- ions are leached from C_3S grains into the solution, the rate of dissolution decreases as the solution becomes saturated and its chemical potential increases (hence, the slowing down of C_3S reaction). This

thermodynamic barrier is lifted when the solution becomes sufficiently supersaturated with Ca^{2+} and OH^- ions for calcium hydroxide to nucleate and grow. C_3S hydration is reactivated as a result of the reduction in Ca^{2+} ions in solution (end of induction period).

Young[46], in studying the Ca^{2+} and OH^- concentration in the liquid phase, with respect to time, found that the time of maximum Ca^{2+} ion concentration coincided with the end of the induction period (Figure 2.4) and the onset of calcium hydroxide nucleation. The following chemical reactions have been suggested by Young[46]:

Initial hydrolysis:

$$C_3S + H \longrightarrow C_2S^* + Ca^{2+} + OH^- \quad ...(2.3)$$

$$C_2S^* + H \longrightarrow 2Ca^{2+} + H_2SiO_4^{2-} + 2OH^- \quad ...(2.4)$$

Where C_2S^* is considered as a lime-deficient C_3S after initial hydrolysis.

$$2H_2SiO_4^{2-} + 2OH^- \longrightarrow Si_2O_7^{6-} + 3H_2O \quad ...(2.5)$$

At the end of the induction period:

$$Ca^{2+} + 2OH^- \longrightarrow CH \quad ...(2.6)$$

$$2SiO_4^{4-} + H \longrightarrow Si_2O_7^{6-} + 2OH^-$$

$$\longrightarrow [SiO_3]_n^{2-} + 2nOH^- \quad ...(2.7)$$

The increase in the ionic products within the solution after CH nucleation is accounted for by the increase in OH^- ion concentration caused by the polymerisation of the silicate species formed during the renewed chemical activity of C_3S (equation 2.7).

Sleger[47], in agreement with Berger[48], confirmed that the solution is supersaturated when Ca^{2+} ion concentration is at its peak (Young[46]), however, they detected $Ca(OH)_2$ crystals in the solution long before supersaturation, but explained that $Ca(OH)_2$ could crystallise near C_3S grain surface, where Ca^{2+} ion concentration is relatively high long before supersaturation of the aqueous phase with Ca^{2+} and OH^- ions. Tadros et al[49] conducting studies on concentrations of ions within the aqueous phase concluded similar findings, they proposed that $Ca(OH)_2$ crystals also act as neucleation sites for C-S-H. This is because $Ca(OH)_2$ crystals incorporate silicate ions.

The hydration stages following induction contributes to the development of the main characteristics and properties of the hydration products. Unfortunately, because of the complexities of the hydrates and inadequate instrumentation to monitor the events taking place, there is a lack of knowledge in this area. There are many conflicting views as to the nature and morphology of the hydrates produced, in particular C-S-H.

It is known that C-S-H converts as C_3S reaction progresses, it forms a rigid network to replace:

a) the aqueous phase along with $Ca(OH)_2$ nucleation between the grain.

b) the anhydrous core within the grain.

Glasser[50] proposed a mechanism for C_3S hydration which is given in Figure 2.7. CH and Type I C-S-H nucleate, which ends the induction period; as the reaction proceeds, Type I C-S-H and CH hydroxides are engulfed by Type III C-S-H. This mechanism has much in common with those suggested by Young[45,46] and Tadros[49].

Taylor[51] proposed a mechanism based on his own observations along the findings of Tadros[49], Glasser[50] and Young[45,46] which is reproduced in Figure 2.8. As the hydration progresses, a semi-solid low calcium/silica ratio layer surrounds the grain (Figure 2.8(b)), which in time advances into the diminishing C_3S grain (Figure 2.8(c)). Some of the Ca^{2+} ions released from the reacting C_3S pass through this layer to form outer products of C-S-H and CH, others are trapped in this layer and react with silica to form the inner C-S-H product. This hypothesis, as suggested by Taylor[51], requires additional experimental proof.

2.4.3 Hydration of Dicalcium Silicate (C_2S)

Generally, hydration of C_2S has not received the amount of attention given to the hydration of C_3S. The reason lies with the fact that C_2S hydrates in a similar way to C_3S and produces the same hydration products, however, the reaction rates are much slower:

$$2C_2S + 5H \longrightarrow C_3S_2H_4 + CH \qquad ...(2.8)$$

Monitoring the hydration of C_2S by measuring the rate of heat liberation is more difficult, because C_2S liberates less heat during its hydration and the reactions take place at a much slower rate. Precipitation of C-S-H around the grain boundaries have been observed[52] as early as 15 seconds after gauging with water, but subsequent development to other morphologies of C-S-H hydrates take much longer. Supersaturation Ca^{2+} and OH^- in solution is not to the same extent as with C_3S hydration, large $Ca(OH)_2$ crystals are formed during the late hydration period.

Lately, because of the realisation of the important role which C_2S hydration plays in the structure building processes of cement, more effort has been directed towards effective ways of monitoring C_2S hydration.

2.4.4 Hydration of Tricalcium Aluminate (C_3A)

The mechanism of C_3A hydration is, in principle, similar to that of C_3S, although the reaction rates vary. The products of hydration have different chemical composition and morphologies, and a much higher rate of heat evolution is experienced. However, like C_3S, when C_3A reacts with water, calorimetry studies[53] show vigorous reactions taking place within minutes of contact with the gauging water. There follows a period of little or no apparent chemical activity proceeded by renewed reaction and subsequent slowing down.

Pure C_3A grains, when reacting with water produce unstable hexagonal hydrates (C_4AH_{13} and C_2AH_8) which convert to stable cubic hydrate (C_3AH_6).

$$2C_3A + 21H \longrightarrow C_4AH_{13} + C_2AH_8 \quad \text{(hexagonal hydrate)} \quad ...(2.9)$$

$$C_4AH_{13} + C_2AH_8 \longrightarrow 2C_3AH_6 + 9H \quad \text{(cubic hydrate)} \quad ...(2.10)$$

The conversion takes place either when sufficient C_3AH_6 nuclei are available, or when the temperature of the hydrating system is raised above $30^{\circ}C$ (by the exothermic nature of the reaction forming hexagonal hydrates), once C_3AH_6 is nucleated, crystal growth will take place and continue even at temperatures below $30^{\circ}C$. Direct formation of C_3AH_6 from C_3A is possible at temperatures above $80^{\circ}C$. However, it is the hydration of C_3A in the presence of sulphate ions that is more relevant to cement hydration. Calcium sulphate $CaSO_4.2H_20$ (known as gypsum) is added to cement clinker during its manufacturing process, to control cement setting. In the presence of gypsum, during the first few minutes, an almost impermeable coating of ettringite ($C_6AS_3H_{32}$) covers the C_3A grains and prevents further dissolution and hence the diffusion of SO_4^{2-} and Ca^{2+} ions into the liquid phase. Ettringite remains stable so long as there are sufficient amounts of SO_4^{2-} available in the liquid phase to prevent conversion to the more stable $C_4A\bar{S}H_{12}$ (monosulpho-aluminate) hydrate:

$$C_3A + 3C\bar{S}H_2 + 26H \longrightarrow C_6A\bar{S}_3H_{32} \quad \text{(ettringite)} \quad ...(2.11)$$

$$C_6AS_3H_{32} + 2C_3A + 4H \longrightarrow 3C_4A\bar{S}H_{12} \quad \text{...(2.12)}$$

(monosulpho-aluminate)

The first peak in the heat evolution profile is the consequence of the initial dissolution of C_3A and the formation of ettringite (Stage 1, Figure 2.9(a)). The subsequent period of inactivity (Stages 2 and 3, Figure 2.9(a)) is the result of reduction in the SO_4^{2-} and Ca^{2+} ion concentration in the liquid phase, which controls the rate at which ettringite is formed. Stage 4 is the onset of the conversion of ettringite to monosulpho-aluminate, initiated by a sufficient reduction in SO_4^{2-} ion concentration of the liquid phase. The conversion fractures the ettringite layer, and exposes unhydrated C_3A core to further hydration. Figure 2.9(b) illustrates the sequence of C_3A hydration as suggested by Jawed and co-workers[33]. A new mechanism of hydration has been suggested by Tadros[54] and Skalny[55] based on their dissolution and electrokinetic data, which is not unlike the mechanism proposed by Skalny[32] and Fujii[39] for C_3S hydration. They postulate C_3A to dissolve in water, leaving a negatively charged alumina rich layer around the anhydrous core, positively charged Ca^{2+} ions are adsorbed to this layer, the formation of this charged layer reduces the rate of C_3A dissolution. In the presence of sulphate ions, C_3A particles with their positively charged layer will adsorb negative SO_4^{2-} ions which results in further reduction in the dissolution of C_3A (Figure 2.10).

2.4.5 Hydration of the Ferrite Phase (C_4AF)

C_4AF hydration is similar to that observed by C_3A hydration in

the presence or absence of gypsum. However, the reaction rates are slower and the amount of heat that is evolved is much less. The mechanism of hydration is the same as that for C_3A hydration, only iron oxide plays the role of aluminium oxide. As the amount of iron is increased, the reaction slows down.

2.4.6 Setting and Hardening Processes in Cement Paste

The hydration of Portland Cement is a complex chemical interaction of several individual compounds hydrating simultaneously at varying rates, each being influenced by each other's hydration. The most reactive compound forming Portland Cement clinker is C_3A followed by C_3S, C_4AF and C_2S. C_3S forms the greatest part of Portland Cement clinker and, as such, its hydration dominates the early hydration of Portland Cement. The mechanism of early Portland Cement hydration is believed to closely follow that of C_3S hydration[32], therefore, the theories suggested by Skalny[32], Fujii[39], Double[40-42] and Powers[44] would, in principal, apply to Portland Cement hydration. To date, a precise mechanism for cement hydration has not been fully understood and, although the postulated theories are more often complimentary than contradictory, they are still the subject of controversy. However, several different time stages in the process of cement hydration can be distinguished and be related to the formation of different chemical hydrates. A convenient method to follow the various stages of cement hydration is to use the heat evolution profile during hydration (Figure 2.11).

The first stage of hydration lasts for a few minutes and the first peak in the heat evolution graph (Figure 2.11) is the

direct result of the following exothermic reactions. Immediately upon contact with water, C_3A and gypsum interact with water and as a result gypsum starts dissolving, sulphate ions (SO_4^{2-}) migrate to the rapidly hydrating C_3A, encouraging the formation of ettringite ($C_6AS_3H_{32}$) around the unhydrating core of C_3A which will act as an inhibiting layer, preventing further hydration of C_3A. The C_3S component of the grain also dissolve releasing calcium (Ca^{2+}) and hydroxyl (OH^-) ions into the solution. The calcium ions are then partially readsorbed to the silicate-rich outer layer, this, along with further hydration of C_3S, results in the formation of a thin layer (50-100 angstroms) of C-S-H hydrate with calcium to silicate ratio of between 1 and 3, called gel, beneath the readsorbed Ca^{2+} layer. This is an amorphous calcium silicate hydrate, which can last for several seconds or up to a few minutes. It is sometimes referred to as Type 0 C-S-H.

Following these initial exothermic reactions, there is a period of 30 minutes to several hours when there is little or no heat liberation (Stage 2, induction period), however, the chemical reactions have not ceased completely, water is adsorbed by the unhydrated core and Ca^{2+} ions are slowly released into solution. During the induction period, the morphology of C-S-H changes and acquires a more definite crystalline form (Type II, C-S-H). According to one of the hydration theories[40-43], the C-S-H overlayer acts as a semi-permeable membrane which allows water molecules to diffuse into the anhydrous grain core but greatly slows down calcium and hydroxyl ion migration into solution. Therefore, the osmotic pressure continuously builds during this

dormant period. When a critical pressure is reached, the C-S-H protective layer bursts and exposes unhydrated C_3S core for further hydration.

The second heat liberation peak (Figure 2.11) marks the beginning of renewed chemical activity. It corresponds to the formation of calcium hydroxide crystals within the now supersaturated liquid phase, moreover, the morphology of silicate hydrates are modified, new C-S-H hydrates are formed (Type I C-S-H) and others convert to fill the spaces vacated by water used by hydration. Most of the C_3A would have been hydrated to form ettringite, using available SO_4^{2-} ions, which would also contribute to the amount of heat evolved. However, if SO_4^{2-} ion concentration in the liquid phase is depleted, ettringite will dissolve to form monosulpho-aluminate. Because this reaction is dependent on the relative availability of aluminate and sulphate ions, it could take place any time after the end of the induction period.

After the second peak in the rate of heat evolution is reached, the overall rate of reaction drops as the reactions become diffusion controlled. At this stage hydration of C_2S and C_4AF compounds becomes more prominent, their reaction following an essentially similar hydration mechanism to those of C_3S and C_3A respectively. They would proceed as long as space and reacting species are available.

In this brief synopsis of the Portland Cement hydration process, the C_3S hydration phase has been emphasised, this is for the simple reason that C_3S hydration is judged to be the main

reaction phase[7,21] in Portland Cement hydration and the principal contributor to setting[33]. It is during Stage 3 that the paste changes from fluid to rigid state and it is over this transition period that the terms "initial set" and "final set" are used to define arbitrary degrees of firmness of the paste. Traditionally the Vicat Needle[56] has been used to quantify these terms.

2.5 RETARDATION AND ACCELERATION IN SETTING TIME

As stressed before, the chemical composition of cement clinker has a direct influence on its setting and hardening properties. Therefore, controlling the composition of the dry cement and the manufacturing process becomes important. The setting time of cement is adjusted during the manufacturing by:

a) composition adjustment (i.e. C_3S to C_3A ratio),

b) particle size distribution (altered by grinding process), cement will set slower when coarsely ground,

c) the cooling rate of the cement clinker which determines, to some degree, the amount of C_3A available for hydration - the faster the clinker is cooled, the less C_3A is formed and the slower the setting time.

It is common practice to use several of the above methods when producing special cements.

Field retardation or acceleration of cement hydration is common and accomplished by introducing chemical additives, which alter

the hydration process of cement. The use of admixtures becomes necessary when environmental conditions, local conditions, and design constraints demand particular characteristics from cement. Recently, the use of admixtures by the construction industry has increased[57], as a substitute to using special cements.

A variety of admixtures are in use, and they are often classified according to the purpose for which they are being used[8]. The most common are retarders, accelerators and water reducing (superplasticisers), the less common admixtures are air entrainment, air detrainment, fungicidal and water proofing admixtures. Details of how admixtures chemically affect the hydration of Portland Cement can be found in References 7, 8, 45, 58 and 59.

a) Celluloses, lignosulfonates and sugar[60,61] derivatives are widely used as retarders, they inhibit hydration and precipitation of calcium hydroxide. Care must be taken with retarders to make sure that they do not interfere with strength development of the cement.

b) Amongst a number of chemicals used as accelerators, sodium chloride and calcium chloride are the most common[62]. These inorganic chemical accelerators increase the ionic character of the aqueous phase, this encourages the rapid hydration of C_3A, C_3S and C_2S phases, the nucleation of calcium hydroxide, and the formation of calcium-silicate-hydrate, hence faster setting time.

c) Lignosulphonic acids, hydroxylated carboxylic acids are used as water reducing admixtures[63,64,65]. These admixtures

help to disperse cement particles and hence expose a greater surface area of the cement to hydration, this will result in an early gain in the strength of the mix. Because of the entrained air introduced by the admixture, the quantity of the mixing water could be reduced without affecting workability. The reduction varies between 5-15%[65].

Superplasticisers are modern equivalents of water-reducing admixtures[66], they are more effective in dispersing the cement particle, hence improving workability and the increase in the rate of hydration.

Although manufacturers of additives describe the effect and properties of their products, care must be taken when using admixtures. Their effect is not similar on cements of different chemical composition, and age. Their use, therefore, must be based on personal experience or ad hoc tests and the adherence to Code recommendation (BS 5075: Part 1, 1982 and ASTM Standard C494-79) until theoretical information on a scientific basis becomes available to permit a reliable quantitative prediction of the behaviour of admixtures in concrete under various possible circumstances.

2.6 CONCLUDING COMMENTS

- Despite all research in the field of cement hydration, divergence of opinion exists between the presented theories as to the mechanism of cement hydration.

- There are limitations as to the use of any one of the experimental techniques in studying cement hydration.

- Much information has been gained on the hydration mechanisms of the individual cement minerals. This information provides a necessary basis for the understanding of cement hydration, however, care must be taken to consider the cross-reactions that will take place between various major and minor compounds.

- There is a need for the development of accurate techniques to continually monitor:
  a) the hydration of cement paste,
  b) chemico-physical changes of cement paste,
  c) pore structure development.

- The need for the use of new techniques for monitoring and assessing such engineering properties of cement and concrete as:
  a) Strength,
  b) Setting time,
  c) The influence of admixtures,
  d) Durability,
  e) Permeability.

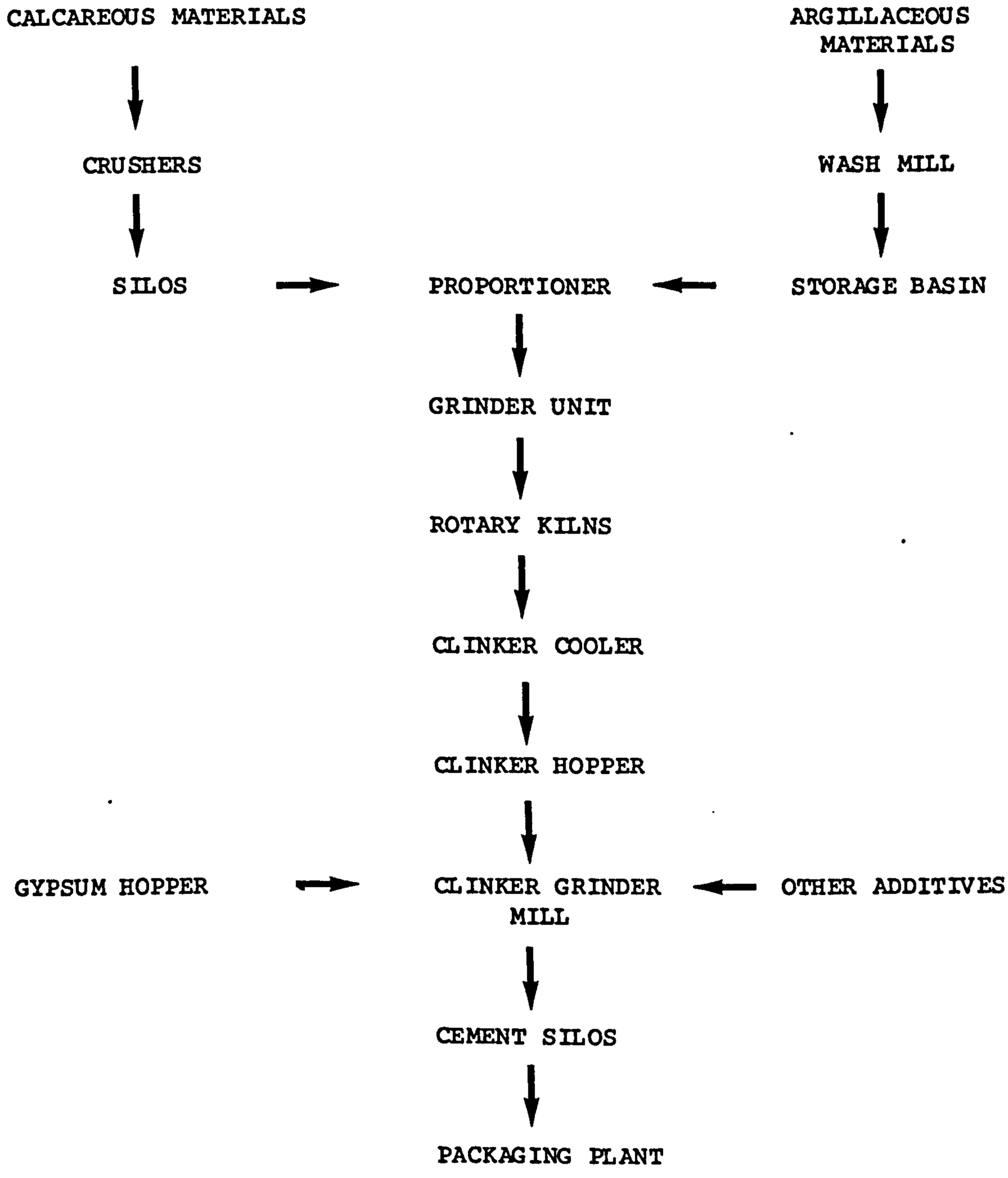

FIGURE 2.1 PORTLAND CEMENT MANUFACTURING DRY PROCESS

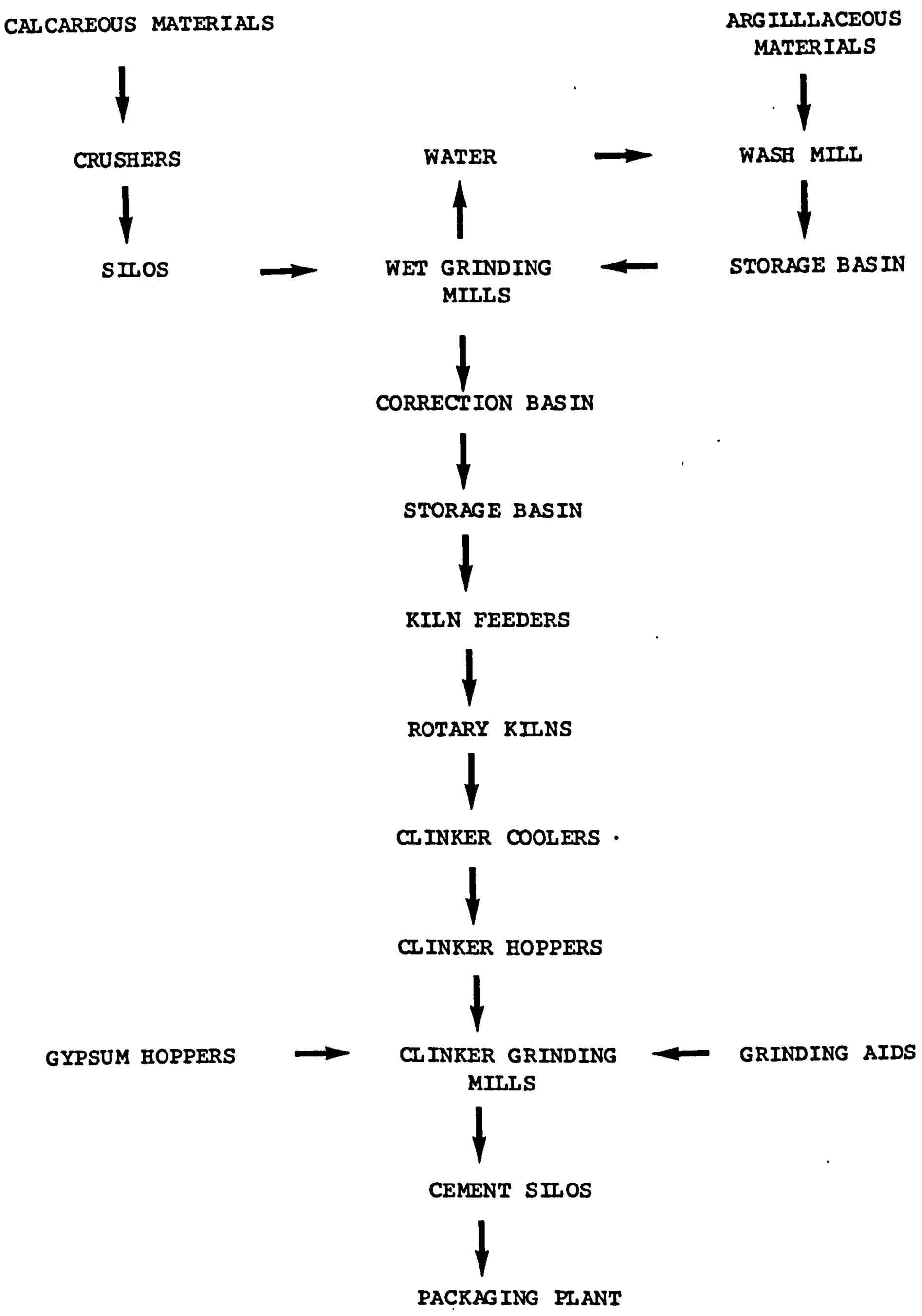

FIGURE 2.2 PORTLAND CEMENT MANUFACTURE WET PROCESS

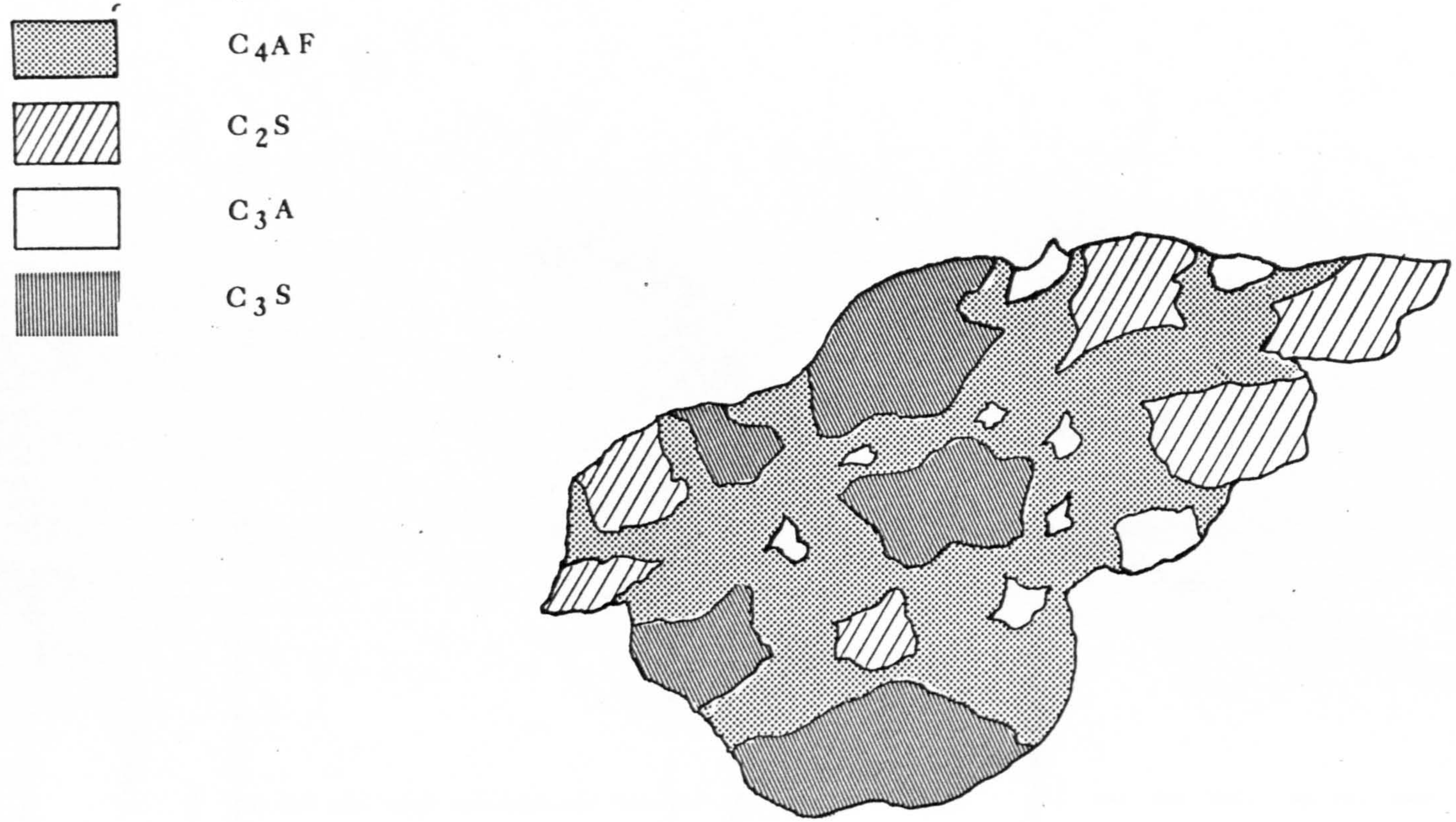

FIGURE 2.3 SUGGESTED CLINKER GRAIN STRUCTURE[26]

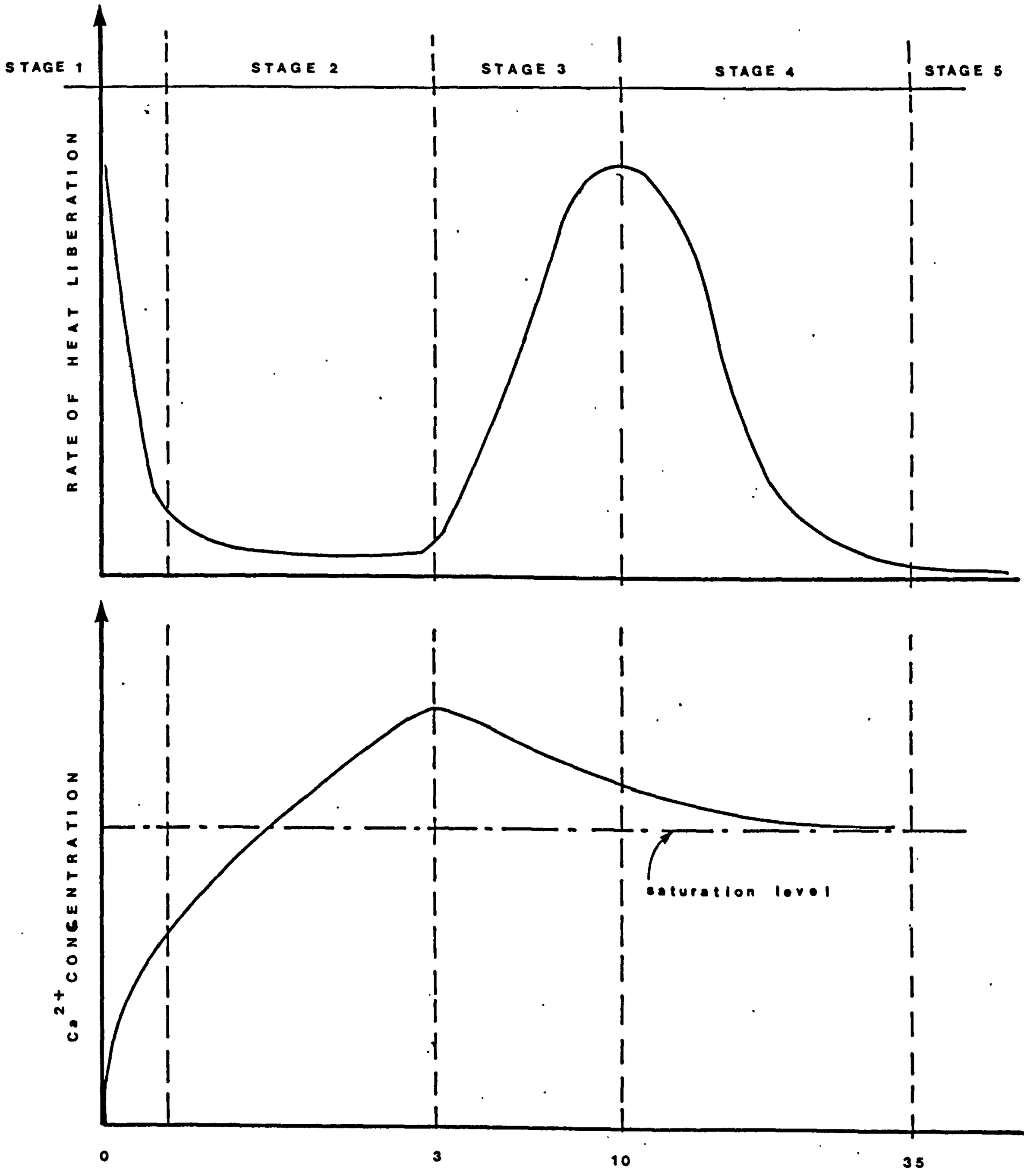

FIGURE 2.4 CLASSIFICATION OF HYDRATION STAGES OF C_3S ON THE BASIS OF HEAT EVOLUTION AS MEASURED BY CONDUCTION CALORIMETRY AND ITS CORRELATION WITH CA^{2+} ION CONCENTRATION IN THE LIQUID PHASE (MODIFIED FROM KONDO AND VEDA[31]) WATER/CEMENT RATIO ≈ 10:1

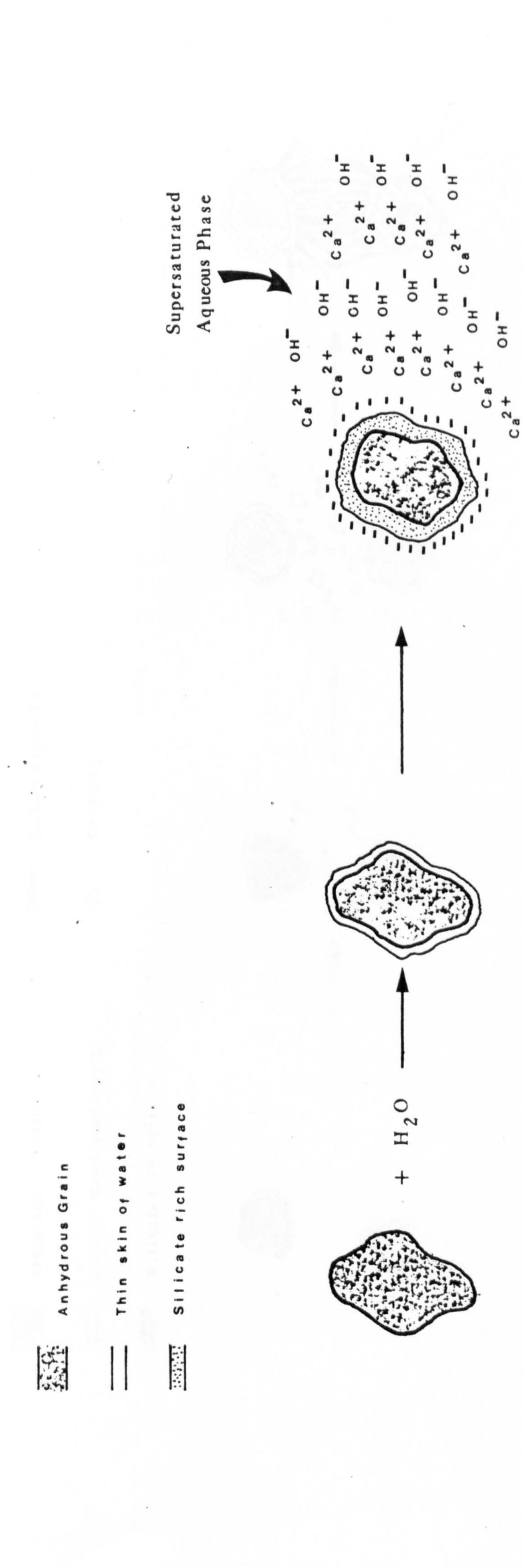

POSSIBLE SCENARIO FOR EARLY HYDRATION OF C_3S. SKALNY[32] AND FUJII[39]

FIGURE 2.5

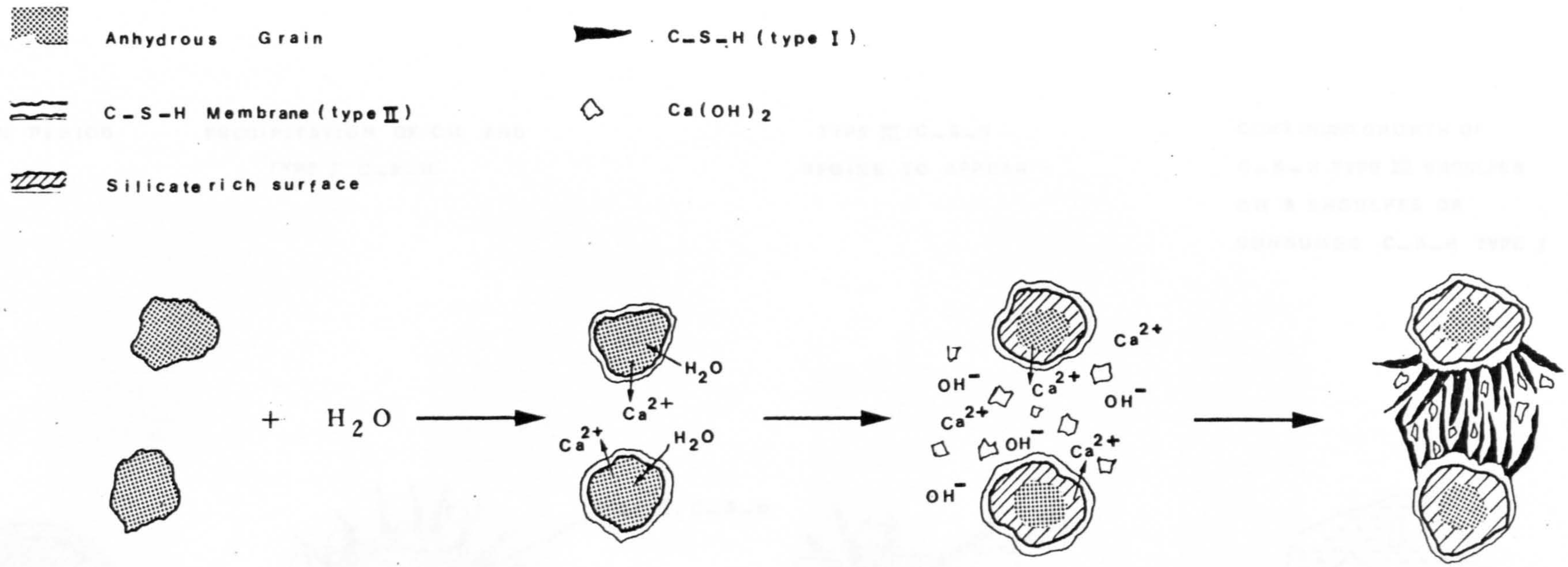

FIGURE 2.6 POSSIBLE SCENARIO FOR EARLY HYDRATION OF C_3S. DOUBLE[40-42] AND POWERS[44]

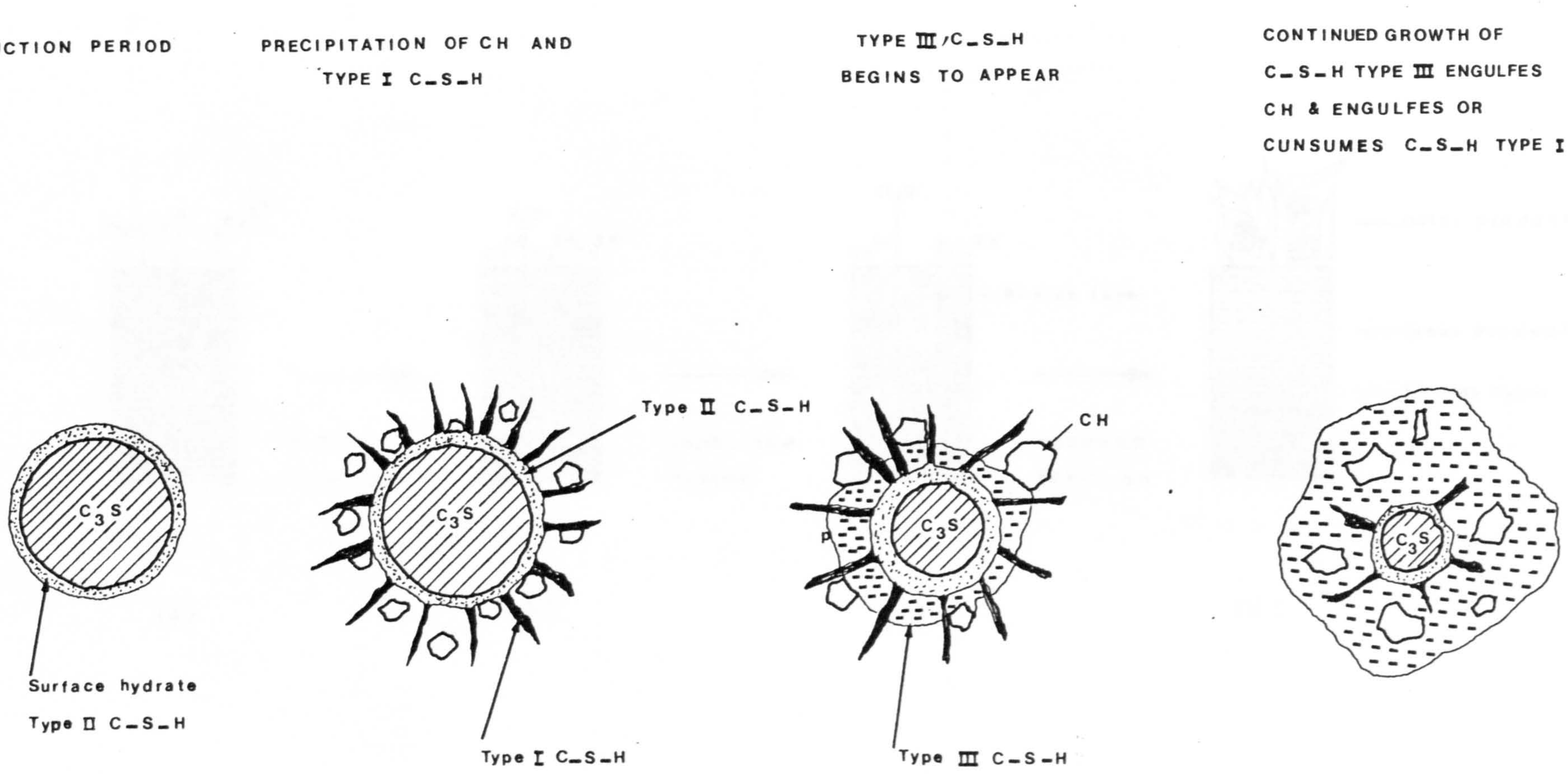

FIGURE 2.7 SUGGESTED MECHANISM OF C_3S HYDRATION PROPOSED BY GLASSER[50]

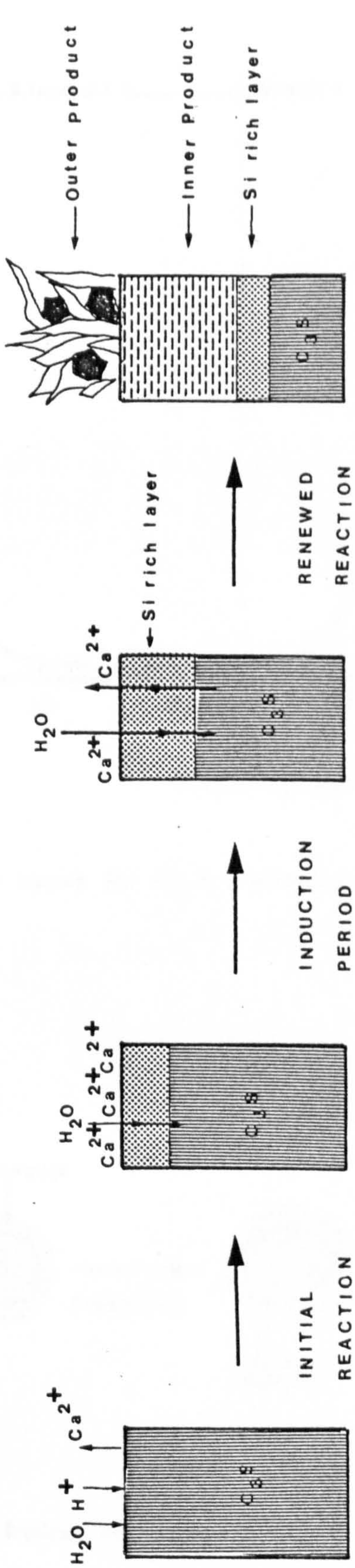

FIGURE 2.8 SUGGESTED MECHANISM OF C_3S HYDRATION PROPOSED BY TAYLOR(51)

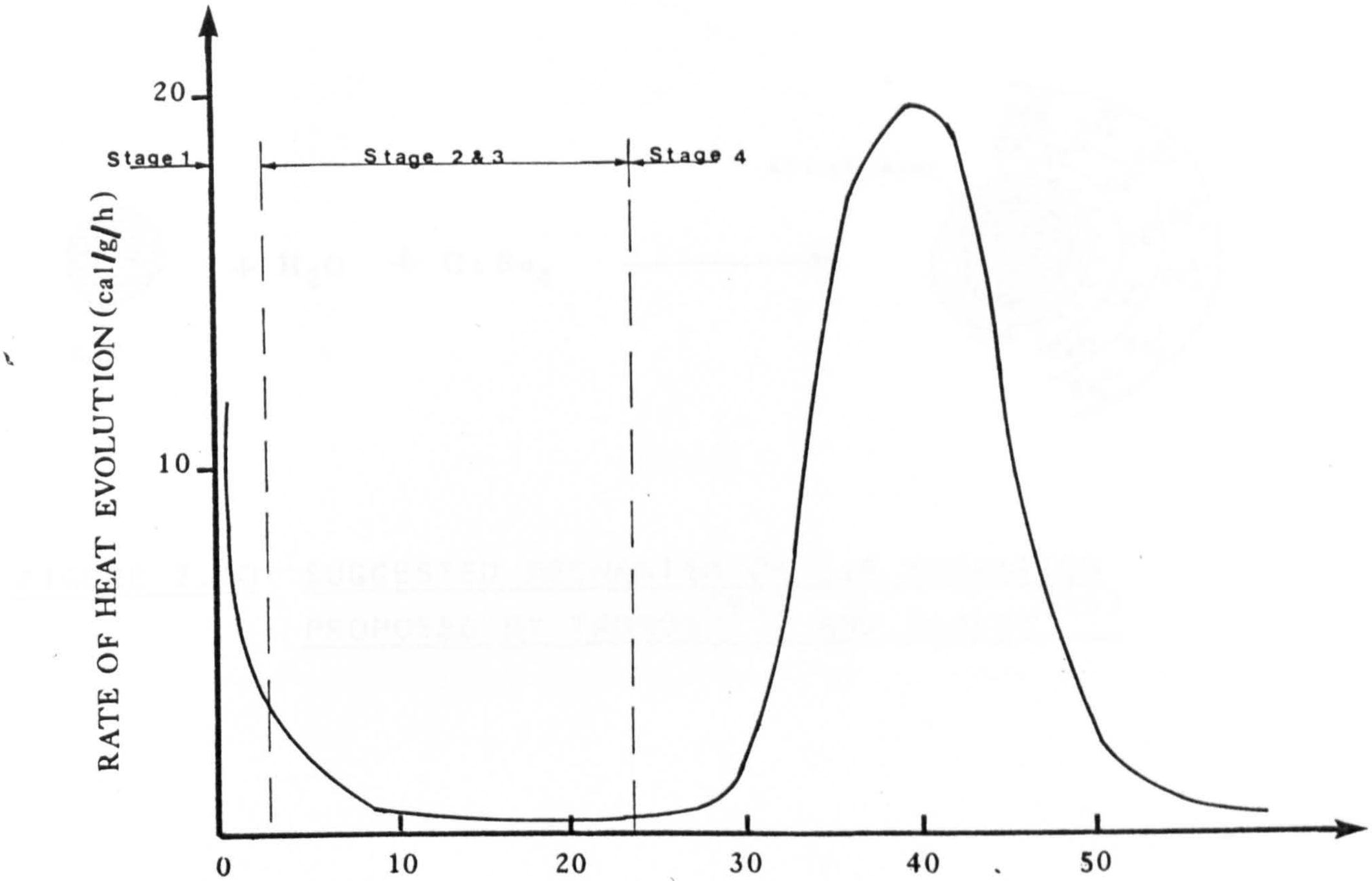

a) calorimetric curve for C_3S hydration

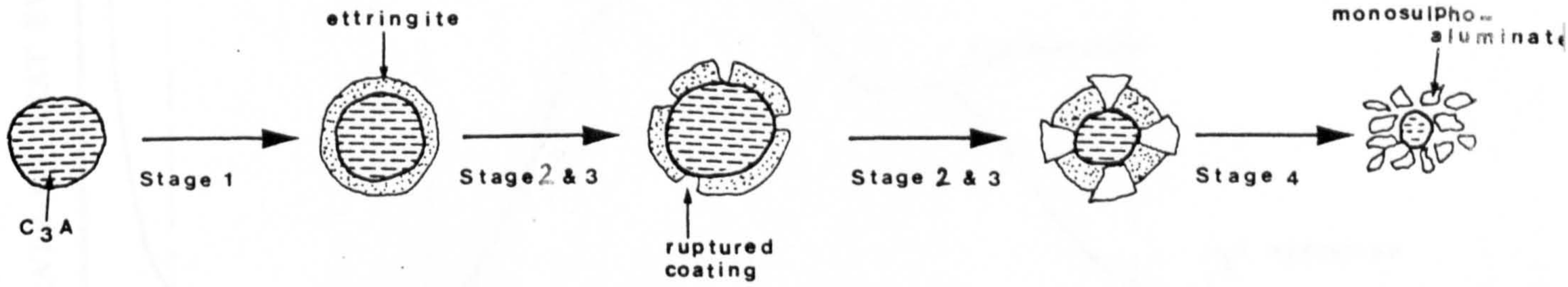

b) sequence of hydration

FIGURE 2.9 SUGGESTED MECHANISM OF C_3A HYDRATION PROPOSED BY JAWAD ET AL[33]

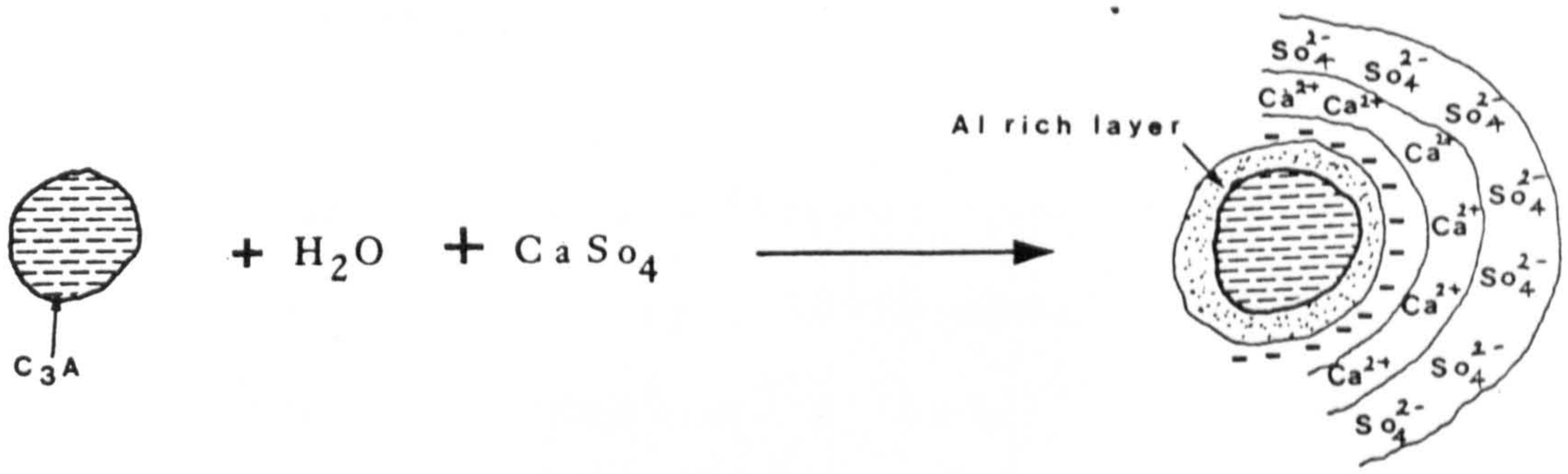

FIGURE 2.IO SUGGESTED MECHANISM OF C_3A HYDRATION PROPOSED BY TADROS[54] AND SKALNY[55]

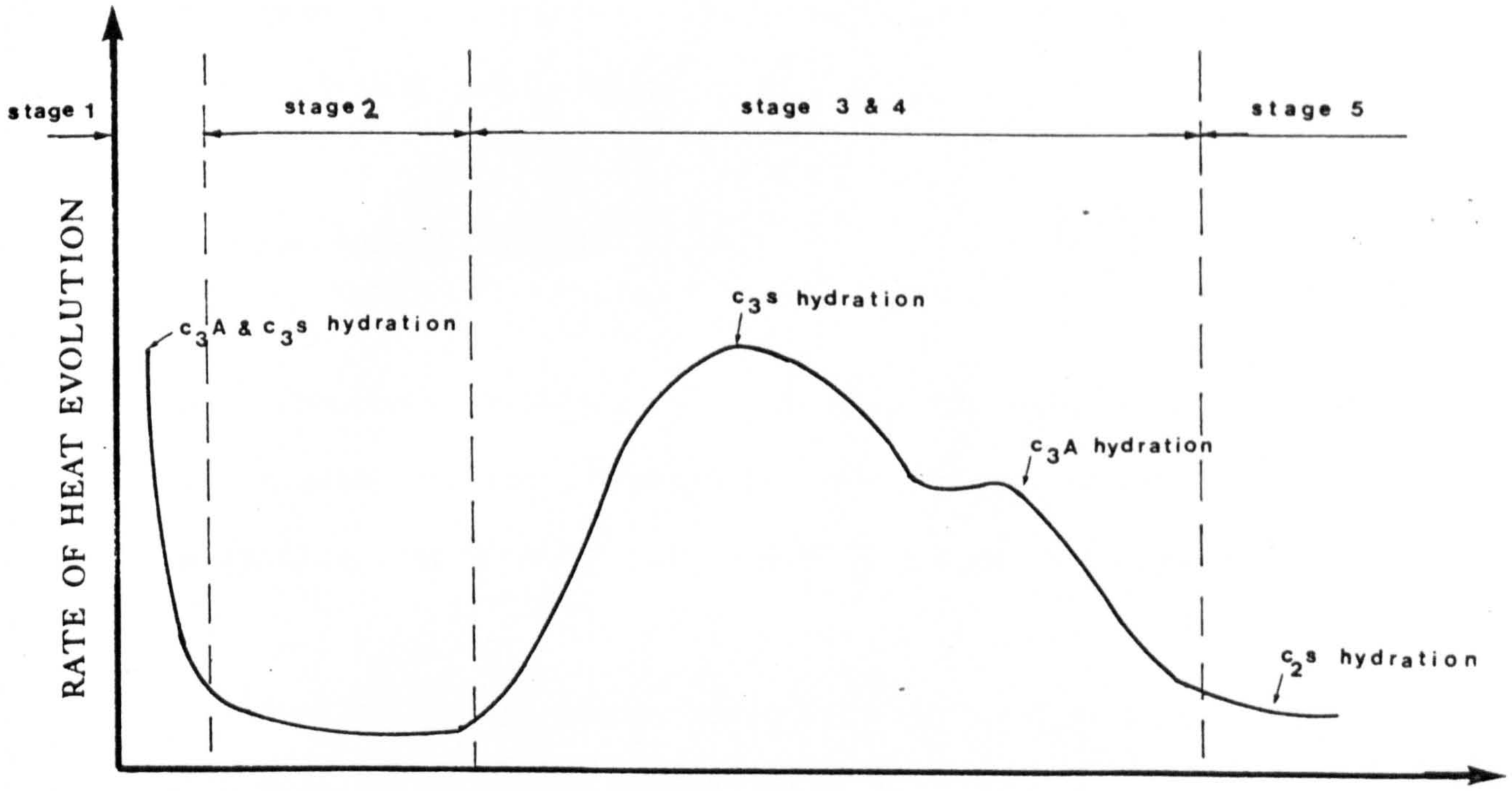

FIGURE 2.II SCHEMATIC REPRESENTATION OF CEMENT CLINKER HYDRATION

CHAPTER 3

METHODS OF TESTING CEMENT AND CONCRETE

3.1 INTRODUCTION

As mentioned in the previous chapter, cement is a non-homogeneous material formed by finely grinding several minerals, hence the performance and properties of cement is dependent on the percentage and properties of its individual constituents; the manufacturing process; the storage conditions of cement before use; the mix design and quality control. Stringent control takes place and tests are performed in a cement work's laboratory to ensure that the cement is of the desired quality and conforms to the various national standards. However, it is essential for the cement user to conduct independent tests at more frequent intervals to ensure that his, and the requirements of the various standards, are satisfied. In Britain, the relevant standards are BS 12, BS 4550 and BS 1881.

3.2 LABORATORY TESTING

The laboratory analysis of cements, and the methods used to investigate cement hydration, can be divided into three categories, depending on the state of cement for testing:

a) Testing of dry cement powder and wet chemical analysis.

b) Testing of liquid cement paste.

c) Testing of hardened cement paste.

There are universally accepted and recognised tests which conform to various international standards and cover the above. In addition, there are rheological and other unconventional tests

available which, although not universally recognised, give an insight into the hydration of cement. The electrical method, described here, falls within the latter category.

3.2.1 Testing of dry cement powder and wet chemical analysis

Testing of cement powder involves chemical analysis in order to ascertain the chemical composition of the cement and the properties of the individual constituents. A number of established tests are available[26], a brief description of these methods is given here.

a) Scanning Electron Microscopy

Scanning Electron Microscopy and Energy Dispersive Analysis can provide qualitative indication of the presence of the various elements, this has been extensively used[42,43,67-79] to monitor microstructure development of cement paste during hydration. In most cases[67-78], prepared fracture surfaces of cement paste from the bulk hydrated sample are dried under a low pressure and the surface sputtered with a thin layer of gold to render them electrically conducting, hence avoiding the build-up of charge on the surface. It has been argued[42,43,79] that there will be some disruption of the microstructure through the drying process. Double et al[42] developed an environmental chamber and studied the hydration process continuously. The shortcomings of this method are the high water/cement ratios required in order to obtain transmission through the hydrated products surrounding the cement grain, and loss of clarity in the final image caused by the movement of the cement particles.

b) X-ray Diffraction

This process yields quantitative results by relating various peak areas obtained[80,81]. Diffracted X-rays from the cement sample are detected by a proportional counter and the resultant signal recorded on a strip chart recorder. Each crystalline compound within the sample has its own particular diffraction pattern, which can be considered as a fingerprint of the compound; by identifying the numerous intermixed fingerprints on a strip chart of considerable length, the experienced laboratory technician can determine which, and approximately how much, of each chemical compound exists within the original sample.

c) Flame Atomic Absorption Spectrophotometry

In this process, a prepared solution of the material to be analysed is atomized in a very hot flame (2000 - 3000^{o}F), while a lamp, the cathode of which is made of the element to be measured, emits light of specific wavelength through the flame. The light absorbed by the atomized element is then measured, providing a reading that is directly proportional to the concentration of the element in the original solution[26].

d) Solubility Test

C_3S and C_2S are both soluble in a blend of salicylic acid and methanol; C_3A is soluble in a solution of cane sugar and C_4AF is insoluble in either solution. From this information, and using standard laboratory apparatus, the percentages of various phases can be determined by carrying out a series of filtrations.

The physical properties of cement powder are directly related to

its particle size or fineness. The standard equipment for measuring fineness is the Blaine Permeameter[26]; the air permeability through cement powder is measured and then converted to a value of specific surface area, expressed in square centimetres per gram of cement.

3.2.2 Testing of Liquid Cement

The hydration of cement is an exothermic reaction, and hence energy is evolved in the form of heat. Conduction calorimetry has been used to study the hydration of cement for some time. Much of the early work was carried out by Tian[82] and Carlson[27,83], others[28-30,84,85] have modified and developed apparatus (conduction calorimeter) to deal with not only the total heat of hydration over a few days[27,82,83], but to estimate the instantaneous rate of heat liberation at any particular time. Through detailed measurements of the heat evolution, chemical properties of cement are related to its physical performance.

3.2.3 Testing of Hardened Cement

The chemical analysis of set cement samples can be performed using X-ray diffraction methods, however, as yet, no standard test method has been defined and accepted. In general, it is difficult to quantitatively estimate the new compounds that are formed during the process of cement hydration (e.g. calcium-silicate-hydrate gel or sulphoaluminate-silicate-gel), because their chemical composition and nature are altered upon the environmental conditions to which they are subjected. The investigation of the physical properties of a set cement can

involve any one, or a combination of, the following tests:

a) Compressive strength.

b) Setting time.

c) Bonding strength.

d) Expansion.

e) Pore size distribution.

f) Permeability.

Amongst the tests mentioned above, compressive strength and setting time are the most commonly used. The former is simply the measurement of the force needed to crush a sample of defined geometry under unrestrained uniaxial compression. The latter relates to the time taken for wet cement, in static state, to reach a conventional cohesive strength. The traditional methods are Gillmore and Vicat needles, in which measurements are made according to the penetration into the sample of wet cement by a needle of specific weight and cross-sectional area. There are other methods in existence such as the use of acoustic and ultrasonic wave propagation (used mainly by various oil companies[86]). These techniques are still in the early stages of commercialisation and are not yet in common use, however, it seems likely that they will in the future be used to further supplement the standard tests.

3.3 THE ELECTRICAL METHOD

Previous studies on the a.c. electrical properties of cement and concrete[87-94] has concentrated on the changes in the electrical

resistivity of prisms in the hardened state (i.e. after 24 hours) to periods in excess of 200 days. Early research[96-101] on electrical methods used by the oil industry to determine soil fabric and properties of oil-bearing rocks has been beneficial to researchers working on the electrical response characteristics of cement and concrete.

The variation in electrical resistance has been monitored and in most cases[87-89] attempts were made to relate these changes to the physical characteristics and state of the specimen. Little effort was made to relate changes in electrical resistance with chemical processes of setting and hardening. More recently, attention has been drawn to the use of the electrical resistivity characteristics of cement paste as a technique for measuring the degree of hydration, and hence hardening and strength of the paste[91-94], however, the studies only covered the resistivity measurements of hardened specimens. Some early work[102-104] was undertaken to obtain information on the changes in electrical resistance during the first 24-hours of the setting process in cement paste, however, specimens of differing sizes, differing electrode configurations, measuring techniques, and test conditions together with a general lack of data points makes the results presented vary within wide limits.

The previous work outlined above has used a resistive model for cement paste, mortar and concrete with aggregate and cement paste represented by a parallel combination of resistive elements. It is said that this model is more applicable to relatively mature specimens. Cement paste, mortar or concrete can be more

accurately modelled using an electrical network consisting of a capacitive element, C, and a resistive element, R. Such a model was introduced relatively recently[105-112], however, the research concentrated on the hardened state.

The electrical model used in the present study[113-117] to represent the macroscopic response of a colloidal dispersion such as cement paste, is a modification of a model developed by McCarter[109], it includes a capacitive element, C, in parallel with the resistive element, R, (Figure 3.1). This study concentrates on the electrical response changes of cement paste and mortar specimens over the initial 24-hours after gauging. It is during this period that, as a result of chemical reactions taking place, the paste changes from a fluid to a solid.

Electrical response of cement paste to the application of an alternating electrical field can be measured in terms of resistance, R, and capacitance, C; the measurements can be taken irrespective of whether the system chosen is a parallel combination of resistance and capacitance, Figure 3.1; a series combination of resistance and capacitance, Figure 3.2; or a combination of both, Figure 3.3, provided the applied potential and therefore the subsequent current is sinusoidal.

The values of capacitance, C, and resistance, R, are converted to more meaningful electrical parameters, dielectric constant ε, and electrical resistivity, ρ, these parameters account for the geometry of the specimen using the following relationships:

$$\varepsilon = \frac{C}{C_o} \qquad ..(3.1)$$

$$\rho = \frac{RA}{L} \quad \text{ohm-m} \qquad ..(3.2)$$

where, L = length of specimen in metres

A = cross-sectional are of the specimen in m^2 (assumed uniform)

C_o = the capacitance of the system when vacuum occupies the space between the electrodes (in Farads).

It should be emphasised that the values of capacitance and resistance depend upon the size and shape of the specimen, whereas, the dielectric constant and resistivity values are constants for the particular material and independent of shape and size of the specimen, therefore, the values of these parameters could be compared for various materials.

Loss angle, tan δ, is another electrical term used in measuring the combined effects of dielectric polarization and electrical conduction, and is defined numerically as

$$\tan \delta = \frac{1}{2 \pi f RC} \qquad ..(3.3)$$

where f is the frequency of the applied field and is the ratio of the current flowing through the resistive element to the current flowing through the capacitive element.

3.3.1 Polarization

The structure and composition of the material has a direct effect on the values of the above measured electrical parameters. In a

fine grained material, such as cement, there will be a concentration of electrical charges adjacent to the surface of the individual particles. The amount of charge and the strength by which it is held to the particle depends on such factors as particle surface texture, the number of unsatisfied surface bonding sites, and the net electrical charge on the particle itself. When an alternating electrical field is applied, the charges next to the particle surface tend to oscillate back and forth with a certain amplitude. The amplitude of oscillation will vary with such factors as:

a) the type of charge,

b) the degree of association of the charge with the particle surface,

c) particle orientation,

d) temperature of the system, and,

e) strength and frequency of the electrical field.

The oscillation, or movement, of charges in an electrical field (without conduction) is called polarization. The magnitude of the oscillation of charges in a material is measured as a polarization current. The number of charges per unit volume multiplied by the average displacement is the polarizability of the medium. The magnitude of the polarizability of a material is reflected by the value of capacitance, C, and hence the dielectric constant, ε.

Some charges, usually in the form of ions in solution, which are not bound to particle surfaces, are free to drift through the solution and discharge at the electrodes. This produces a

conduction effect that is reflected by the resistance, R, and hence resistivity, ρ.

3.2.2 Types of Polarization

The polarization (on a microscopic scale) produced by an alternating electrical field in a cement which includes both bound and unbound charges can be classified under the following headings:[100,109-111]

a) Rotation of dipoles and polar molecules in sympathy with the applied electrical field, Figure 3.4(a). When an alternating field is applied, asymmetric (polar) molecules having a permanent dipole moment become preferentially orientated in the direction of the applied electrical field[118-120] (dipole polarization).

b) Accumulation or the build-up of charges (ions) at the interface of the particles and crystal boundaries. Figure 3.4(b), and inhomogeneities due to differences in the properties forming the system[121,122] (Maxwell-Wagner effect).

c) Induced polarization in the field direction because of (i) displacement of ions from their zero field equilibrium positions[123] (atomic polarization), Figure 3.4(c); (ii) displacement of double-layer charges adjacent to particle surfaces[124,125] (double-layer polarization), Figure 3.4(d).

d) Displacement of electron clouds relative to an atomic nucleus in an applied field[126] (electronic polarization), Figure 3.4(c).

The frequency of the applied electrical field has a significant influence on the polarization mechanism, this is reflected by the value of capacitance, C, and hence the dielectric constant, ε . Resistance, R, and hence resistivity, ρ , is not as sensitive to frequency changes. However, in general, resistivity decreases with increase in frequency. If changes in the values of the dielectric constant, ε , and conductivity, σ , (the reciprocal of resistivity) are monitored over a spectrum of frequencies, then, as the frequency increases, the conductivity, σ , Figure 3.5, increases and the dielectric constant, ε , decreases.

3.3.3 Representation of Polarization Data

Because of the possibility of a phase lag developing between the applied field and the instantaneous polarization, the complex dielectric constant is expressed in terms of real and imaginary parts ε' and ε'' respectively, where by Debye's[118] equation, the dielectric constant, ε, is,

$$\varepsilon = \varepsilon' - j\,\varepsilon'' \qquad ..(3.4)$$

where ε' is the real part (dielectric polarization), and,

ε'' is the imaginary part (or the dielectric loss).

The imaginary part of the dielectric constant, ε'', is a measure of both the energy dissipated by the motion of the charges and ionic conduction processes in the applied electrical field and is related to the conductivity;

$$\varepsilon'' = \frac{\sigma_{AC} - \sigma_{DC}}{2\,\pi f\,\varepsilon_v} \qquad ..(3.5)$$

where σ_{AC} = the conductivity at a particular frequency,

σ_{DC} = the low-frequency or DC conductivity,

ε_v = the absolute dielectric constant of a vacuum,

8.854×10^{-12} farads/m,

f = frequency of the applied electrical field (Hz).

The energy dissipation represents a dielectric loss. The real part of the complex dielectric constant, ε', decreases with increase in frequency, the drop in dielectric constant with increasing frequency is termed the dielectric dispersion, Figure 3.6(a). The region AB is referred as the region of dielectric dispersion. In the region of normal dispersion, ε'', is small, whereas in the region of dielectric dispersion it rapidly increases to a maximum and then decreases , Figure 3.6(b). The maximum value of ε'' occurs at a frequency which is termed the characteristic frequency, f_o.

For a given material, there may be several regions of dielectric dispersion over a spectrum of frequencies as shown in Figure 3.7, and are indicated by regions a, b, and c. At low frequencies, there may be adequate time available for several polarization mechanisms to contribute to the dielectric constant, however, as the frequency increases, the time available for charge distortion during any single current alteration decreases and may not be sufficient for one or more of the polarization mechanisms to operate. Different polarization mechanisms may cease to be effective at different frequency ranges, thus accounting for curves in Figure 3.7.

Mitchell[100] has used the features in the dielectric dispersion and conductivity dispersion curves in characterising the structure state of the material.

a) The dielectric constant at low-frequency, ε_o', Figure 3.6(a), is a measure of the amount of polarization that can develop when a relatively long time is available. It therefore reflects the number of bound charges and the maximum amplitude of their displacement in an electric field.

b) The value of $\Delta\varepsilon_o'$ reflects the magnitude of polarization that can develop only in the low-frequency range and, therefore, is a measure of the mechanisms requiring relatively long times for oscillation, such as the displacement of double-layer charges adjacent to particle surfaces.

c) The extent of polarization that can develop due to mechanisms requiring relatively short times is measured by $\varepsilon_o' - \Delta\varepsilon_o'$.

d) The characteristic frequency, f_o, measures the average time required for a particular polarization process. The characteristic frequency is the measure of the distance the charges can move, the ease of movement and the size of charges. The more easily charges can follow the electrical field alternation, the higher the characteristic frequency .

e) The DC conductivity of the material, σ_{DC}, measures the amount of free charge and the ease with which it can pass through the material.

3.3.4 Polarization in Cement Paste

The electrical dispersion characteristics of cement paste can be related to its micro-structure by the use of a simple electrical model.

The micro-structure of cement gel may be considered as being composed of several main components[5] at any particular time:

a) grain particles surrounded by an ion atmosphere (double-layer) which are assumed to behave as integral units,

b) segmented grains,

c) solid particles in contact with each other,

d) continuous and discontinuous pores filled with water,

e) gel pores.

When a voltage is applied to a cement paste matrix, current is considered to be conducted along three paths:

1) through solution and conducting particles,

2) through particles in contact with each other,

3) through the solution in the continuous interstitial path.

Nikkannen[127] has suggested that conduction through moist concrete is essentially electrolytic in nature and tests by

Hammond and Robson[128] support the view that conduction is by means of the available ions in the evaporable water within the cement paste. The principal ions being Ca^{+}, Na^{+}, OH^{-} and SO_4^{2-}.

The simplified electrical model, Figure 3.1, used in this study treats cement paste as a lossy dielectric, where conductive mechanisms are accounted for by a resistive element set in parallel with a capacitor to account for the various polarization mechanisms. However, the more precise model will account individually for each conductive path and represent them by a network consisting of a resistor and capacitor arranged in parallel or serial configuration.

The main polarization mechanisms operative within cement paste are:

a) Double-layer[124,125] or colloidal layer polarization, in which charges adjacent to grain surfaces can be displaced, thereby inducing a large effective dipole moment, Figure 3.4(d).

b) Interfacial polarization or Maxwel-Wagner[121,122] effects, which results in an accumulation or build-up of charges at crystal boundary interfaces, Figure 3.4(b).

The total sum of all the polarization mechanisms is reflected by the value of the capacitance, C, and hence the dielectric constant, ε . It is evident that the values of dielectric constant and electrical resistivity will be dependent upon:

i) Changes in the physical state of the water and the ionic concentrations within the gauging water.

ii) The ease with which dipoles and polar molecules can be polarized within the paste.

iii) The degree of association of charges with grain surfaces and the temperature of the system.

Therefore, since definite chemical and structural changes occur within the cement paste, then these should be reflected by changes in the measured electrical parameters.

3.4 SUMMARY

- A brief outline has been given of the present and the developing techniques for monitoring changes in, and assessment of, the properties of cement paste, mortar and concrete.

- The electrical method has been introduced as a developing technique in monitoring cement hydration. A modified electrical model has been presented; unlike previous models, it includes a capacitive element as well as a resistive one. The capacitive element accounts for the polarization that can develop within the paste. The advantages and the full implications of the use of this electrical method are detailed later.

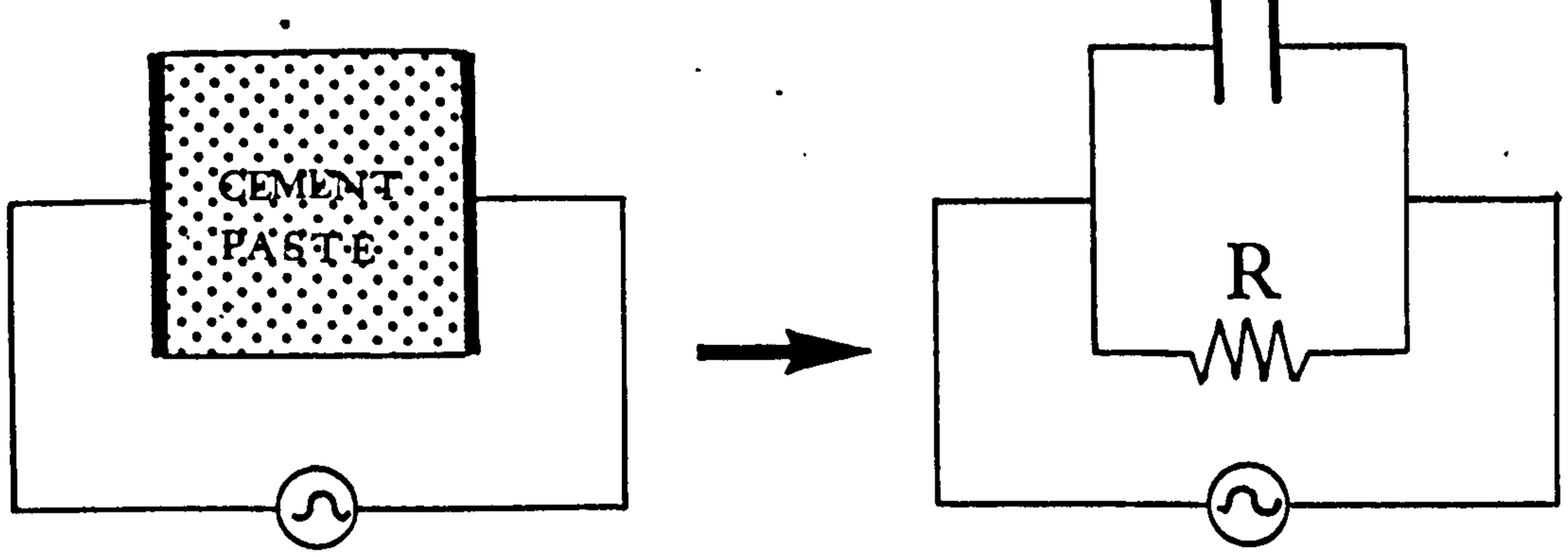

FIGURE 3.1 PARALLEL ELECTRICAL MODEL FOR CEMENT PASTE

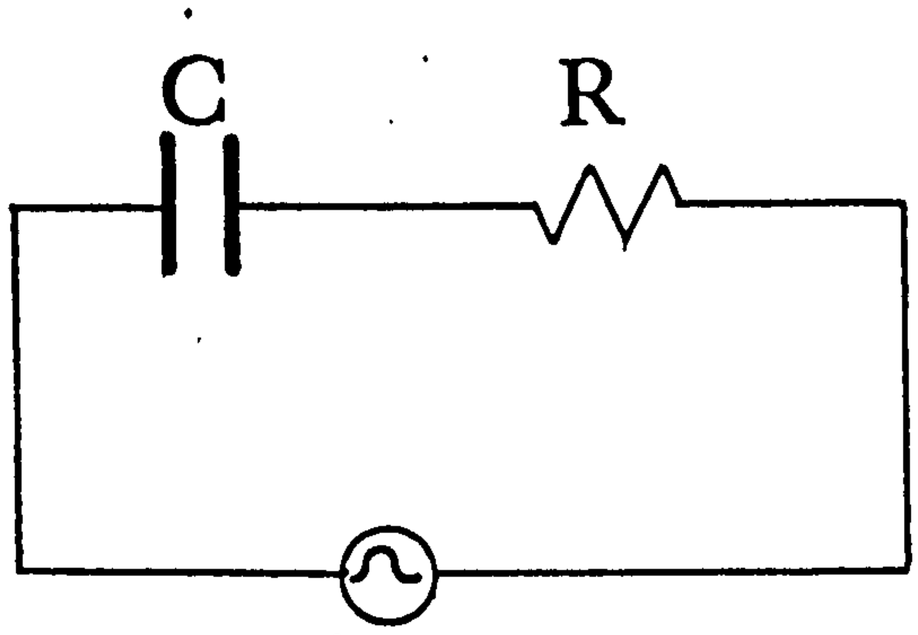

FIGURE 3.2 SERIES ELECTRICAL MODEL FOR CEMENT PASTE

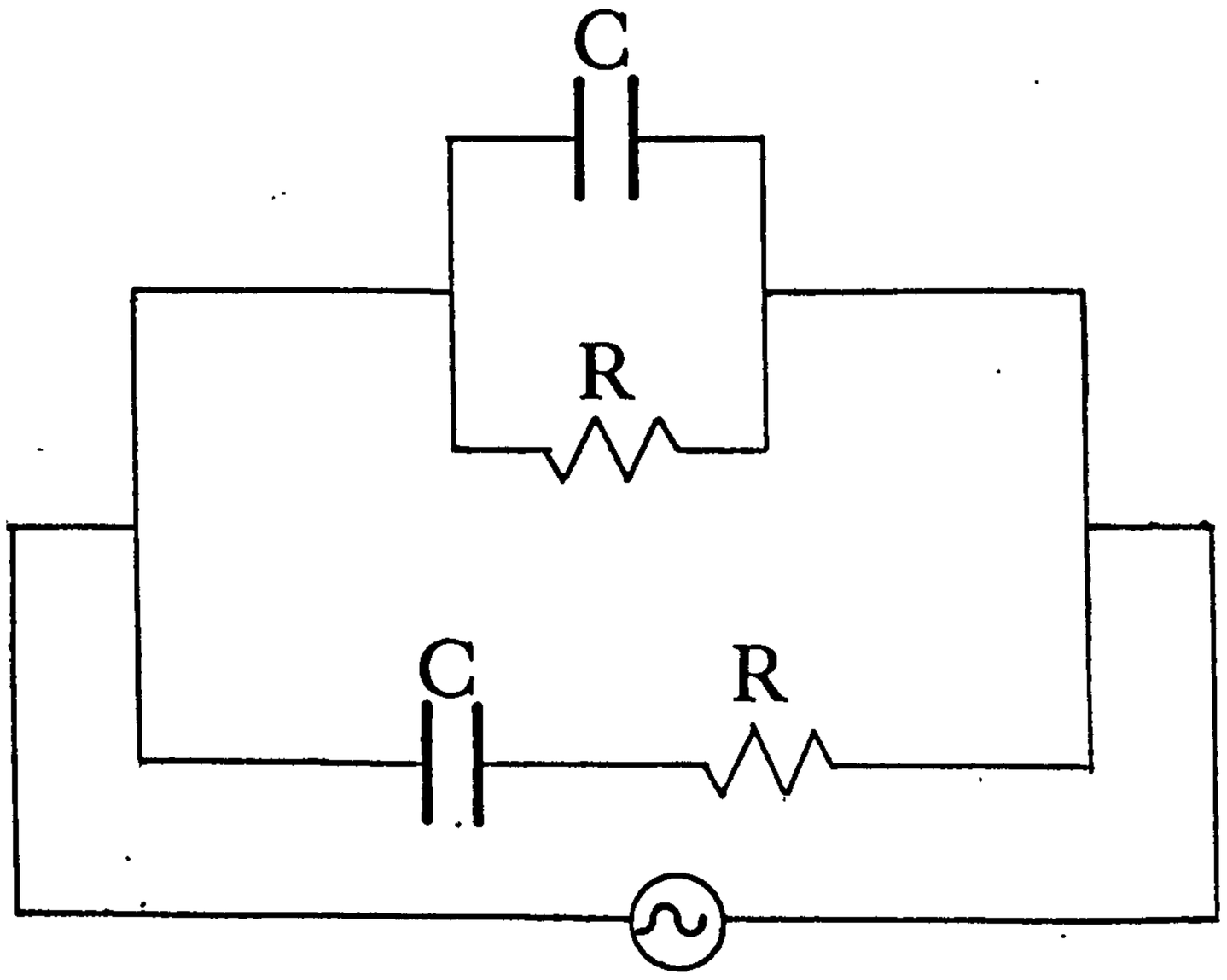

FIGURE 3.3 AN ELECTRICAL MODEL BASED ON A COMBINATION OF SERIES AND PARALLEL MODELS

NO FIELD

APPLIED FIELD

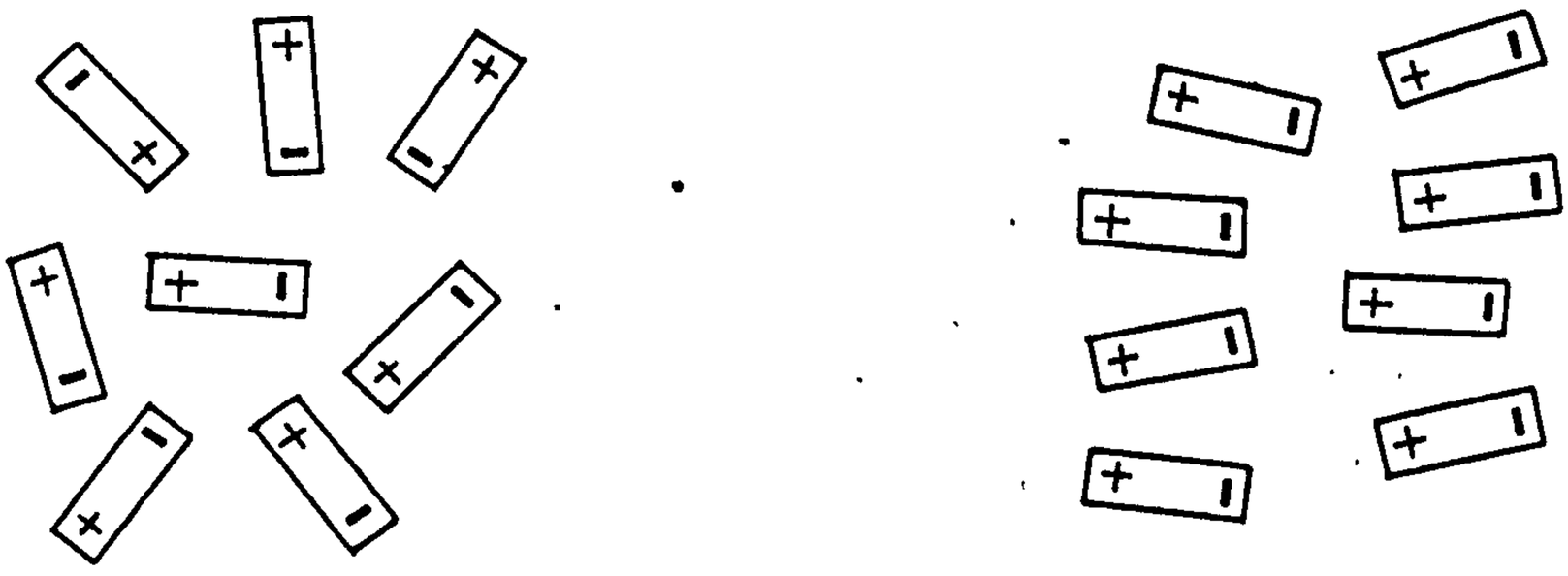

a) DIPOLE POLARIZATION

b) INTERFACIAL POLARIZATION

C) ATOMIC POLARIZATION

d) DOUBLE-LAYER POLARIZATION

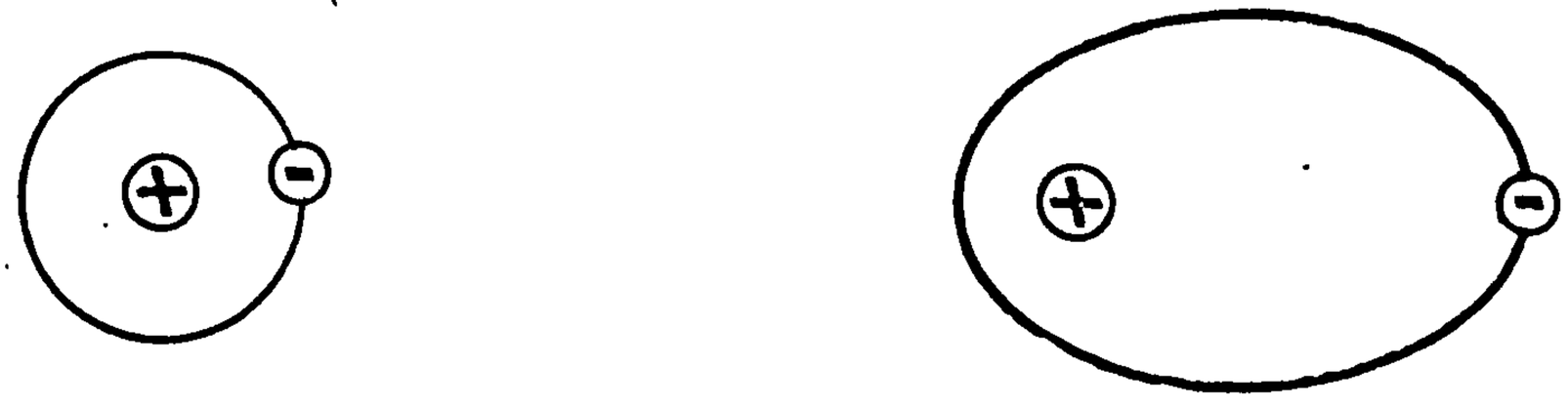

c) ELETRONIC POLARIZATION

FIGURE 3.4 POLARIZATION MECHANISMS

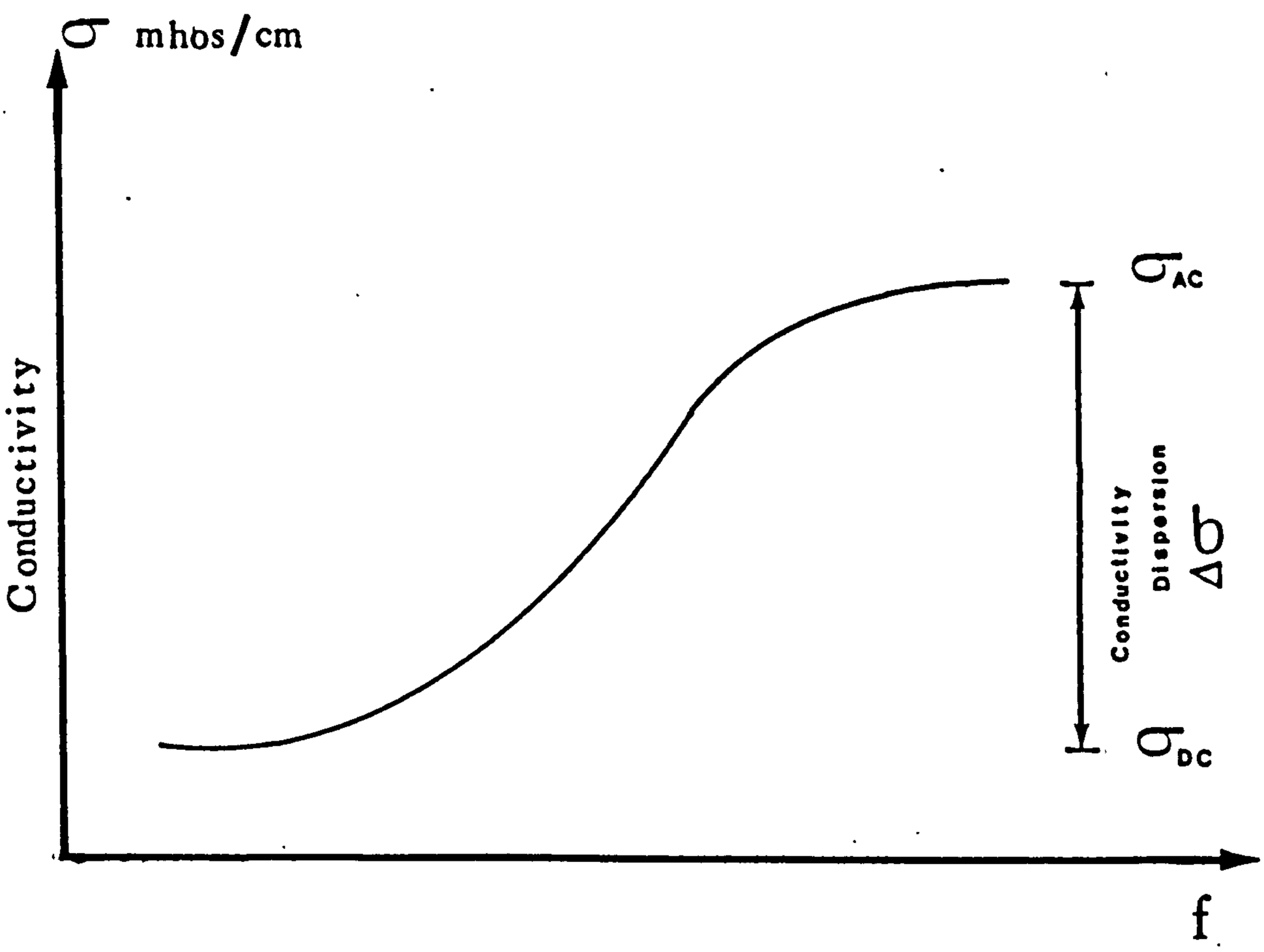

FIGURE 3.5 CONDUCTIVITY AS A FUNCTION OF ANGULAR FREQUENCY, DEBYE[67]

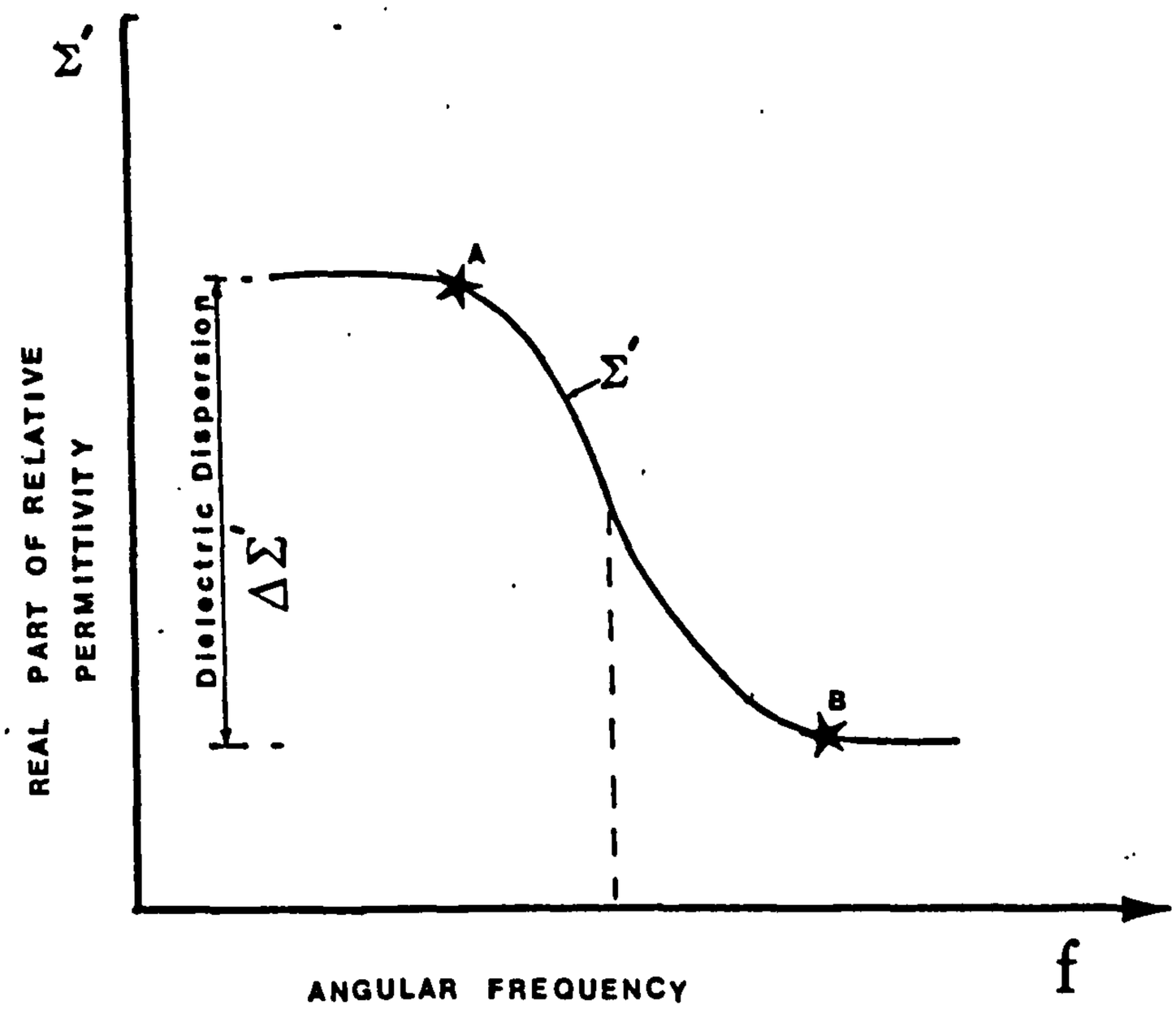

(a)

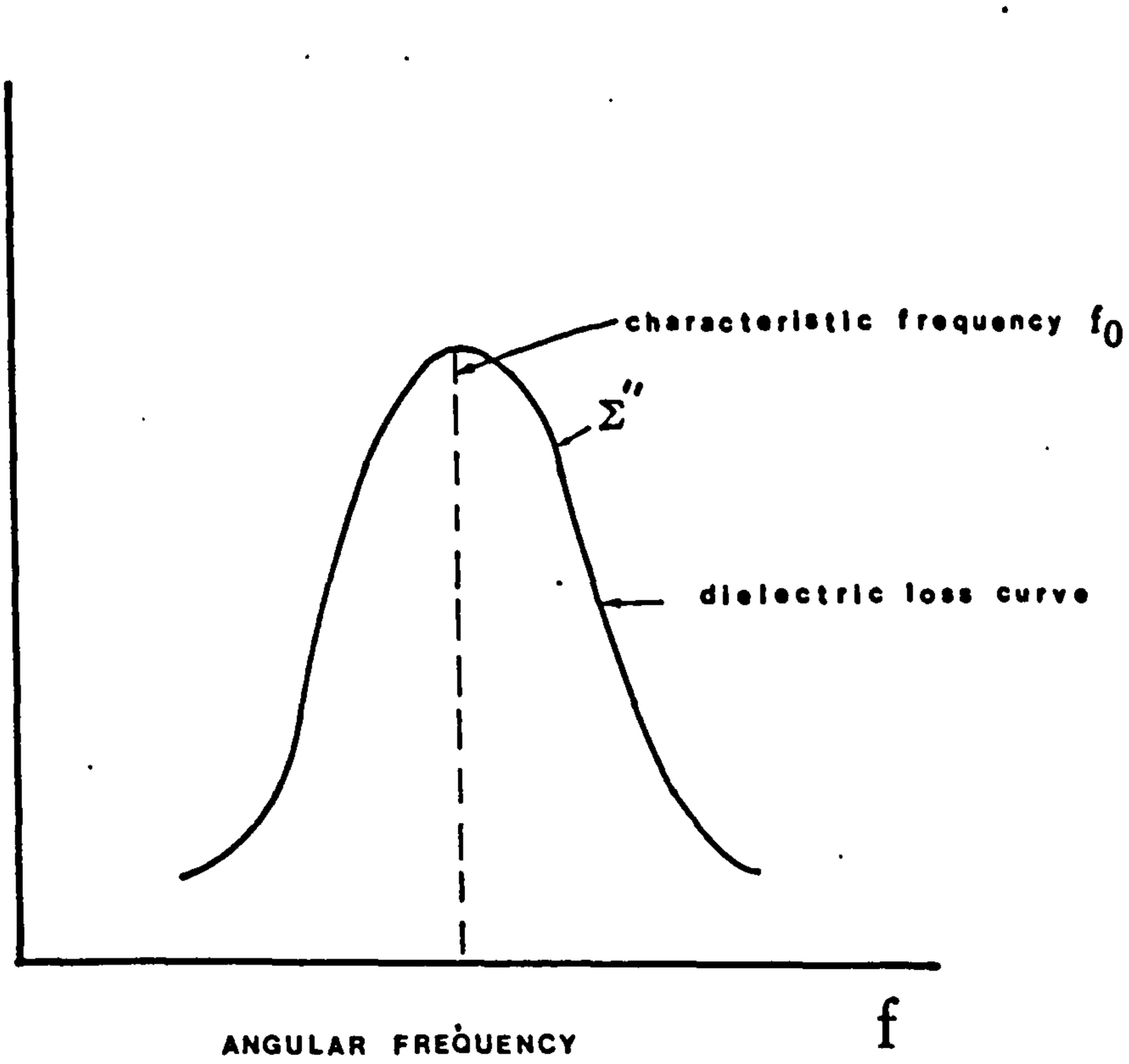

(b)

FIGURE 3.6 REAL AND IMAGINARY PARTS OF RELATIVE PERMITTIVITY AS A FUNCTION OF ANGULAR FREQUENCY DEBYE[67]

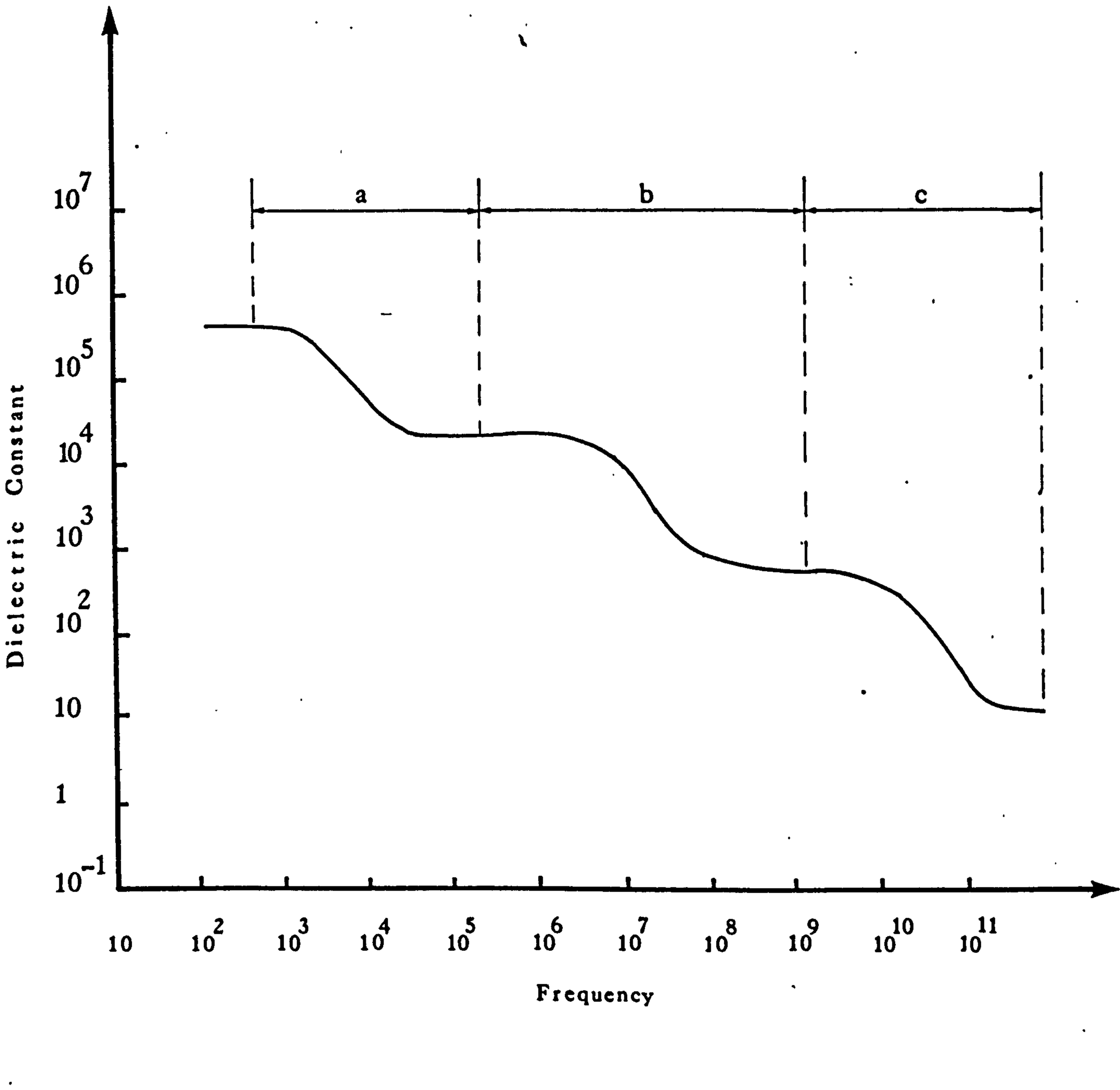

FIGURE 3.7 ZONES OF DIELECTRIC DISPERSION (IDEALISED)

CHAPTER 4

EXPERIMENTAL DESIGN AND DATA ACQUISITION

4.1 INTRODUCTION

The experimental programme was developed on two fronts; quantitative information on the progress of hydration was obtained by monitoring the electrical response characteristics of cement paste, and qualitative information on the morphology of hydrate development and topography of grain surfaces was obtained by scanning electron microscopy.

Pilot studies that were carried out to validate the effectiveness of using the electrical response characteristics of cement paste as a means of monitoring the hydration processes, revealed the need for the development of a microcomputer system for experimental control, data acquisition retrieval and analysis. In order to monitor the changes in electrical parameters, measurements had to be taken at frequent time intervals during the test period. The variables to be measured were; the electrical resistance (R), capacitance (C) and the specimen's internal temperature at predetermined time intervals. Therefore, the requirements for such a system were:

a) to monitor the experiment and control the various peripherals which comprise the system over a period of 24-hours or more.

b) to initiate a reading cycle, under clock control, and log, process and store the incoming data.

c) to process and store data from each experiment which had to be easily accessible for analysis and plotting purposes.

The test duration was to be 24 hours, hence, with the interval of 300 seconds between each cycle, approximately 340 reading cycles were triggered. The data recorded comprised:

a) the time the reading cycle was triggered after the start of the experiment,

b) the internal temperature of the specimen,

c) the electrical resistance at various frequencies,

d) the capacitance at various frequencies.

In order to meet these requirements, a microcomputer control system was developed.

4.2 INSTRUMENTATION

Details of the electrical parameters measured are given in the previous chapter. Plate 4.1 shows an overall view of the instrumentation and a schematic diagram of the system architecture is shown in Figure 4.1, with arrows indicating the flow of information. A Wayne Kerr 6425 multi-bridge[129] was used to measure the parallel resistance and capacitance for the electrical model[109,116] over an extended frequency spectrum. The bridge was fitted with IEEE bus interface; this is a parallel bus system permitting a number of different instruments and peripheral devices to be operated by a common controller. Fitted with the IEEE interface, the instruments can be operated as a basic talker/listener and can output data onto a common bus, as well as being fully controlled from the bus.

A Hewlett Packard HP3456A digital voltmeter[130] was used in conjunction with a compatible thermistor to measure internal temperature changes within the specimens. The HP3456A is also equipped with an IEEE interface bus which will enable it to be controlled remotely with full handshake capability.

The controller employed to manage the overall running of the experiment, control of individual peripherals, process and store the incoming data, was a Hewlett Packard HP9836U modular computer[131] fitted with integral flexible disc drives and CRT display. A Hewlett Packard interface bus HP-IB[132] was used to interface all peripherals. The interface bus provides for messages in digital form to be transferred between two or more HP-IB compatible devices.

In the initial stages of the research programme, pilot studies were carried out using a similar system[117] as that outlined above. A Wayne Kerr automatic precision bridge B905[133], the HP3456A digital voltmeter and a Hewlett Packard HP9915 modular computer[134] fitted with optional components (HP98155A keyboard, CRT display, HP82905B printer, Seikosha GP.100A printer and HP82901M/S flexible disc drives) were the components of this system. In order to extend the operating frequency range offered by the B905 (100Hz - 10kHz) and provide extended storage facilities on the controller, it was up-dated to that presented above. The combined facility offered by the two systems allowed measurements to be taken at a range of frequencies between 20 Hz to 300 KHz at over 27 spot frequencies. A facility is also available to output raw data via a RS232

interface onto a printer.

In order to have an independent system dealing with data analysis, so that the controller system could operate continuously, a Hewlett Packard HP-85 microcomputer was used to drive a Calcomp model 84 X-Y eight pen plotter[135]. This means that data analysis, graph plotting and software development could be carried out without interruption to the controller's operation over the experiment. This, however, did not prevent the plotter being integrated into the main system, if required; indeed, incorporated in the modified system there is a HP 7475A graphics plotter.

4.2.1 Software Development

Programmes were developed for the controller to manage the running of the experiment, log and process the raw data, store the computed data, and finally, present the results in graphical form.

Either computers and a HP-IB interface were set up as system controller. The first operation necessary for the HP-IB system is to assign a binary code number to all devices on line and programme them for remote operation via the bus. To prevent any of the system devices from being returned to local operation from the front panel, a lockout message is sent, e.g.

```
10  REMOTE  722
20  LOCAL LOCKOUT  7
```

The system is now set up for remote control. The next step is to programme each device for the desired mode of operation. This is

generally accomplished by means of simple output statements directed to the device to be programmed. A sequence of ASCII characters sent by the 'Output' statement to the device via the bus has the effect of setting the appropriate front panel controls on the machine:

```
30  OUTPUT  722;  "NORS;PAR;SIN;C;R;FREQ300E3"
```

Once the system devices are programmed for operation, it is possible to address them sequentially. This is achieved using a trigger statement followed by the enter statement, e.g.

```
40  OUTPUT 722; "TRG"

50  ENTER  722;  A1,C,R,A2
```

Statement 30 addresses the peripheral (component bridge) code numbered 22 via interface selection code 7 to listen and receive the control codes; statement 40 triggers the peripheral to initiate a reading; and statement 50 sets the peripheral to talker mode and sends the readings to the controller. Output from the bridge comprises four numerical values and the storage location labelled A1, C, R and A2 are allocated to them. The relevant incoming variables are C and R (capacitance and resistance), the remaining two being encoded messages

```
60 C(28)  =  1.4138 E12*(C-3.356E-13)

70 R(28)  =  R*0.098
```

Statement 60 and 70 convert C and R to dielectric constant and electrical resistivity respectively. The address sequence for a complete reading cycle is shown in Figure 4.2 and a typical control programme is presented in Appendix 1.

4.2.2 Data Storage and Retrieval

Over the duration of each test, 340 reading cycles are initiated

with 56 pieces of data logged per reading cycle. The raw data generated are processed and stored on floppy discs and on a cassette tape in the form of a dielectric constant/time matrix (28 columns, 340 rows); a resistivity/time matrix (28 columns, 340 rows) and a temperature/time matrix (2 columns, 340 rows). This allows easy access to the data, in particular when plotting graphs. If, for example, the internal cube temperature was to be plotted as a function of time, the controller would take the appropriate variables from the row and columns in the data matrix and plot the resulting set of coordinates.

Graphical representation of the processed data is presented as the experiment progresses on the CRT display unit of the HP9836U computer and a hard copy of the processed data at selected frequencies on a HP82905B printer. Having continuous access to the results, both graphically and numerically throughout the experiment, allows for a better understanding and appreciation of the on-going processes of hydration. A hard copy of the graphs produced on the CRT display during the experiment is dumped on to the printer at the end of the experiment. A sample of this output is given in Appendix 1.

Customised programmes were developed to analyse the data and plot the results. Incorporated within the main plotting programmes are axis plotting, scaling and labelling subroutines. A typical plotting program is presented in Appendix 1. The analysis of the results and the plotting of graphs are carried out using an independent system comprising of a HP85 microcomputer linked via a RS232 serial interface to a Calcomp 84 plotter. Within minutes

of completion of an experiment, the following graphs could be obtained at any one of 27 frequencies:

a) Temperature vs Time,

b) Resistivity vs Time at any one of 27 frequencies,

c) Dielectric constant vs Time at any one of 27 frequencies,

d) Loss tangent vs Time at any one of 27 frequencies, and,

e) Dielectric dispersion curve at any point in time.

For ease of interpretation of the graphs, at each particular frequency, the internal temperature, resistivity and dielectric constant are plotted against time on the same set of axes (Figure 4.3). The variable, time, is measured in minutes and is the period from when gauging water is mixed with the cement. Resistivity is measured in ohm-metre and dielectric constant is dimensionless. Internal temperature of the specimen is measured in degrees Centigrade.

Loss tangent, which shows the combined effects of dielectric polarisation and electrical conduction, can be plotted against time at any required frequency (e.g. 100 Hz, 1 kHz, 10 kHz) on the same set of axes (Figure 4.4).

4.3 THE DIELECTRIC TEST CELL

The cell used to contain the specimen is designed so as to contain 100 mm^3 of cement paste, this will make the sample comparable to the British Standard 100mm cube. The cell was constructed from 12mm thick perspex, fitted with 100mm x 100mm x 3mm brass or stainless steel plates as electrodes. The

electrodes are attached to opposite faces of the cell as shown in Plate 4.2 and Figure 4.5. Electrical contact points are positioned at the centre of the electrode plates through the perspex sides. The cell is designed for easy demoulding and cleaning. In order to eliminate the errors introduced by field fringing effects around the electrodes and to account for the capacitance of the cell itself, the cell is calibrated at the test frequencies using a liquid of known dielecric constant, in this instance, Cyclohexane (ε = 2.025 at 20^{o}C). The total capacitance of the system is:

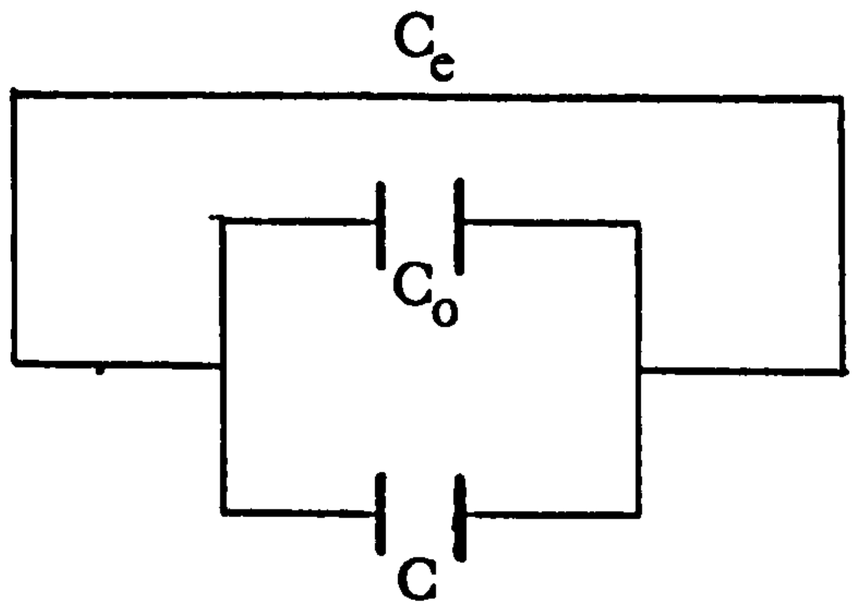

Now,

$$C_e = C + C_o \qquad ..(4.1)$$

$$C_F = C + C_x \qquad ..(4.2)$$

by definition, (see equation 3.1)

$$C_x = C_o \varepsilon_x \qquad ..(4.3)$$

Substitute for C_x in equation (4.2) from equation (4.3),

$$C_o(\varepsilon_x - 1) = (C_F - C_e) \qquad ..(4.4)$$

$$C_o = \frac{C_F - C_e}{\varepsilon_x - 1} \quad \text{(air capacitance)} \qquad ..(4.5)$$

Substitute for C_o in equation (4.1) from equation (4.5)

$$C = C_e - \left\{\frac{C_F - C_e}{\varepsilon_x - 1}\right\} \qquad \text{(cell capacitance)} \qquad ..(4.6)$$

The measured capacitance of the cell when filled with paste is equal to:

$$C_m = C + C_p \qquad ..(4.7)$$

Substitute for C in equation (4.7) from equation (4.6)

$$C_p = C_m - C_e + \left\{\frac{C_F - C_c}{\varepsilon_x - 1}\right\} \qquad ..(4.8)$$

the dielectric constant of the paste is then,

$$\varepsilon_p = C_p/C_o \qquad ..(4.9)$$

Substitute for C_p and C_o in equation (4.9) from equation (4.8) and (4.5) respectively, therefore, the dielectric constant ε_p for the paste is:

$$\varepsilon_p = \left[(C_m - C_e) + \left\{\frac{C_F - C_e}{\varepsilon_x - 1}\right\}\right] / \left\{\frac{C_F - G_e}{\varepsilon_x - 1}\right\} \qquad ..(4.10)$$

where C = cell capacitance in farads,

C_e = cell and air capacitance in farads,

C_o = air capacitance in farads,

C_F = cell and Cyclohexane capacitance in farads,

C_x = Cyclohexane capacitance in farads,

C_p = paste capacitance in farads,

C_m = cell and paste capacitance in farads,

ε_x = dielectric constant of Cyclohexane,

ε_p = dielectric constant of the cement paste.

4.4 MATERIALS USED

4.4.1 Cement

Four types of cement were used:

a) Ordinary Portland Cement (OPC)

b) Rapid Hardening Portland Cement (RHPC)

c) Sulphate Resisting Portland Cement (SRPC)

d) High-Alumina Cement (HAC)

The cements used were supplied by the local merchants in 50kg standard bags unless otherwise stated. During the period in use, the bags of cement were stored in airtight containers to limit moisture absorption.

Typical chemical composition of the cements used are given in Table 4.1, showing their oxide composition.

4.4.2 Water

Tap water and distilled water were used with a temperature of $19^{o}C \pm 2^{o}C$. The tap water used had an electrical resistivity $\simeq$100 ohm-m and dielectric constant $\simeq$80.

4.4.3 Sand

Zone 3 grading, building sand was used, with grading limit shown in Figure 4.6. The sand was oven dried prior to use.

4.4.4 Admixtures

Calcium chloride ($CaCl_2$), Calcium sulphate ($CaSO_4$), and table sugar were used, all in granular form, and added to the mixing

water (by percentage weight of cement) before gauging.

Water-cement ratios for the mixes were varied between 0.27 and 0.5 by weight (water-cement ratio of 0.27 produces a paste of standard consistency to BS 4550: Part 3: Section 3.5: 1978 "Methods of Testing Cement"[136]). In the case of mortar samples, sand-cement ratio was varied from 0.1:1 to 3:1 and water-cement ratio was varied between 0.35 and 0.6 by weight.

4.5 EXPERIMENTAL PROCEDURE

4.5.1 Electrical Test

The test period of all experiments was confined to the hydration over the initial 24-hours after gauging with water as it is during this time when the viscosity of the paste decreases as it changes from a fluid to a solid. All samples were placed in the confines of a humidity cabinet to maintain constant ambient air conditions ($20^{o}C \pm 2^{o}C$ and relative humidity of 80%). The laboratory also had constant ambient air conditions. The specimens were made from single batches of cement to minimise the effects of variability in materials.

The ingredients for the mix were weighed out to the appropriate percentages by weight, the cement and sand (when used) were placed in a mixing bowl and pre-mixed using a Hobart Planetary Motion Rotary Mixer before gauging water was added. The admixture (if used) was dissolved in the gauging water before mixing. Mixing time was kept constant at 2 minutes for all experiments, the paste was placed in the dielectric cell and was

vibration compacted, using a table vibrator, in three, approximately equal, layers. The surface of the specimen was then trowelled smooth and levelled with the top of the cell. Two dielectric cells were prepared in this way and placed in the humidity cabinet (Plate 4.1), one cell was connected to the precision bridge to measure the in-phase component (resistance, R) and the quadrature component (capacitance, C) of the electrical impedance. Care was taken to earth the metal rods holding the cell together in order to minimise inductance effects. The humidity cabinet was also connected to a common earth to prevent earth loops. The inductance and capacitance associated with the connecting leads were also trimmed off the incoming data using a trim facility on the instrument. The other cell was used to measure internal temperature variations within the paste, this was achieved by placing a thermistor (Fenwal Electronics 0837-0164) connected to the HP3456A digital voltmeter, in the centre of the paste within the cell.

Appropriate information relating to the particular experiment is entered into the computer to label the data, cement type, time etc. The experiment is then started, and readings of resistance (R) and capacitance (C) are taken through the component bridge at 27 frequencies and the temperature through the voltmeter.

The raw data from the bridge is processed by the controller. This, and the print-out of the processed data, plus the continually updated graphs being plotted on the HP9836U computer's CRT display, enables the operator (or the controller) to take operational decisions during the experiment. On

completion of the experiment, the data is transferred onto tape and used on HP85 to display digital data in graphical form.

The cells are demoulded, the cubes are marked for later identification and immediately submerged in a tank of clean water maintained at a temperature of $20^{o}C \pm 2^{o}C$. The cubes were tested at 28 days using a Denison cube crusher to determine their compressive strength. In parallel with the electrical experiments, physical and chemical tests were performed on the matrix and its components to establish their characteristics and elemental constituents.

a) Vicat Needle tests were carried out to BS 4450: Part 3: Section 3.5: 1978 to determine the consistency of the cement paste, times at which the conventional 'initial set' and 'final set' took place were noted.

b) To determine the gain in strength for the cement paste, an EL25-220 series multi-speed drive, triaxial load frame (Plate 4.3) was adapted to measure the crushing strength of the cement paste during the first 24 hours of hydration. 50mm cubes were cast using cast iron three gang moulds (Plate 4.4) to BS 4550. The cubes were carefully demoulded at appropriate time intervals during the 24 hour test period and were tested using the load frame at a constant load rate to BS 1881, Part 4, Section 2.2.3 and BS 4550. A minimum of 10 tests were carried out at each time increment and the results are presented in graphical form as strength (N/mm^2) versus time (minutes).

4.5.2 Scanning Electron Microscopy

A Cambridge Stereoscan model 250 MK2 scanning electron microscope, with maximum accelerating voltage of 40KV and ultimate resolution of 4.5nm (Plate 4.5), was used to examine samples of cement paste[137].

A resolution of the Stereoscan is about 200 A^{o} (2×10^{-8}m), which is approximately a factor of 10X better than the best optical microscope. A useful range of magnification lies between 20X and 30,000X with a depth of field that is at least 300X better than an optical instrument. The instrument requires a vacuum of at least 10^{-4}mm of mercury for it to operate, and this is accomplished by means of two diffusion and one rotary pump. The scanned area can be varied between 5mm to 1 µm square and photographic records of the image are produced using a 35mm camera mounted on a cathode ray tube.

Small fracture surfaces (approximately 5mm diameter, 5mm thick) of cement paste taken from the bulk hydrating sample at appropriate times during the first 24-hours of hydration were mounted onto an aluminium stub holder (Plate 4.6) with a suitable adhesive. The specimen had to be evacuated under a low pressure and the surface sputtered by vacuum deposition with a thin layer of gold (approximately 500 A^{o} thick) to render it electrically conducting (so as to neglect build-up of charge on the surface due to the electron beam). The stub containing the specimen is then placed in the microscope's chamber and photographic records are taken of the hydrate development on the cement grain surface. Typical sample photographs are presented in the following chapters.

4.6 CONCLUDING REMARKS

In adhering to the design requirements of the experimental programme, an automated microcomputer system was developed, with customised software to manage the overall running of the experiment and the processing and logging of data. The system requires minimum input from the operator, minimises the data acquisition time and delay time between experiments, and maximises the freedom of manipulating the data to reach a conclusion. Moreover, although the system has been designed to cater for the specific requirements of this research programme, there is no reason why the system could not be adapted and the software modified to match other requirements.

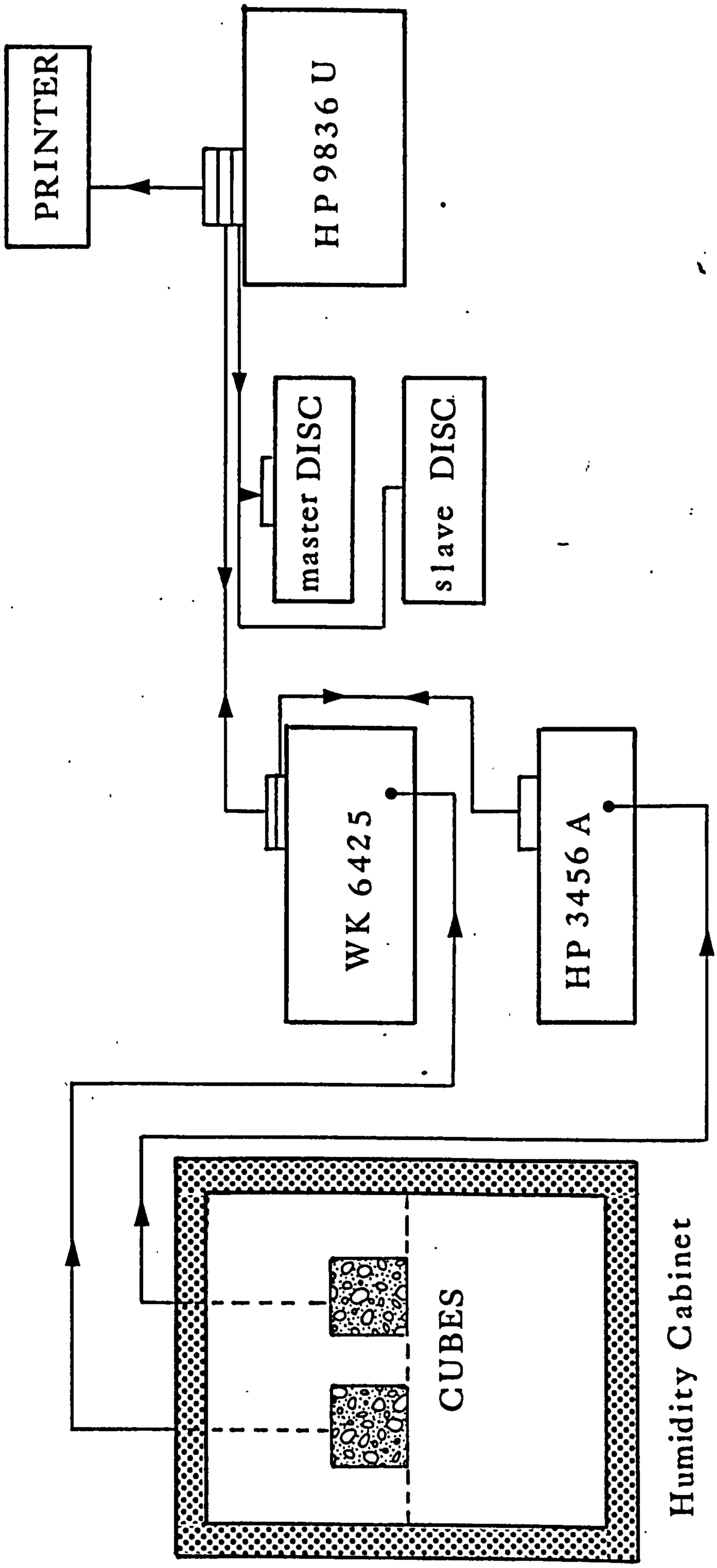

FIGURE 4.1 SCHEMATIC DIAGRAM OF SYSTEM ARCHITECTURE

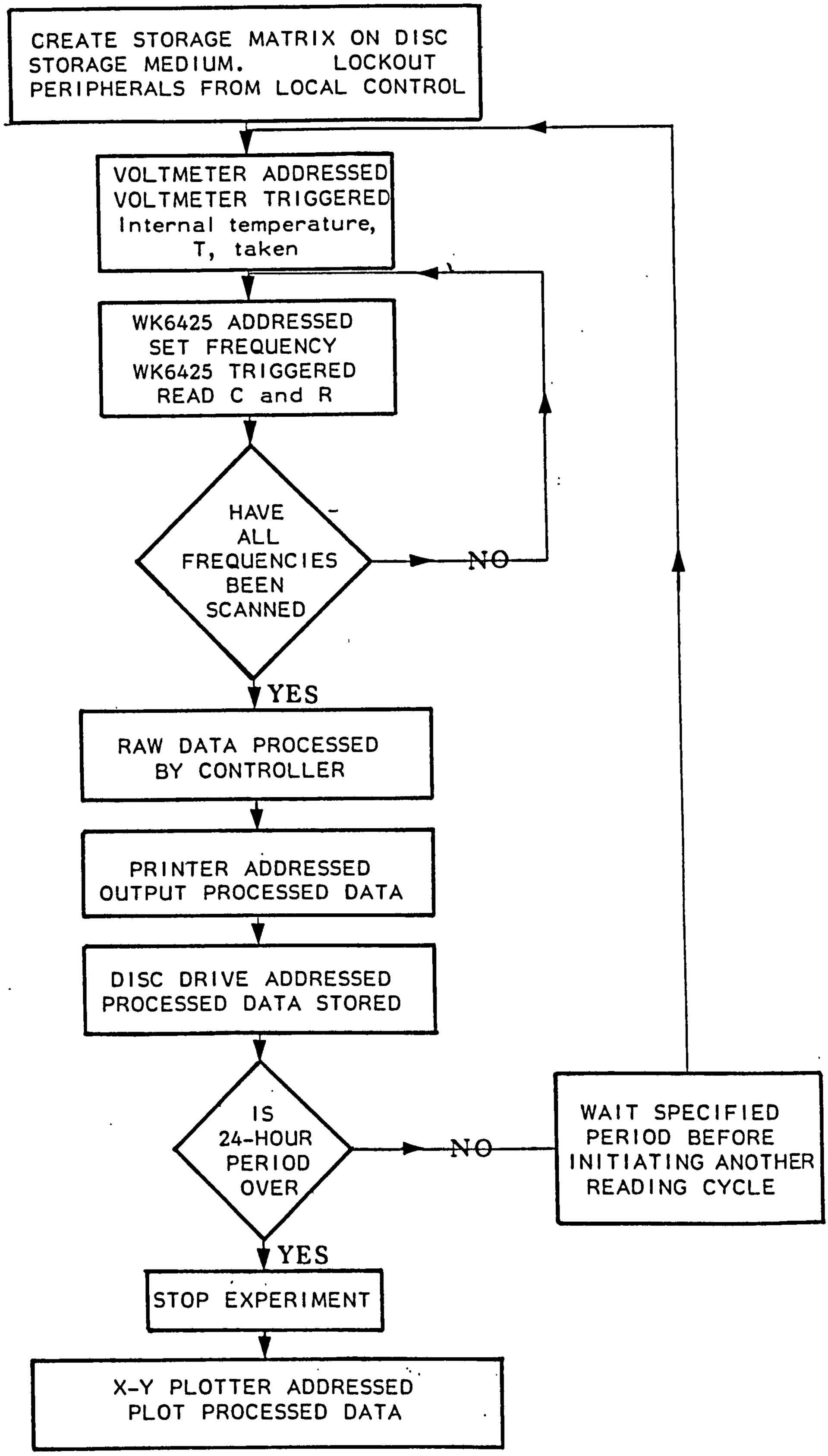

FIGURE 4.2 ADDRESS SEQUENCE OF PERIPHERALS

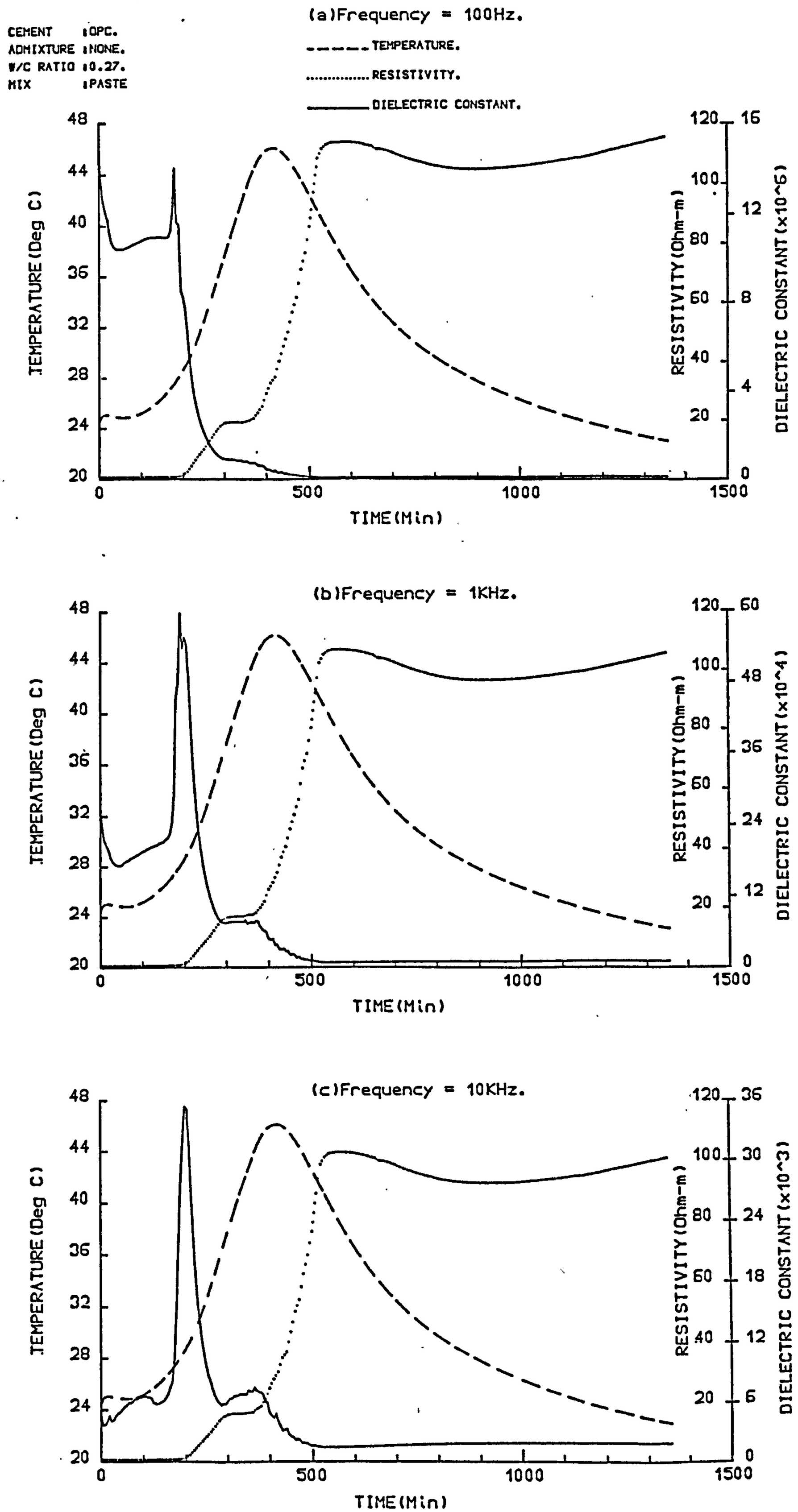

FIGURE 4.3 TYPICAL GRAPHS REPRESENTING THE ELECTRICAL RESULTS

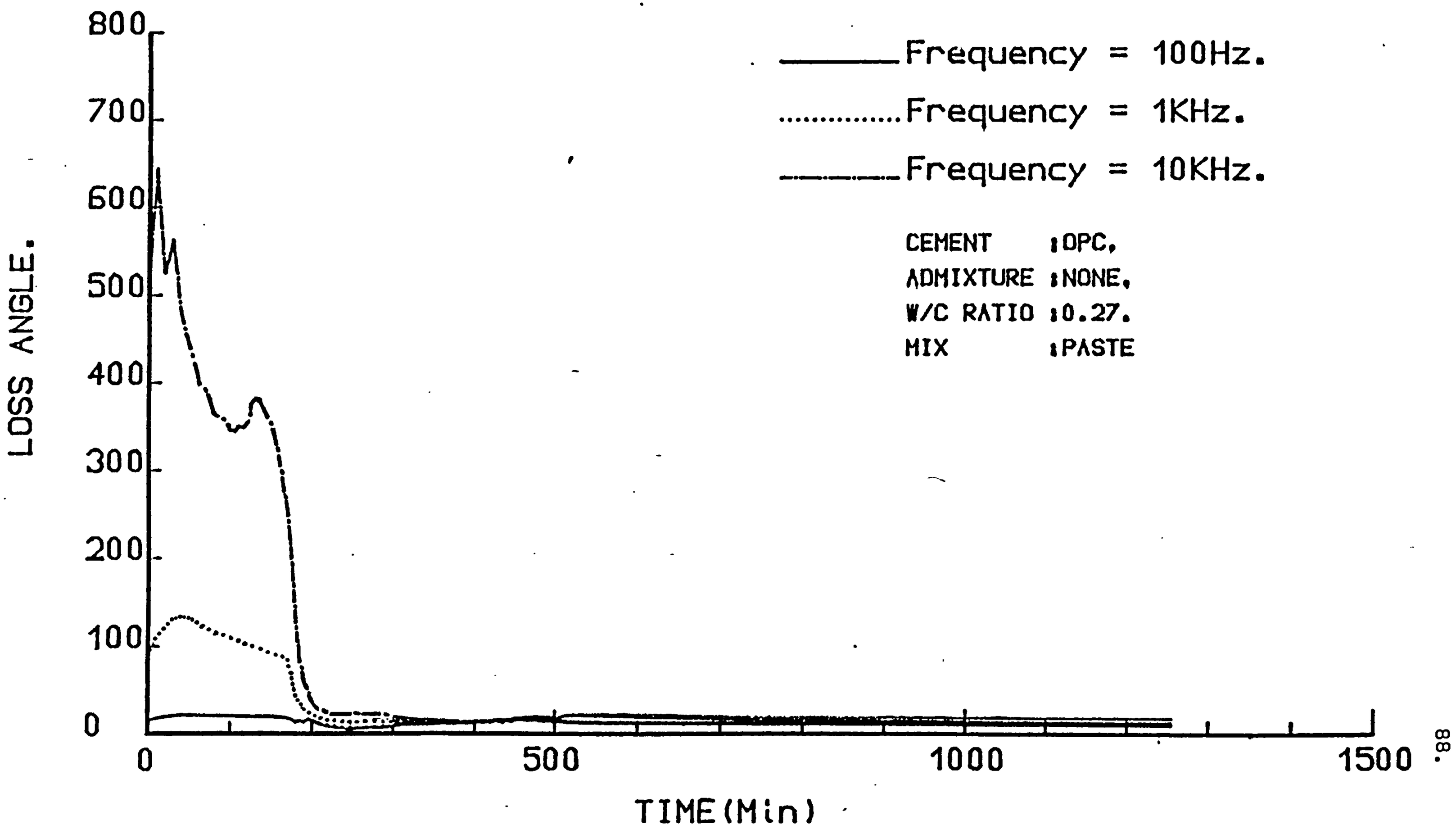

FIGURE 4.4 TYPICAL LOSS ANGLE GRAPH

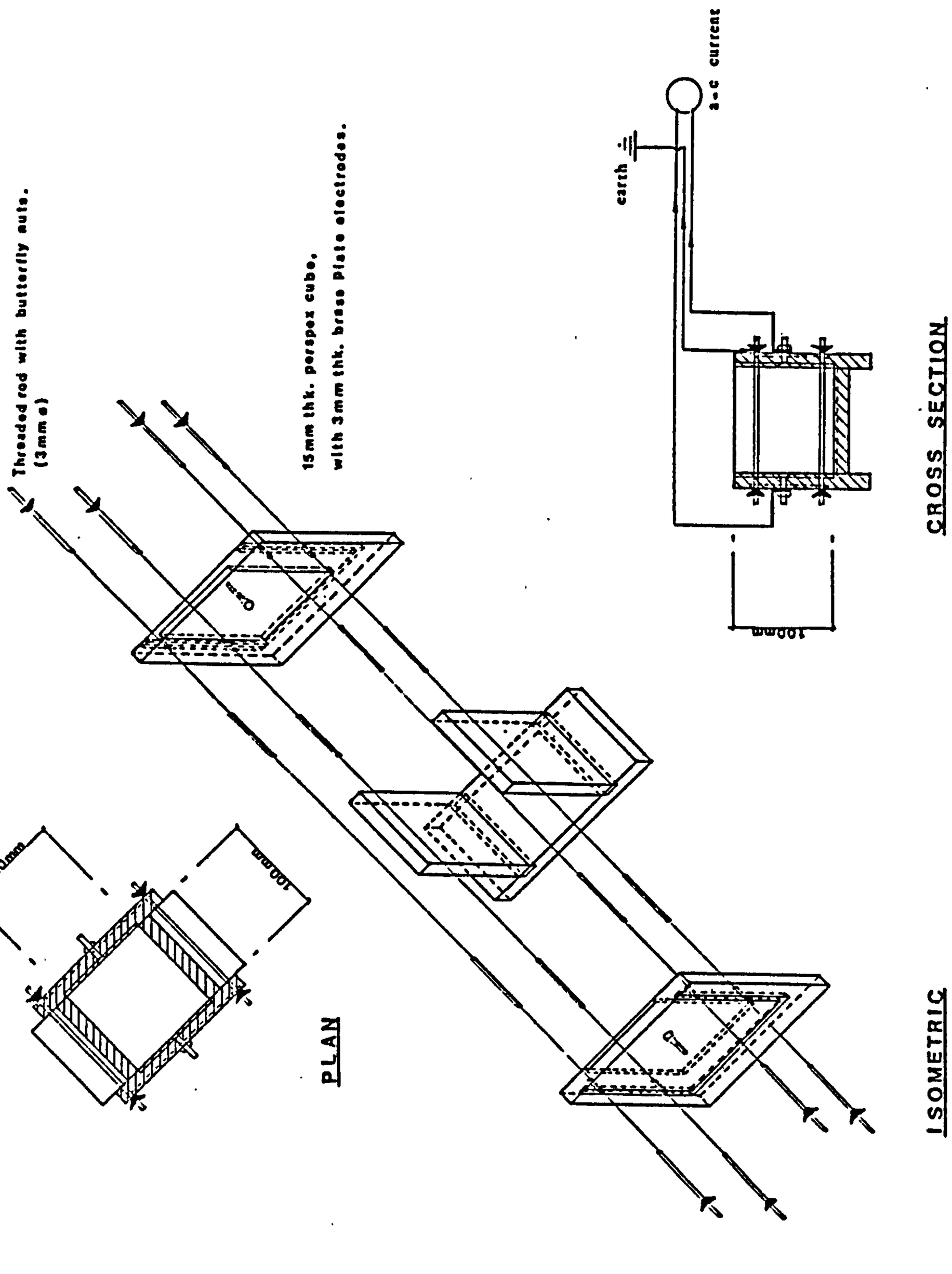

FIGURE 4.5 DIELECTRIC CELL

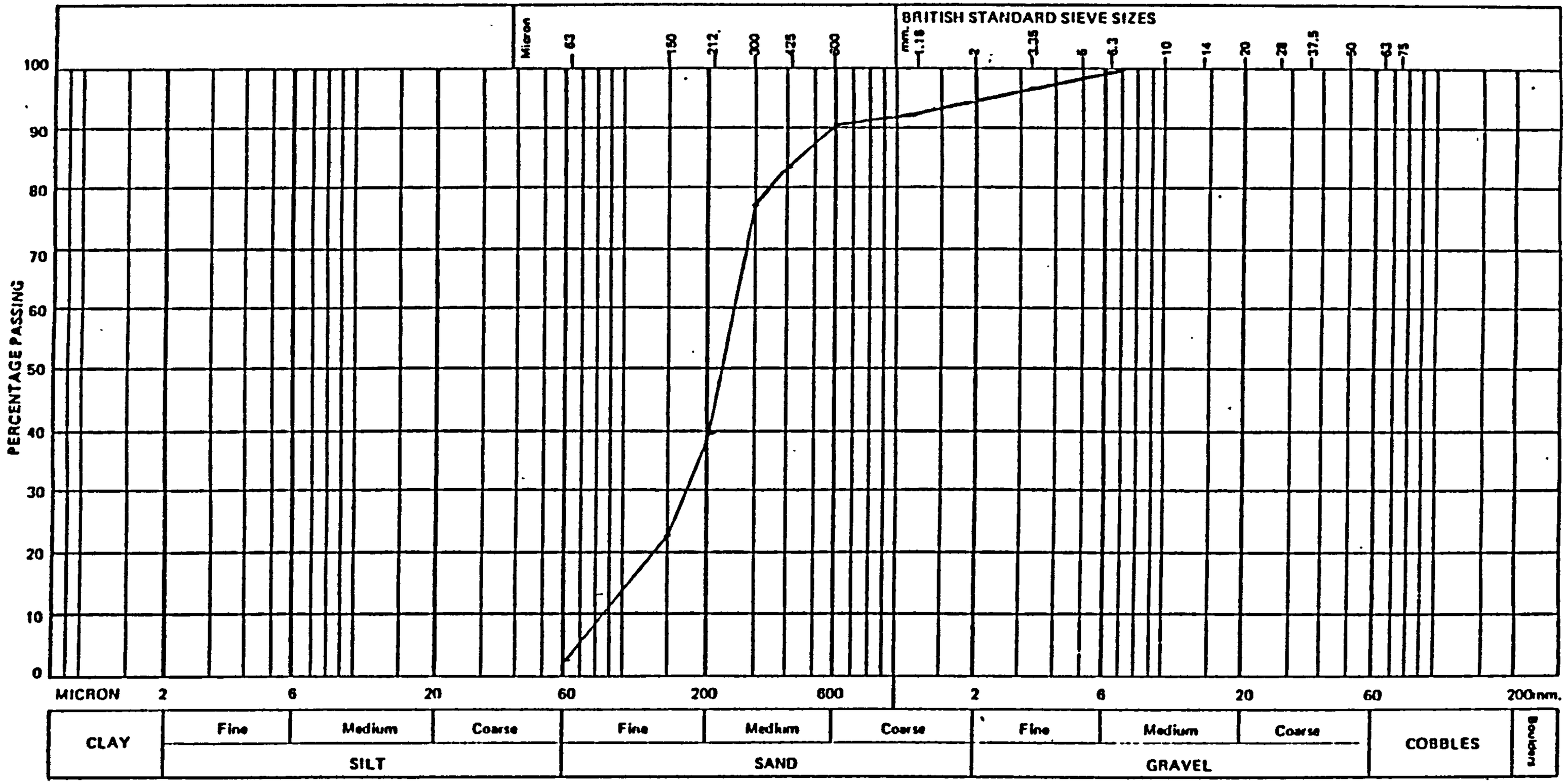

FIGURE 4.6 PARTICLE SIZE DISTRIBUTION (BUILDING SAND)

CHEMICAL COMPOSITION	CEMENT TYPES				
	OPC	RHC	SRC	HAC	CHEMICAL COMPOSITION
SiO_2	19.2	19.34	20.2	5	SiO_2
Al_2O_3	5.7	5.44	3.8	39	Al_2O_3
Fe_2O_3	3.4	3.09	4.9	9	Fe_2O_3
CaO	63.9	63.84	64.3	38	CaO
MgO	2.6	2.73	2.1	5	FeO
SO_3	2.6	3.16	2.2	2	TiO_2
Na_2O	0.07	0.09	0.11	1	MgO
K_2O	0.44	0.51	0.54	1	Insoluble residue
Free CaO	2.2	2.2	3.0	-	
Loss on ignition	1.1	1.16	1.3	-	
Insoluble residue	0.5	0.32	0.4	-	

TABLE 4.1 OXIDE COMPOSITION OF CEMENT TYPES

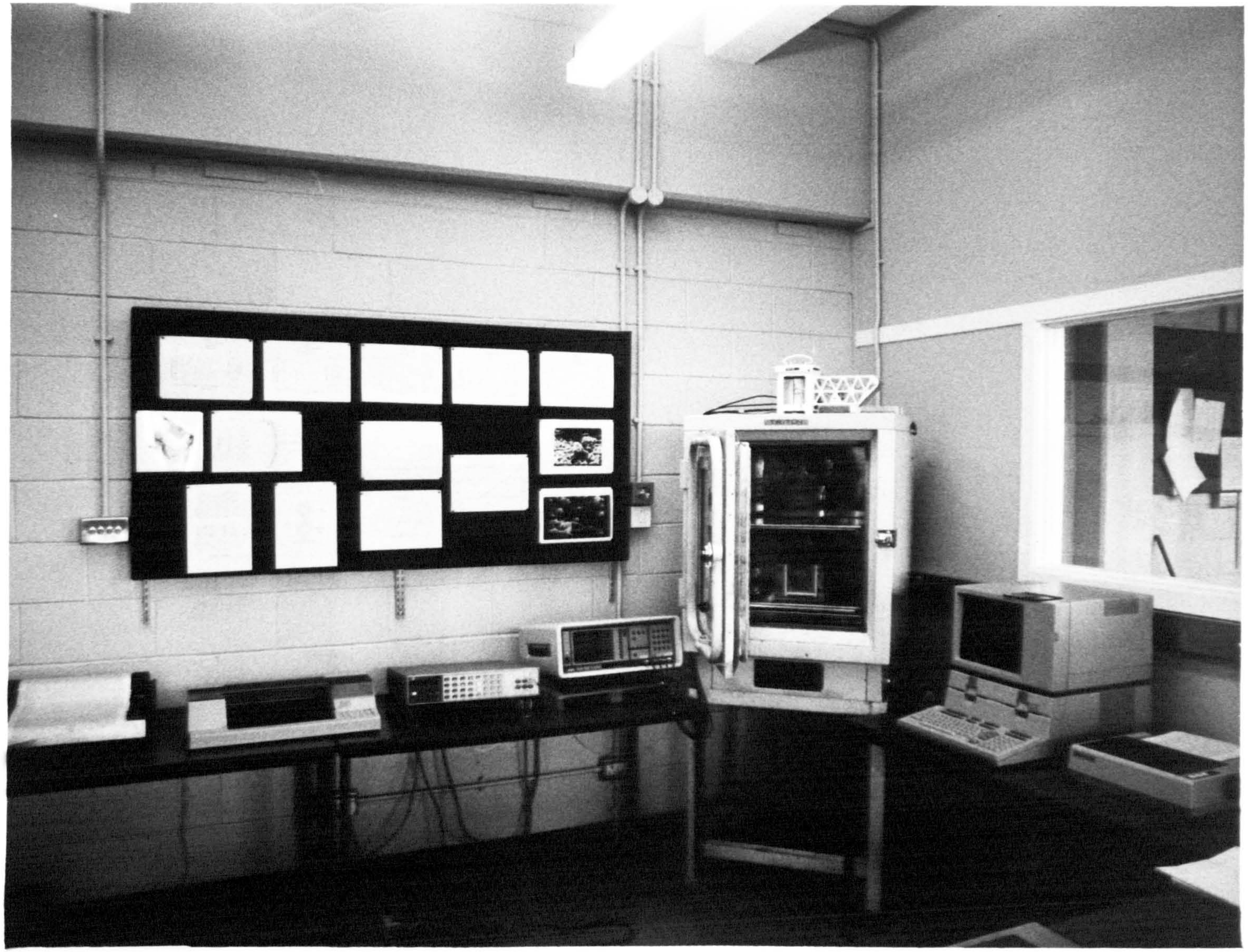

PLATE 4.1

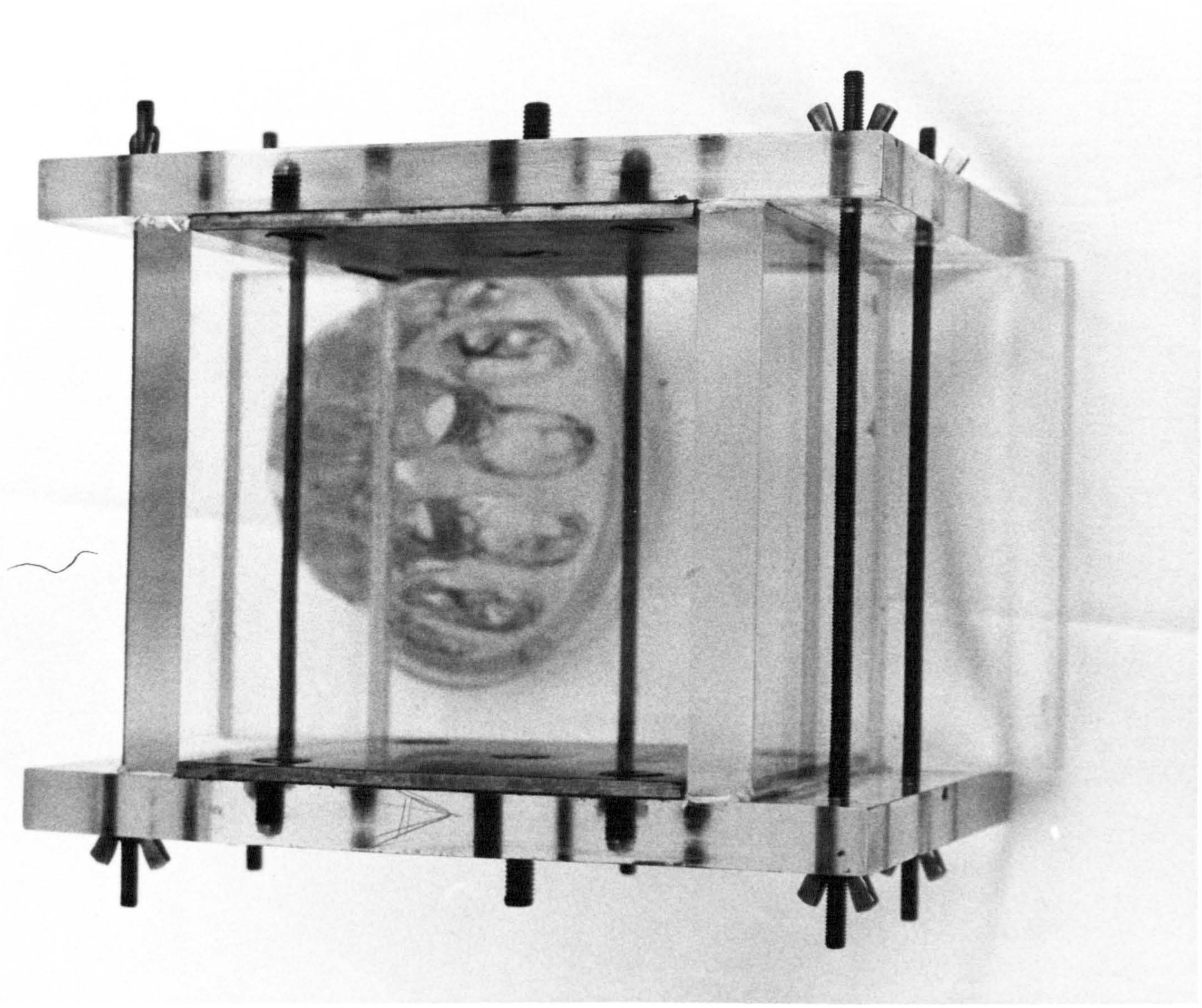

PLATE 4.2

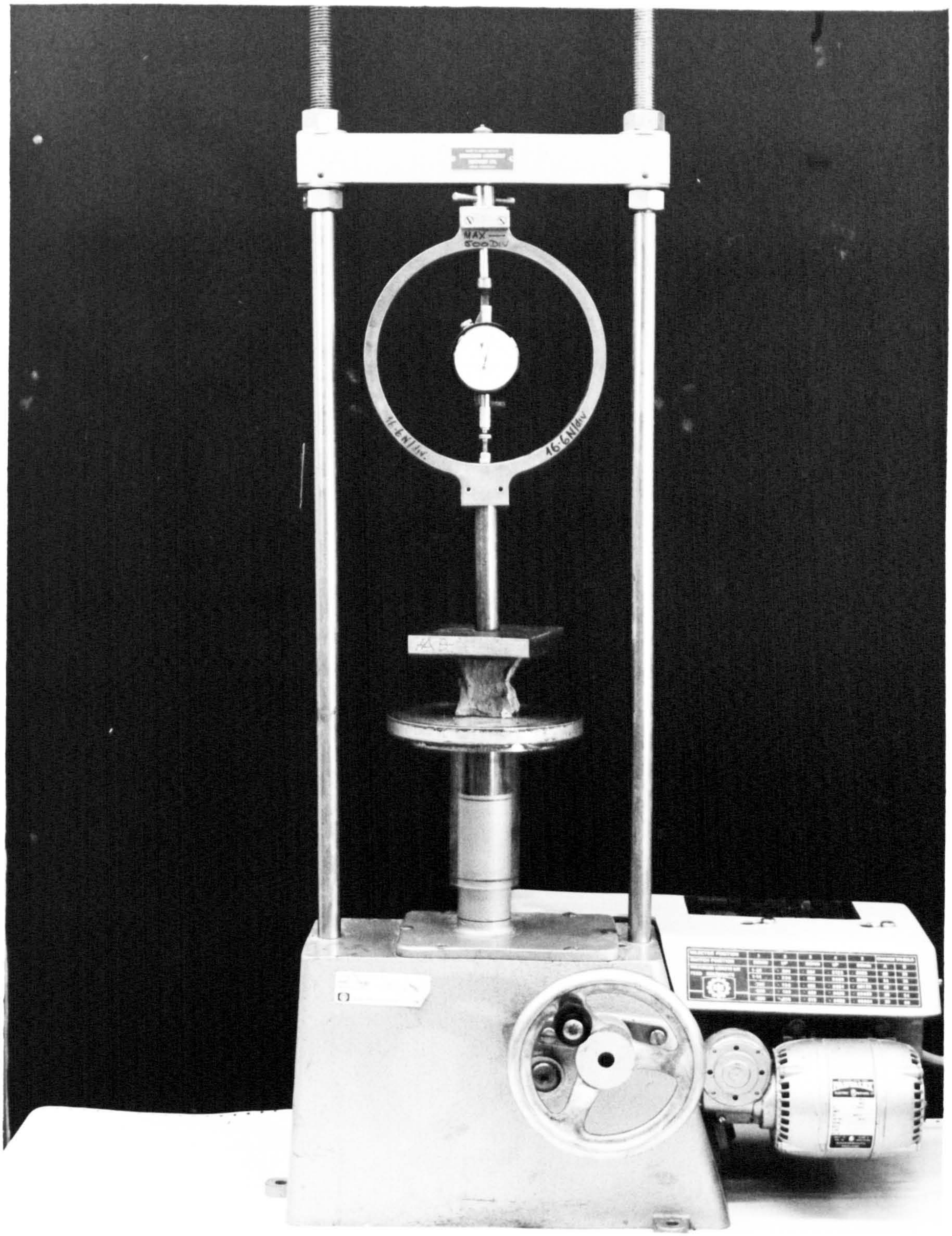

PLATE 4.3

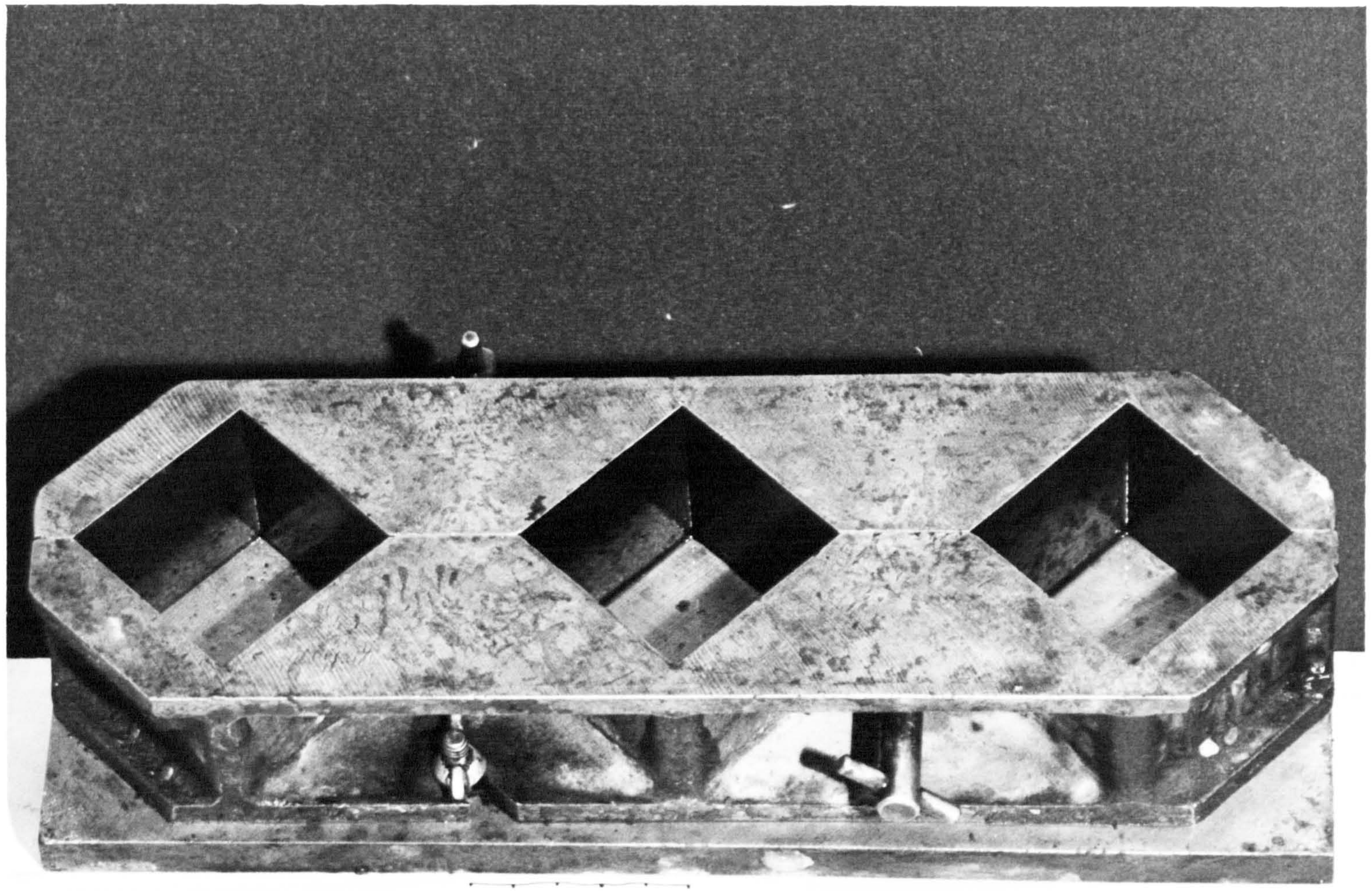

PLATE 4.4

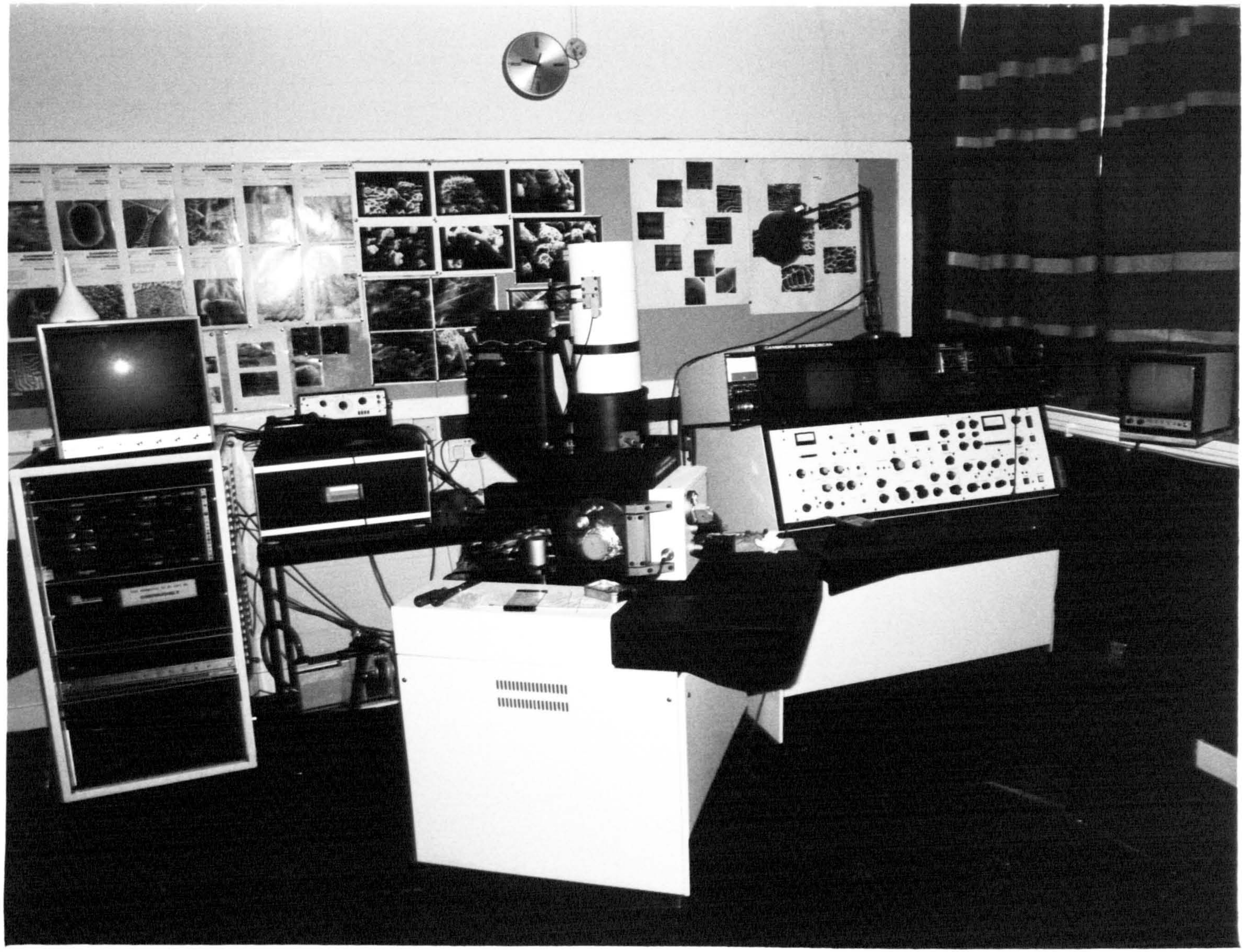

PLATE 4.5

PLATE 4.6

CHAPTER 5

EXPERIMENTAL RESULTS AND DISCUSSION

5.1 INTRODUCTION

Although cement is one of the most important building materials, and in spite of the amount of research carried out on the subject worldwide, disagreement and uncertainty remains as to the precise nature of the chemical processes involved in cement hydration and the effect of these processes on its engineering properties. Over the last four decades, with the introduction of modern instruments and techniques (e.g. SEM, TEM, and X-ray diffraction), our knowledge of the hydration processes has grown considerably, but a universally accepted view of hydration still awaits formulation.

The results of the experimental studies described and discussed in this chapter are intended to demonstrate how, for example, chemical composition; age of cement; introduction of admixtures, and environmental conditions affect the electrical response characteristics of cement paste. The observations are interpreted in terms of electrical conduction and polarization mechanisms, however, the primary objective is to demonstrate that the hydration mechanisms of cement paste can be effectively monitored by its response to an alternating electrical field.

5.2 PRESENTATION

An extensive experimental programme was carried out using the experimental system and equipment described, and as explained in the previous chapter. Results from the experimental programme have been presented,

a) to introduce a new method for continuously monitoring cement hydration without disruption to the microstructure;

b) to demonstrate the use of electrical response techniques of cement paste for elucidating hydration mechanisms;

c) to demonstrate and assess the influence of chemical composition, mix properties and admixtures on the electrical response and hence hydration characteristics.

It is also shown that tentative links can be made between crystal growth and development within cement paste and electrical response. Cross-correlation of electrical response data with results from conduction calorimetry(31,33-39,43) and SEM work is used to corroborate findings.

The electrical response graphs and SEM micrographs presented here are typical from over 300 tests. Each curve represents over 300 data points taken over 24-hours duration.

5.3 DISCUSSION OF RESULTS

5.3.1 Electrical Response

The in-phase (resistance) and quadrature (capacitance) components of the admittance, and the internal temperature, were measured over the initial 24-hours of hydration at predetermined time intervals (every 300 seconds). The raw values of resistance and capacitance were converted to resistivity, dielectric constant and loss angle using the equations in Chapter 4. Their variation is presented here in graphical form.

5.3.1.1 Variation in resistivity, dielectric constant and temperature with time

The changes in resistivity, ρ, and dielectric constant, ε, are plotted as a function of time and frequency and the internal temperature changes have been plotted on the same axis for comparative purposes. A representative graph is shown in Figure 5.1 (a)-(g).

A general feature of the electrical response curves over the test period is the considerable drop in the dielectric constant value and the rise in resistivity value, which, in broad terms, can be attributed to an irrotational binding of charges as the viscosity of the paste decreases. Within minutes after gauging, as a result of the initial dissolution of the surface of the grains and the subsequent release of silica (SiO_2, SiO_4^{4-}, $HSiO_4^{3-}$), Ca^{2+}, OH^- and other minor ions into the bulk aqueous phase (Figure 5.2(b)), an amorphous, gel membrane of calcium-silicate hydrate (C-S-H) forms around and close to the surface of the grain (Figure 5.2(c)). This semi-permeable C-S-H membrane allows water from the bulk aqueous phase to penetrate through and dissolve the unhydrated core further, releasing additional ions into the restricted space within the C-S-H shell. The larger sterically hindered hydrosilicate ions are denied passage through the thickening gel membrane; the smaller Ca^{2+} and OH^- ions pass through the membrane while others are held back by the negatively charged silica rich grain surface. Associated with the unhydrated cement core, the silica rich surface layer and gel membrane, there will exist an electrical double layer comprising

Ca^{2+} and OH^{-} ions which will be physically separated from the grain by a gel membrane.

It is evident that charges present within the system during the early stages of hydration have varying degrees of mobility:

1. mobile unbound charges in the bulk aqueous phase,
2. electrostatically bound charges of varying mobility associated with the:
   a) diffuse double layer,
   b) gel membrane,
   c) silica rich grain surface layer.

The electrical response of the matrix is directly related to the mobility of charges within the system. The mobile unbound charges within the bulk aqueous phase, outwith the grain and surrounding double layer, will give rise to ionic conduction on application of an electrical field and will be reflected in the resistivity values. Electrostatically bound charges, while not available for conduction, can be polarized by the applied alternating electrical field to induce large dipole moments, giving high dielectric constant values[123,124]. The mobility of the electrostatically bound charges (Figure 5.2(c)) varies, depending on their position in relation to the unhydrated cement core. During early hydration, the degree of association/attraction of charges on the grain varies as the inverse square of the distance from the surface of the grain. Since the mobility of charges within the membrane shell are restricted by the confined space and large electrostatic forces,

those charges outwith the protective membrane and further away from the core are more easily polarized by the alternating field, particularly as the frequency of the applied electrical field increases.

On gauging, the resistivity of the paste attains a relatively low value (compared with that of the original mixing water) and continues to decrease during the initial 40 minutes by around 2% of its original value (this feature is obscured by scale) which would indicate that ions are continually passing into solution as the grains dissolve. The formation of a gel membrane will slow, and hinder, the passage of ions into solution; following the initial drop over the first 40 minutes, the resistivity begins to increase albeit very gradually, indeed by ≈ 180 minutes it is increased by only 8% of its initial value, indicating a combination of:

a) a reduction in ionic concentration within the continuous aqueous phase, and,

b) slow build-up of gel and some initial contact between grains.

The formation of the gel membrane is also marked by the variation in the dielectric constant curve (the value of the dielectric constant at any time and frequency reflects the sum of all the polarization mechanisms operating in the system at that frequency). On gauging, the dielectric constant value represents the polarization of all electrostatically bound charges associated with the grain, the dielectric constant value increases at all frequencies over the initial 40 minutes (Figure

5.1(a)-(g), indicating the dissolution of grains and release of ions into the double layer and the build-up of gel. The peak at 40 minutes, coinciding with the minimum value of resistivity, marks the formation of C-S-H gel membrane and double layer around the grain and the onset of a period of reduced chemical activity as inferred from the rate of change of electrical parameters which are indicative of the rate at which reactions are progressing.

The suggested mechanisms governing the induction period and its termination are presently the subject of much discussion, and are centred around two main theories. The first attributes the induction period to delayed nucleation of CH and/or C-S-H[45], the period ending when nucleation commences. In the second theory, the induction period commences with the formation of a protective surface layer on the cement grains and ends when the layer is ruptured due to osmotic pressures[42]. As will be explained, the electrical response results would tend to favour the protective membrane theory, however, the belief is that a combination of both theories is responsible for the onset and termination of the induction period.

Figure 5.3 shows the dissolution of the grain and the formation of the protective membrane. During the induction period, water penetrates the semi-permeable C-S-H gel membrane and dissolves the unhydrated cement core from within, the majority of the released Ca^{2+} and $HSiO_4^-$ ions remain within the shell formed around the cement grain by the C-S-H membrane (Figure 5.3(c)). At low frequencies (up to $\simeq$10 kHz), the charges within the

protective membrane can follow the alternation of the electrical field and can thus be polarized, therefore there is an increase in the dielectric constant value over the period (40-180 minutes), Figure 5.1(a)-(d)).

The continuous release of ions into the confined space within the shell would:

a) give rise to osmotic pressure caused by the increase in the silica ion concentration within the gel and close to the grain surface, and

b) supersaturation of Ca^{2+} and $HSiO_4^-$ ions within the shell.

A combination of sufficient generation of osmotic pressure and precipitation of C-S-H 'inner product'[51] within the shell (whose volume exceeds that of the dissolved anhydrous material) weakens and finally ruptures the protective membrane, either by heat and/or mechanical stresses associated with the formation of C-S-H (Figure 5.3(d)). Once the protective membrane is ruptured, more water will reach the unhydrated core and releases Ca^{2+}, OH^- and $HSiO_4^-$ ions, this renewed activity is marked by the sudden rise in the value of the dielectric constant (≃ 180 minutes). From the frequency range considered, it was found that this peak is more prominent over the range 80 Hz - 60 kHz (Figure 5.1(a)-(e)). The charges associated with this renewed activity are held within the protective membrane and the immediate vicinity outwith the gel, and can only be polarized at relatively low frequencies. If these charges were released into the bulk aqueous phase, they would be available for ionic conduction and

thus the resistivity would be expected to decrease. From the data presented this is not the case. This event is seen as the termination of the induction period.

As the released Ca^{2+} and $HSiO_4^-$ charges squeeze out through the ruptured surfaces, they quickly combine with charges in the double layer resulting in the nucleation of C-S-H and CH (Figure 5.3(e)). The consequence of this renewed activity is that the conduction paths become blocked and more tortuous as crystals grow and the gel extends into the water-filled capillaries. The sudden drop in the dielectric constant (observed at all frequencies) coincides with the rise in resistivity, indicating an irrotational binding of charges and an increase in rigidity of the paste.

Further formation of C-S-H and their conversion to more crystalline C-S-H hydrates would take place over the period 180-600 minutes. During this period, the resistivity rises quite sharply indicating that conduction paths through capillary pores in the paste are becoming restricted as ionic concentration decreases with crystallisation and grain segmentation. There is an increase in temperature associated with this renewed chemical activity marked by the rise in the temperature/time curve which peaks at 350 minutes (Figure 5.1), similar temperature increases have been reported[31,33-39,43] using calorimetry techniques, however, the peak usually occurs at a later time (≃400 minutes), this is the result of the high water-cement ratios used in these tests (≃10:1).

At 600 minutes, the electrical parameters undergo yet another change, the resistivity decreases coupled with an increase in the dielectric constant value (although slightly obscured by scale) but more noticeable at higher frequencies. This could indicate further activity within the paste, the slow rate of change of electrical parameters suggests much reduced rate of reactions during this period. At this point in time (600 minutes), the paste has gained considerable strength and the grains have segmented to a rigid matrix. The renewed chemical activity must release charges into;

a) the continuous capillaries, thereby reducing the electrical resistivity,

b) the blocked capillary and gel pores, thereby increasing the dielectric constant by interfacial polarization.

The period following 600 minutes is regarded as the beginning of the hardening process, the change in the value of resistivity and dielectric constant from this point on are associated with, and indicate, renewed activity on the C_3A phase, with the formation of ettringite (AFt) and its conversion to monosulpho-aluminate (AFm). During this conversion reaction, two moles of Ca^{2+} and So_4^{2-} are formed per mole of ettringite, this could corroborate the work by Tamas[148];

$$C_3A + 3CSH_2 + 26H \longrightarrow C_6A\bar{S}_3H_{32}\ (AFt) \qquad ..(5.1)$$

$$C_6A\bar{S}_3H_{32}\ (AFt) \longrightarrow C_4ASH_{12}(AFm) + 2C + 2S + 2OH \qquad ..(5.2)$$

$$2C + 2S + 2OH + 2C_3A + 4H \longrightarrow 2C_4A\bar{S}H_{12}\ (AFm) \quad ..(5.3)$$

The sum total of equations (5.2) and (5.3) will result in equation (5.4), which was discussed in Chapter 2, equation (2.12).

$$C_6AS_3H_{32} + 2C_3A + 4H \longrightarrow 3C_4A\bar{S}H_{12} \quad ..(5.4)$$

The magnitude of the decrease in resistivity during this period indicates the reactivity of this phase which depends on the chemical condition of the matrix (i.e. the SO_4^{2-} concentration).

From the electrical response curve, four stages in the early hydration of Portland Cement have been identified, this corroborates previous theories of cement hydration[31] using heat evolution curves discussed in Chapter 2. However, the proposed times at which each stage commence and terminate are different. The various stages are marked on Figure 5.1(c).

STAGE 1 Initial build-up of amorphous hydrates on the grain surface (0-40 minutes),

STAGE 2 A dormant period of little chemical activity (40≃180 minutes) during which the protective gel membrane is formed and thickens,

STAGE 3 A period of renewed chemical activity and gain in rigidity of the paste (180≃500 minutes),

STAGE 4 A reduction in the rate of chemical activity and a general slowing-down of reactions, renewed reaction on C_3A phase (depending on SO_4^{2-} availability), formation

of ettringite and its conversion to monosulpho-aluminate.

5.3.1.2 The effect of frequency of applied field on electrical response

a) Dielectric Constant

It is evident that, as the frequency increases, not only does the shape of the dielectric constant curve change quite markedly but absolute values reduce. Indeed, at any particular point in time, the high frequency value (300 kHz) of dielectric constant is almost three orders of magnitude lower than the low frequency (20Hz) value. The fall in dielectric constant with increasing frequency can best be presented by a dielectric dispersion curve plotted at various points in time over the frequency range employed. Figure 5.4(a),(b) shows dispersion and loss angle curves plotted at 100, 200, 400, and 1000 minutes after gauging.

It is apparent that over the frequency range considered, a region of dielectric dispersion exists. As the rigidity of the paste increases, its polarizability decreases due to irrotational binding of charges and results in a displacement of the dispersion curve with time. The value of the low frequency dielectric constant ε_o' (i.e. at 20 Hz) and the dielectric dispersion $\Delta\varepsilon_o'$ (i.e. $\varepsilon_o' - \varepsilon_{AC}'$), reflects the amount of low frequency polarization mechanisms that can develop. It is apparent that as the grains segment and the paste increases in rigidity, ε_o' decreases, the slope of dispersion curve is reduced and, as a result, $\Delta\varepsilon_o'$ decreases. Polarization mechanism changes

from a predominantly double layer[124,125] (where relatively long time is required for bound charges to be displaced) to interfacial and Maxwell-Wagner[121,122] effects. The extent of the latter type of polarization is measured by $\varepsilon_o' - \Delta\varepsilon_o'$, and decreases as the paste sets.

The peak in the loss curve (Figure 5.4(b)) represents the characteristic frequency, f_o, it occurs in the region of dielectric dispersion and measures the mobility of charges. Figure 5.4(b) shows that as the paste sets, the magnitude of the loss curve peak reduces, and indicates a loss in polarizability. This is the result of grain segmentation and increase in the rigidity of the paste. As hydration progresses the characteristic frequency (peak loss) shifts to a higher frequency indicating a change in the polarization mechanism from predominently double layer to interfacial effects.

The dielectric dispersion at 1000 minutes displays a higher value at all frequencies than the dielectric dispersion at 400 minutes, this is the result of the AFm-AFt conversion which releases charges, hence the reduction in resistivity and an increase in dielectric constant values (although obscured by scale in Figure 5.1(c).

b) Resistivity

The resistivity of the paste, unlike its dielectric constant, is not as sensitive to the change in the frequency of the applied electrical field over the test period. In general, the resistivity value decreases with increasing frequency, this

feature is more noticeable after the sudden rise in resistivity and dielectric constant (approximately 200 minutes) when cement paste begins to gain rigidity. The resistivity curves in Figure 5.1(a)-(g) demonstrate this feature.

Water is held in hydrated cement in a variety of ways as:

a) free water,

b) gel water, and,

c) chemically combined water.

Free, unbound water held in capillary pores will contribute to ionic conduction processes through the cement paste during early hydration and could be assumed to be the primary conduction mechanism. The chemically combined water, forming a definite part of the compounds of hydration increases as more hydration products are formed within the capillaries, it could also be assumed that chemically combined water will not contribute significantly to conduction. Gel water, however, is held in varying degrees of firmness, (Figure 5.5):

a) adsorbed water held to the gel particles by surface forces (Van-der-Waals forces),

b) interlayer water held between the Tobermorite sheets.

As hydration progresses, the volume of hydration products (gel) increases and extends to fill the water-filled capillaries, thereby reducing the available capillary water which is responsible for ionic conduction. The continually increasing gel also adsorbs the evaporable capillary water onto its surface.

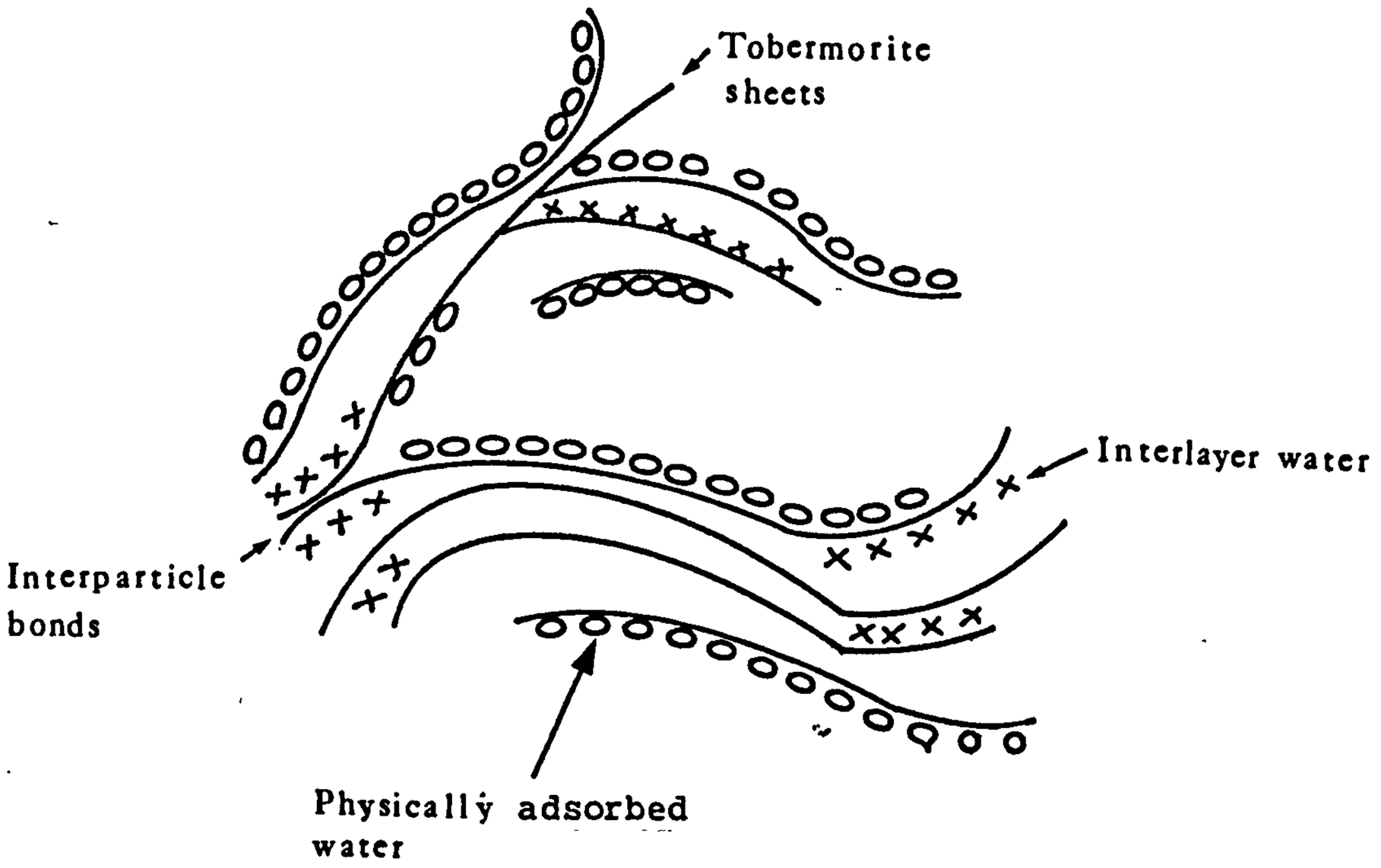

Figure 5.5 Probable structure of hydrating silicates[149]

The result of this is:

a) a reduction in the cross-sectional area for ionic conduction processes, and,

b) an increase in surface ionic conduction processes by means of the adsorbed gel water.

The consequence of (a) and (b) above would mean that the conductivity for cement paste could be explained by a parallel conduction model represented by:

$$\sigma(f) = \sigma_{dc} + \sigma_{ac} \qquad ..(5.5)$$

where $\sigma(f)$ is the conductivity at any frequency of applied electrical field,

σ_{dc} is low frequency (dc) conductivity, and

σ_{ac} is the frequency dependent conductivity.

At low frequencies, conduction is primarily ionic and therefore,

$$\sigma(f) \simeq \sigma_{dc} \text{ (at low frequency)} \qquad ..(5.6)$$

However, as the frequency increases, the surface ionic conductivity associated with gel water will affect the overall measured conductivity for the paste, thus the frequency dependent or enhanced conductivity element can be expressed as:

$$\sigma_{ac} = \sigma_{dc} - \sigma(f) \qquad ..(5.7)$$

Figure 5.6(a)-(d), shows the variation in resistivity values as the frequency of applied electrical field increases. It is noted that the variation is more pronounced following the grain segmentation, it is also noticeable that resistivity decreases with increasing frequency at all water-cement ratios. The difference in the high frequency value and low frequency value of resistivity is greatest at low water-cement ratios.

Summarising the low frequency electrical resistance of cement paste will be dominated by ionic conduction, as the frequency of the applied electrical field increases, the surface ionic effects

will influence the overall conductivity or resistivity,

At low water-cement ratios, the fractional volume of gel in paste is greater than at high water-cement ratios (i.e. the gel-space ratio is higher in the former case), hence the surface ionic conduction effects would be more significant in the case of low water-cement ratios. The equation (5.7) has been rearranged in terms of resistivity and a percentage frequency effect (PFE) term has been introduced to quantify the effect of enhanced conduction through the adsorbed gel water, thus

$$PFE = \frac{\rho_{dc} - \rho_{ac}}{\rho_{dc}} \times 100\% \qquad ..(5.8)$$

where, in this case, ρ_{dc} is the resistivity at dc (low) frequency (20Hz) and ρ_{ac} is the resistivity at ac (high) frequency (300kHz).

The PFE term increases with time, but the effect is more noticeable after grain segmentation and is apparent at all water cement ratios (Figure 5.6). The percentage frequency effect could be visualised as a measure of the rate of gel development within the continuous capillaries. As the surface area of the gel increases, so does the volume of the adsorbed water to the gel surface and hence the cross-sectional area available for surface ionic conduction. This feature is noted on the PFE curves shown in Figure 5.6 at all water-cement ratios, the increase is gradual up to the peak in dielectric constant when there is a sudden increase in PFE caused by the formation of gel products associated with C_3S hydration and a consequent dilation

of the gel and an increase in its surface area. The subsequent drop in PFE is the result of crystallization of gel products. Following this drop, the PFE value continues to rise gradually, it is noted that PFE value is higher at lower water-cement ratios. This is due to the increased cross-sectional area available for conduction through the adsorbed gel water, thus a higher proportion of conduction at low water-cement ratios is associated with surface ionic effects. A paste with a relatively low percentage frequency effect would thus represent a more 'open' texture, therefore, as water-cement ratio increases, the structure of the paste becomes more porous (the calculated value from the data presented for PFE at 0.25 water-cement ratio is 60%, compared to 40% for 0.35 water-cement ratio). This term could thus be used to give a measure of the permeability and rigidity of the paste.

Strength is one of the most important engineering properties of concrete, and is said[8] to depend on:

a) the water-cement ratio,

b) the degree of hydration.

However, since strength is directly related to the development of microstructure, and the microstructure development is a function of gel-space ratio, it is more appropriate to assess strength in terms of the degree of hydration. Therefore, PFE could thus be developed to give a measure of permeability, rigidity and strength of the paste.

The variation in electrical response over the test period has been discussed above for standard samples of cement (OPC cement paste with water-cement ratio of 0.27). The electrical response will alter with changes in:

a) water-cement ratio,

b) age of cement,

c) chemical composition of cement,

d) environmental conditions,

and the introduction of:

a) admixtures,

b) aggregate.

The effect of these variables on electrical response will now be discussed.

5.3.1.3 The effect of water-cement ratio on electrical response

Water plays an important role in the micro-structure building processes in cement paste during early hydration, it is believed[138] that the structure and behaviour of C-S-H and CH crystals change according to the amount of water and space available. There is general agreement that as water is removed from the matrix, some rearrangement of the micro-structure with regard to C-S-H and CH crystals takes place. It has been noted that under sustained loads (less than those required to cause failure due to static fatigue) there is a strengthening effect[140]. This may be attributed to an increase under

pressure of the Van der Waals attraction between adjacent crystals. The removal of water from the system may play a similar role, as this will also cause particles to come closer together. Figure 5.7 shows the effect of increasing water-cement ratio on the electrical parameters. Some general features are evident,

a) The rate of change of the resistivity curve decreases as water-cement ratio increases, this indicates that as the water-cement ratio decreases the fractional volume of evaporable water and the number of continuous capillaries are reduced and thus conduction paths become constricted as hydration proceeds.

b) The dormant period is lengthened and the peak in dielectric constant is delayed as the water-cement ratio is increased, the fractional volume of cement particles is less and they are more dispersed. The time taken for rupture of the protective coating is increased and the nucleation of CH is delayed.

5.3.1.4 The effect of age of cement on electrical response

Figure 5.1 shows the electrical response of OPC supplied from a builder's merchant and it was estimated that the cement had been lying in storage for approximately 2 months before delivery. Experiments were also conducted on ex-works cement (Figure 5.7(a)). Similarities between 'old' and 'new' cement are noticeable, but, perhaps, the most significant differences are:

a) the reduction in the length of the dormant period during Stage 2 (by around 100 minutes),

b) a more significant drop in resistivity and rise in dielectric constant associated with Stage 4.

The implication of (a) and (b) is that the 'new' cement hydrates at a much faster rate. The stored cement would have been prematurely hydrated by absorbing moisture from the atmosphere, the hydration products will form a coating on the grain surface which will account for the delay in hydration of C_3S phases in Stage 2 and hence an increase in the dormant period, and the more gradual rate of hydration with regard C_3A phase during Stage 4.

5.3.1.5 The effect of chemical composition on electrical response

When cements of differing chemical composition were tested, similarities in the response graphs to those of OPC were noted. Figure 5.8(a)-(c), display the variation in measured electrical parameters for HAC, RHPC and SRPC respectively for a frequency of 1 kHz.

The principal cementitious phase of high alumina cement (Ciment Fondu Lafarge) is monocalcium aluminate, $CaO.Al_2O_3$ (approximately 78% by weight). Minor constituents comprise iron oxides (FeO and Fe_2O_3) and silica (SiO_2). The hydration of monocalcium aluminate ($CaO.Al_2O_3$) is temperature dependent[6,7,139] and its hydration can be summarised,

$$\text{CaO.Al}_2\text{O}_3 + \text{H}_2\text{O} \begin{cases} <15^{\circ}\text{C} \rightarrow \text{CaO.Al}_2\text{O}_3.10\text{H}_2\text{O} \ (\text{CAH}_{10}) & ..(5.9) \\ \quad \downarrow \text{increase temperature} \\ 15\text{-}25^{\circ}\text{C} \rightarrow \text{Al}_2\text{O}_3 + 2\text{CaO.Al}_2\text{O}_3.8\text{H}_2\text{O} \ (\text{C}_2\text{AH}_8) & ..(5.10) \\ \quad \downarrow \text{increase temperature} \\ >25^{\circ} \rightarrow \text{Al}_2\text{O}_3 + 3\text{CaO.Al}_2\text{O}_3.6\text{H}_2\text{O} \ (\text{C}_3\text{AH}_6) & ..(5.11) \end{cases}$$

At normal ambient temperatures, CAH_{10} and C_2AH_8 would be normal products of hydration. However, if the temperature rises above $25^{\circ}C$, conversion takes place as CAH_{10} and C_2AH_8 are transformed to C_3AH_6.

With reference to data presented in Figure 5.8(a), the absolute values of dielectric constant and resistivity are, respectively, lower and higher than those for OPC paste (Figure 5.1) at the same age. This would indicate an overall reduction in ionic concentration due to low lime content of HAC. Three peaks are observed on the dielectric constant curve; the first peak at 40 minutes is associated with the gradual leaching of ions from the grains, consequently the formation of a weak aluminous hydrate gel on the grain surfaces reduces charge mobility, this could be responsible for the reduction in dielectric constant after the initial 40 minute period. The resistivity reaches a minimum at this time (40 minutes) and is taken to mean that the gauging water has achieved a supersaturated state.

At 100 minutes and up to 200 minutes, the dielectric constant remains constant and the resistivity shows only a very gradual rise. This signifies an overall reduction in the reaction rates as a weak coating forms on the grains, temporarily preventing further hydration and results in a dormant period. At approximately 200 minutes, rupturing of the weak coating initiates renewed hydration of $CaO.Al_3O_3$ resulting in an increase in the polarizability of the paste and subsequent rise in dielectric constant. It is evident that the renewed hydration results in a release of charges which are associated with the grain surfaces and not with the bulk aqueous phase, as no reduction in resistivity is detected at this time, similar, in many respects, to OPC with the peak occurring at the same time. The peak dielectric constant at 260 minutes coincides with a rise in resistivity and an increase in internal temperature of the paste (which is conducive to the formation of $2CaO.Al_2O_3.8H_2O$). At this point in time, the paste is increasing in rigidity. However, due to the exothermic nature of monocalcium aluminate hydration, the temperature of the mix rises considerably (120^{o}) and conversion of the hydrates to $3CaO.Al_2O_3.6H_2O$ must result. The peak in dielectric constant and drop in resistivity noticeable at maximum temperature (350 minutes) is attributed to a combination of C_3AH_6 formation and the rise in the initial temperature of the paste (the dielectric constant and resistivity being temperature dependent[92]). A certain amount of internal dessication must result from this rise in temperature.

The peak and drop in dielectric constant and resistivity is short-lived as the paste rapidly gains rigidity, and the period

of hardening commences. Therefore, the curves follow the same trend as OPC paste, although the values of the measured electrical parameters are an order of magnitude lower, in the case of dielectric constant, and higher in the case of resistivity.

Figure 5.8(b) displays the change in measured electrical parameters for Rapid Hardening Portland Cement (RHPC). RHPC is used when a rapid development of strength is required, the increase in the rate of gain of strength is achieved by increasing the C_3S content and by finer grinding of the cement clinker. Comparing Figure 5.8(b) with Figure 5.1, it is evident that the peak in dielectric constant occurs approximately at the same time indicating a similar 'setting time'. However, certain differences should be noted,

a) the absolute values for resistivity and dielectric constant are higher and lower respectively. Indeed, after the peak in dielectric constant at approximately 200 minutes, the resistivity rises at a faster rate indicating a rapid gain in strength as the cement grains segment and continuous capillaries become blocked by hydration products.

b) The drop in resistivity and rise in dielectric constant after 500 minutes is more considerable than that for OPC, and could indicate an increase in chemical activity on C_3A phase and AFt $\rightarrow$ AFm conversion.

Figure 5.8(c) displays the results for Sulphate-resisting

Portland Cement (SRPC). SRPC has a lower C_3A (≃ 8%) and C_3S (≃ 6%) content and a higher C_2S (11%) content in comparison to OPC. The peak in dielectric constant at 200 minutes is still evident, however, the rate at which the resistivity increases (after this peak) is reduced, possibly due to the reduction in C_3A and C_3S content of the cement. What is also noticeable is the absence of a definite Stage 4 which begins at approximately 600 minutes, which is attributed to the reduction in the C_3A content and AFm → AFt conversion.

It is evident that different types of cement display different electrical response characteristics. In order to highlight this further, a sequence of tests was carried out on blended OPC-HAC cements. Figure 5.8(d) shows the electrical response of a 9:1 OPC/HAC mixture, it is noted that the basic electrical response characteristics are similar to those of OPC and HAC, however, the time of the occurrence of the various peaks has been altered and, in this instance, the gain in rigidity has been accelerated.

5.3.1.6 The effect of admixtures on electrical response

The properties of cement can be conveniently modified by changing the proportions of the basic constituents of the cement to form special cements or by the addition of admixtures to the cement. Monitoring the electrical response offers the opportunity to relate physical changes to chemical reactions taking place during the early hydration period. The variations in resistivity and dielectric constant have been shown to reflect this, and hence it is appropriate at this stage to redefine the peak in the

dielectric constant following the induction period as the 'point of set' (cf Figure 5.1(c), 180 minutes).

Having assumed the point in the dielectric constant curve associated with the 'set' of the paste, then by comparing Figure 5.1 with Figure 5.9, it is evident that the addition of sugar to the mix has the effect of delaying the dielectric peak. Figure 5.9(a) and (b) shows variation in measured electrical parameters when 0.02% and 0.1% sugar is added to the mix respectively; 0.02% sugar delays setting by 220 minutes and 0.1% sugar delays setting by 620 minutes. The retarding agent has the effect of delaying the reaction of the C_3S phase (associated with the peak in dielectric constant) and increasing the induction period; the peak in dielectric constant curve is progressively delayed as the proportion of retarder is increased. The delay in setting is directly proportional to the quantity of sugar added, although it was found possible to kill setting by the addition of more than 0.2%.

The addition of calcium chloride accelerates the setting process; Figures 5.10(a) and (b) show the variation in measured electrical parameters when 1% and 2% of calcium chloride is added to the mix respectively; 1% calcium chloride accelerates the setting by 50 minutes and 2% calcium chloride accelerates setting by 120 minutes. The induction period is reduced and the reaction rates considerably increased. The curves are compressed compared to that of standard mix. If the assumption is made that the nucleation of CH and C-S-H is associated with setting, the addition of calcium chloride will increase the Ca^{2+} ion

concentration within the aqueous phase and subsequently reduce the time required for supersaturation of the aqueous phase and hence nucleation of CH and C-S-H.

Figure 5.11 displays the results of a series of tests obtained by adding various percentages of retarder (sugar) and accelerator (calcium chloride) to the standard paste. In this figure, T_a is defined as the time at which the peak in dielectric constant occurs with admixture added; T_d is defined as the time at which the peak in dielectric constant occurs in the datum mix; and the ratio T_a/T_d is used to quantify the effect of the admixture on the setting of the paste.

Although in this instance, only the graphs for sugar and calcium chloride are presented, similar graphs could be produced for other commonly used admixtures. These graphs can be used to assess the percentage of admixture required to be added to the standard mix to achieve a specified setting time. It is evident from this figure that small percentages of calcium chloride (less than 0.2%) retard setting, this is in agreement with other investigators[7,33].

5.3.1.7 The effect of aggregate on electrical response

The introduction of aggregate to cement paste changes its micro-structure and consequently the electrical response characteristic. An extensive series of tests were carried out to determine the electrical response characteristic of mortar using OPC at various sand-cement and water ratios.

Electrical current is considered to be conducted through mortar along three paths[93]:

a) through the aggregate and paste,

b) through the aggregate particles in contact with each other,

c) through the paste itself.

The electrical resistivity of a typical sand is several orders of magnitude higher than that of mortar. This, therefore, suggests that a high proportion of current is being conducted through the paste (i.e. through the path of least resistance).

Figure 5.12 displays the effect that the addition of various percentages of aggregate has on electrical response. The results shown are for a water-cement ratio of 0.35 (by weight) and a frequency of 1000 Hz.

It is apparent that the general shape of the response curves remain the same, however, certain changes mainly associated with the microstructure variation are noticed:

a) The addition of aggregate with a small dielectric constant (e.g. granite $\simeq$ 10, sandstone $\simeq$ 11) in comparison to that for paste ($\simeq 10^5$) will reduce the overall measured dielectric constant of the matrix and increase its resistivity value as the sand-cement ratio increases. The fractional volume of paste, therefore, will control the overall measured resistivity, dielectric constant and the conduction through the matrix.

The resistivity of cement paste and concrete has been the subject of recent research[94,107,109,116,150], the dielectric properties of cement and concrete on the other hand, has not received much attention. The present work has dealt with the dielectric properties of cement paste and mortar, however, the dielectric theory of heterogeneous substances (e.g. mortar and concrete) is beyond the scope of this thesis and worthy of further research.

From the above test result, it is apparent that the dielectric constant of mortar ε_m is proportional to the fractional volume of the paste (ϕ);

$$\varepsilon_m \alpha \varepsilon_p \phi \qquad ..(5.12)$$

b) The drop in the dielectric constant curve following the peak at ≈300 minutes becomes more gradual and the peak expands. As the fractional volume of paste decreases (due to increasing aggregate content) then the overall $[Ca^{2+}]$ decreases within the aqueous phase. The consequence of which is:

i) much slower rates of reaction after the peak in dielectric constant compared to the neat paste, and,

ii) a more gradual crystallization of CH and C-S-H.

5.3.2 Strength Development of Cement Paste

One of the first physical consequences of cement hydration is its transformation from plastic paste into a rigid matrix, with the

C_3S phase being responsible for normal setting and strength development[33]. It is proposed that the early strength development which is associated with the chemical reactions taking place can be identified by changes in the electrical response.

A series of strength tests were carried out using 50mm cubes cast from samples used for electrical tests, the water-cement ratio of the mixes was 0.27 by weight and the test procedure was that described in the previous chapter. The aim was to investigate the strength development of the paste over the initial 24-hours and to correlate with electrical response curves. Typical results have been given in Figure 5.13, by 200 minutes (the peak in dielectric constant) the paste has gained sufficient strength to be demoulded. The failure pattern when crushed resembles that of stiff clay (Plate 5.1(a)), at 300 minutes with much increased failure load, the failure pattern was 'wedge-like' (similar to one observed in mature concrete specimens), Plate 5.1(b) . This would indicate that the paste during this period (200-300 minutes) takes on the behaviour of the solid material, however it must be appreciated the platen effect could influence failure mode.

The strength increases rapidly over the period 300-1000 minutes, indeed, by the end of this period it has achieved approximately 30% of its 28-day strength (90 N/mm^2).

5.3.3 Scanning Electron Microscopy

Electron microscopy study of cement hydration has received attention by many researchers[32,41,143,144]. The formation and

morphology of the resulting hydrates have, in the past, been related to the various stages of hydration marked by heat evolution curves associated with calorimetery studies[29,30].

The following SEM micrographs were taken at appropriate points in time during the hydration process to investigate the morphology of the hydrates on the grain surface. The times at which the micrographs were taken were identified from, and dictated by, the electrical response curve at identified (critical) stages during hydration. The aim was to follow the micro-structure development using SEM in parallel with electrical response techniques, to correlate the results, and compare them with other methods in use. Typical results are presented, taken from over 200 micrographs.

5.3.3.1 Portland Cement

During storage, cement grains absorb moisture from the atmosphere and prematurely hydrate, this is in evidence (Plate 5.2) when cement grains before gauging with water are viewed under SEM. The small white crystals visible on the grain surface can be identified as CH. Some premature hydration is evident on the grain surface due to moisture absorption and is responsible for the delay in dielectric constant peak and variations in the measured electrical parameters (Figure 5.1(c), Figure 5.7(a)) when old and new cements were used.

A polymineralic fragment of cement clinker (Plate 5.3) was taken at approximately ≃200 minutes, at the end of Stage 2 (Figure

5.1(c)) and at the peak in dielectric constant value. The grain surface is partially coated with the amorphous C-S-H seen at the edge of the grain. Some traces of ettringite (AFt) are evident which would have been formed on the C_3A phase during Stage 1 (Figure 5.1(c)) of hydration; the ettringite appears as fibrillar growths radiating from the grain surface[146]. The dark region in the centre of the photograph is a capillary pore which has been evacuated of water. Examination of grain boundaries on this micrograph show traces of amorphous C-S-H hydrates and Type II C-S-H.

Plate 5.4 was taken at 250 minutes, (following the peak in dielectric constant and the rise in resistivity). Close examination of the micrograph shows the formation of reticulated crystals identified as Type II C-S-H. The net-like crystals bridge the capillary pores between grains and hence increase the rigidity of the paste, this correlates with the increase in resistivity at this time as the conduction paths through the paste become tortuous due to grain segmentation and blocking of pores.

Plate 5.5 taken at approximately 600 minutes shows how the hydration products have now assumed a definite morphology. The short stumpy crystals are identified as C-S-H Type I associated with hydration reactions during Stage 2 and 3, the relatively large white crystal clusters seen amongst the C-S-H are Portlandite (CH), this agrees with findings by Diamond[76], Ciach[74] and Taylor[145].

Plate 5.6 taken at approximately 700 minutes displays a combination of crystals. In the centre, the surface has a coarse texture compared with that of the surroundings. At higher magnification (Plate 5.7), the coarse texture is seen to be composed of hexagonal rods associated with AFt growing on an isolated fragment of C_3A. Closer examination of this micrograph reveals thin plate-like foils[77] identified as monosulpho-aluminate growing through ettringite needle-like crystals. The monosulpho- aluminate develops when SO_4^{2-} ion concentration in the liquid phase is depleted, and ettringite converts to monosulpho-aluminate. At this point in time (Figure 5.1) the rate of change of resistivity reduces considerably, and at the same time there is an increase in the dielectric constant (although slightly obscured by scale). This is the result of renewed chemical activity on the C_3A phase[143], with ettringite converting to monosulpho-aluminate (Plates 5.6 and 5.7), and a subsequent release of charges (equations (5.9)-(5.11).

Plate 5.8 taken at 1300 minutes shows further large-scale formation of ettringite rather than isolated examples seen in Plates 5.6 and 5.7 taken at 700 minutes, and would corroborate the observations of Dalgleish[146].

Calcium hydroxide (CH) appears in the early stages of hydration (200-400 minutes) as thin hexagonal plates, subsequently, deposits of calcium hydroxide grow massive and lose their hexagonal outline, they can be easily recognised by their parallel planes and smooth featureless surfaces.

Plates 5.9 and 5.10 are taken at 800 and 1400 minutes respectively, in both micrographs large-scale formation of calcium hydroxide is evident. It precipitates within capillary pore spaces between C-S-H hydrates and develops to form large crystals. The largest proportion of the total hydration products at this stage is calcium hydroxide and C-S-H Type I, the calcium hydroxide continues development and fills the capillary pores, whereas C-S-H Type I converts to C-S-H Type III and IV. The other hydrate present in large quantity in both micrographs is ettringite.

Dalgleish[146] and Pratt[143] believe that further hydration of the cement core (already protected by a protective membrane) will result in fibres radiating out from the unhydrated core, bridging between the core and the protective shell and the formation of Hadley grains[147]. Plates 5.11 and 5.12 taken at approximately 24 hours show two examples of Hadley grains[147]. In Plate 5.11, a Hadley grain is seen at the top, marked on micrograph H, and in Plate 5.12 is seen in the centre. During fracture, the protective layer has been broken to reveal a partially hollow shell, an unhydrated cement core with C-S-H hydrates in the form of rods bridging the core to the protective layer, also visible in both micrographs are large calcium hydroxide crystals (e.g. in Plate 5.12), a large number of dimple-like C-S-H Type I crystals and clusters of ettringite.

Finally, as the paste reaches maturity, the pores are filled with hydration products, the individual cement particles have dissolved and become more difficult to detect in a general

ground-mass. A fracture surface of a mature cement is shown in Plate 5.13, and reveals areas of calcium hydroxide interspersed with areas of what could be described as C-S-H Type III, and pores are also noted.

5.3.3.2 Portland Cement and the influence of admixtures

The effect of admixtures on the hydration process could also be followed by SEM micrographs taken at various intervals. Plate 5.14 displays a micrograph of OPC cement paste with a water-cement ratio of 0.27 and the addition of .2% calcium chloride ($CaCl_2$) by weight, taken at 200 minutes after gauging with water. Similar reticulated crystals as those found in micrographs of standard mix at 280 minutes (Plate 5.4) are seen here some 80 minutes earlier, this highlights the accelerating effect of calcium chloride. When 0.02% by weight of sugar (retarder) is added (Plate 5.15), the micrograph taken at approximately 200 minutes shows hydration products seen on the grain surface at a much earlier time. No ettringite (AFt) crystals are evident, which suggests that the hydration of C_3A phase has been reduced or retarded.

The above observation further proves the effectiveness of the electrical results and their potential use in monitoring morphological changes in the cement microstructure.

5.3.3.3 High-Alumina Cement

Plate 5.16 shows an unhydrated high-alumina cement grain.

Plates 5.17, 5.18 and 5.19 have been taken at 225, 320 and 425 minutes respectively, these times were dictated by the position of the peaks in the dielectric constant curve recorded for a sample of the same paste (Figure 5.8(a)).

At 225 minutes, Plate 5.17 (the end of the induction period) a dense C-A-H gel (fur-like morphology) has covered the grain, closer examination of the micrograph (centre) reveals crystals radiating to cover the grain and bridge the pores, the hydrate formed during the induction period is the result of reaction associated with equation (5.2).

As the temperature increases CAH_{10} converts to C_2AH_8, resulting in the the second peak in dielectric constant (equation (5.3)), the hydration products formed following this peak have crystals with a more definite morphology (Plate 5.18). The temperature within the paste following the above reactions exceeds the temperature above which C_3AH_8 becomes unstable (25^{o}C) and hence converts to the stable C_3AH_6 (equation (5.4)). Plate 5.19 shows the micrograph following the third peak in dielectric constant, the long slender and the plate-like foils are associated with ettringite and monosulpho-aluminate. These crystals normally form as a result of the reaction of C_3AH_6 with sulphates, they are common in high porosity paste where ettringite formed precipitates in the pores of the material.

5.4 CONCLUDING COMMENTS

The main purpose has been to demonstrate that the electrical response characteristics of cement paste can be used to monitor cement hydration and reflect its physical characteristics. Hydration is the most difficult and complex aspect of cement chemistry and, despite considerable research, controversy remains as to the exact nature of cement hydration.

The observation of the electrical response of cement paste shows the effectiveness of using this method as a means of monitoring hydration. The results are consistent and the time of occurrence of various peaks reflects the changes in chemical composition, water-cement ratio, presence of admixtures, and the age of cement within the matrix. Furthermore, the correlation of results obtained from Scanning Electron Microscopy (SEM) with the electrical response curves and their agreement with previous SEM work done by other researchers[77,143-147] shows that the electrical response characteristics could be developed to monitor micro-structural building processes and morphological changes within hydrating cement paste.

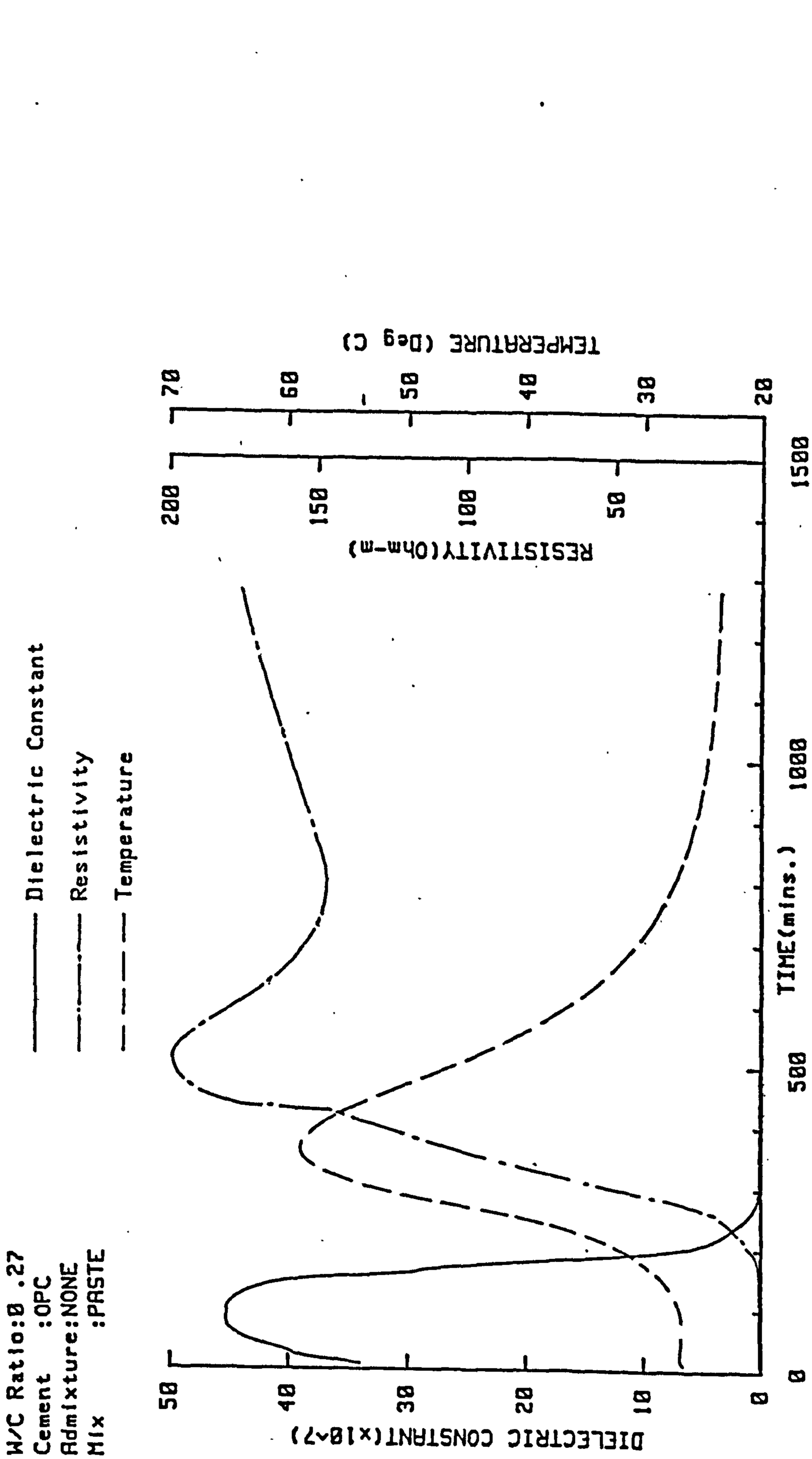

FIGURE 5.1 VARIATION OF MEASURED PARAMETERS DURING INITIAL 24 HOURS GAUGING FOR THE FREQUENCY RANGE 20 HZ - 300 KHZ

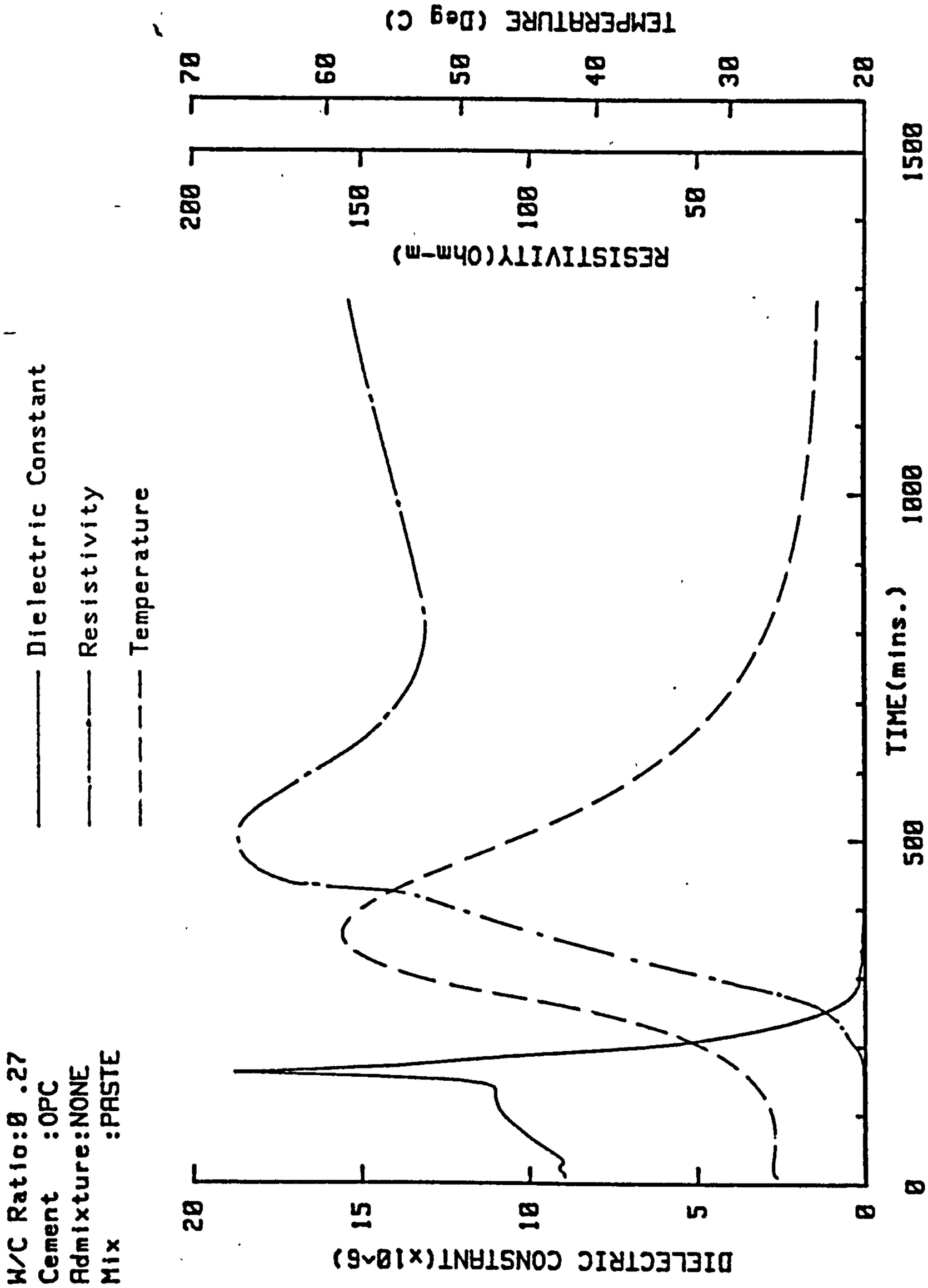

FIGURE 5.1 (CONTINUED)

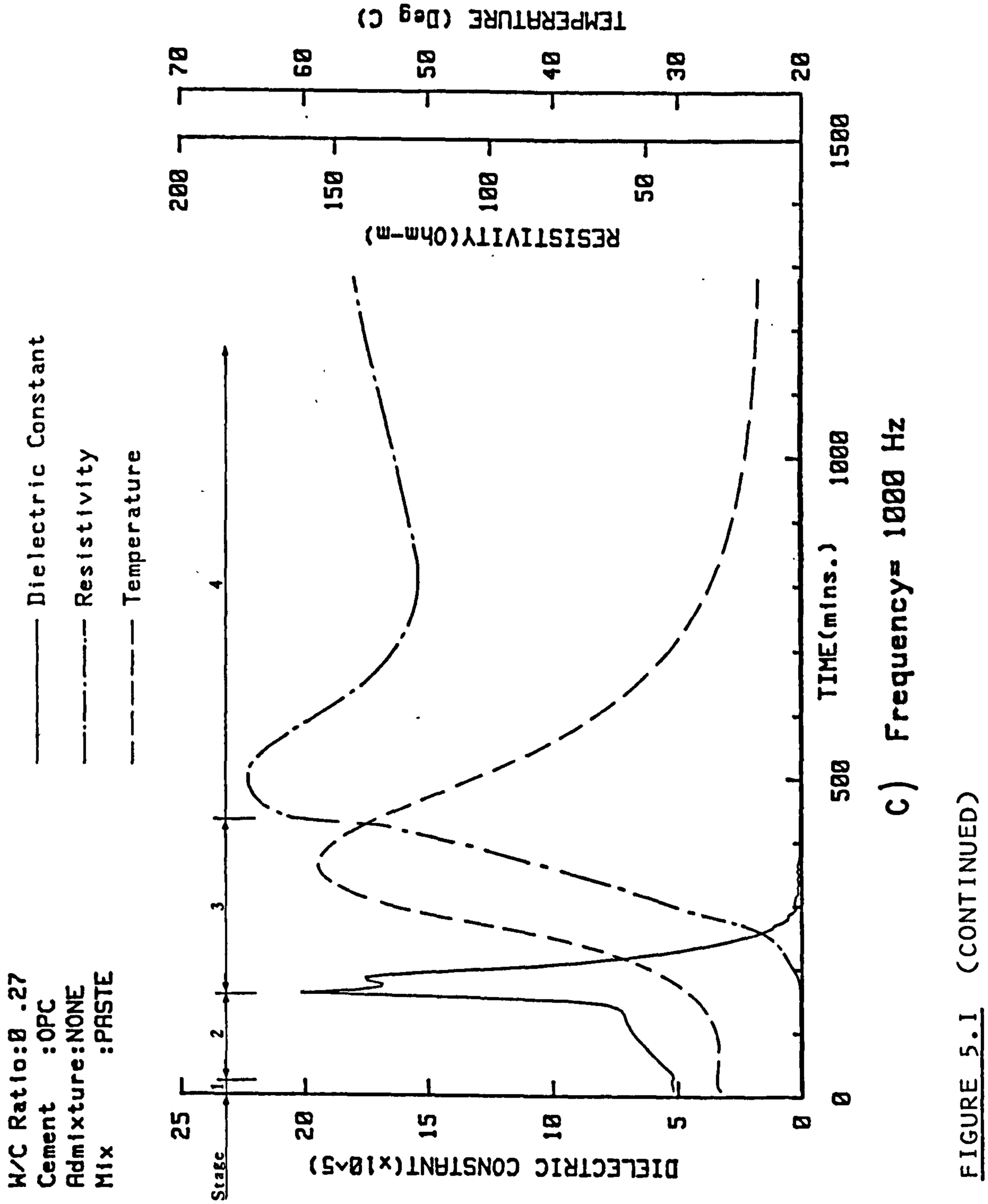

FIGURE 5.1 (CONTINUED)

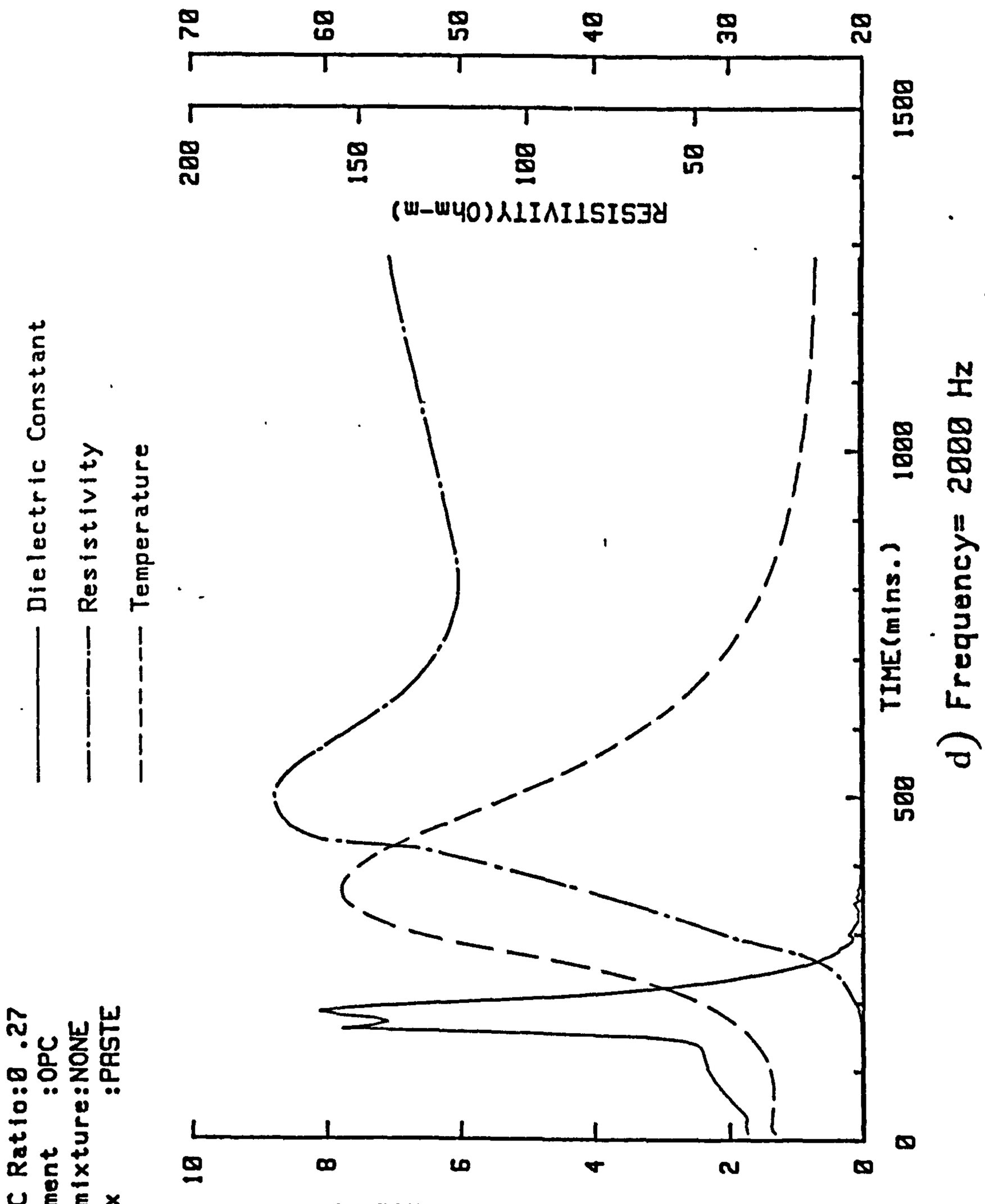

FIGURE 5.1 (CONTINUED)

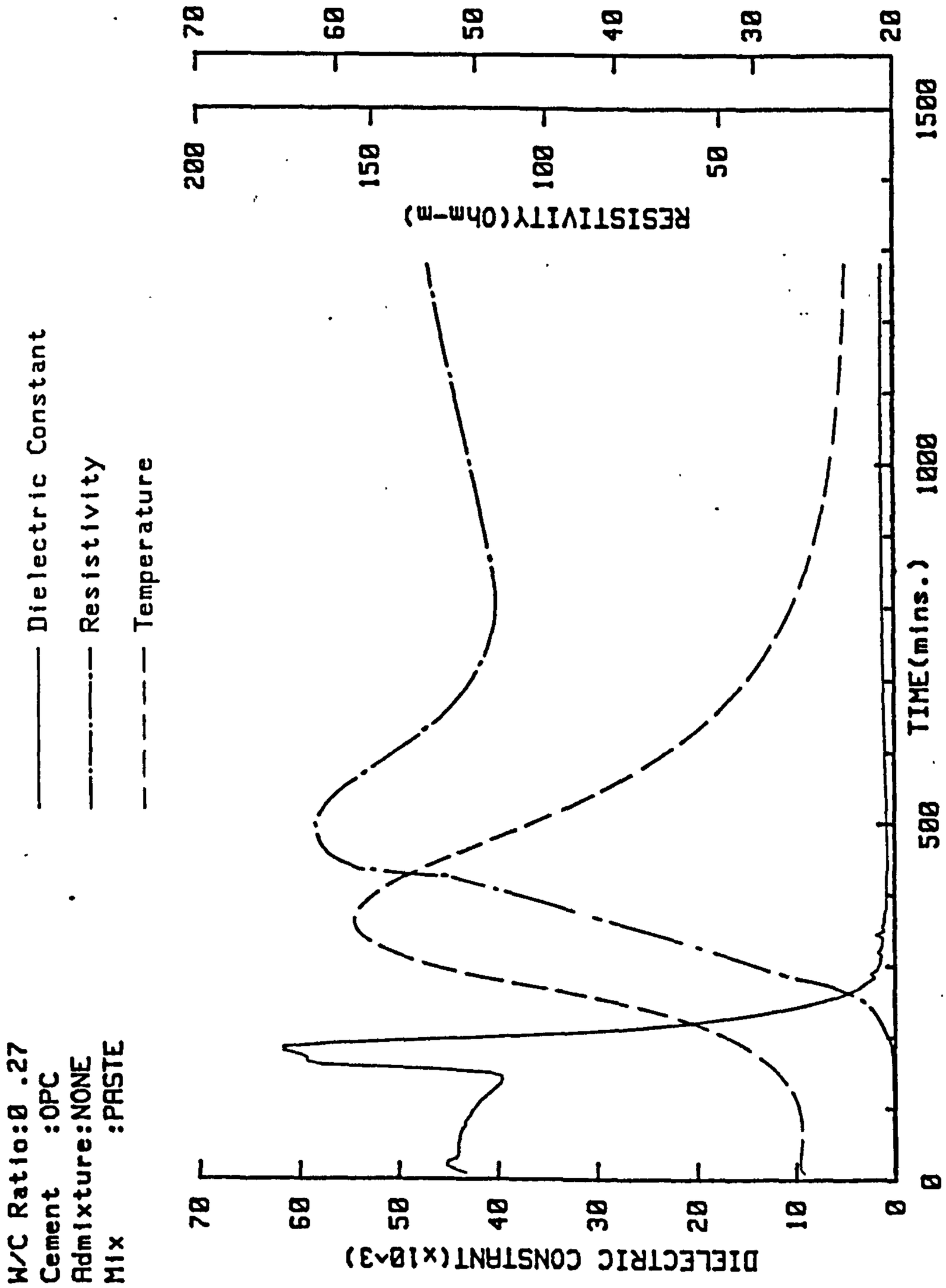

FIGURE 5.I (CONTINUED)

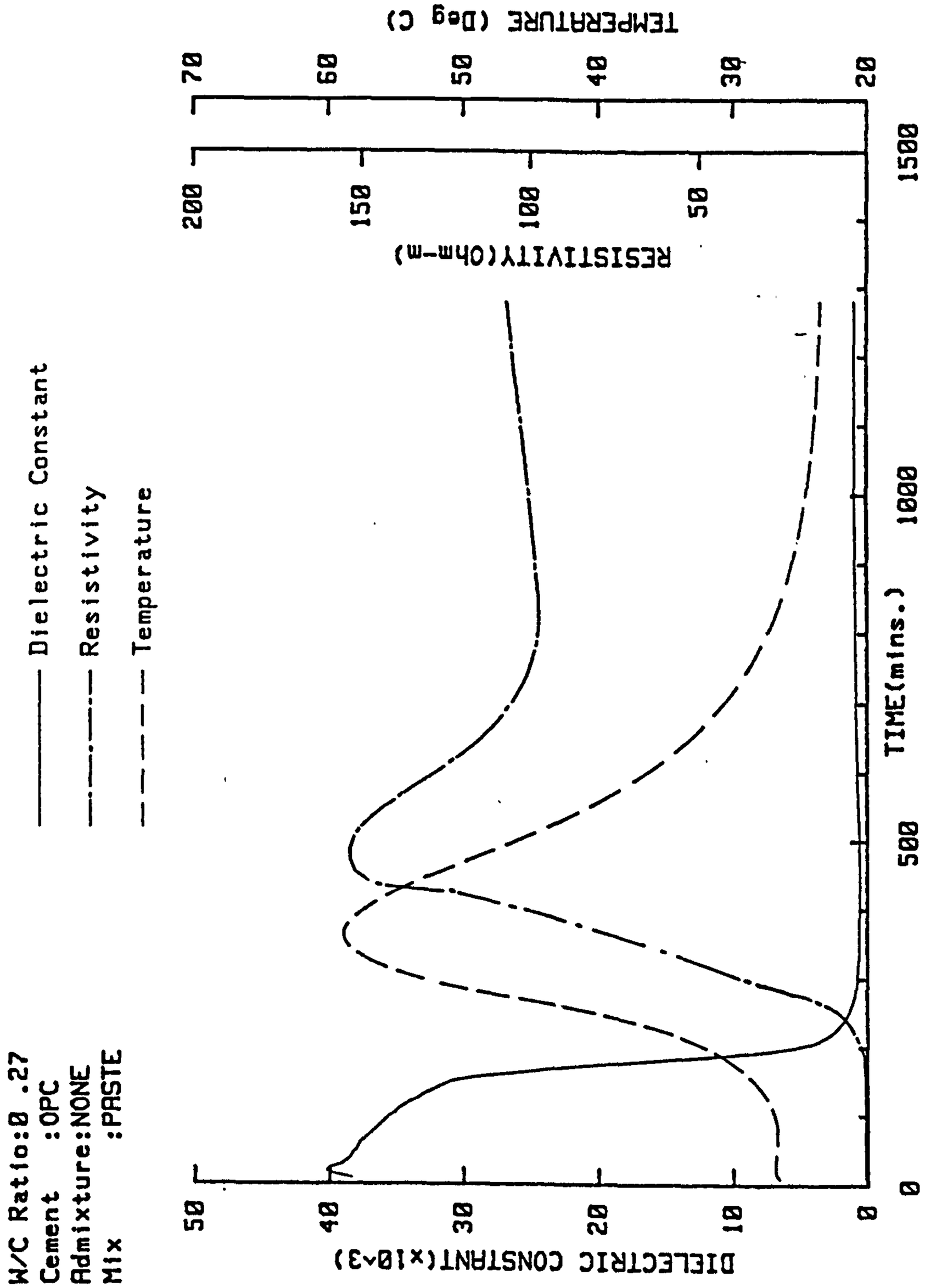

FIGURE 5.I (CONTINUED)

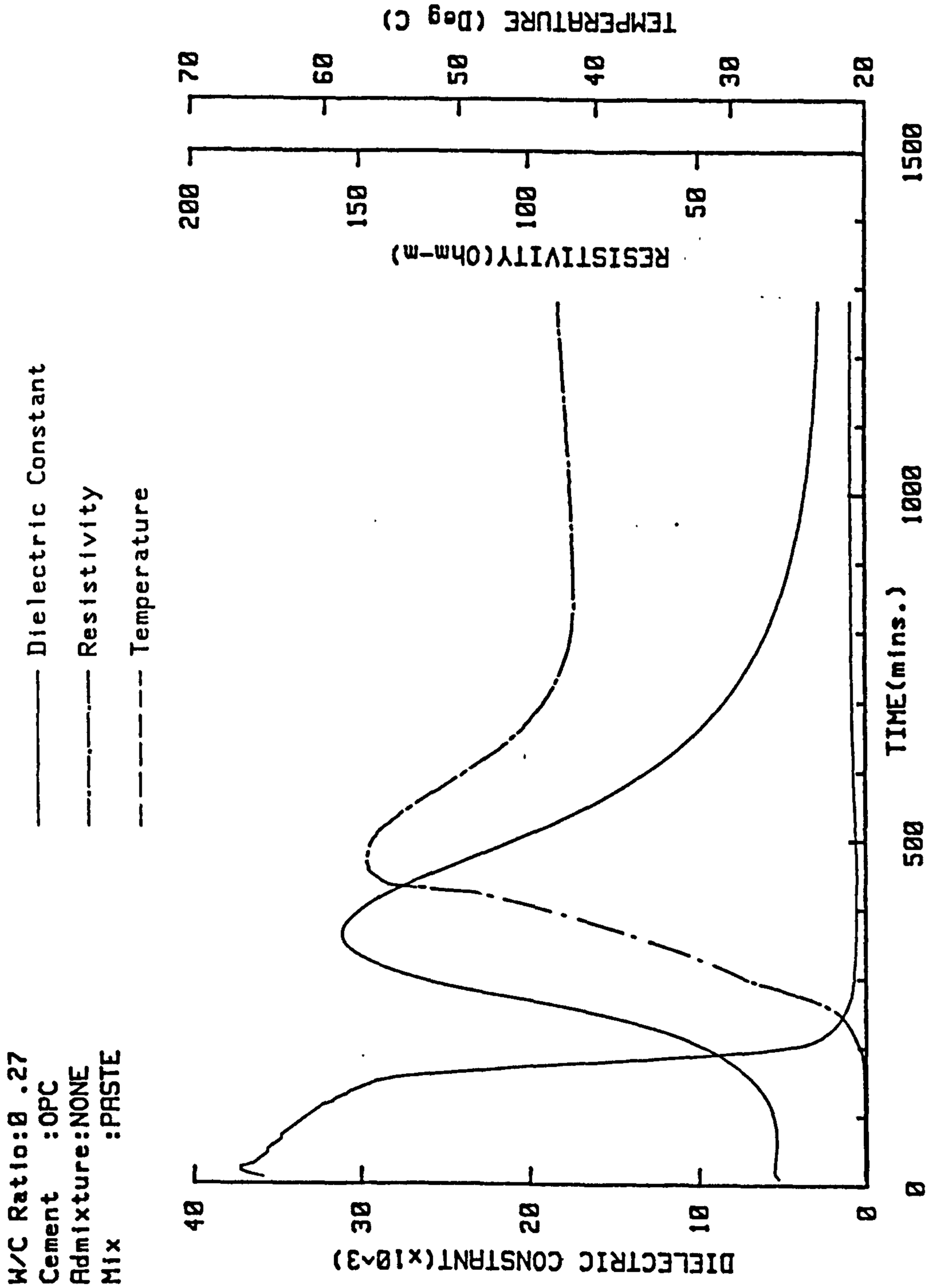

FIGURE 5.I (CONTINUED)

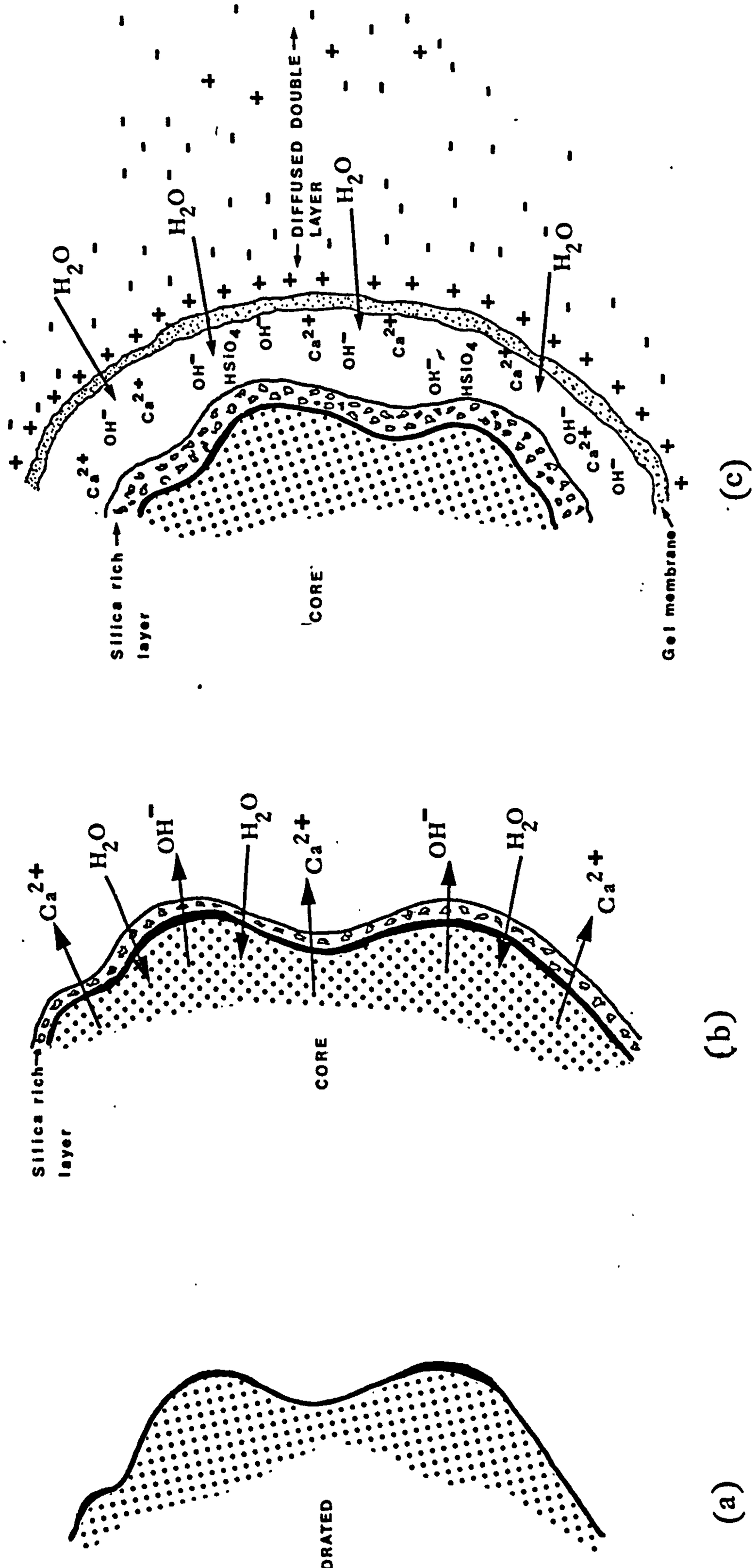

FIGURE 5.2 CEMENT GRAIN ON GAUGING

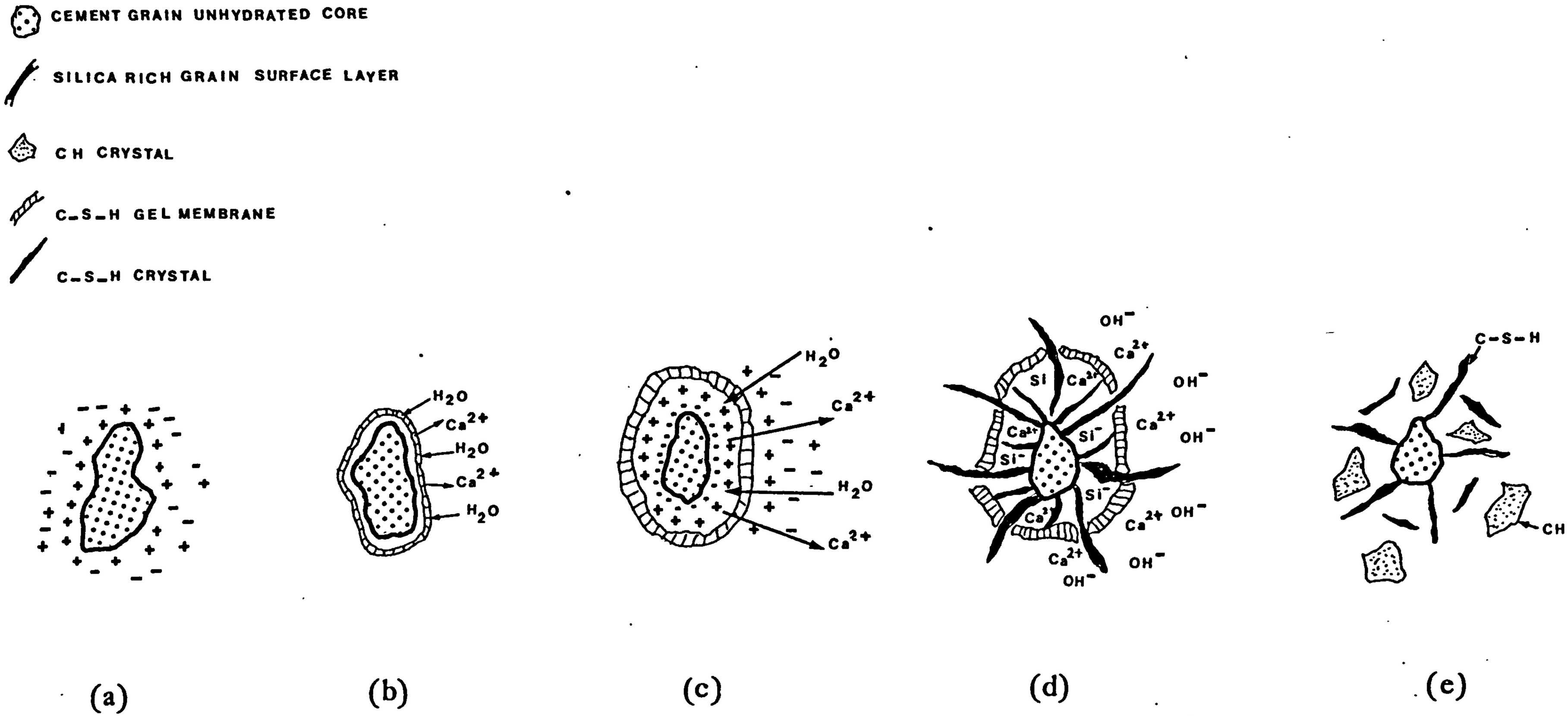

FIGURE 5.3 SUGGESTED MECHANISM OF CEMENT HYDRATION

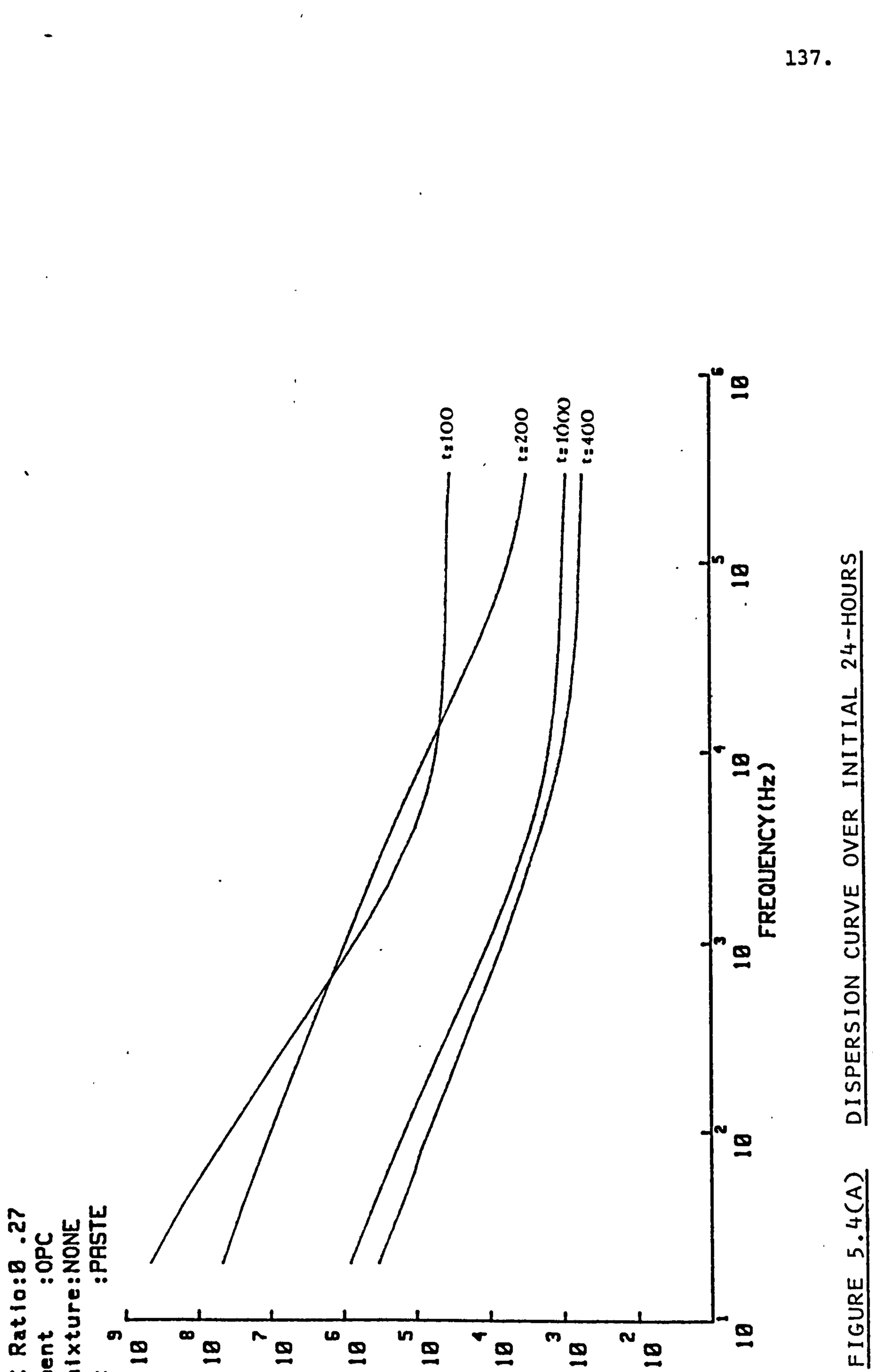

FIGURE 5.4(A) DISPERSION CURVE OVER INITIAL 24-HOURS

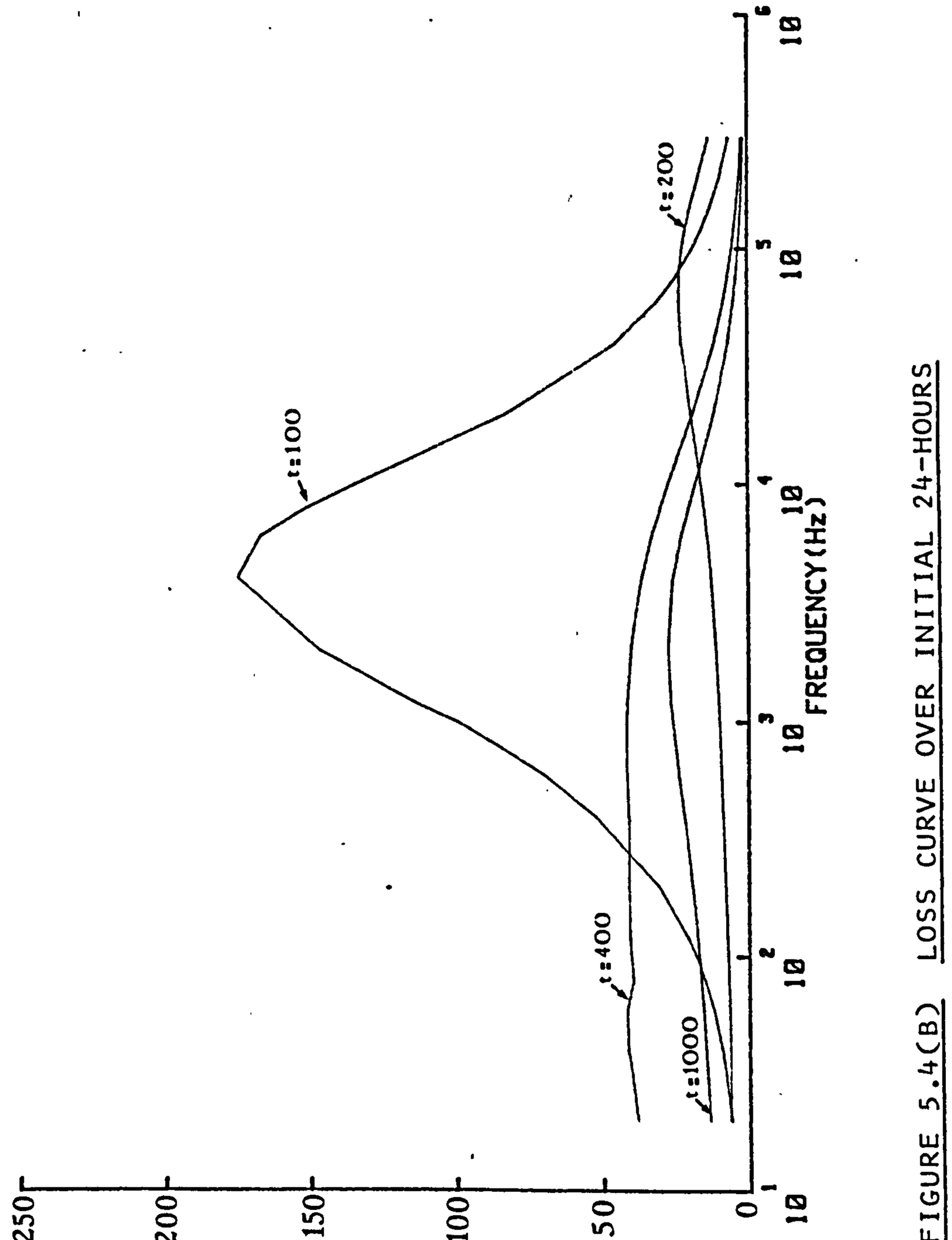

FIGURE 5.4(B) LOSS CURVE OVER INITIAL 24-HOURS

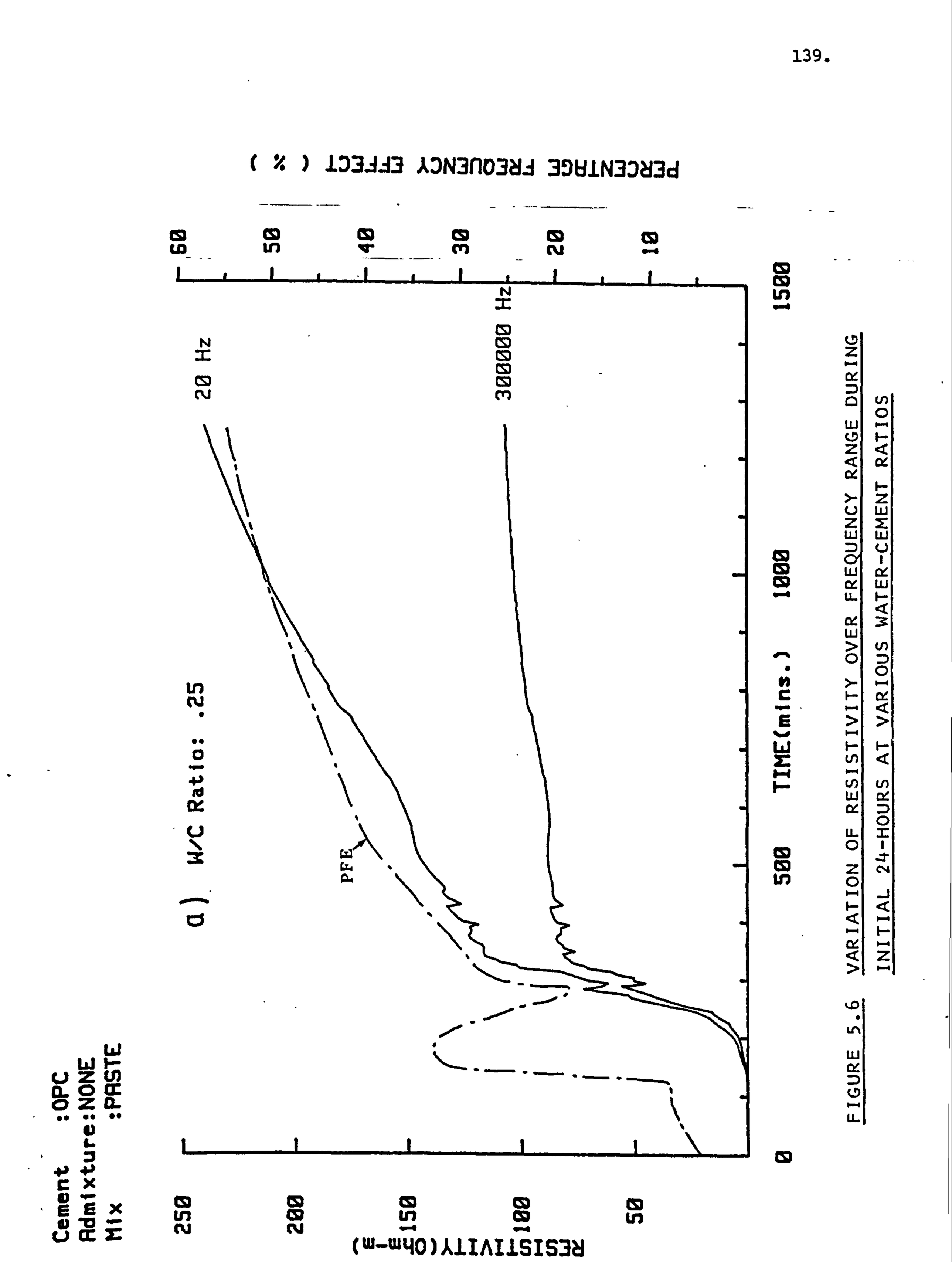

FIGURE 5.6 VARIATION OF RESISTIVITY OVER FREQUENCY RANGE DURING INITIAL 24-HOURS AT VARIOUS WATER-CEMENT RATIOS

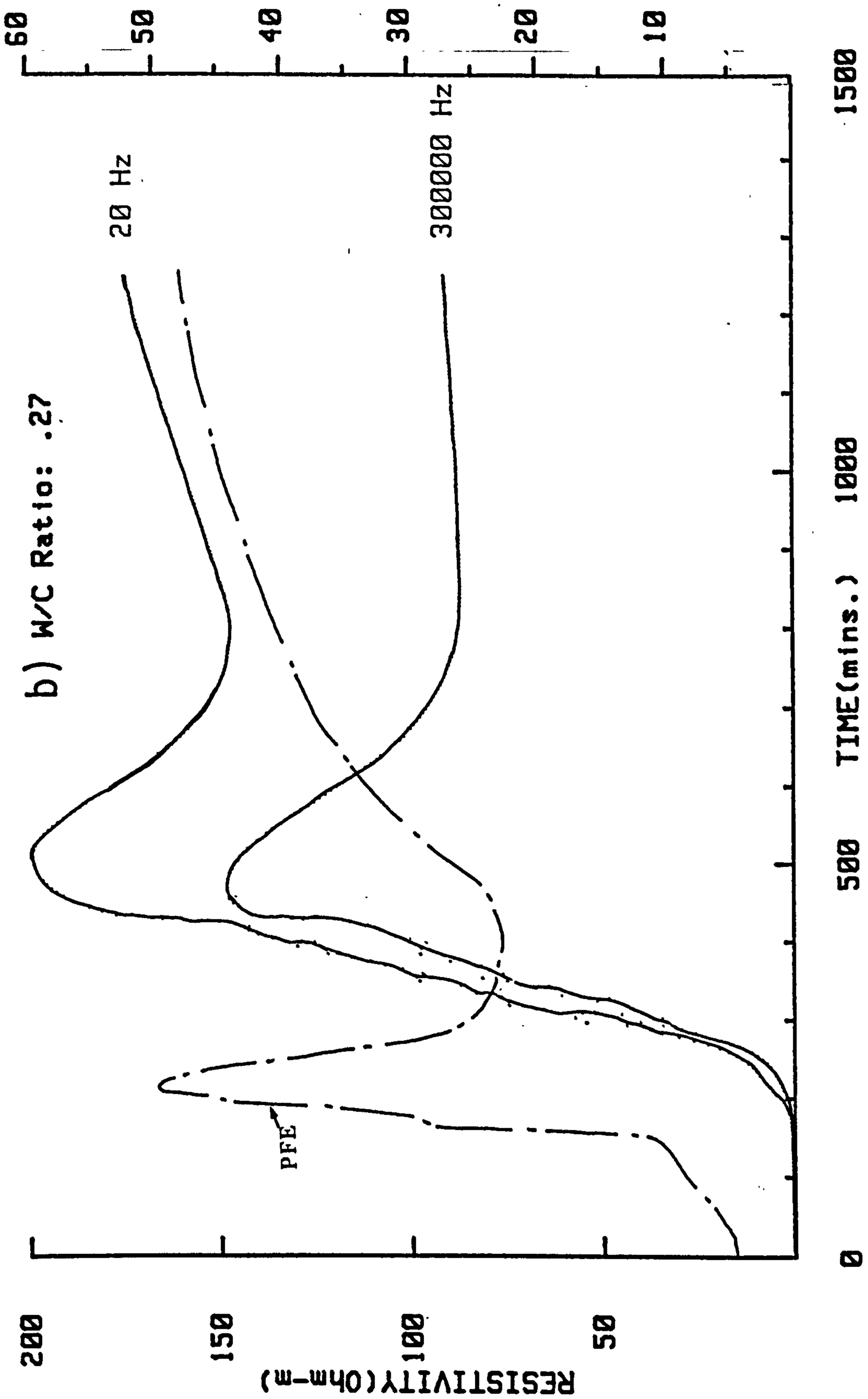

FIGURE 5.6 (CONTINUED)

Cement :OPC
Admixture:NONE
Mix :PASTE

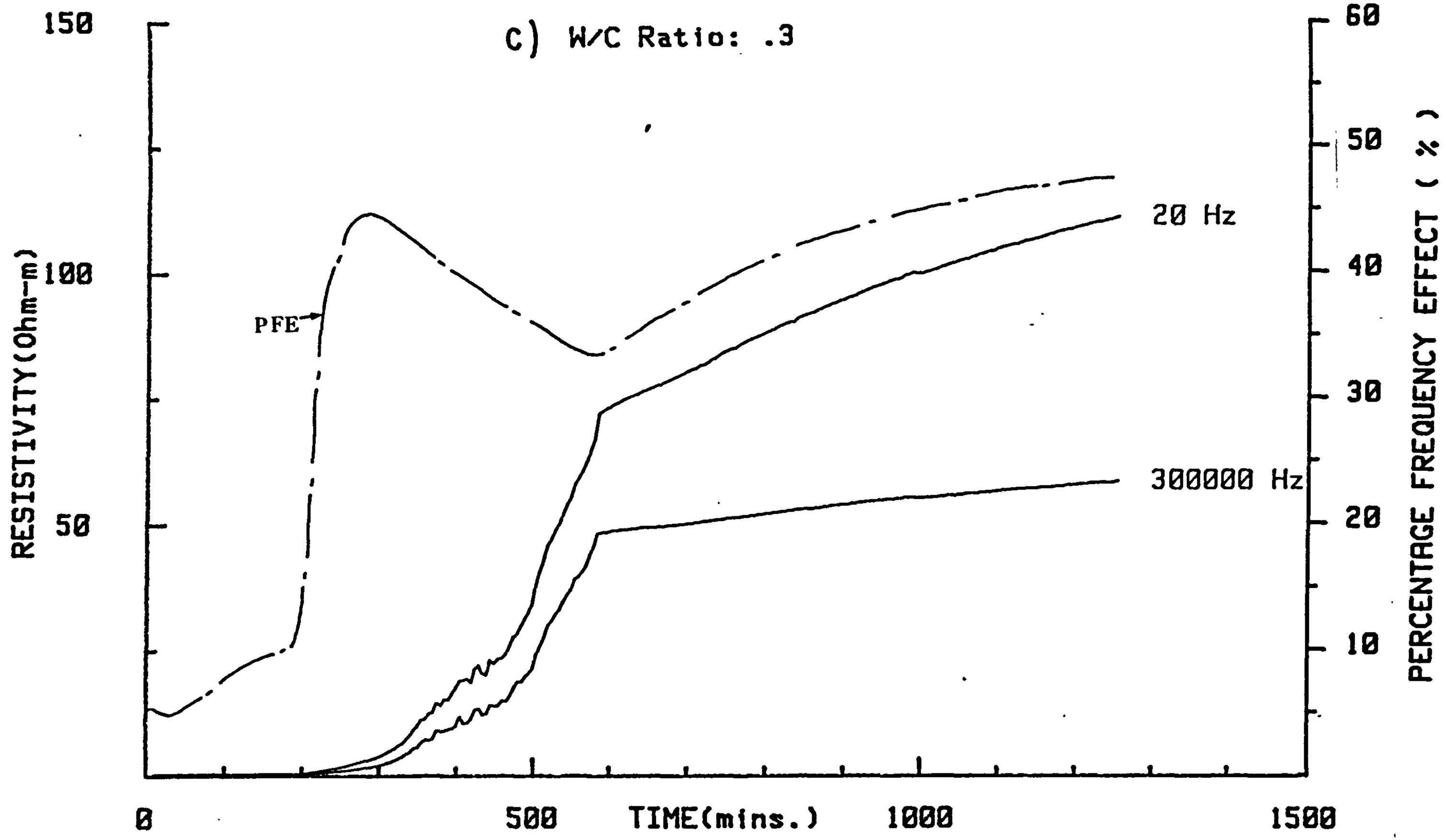

FIGURE 5.6 (CONTINUED)

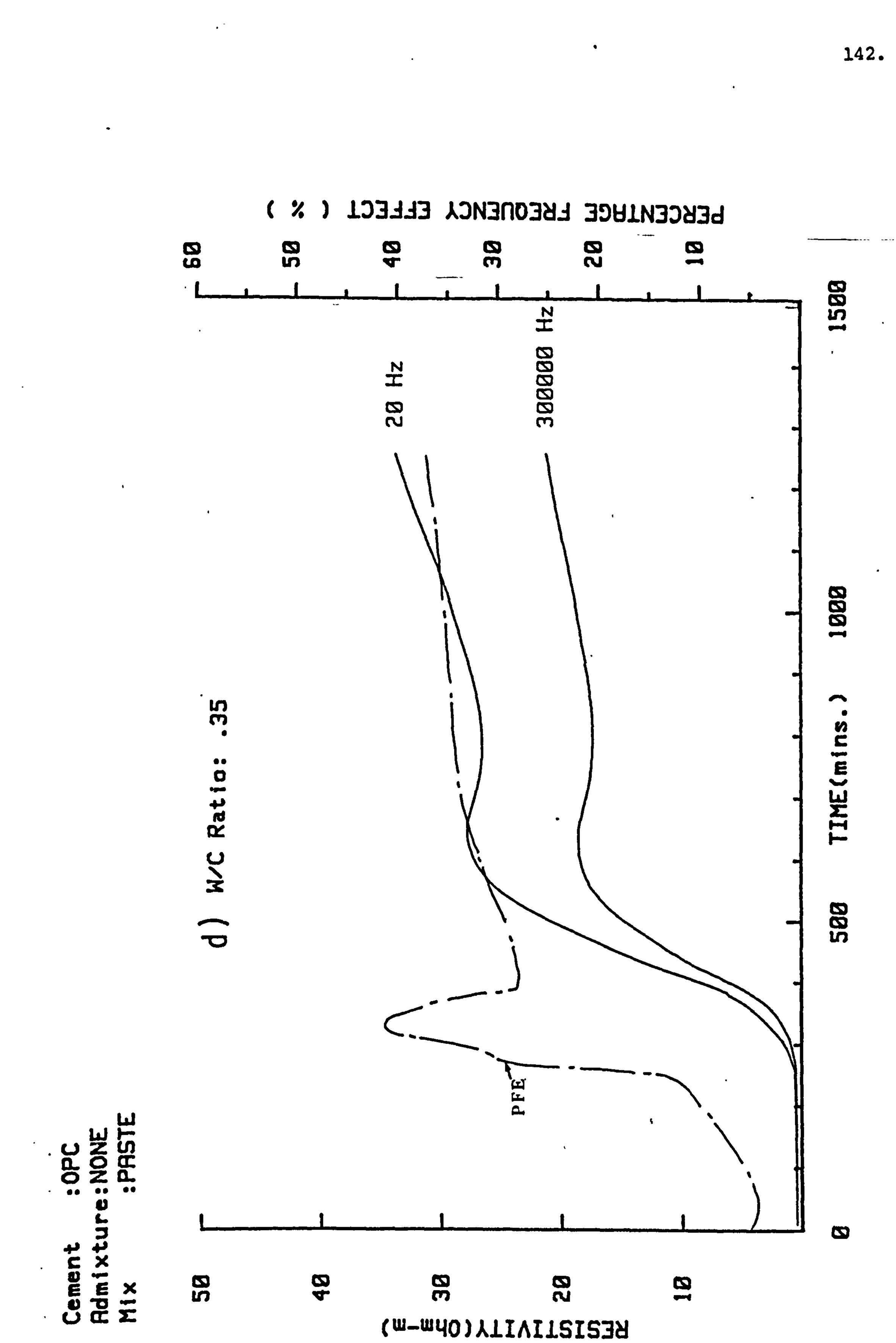

(CONTINUED)

FIGURE 5.6

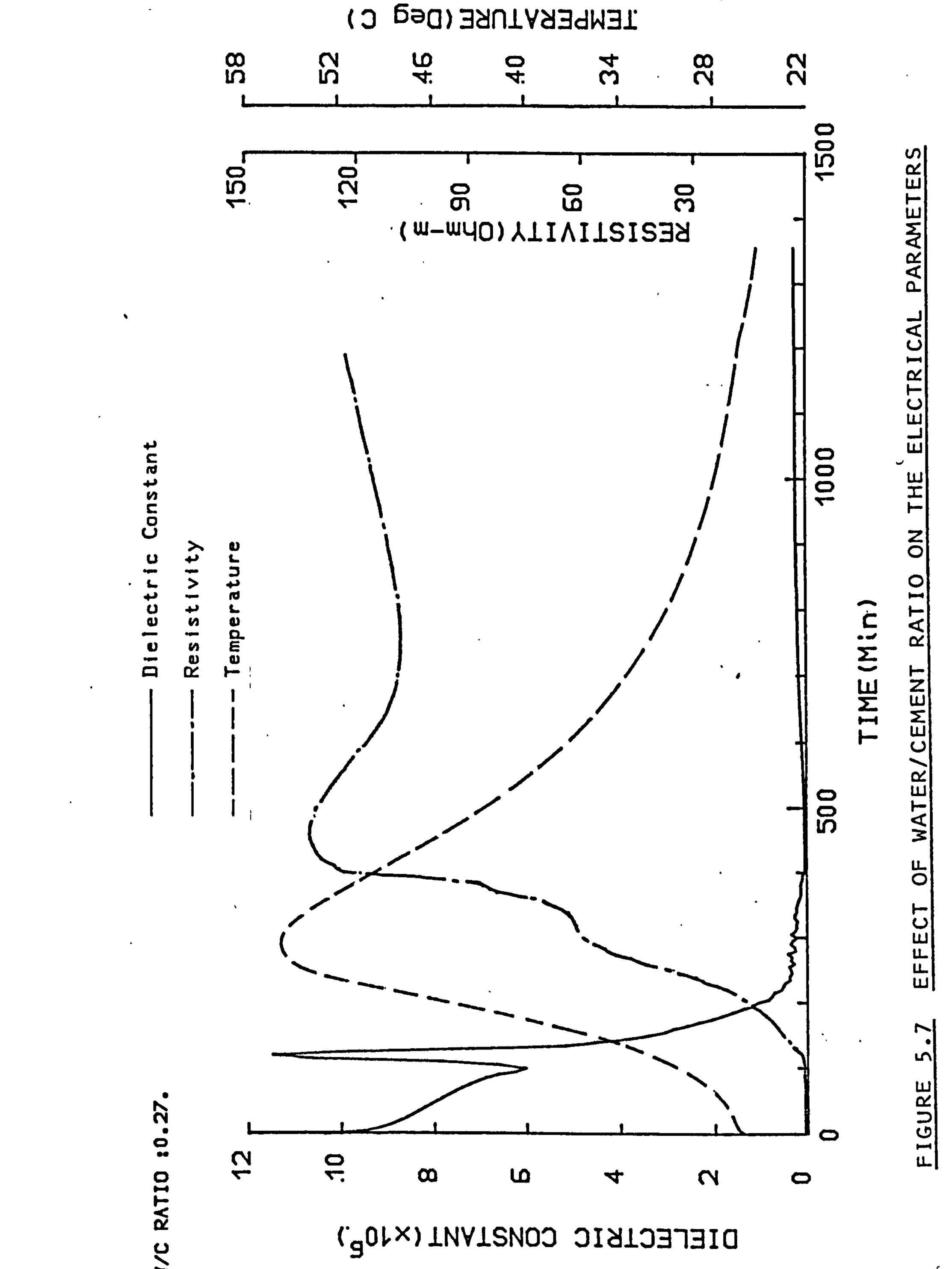
EFFECT OF WATER/CEMENT RATIO ON THE ELECTRICAL PARAMETERS
TIME(Min)
0
500
1000
1500
DIELECTRIC CONSTANT (x10⁵)
0
2
4
6
8
10
12
RESISTIVITY (Ohm-m)
30
60
90
120
150
TEMPERATURE (Deg C)
22
28
34
40
46
52
58
Dielectric Constant
Resistivity
Temperature
a) W/C RATIO :0.27.

FIGURE 5.7

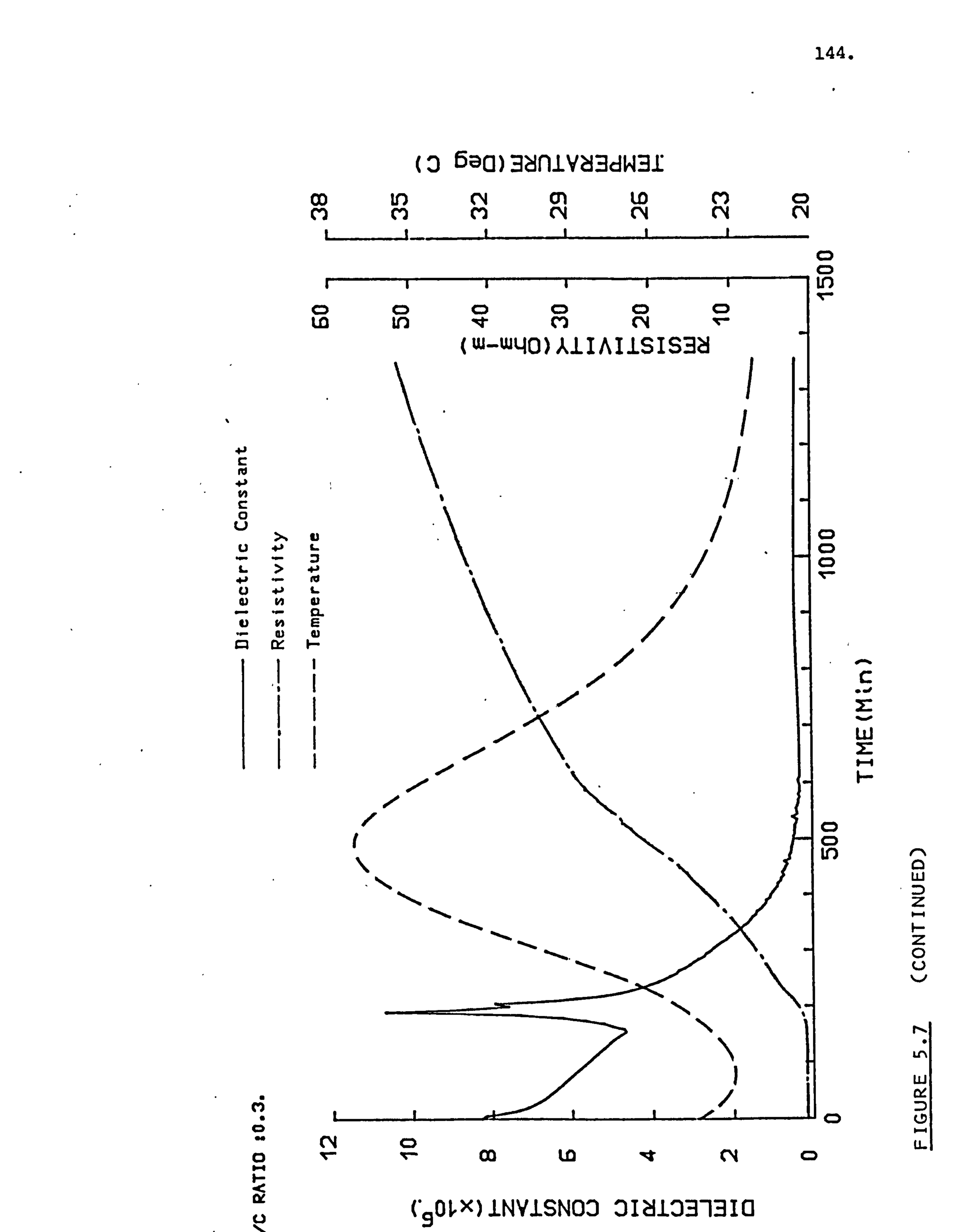

FIGURE 5.7 (CONTINUED)

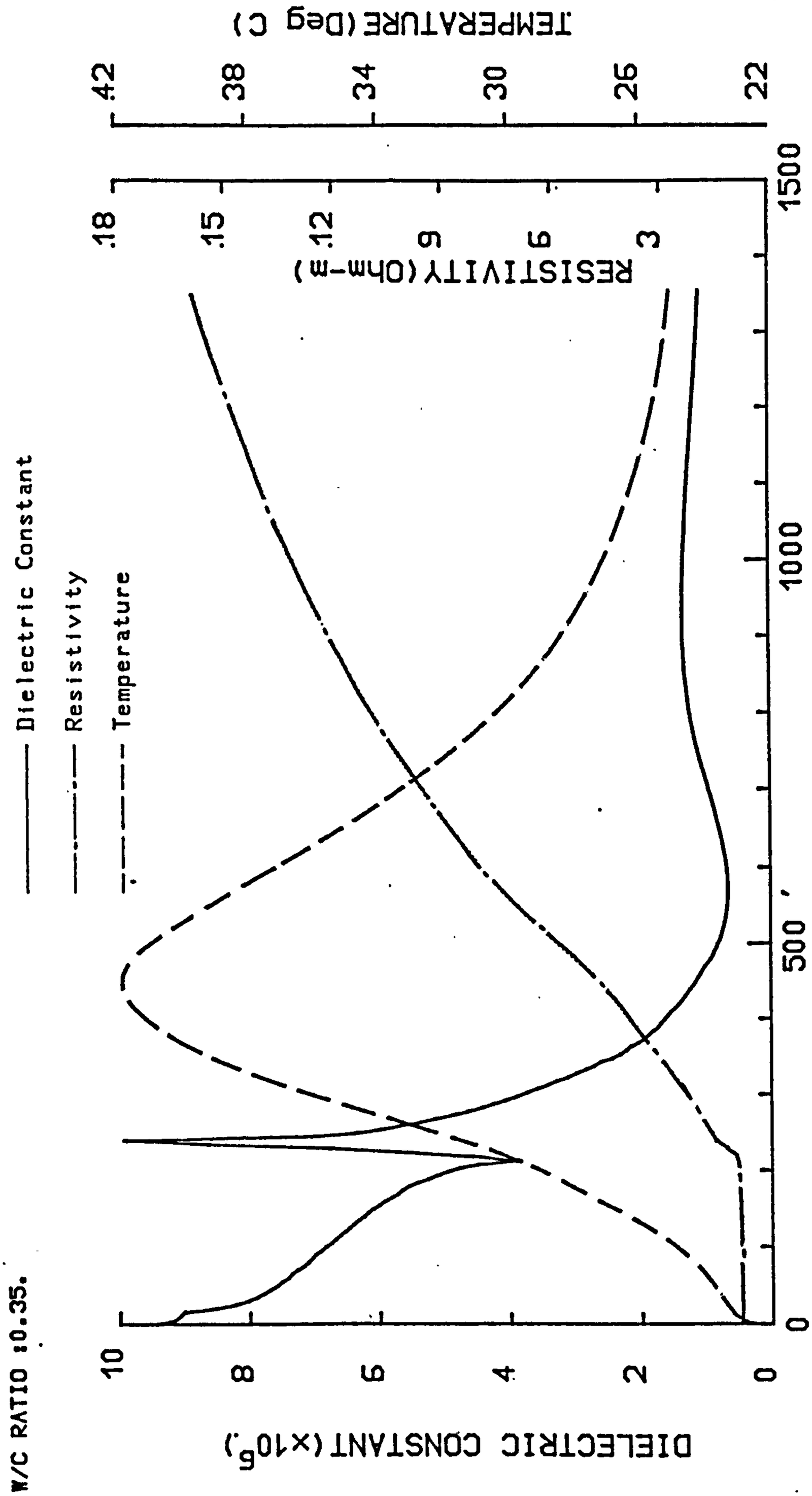

C) W/C RATIO :0.35.

FIGURE 5.7 (CONTINUED)

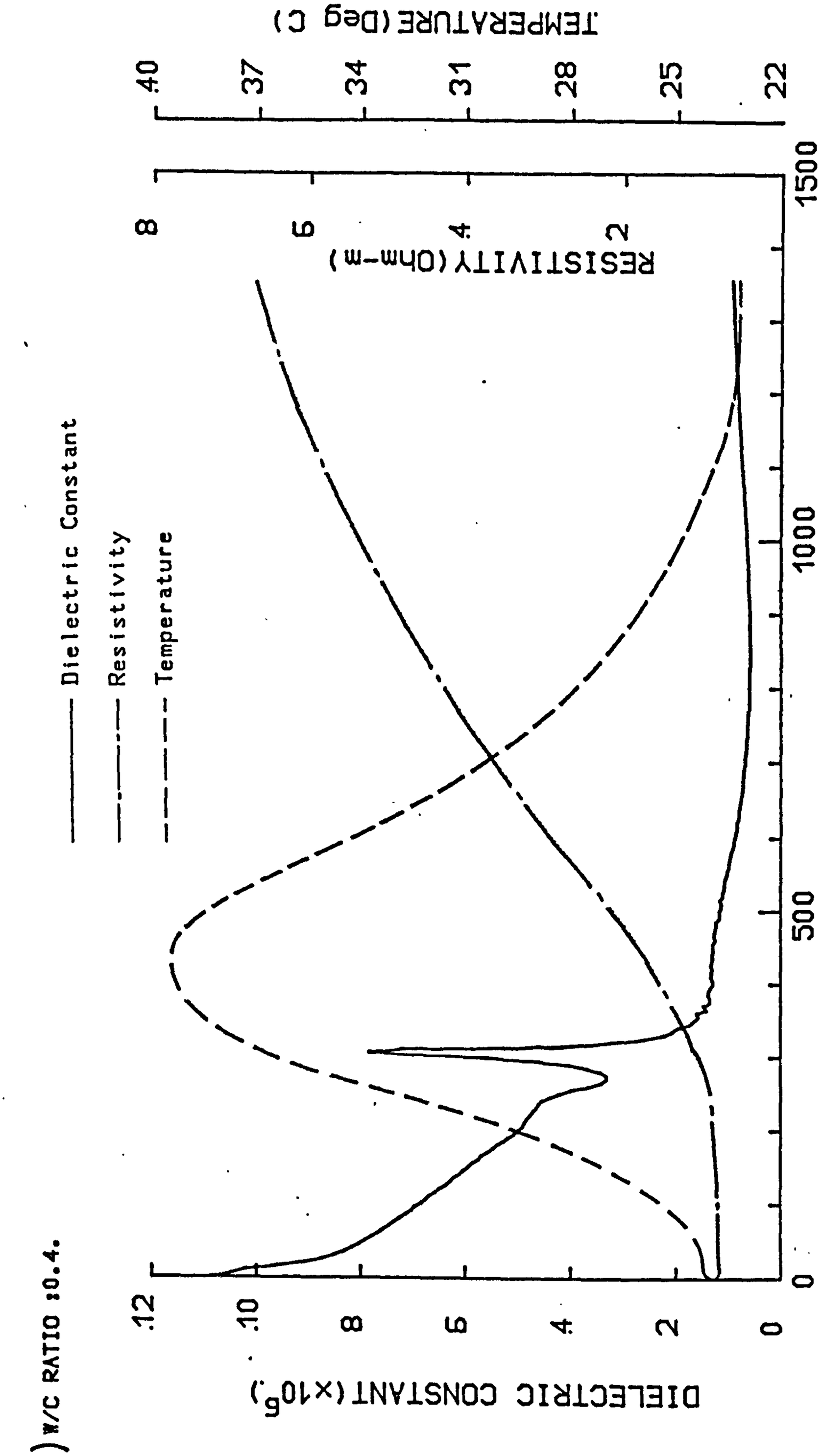

(CONTINUED)

FIGURE 5.7

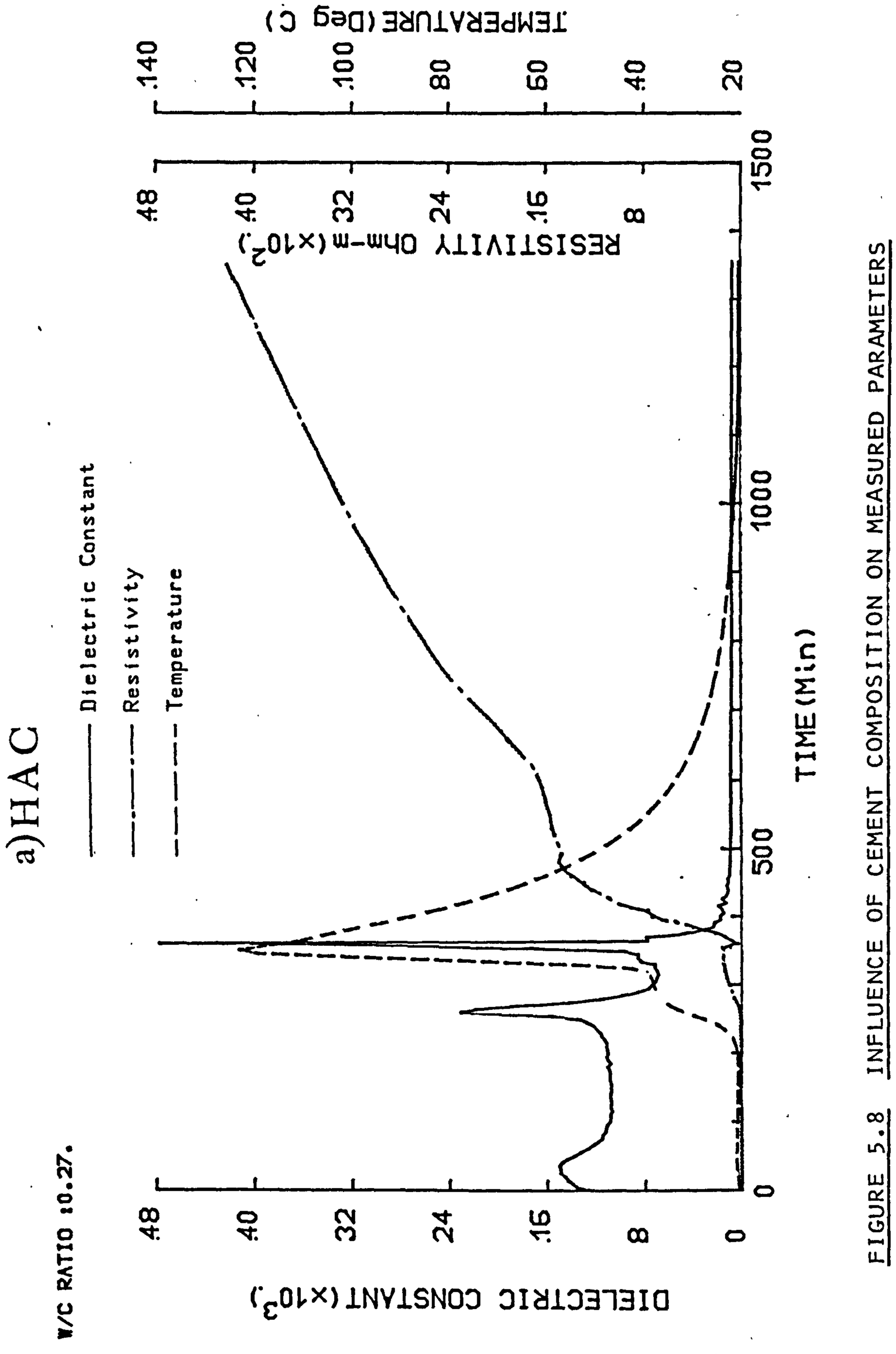

FIGURE 5.8 INFLUENCE OF CEMENT COMPOSITION ON MEASURED PARAMETERS

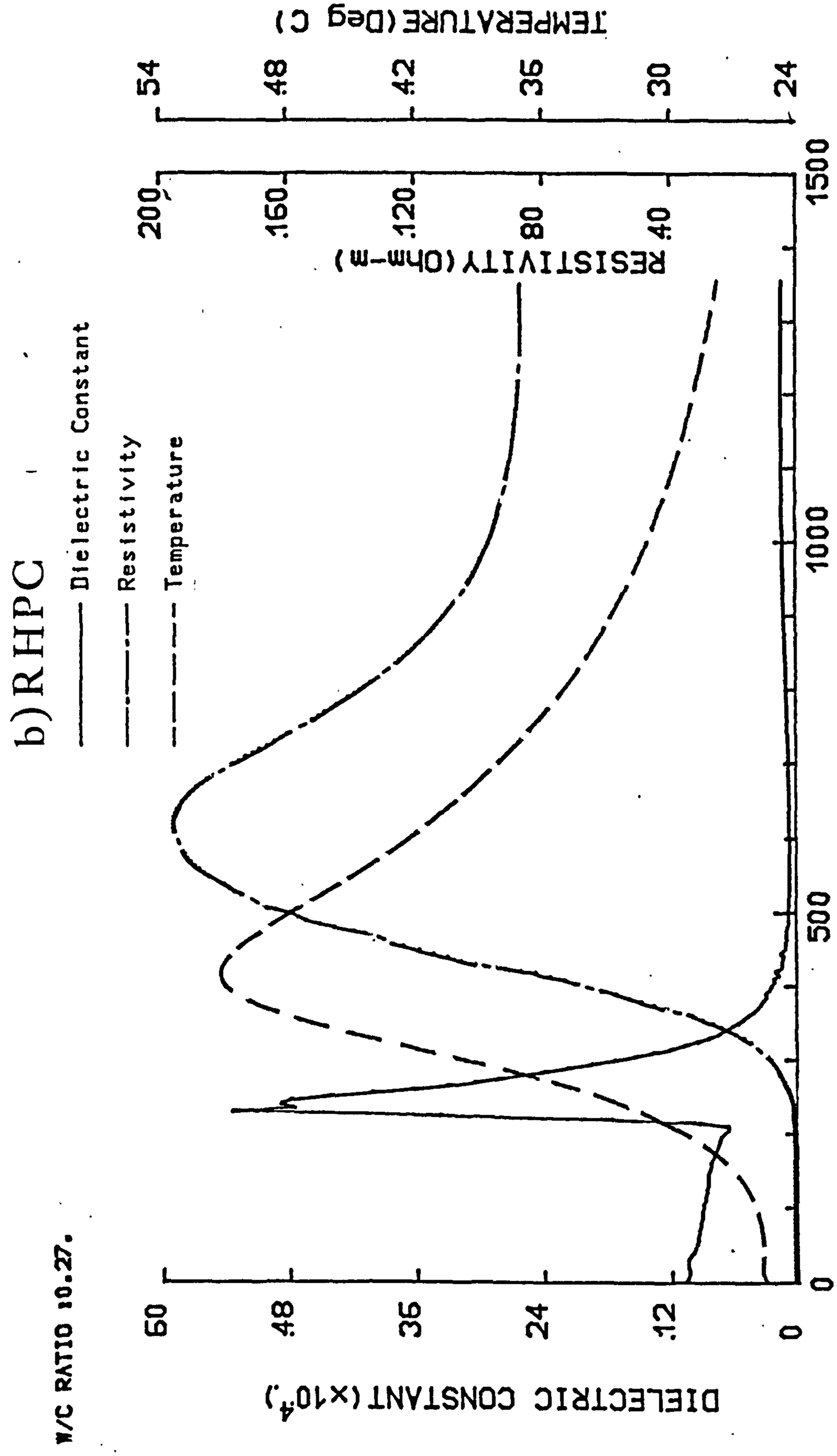

(CONTINUED)

FIGURE 5.8

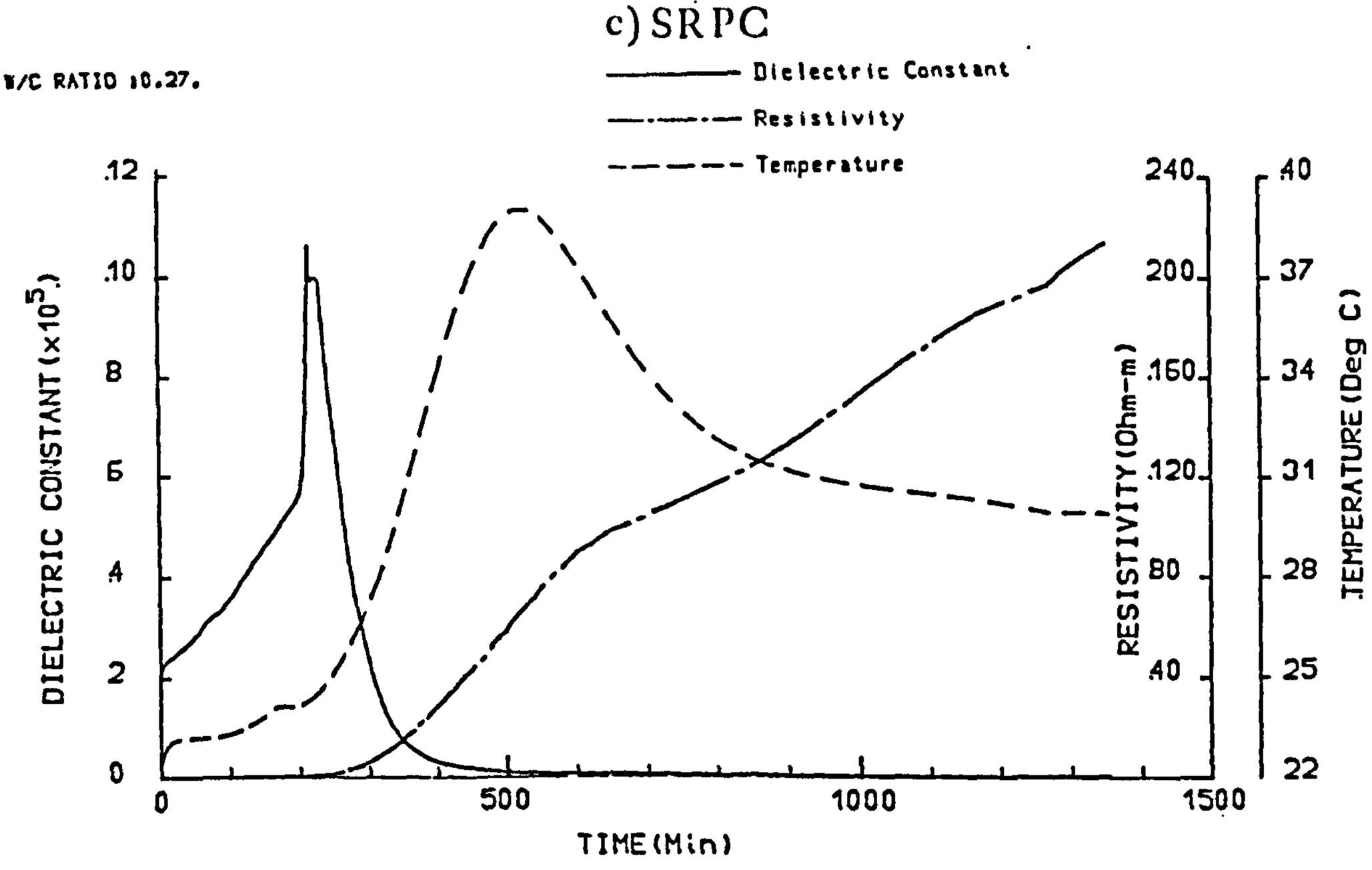

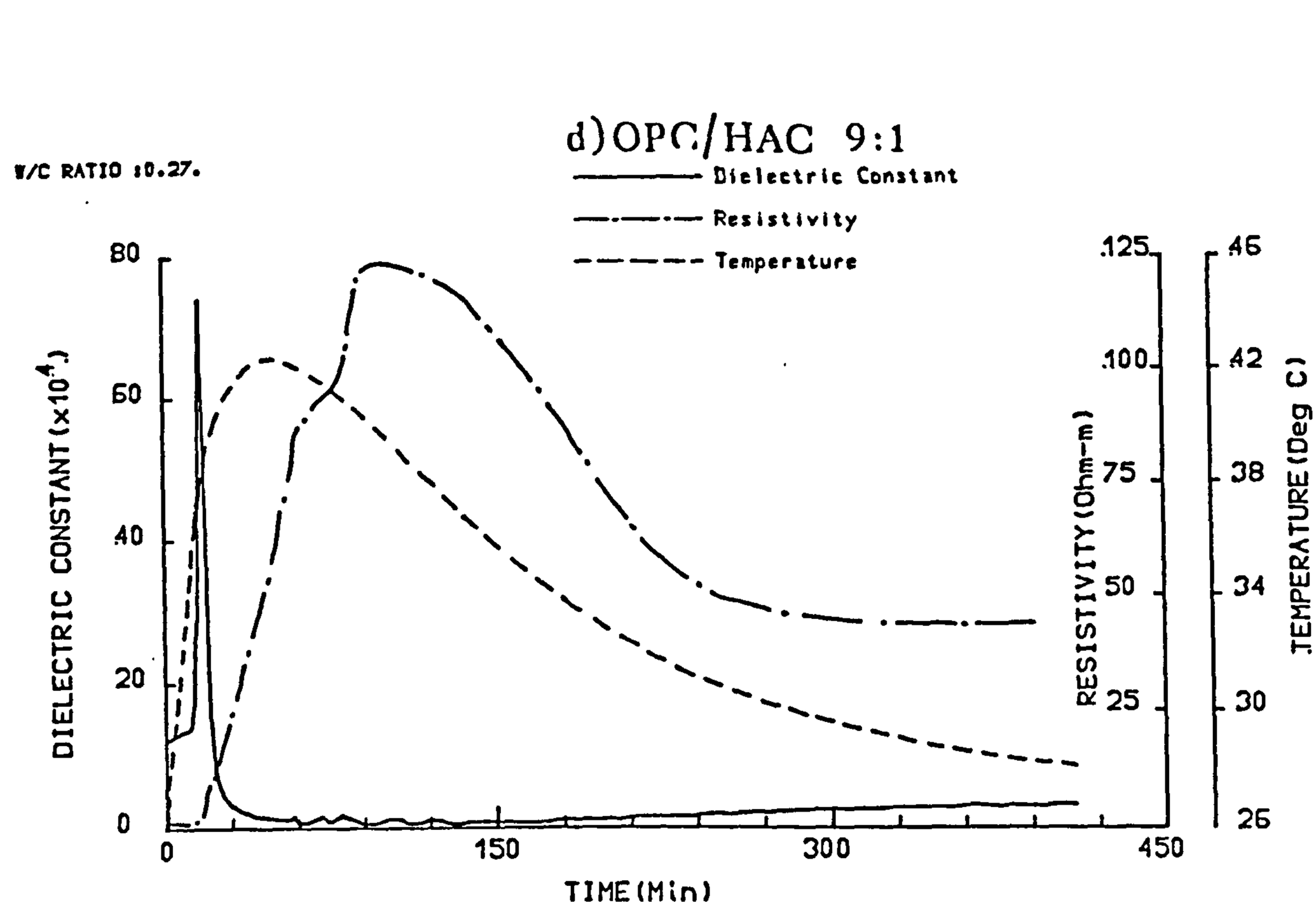

FIGURE 5.8 (CONTINUED)

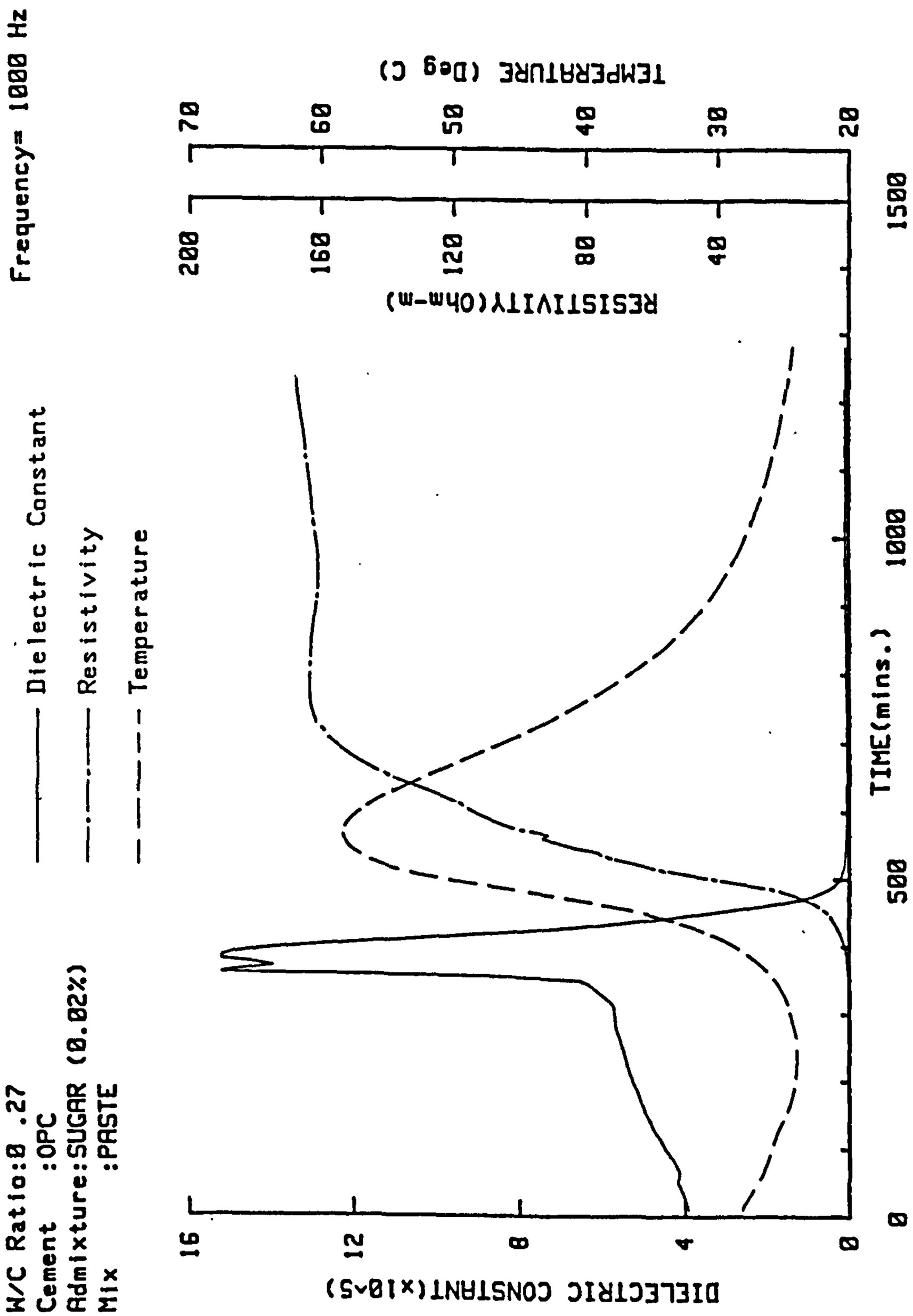

a) Admixture:SUGAR (0.02%)

FIGURE 5.9 THE EFFECT OF RETARDER (SUGAR) ON MEASURED PARAMETERS

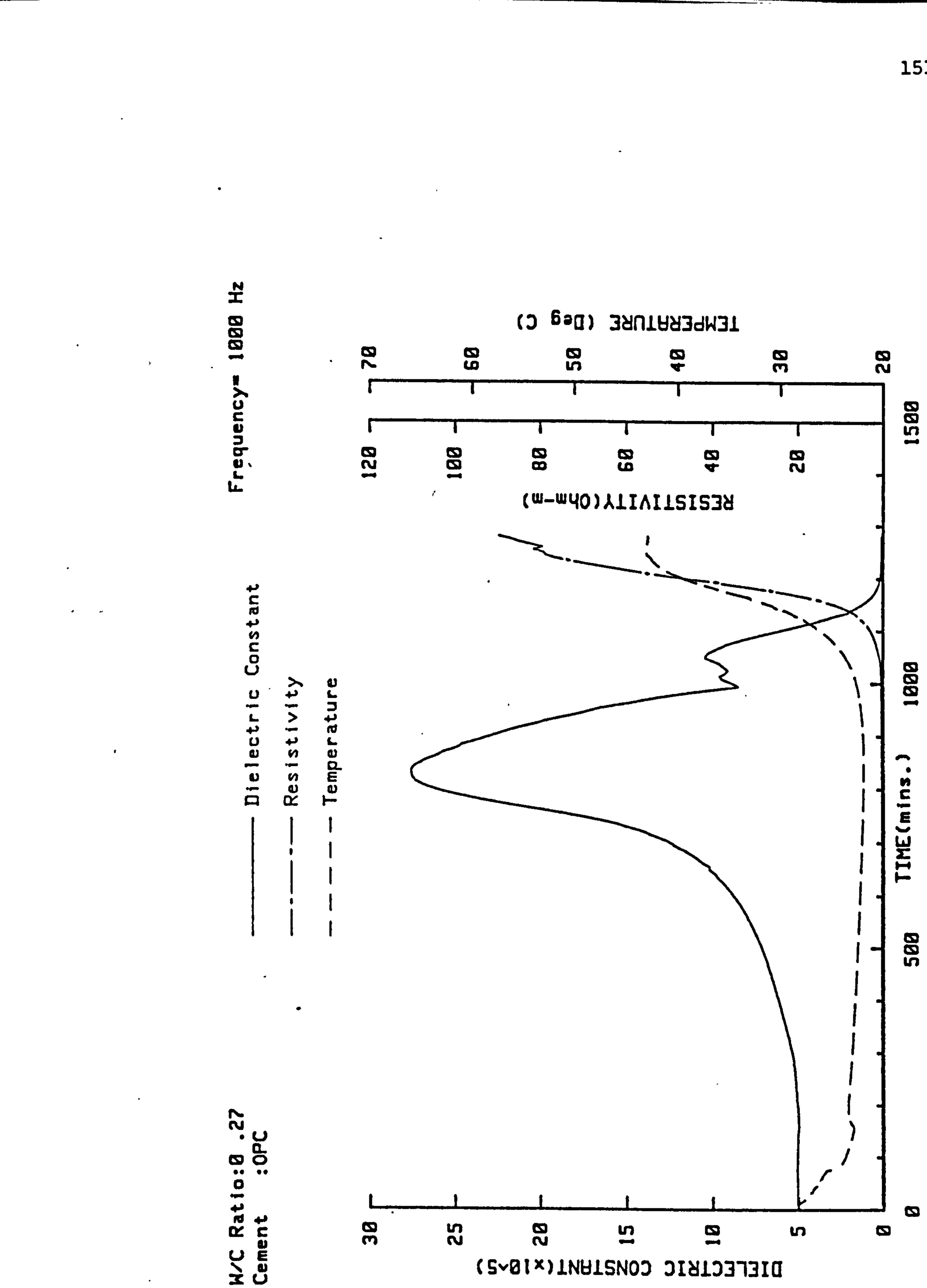

FIGURE 5.9 (CONTINUED)

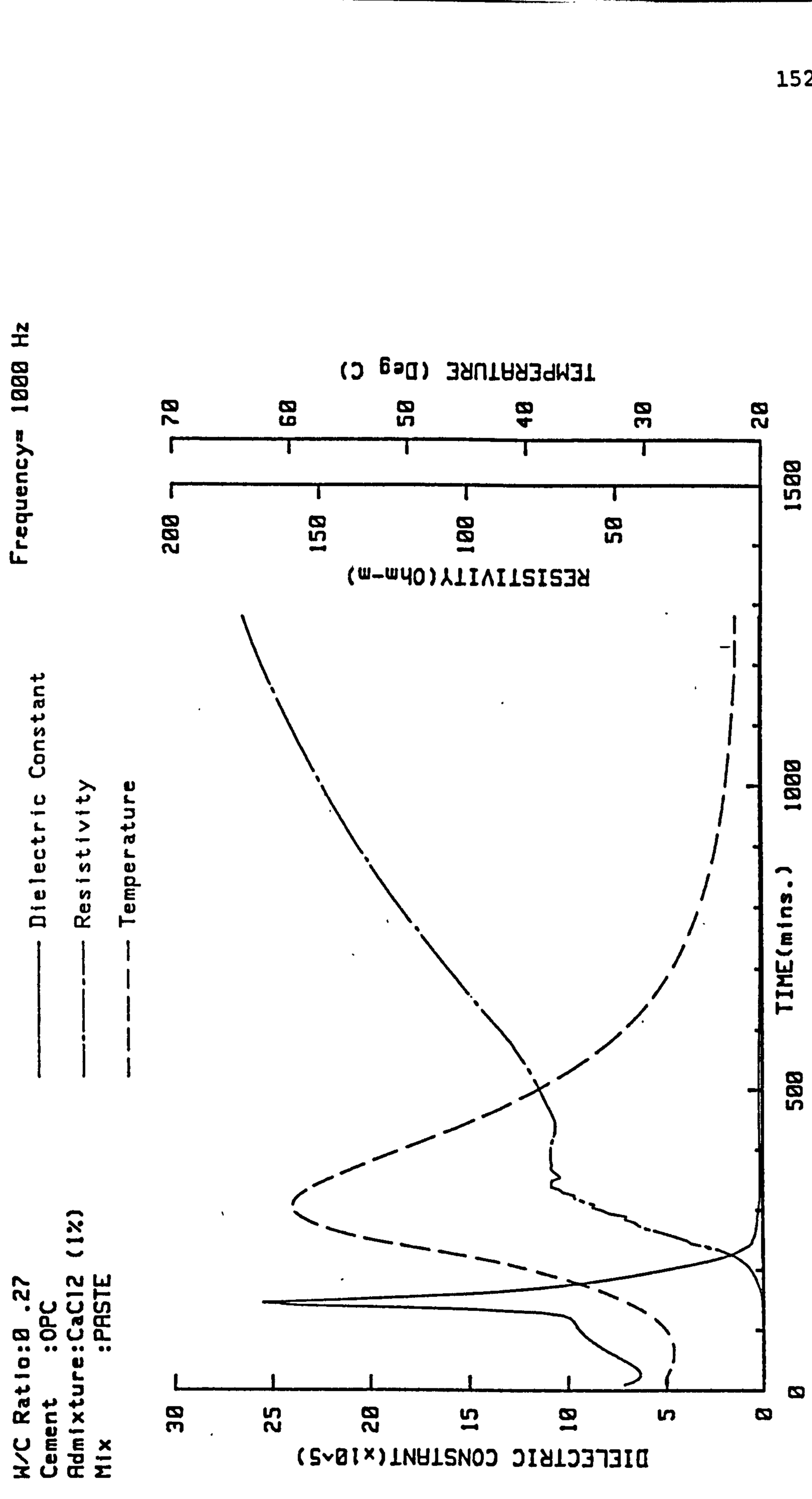

a) Admixture: CaCl2 (1%)

FIGURE 5.10 THE EFFECT OF ACCELERATOR (CALCIUM CHLORIDE) ON MEASURED PARAMETERS

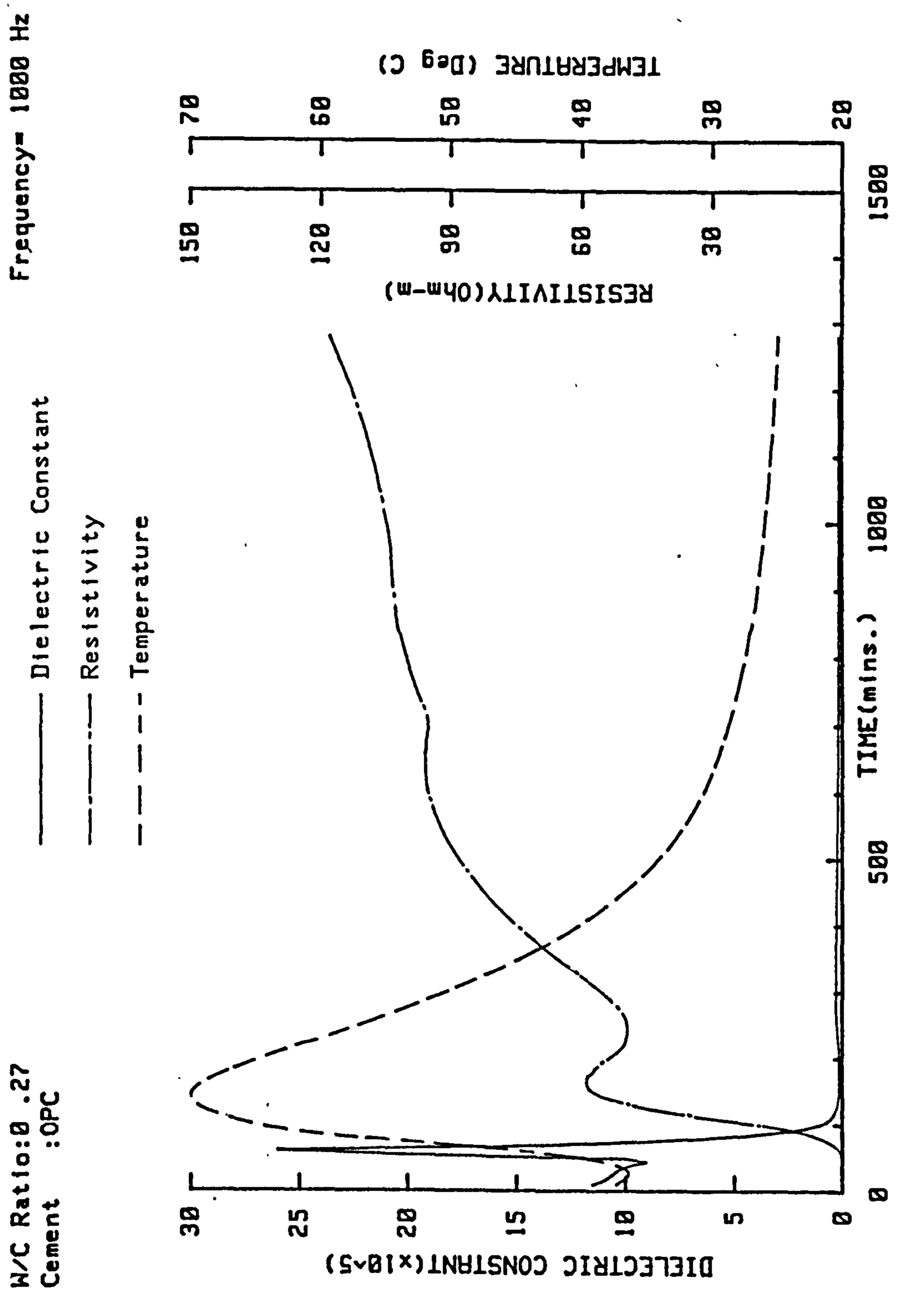

b) Admixture:CaCl2 (2%)

FIGURE 5.10 (CONTINUED)

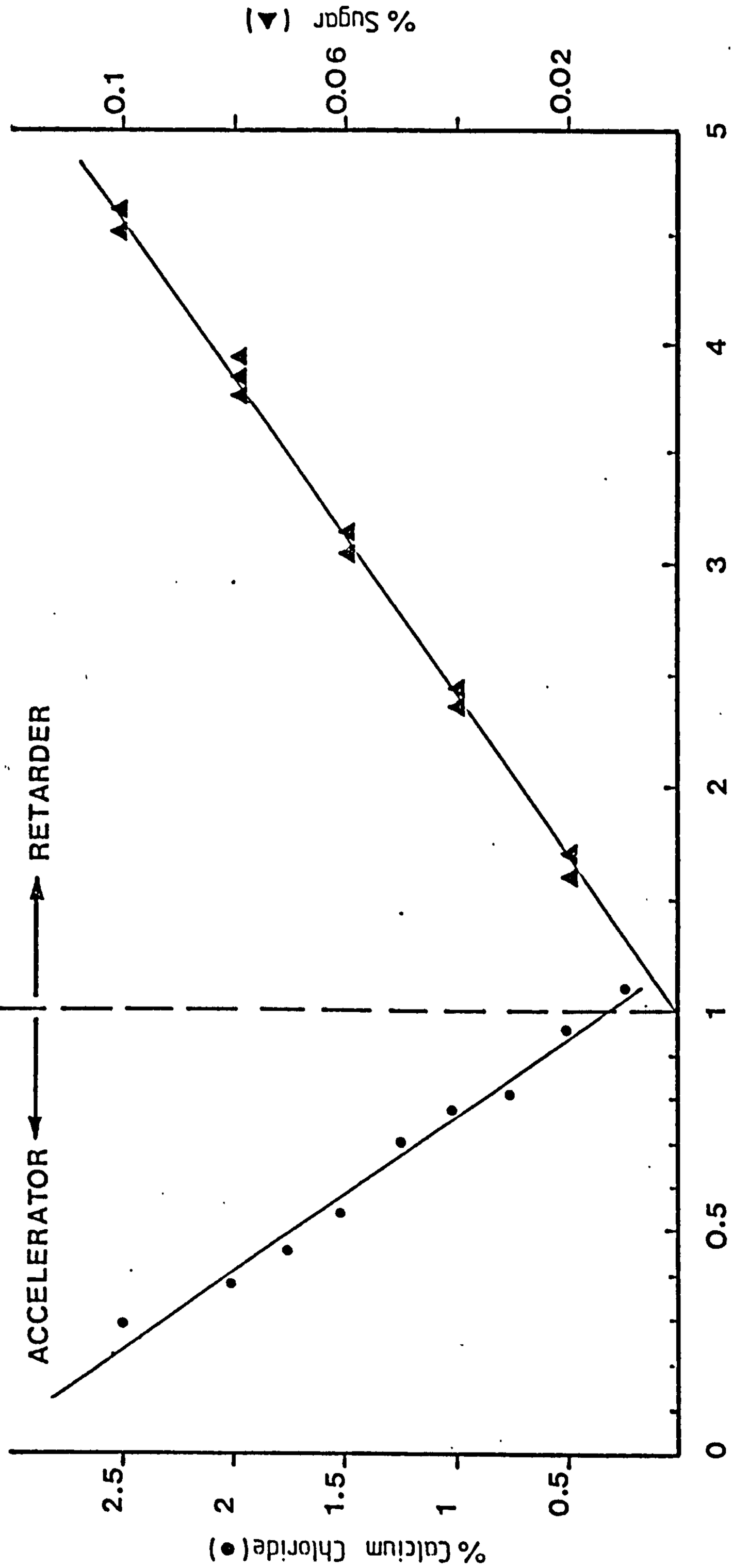

FIGURE 5.II THE RELATIONSHIP BETWEEN SETTING TIME AND THE PERCENTAGE OF ADMIXTURE ADDED

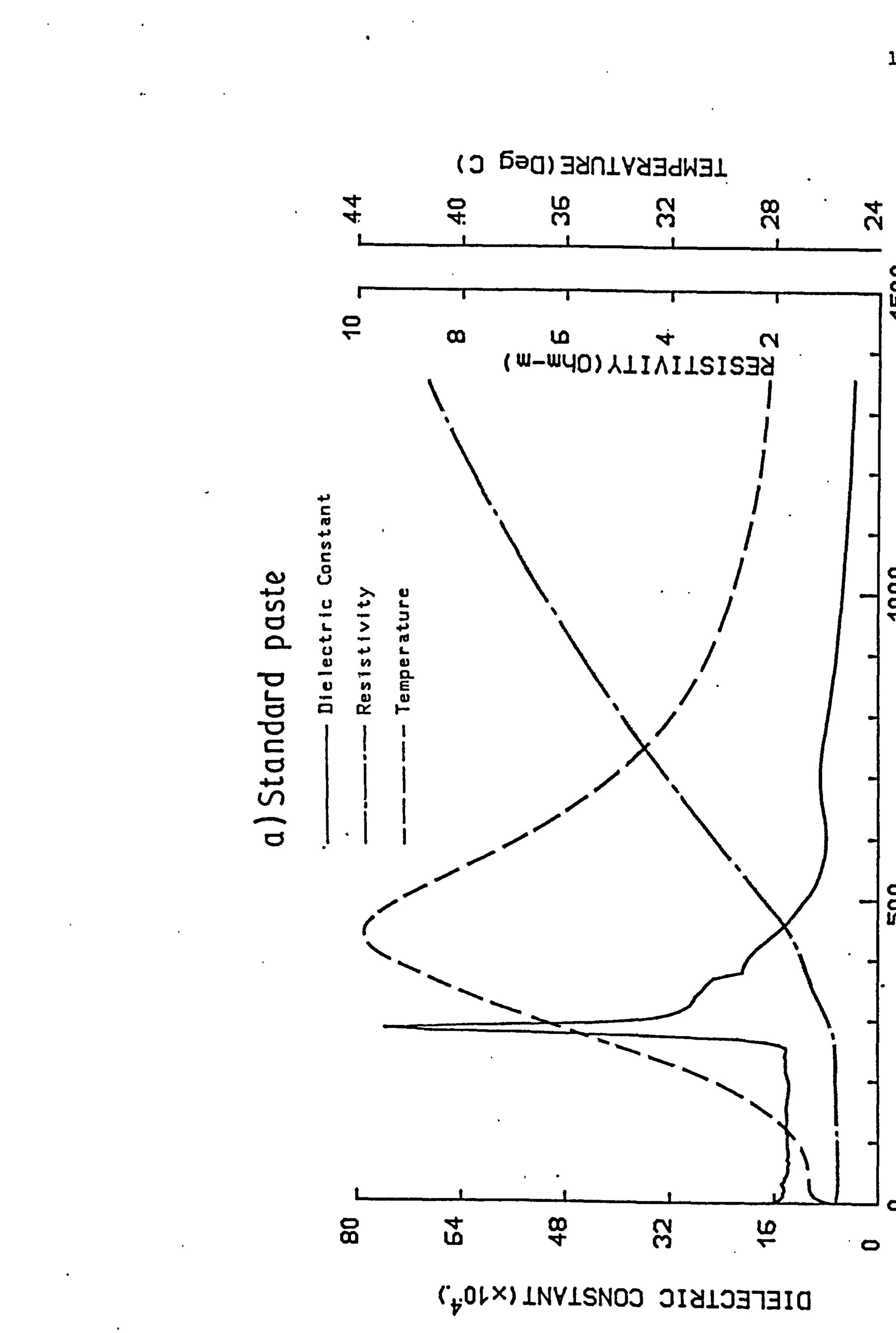

FIGURE 5.12 EFFECT OF AGGREGATE ON MEASURED ELECTRICAL RESPONSE

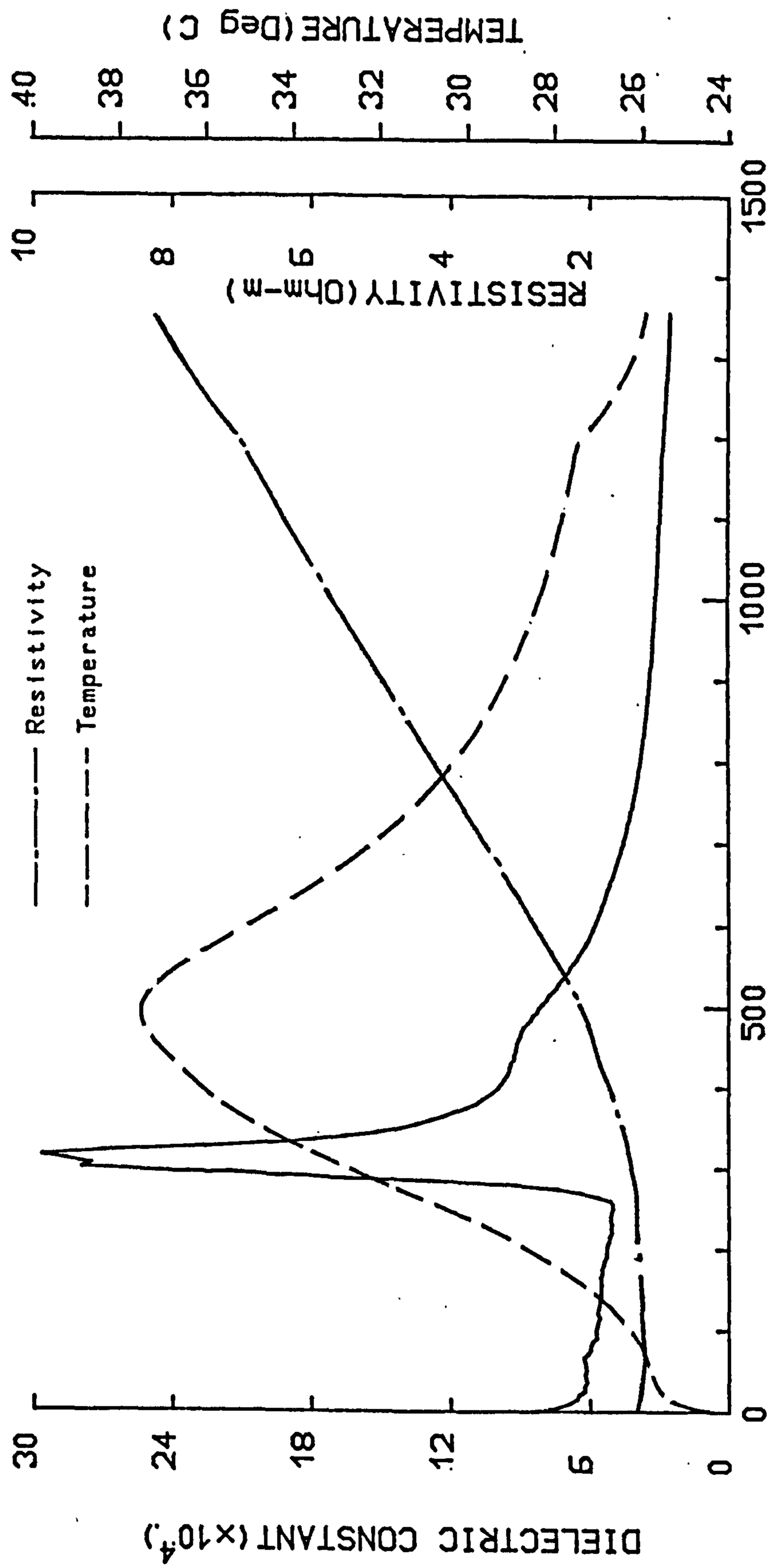

FIGURE 5.12 (CONTINUED)

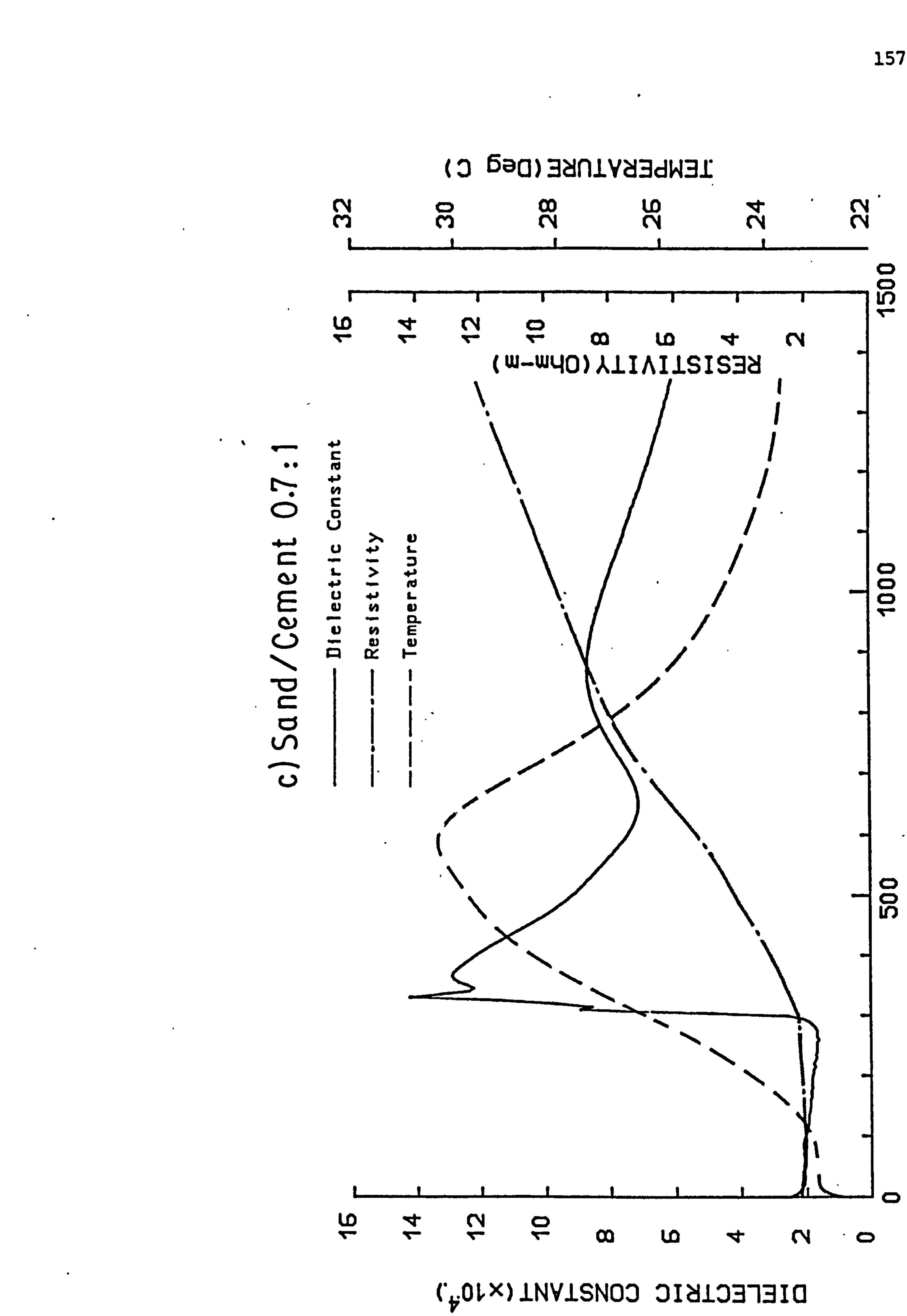

FIGURE 5.12 (CONTINUED)

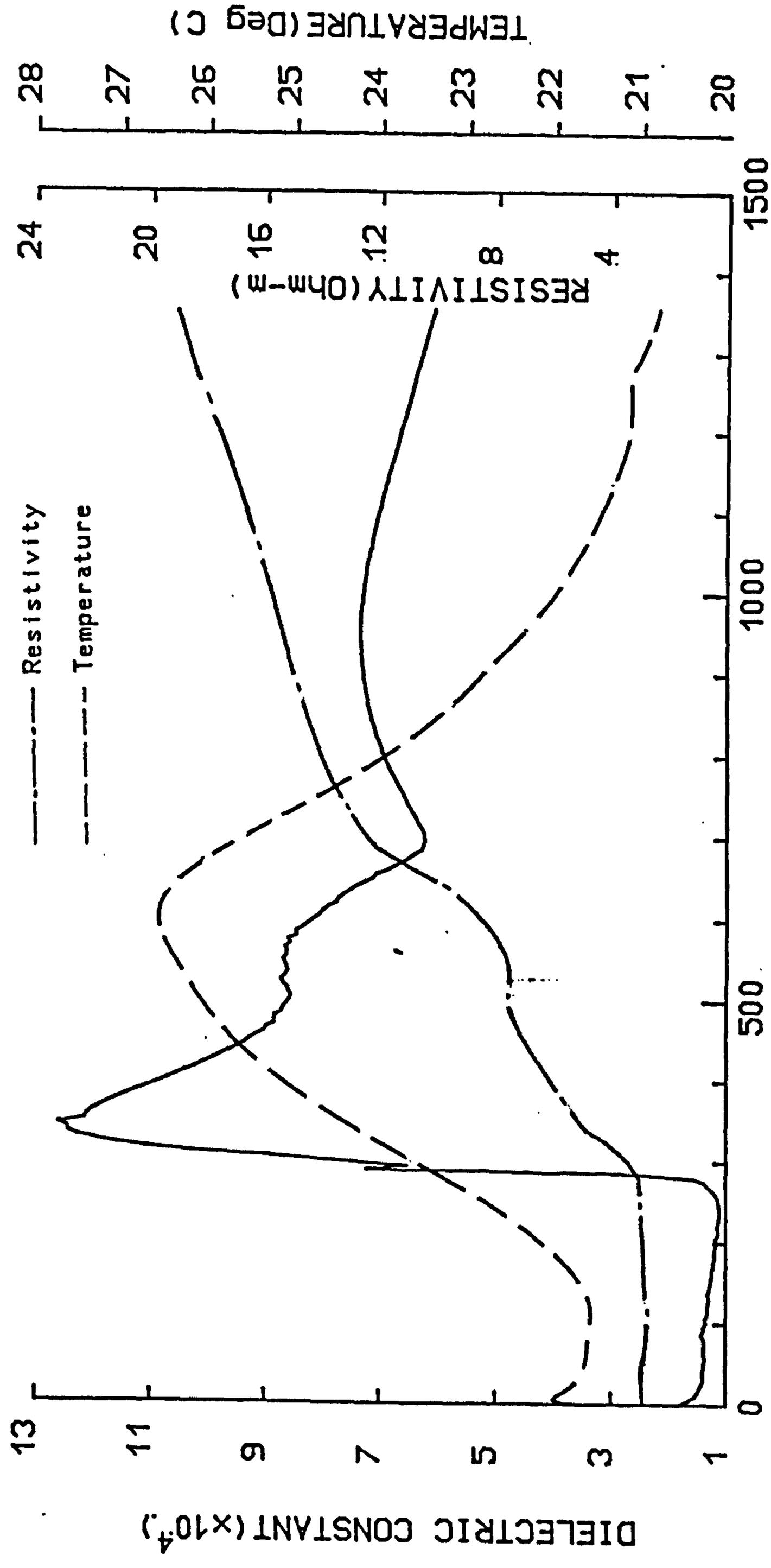

FIGURE 5.I2 (CONTINUED)

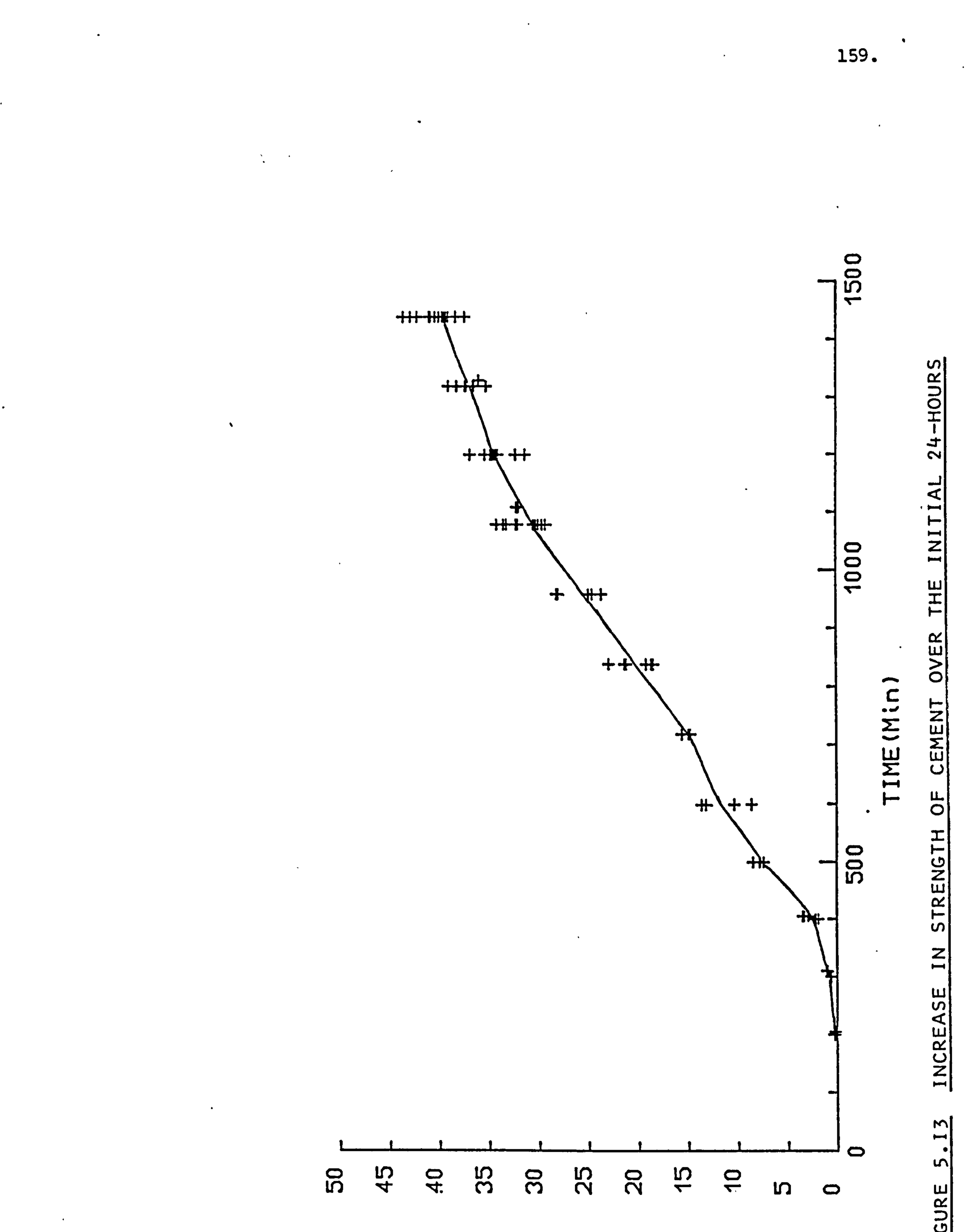

FIGURE 5.13 INCREASE IN STRENGTH OF CEMENT OVER THE INITIAL 24-HOURS

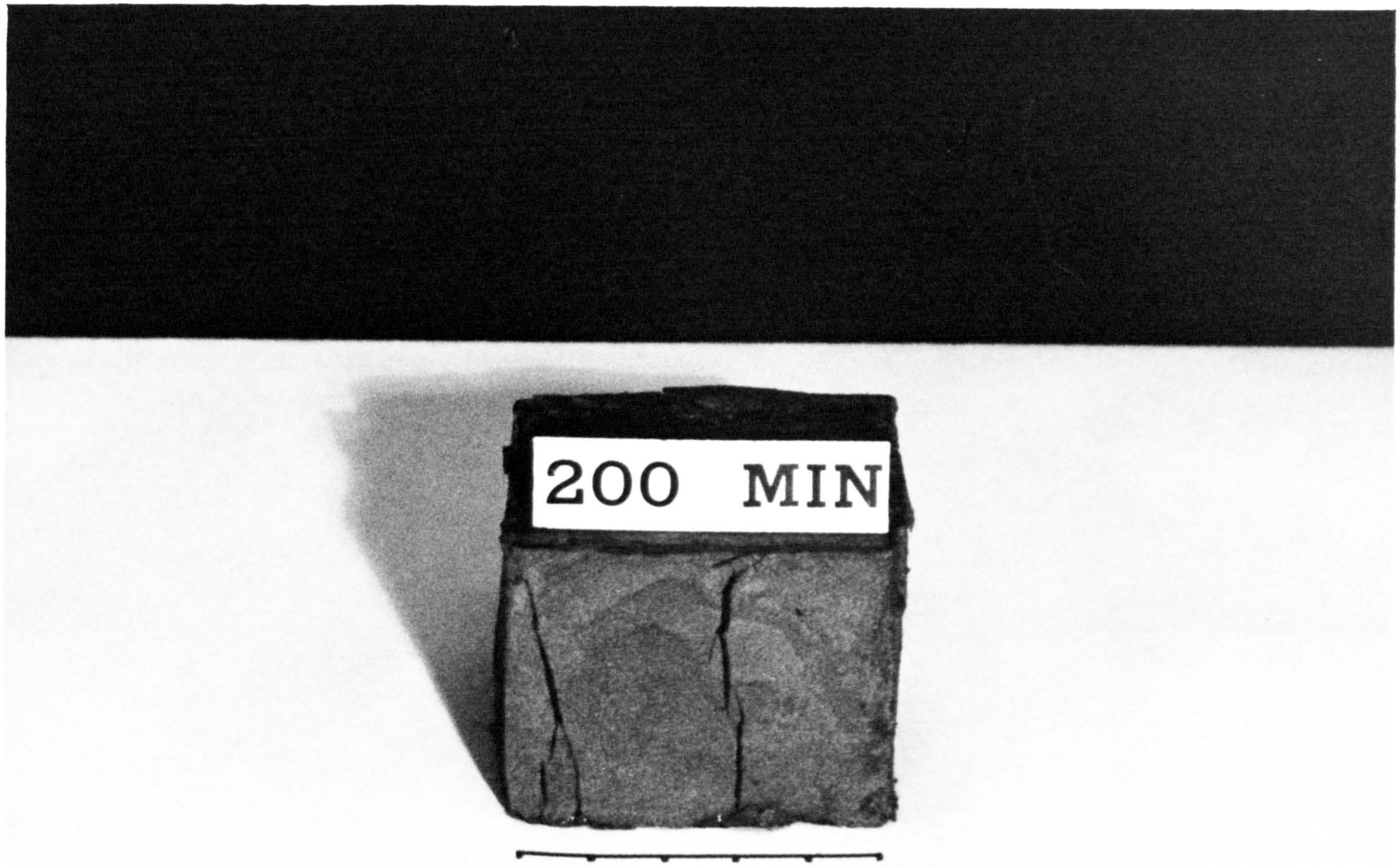

PLATE 5.1a

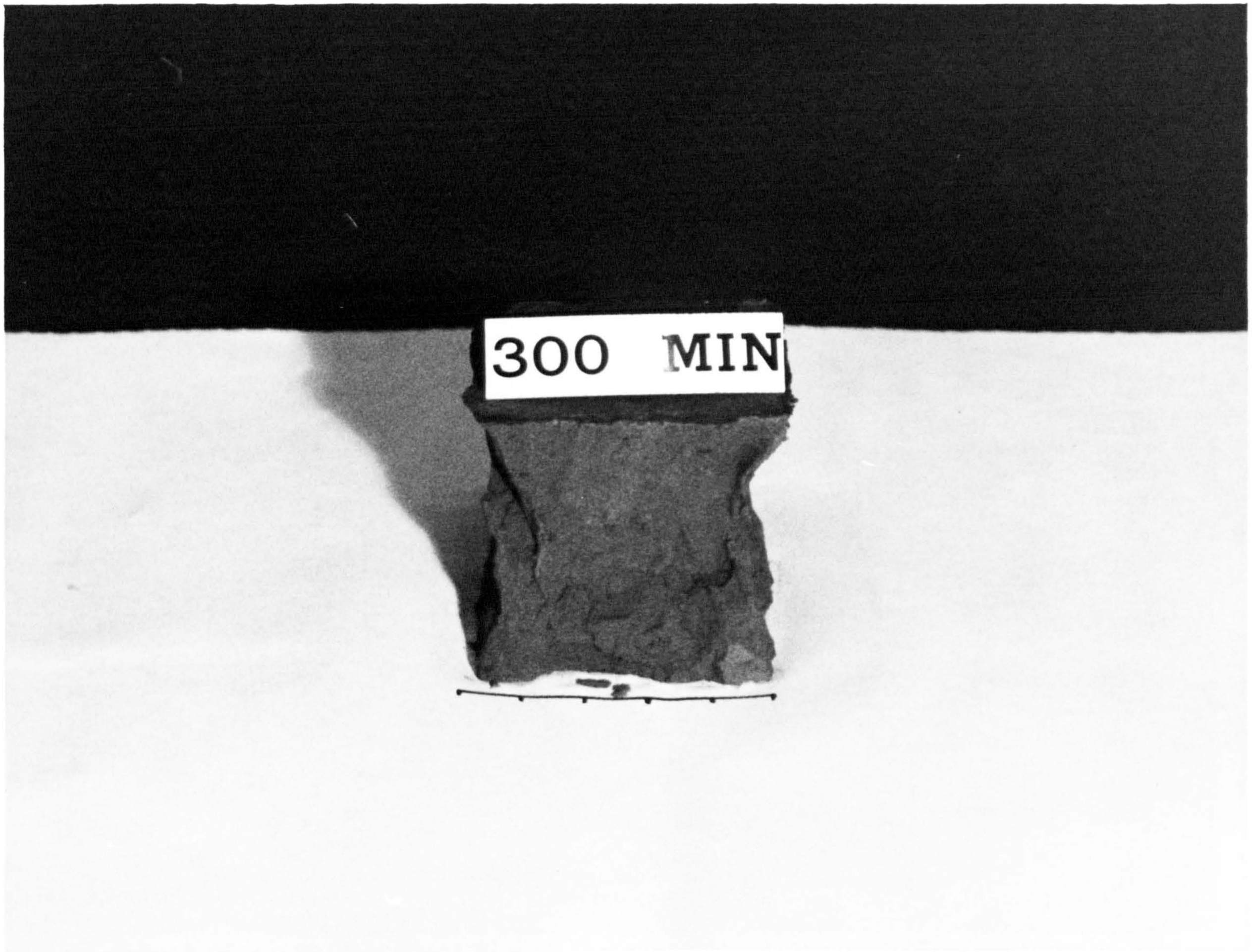

PLATE 5.1b

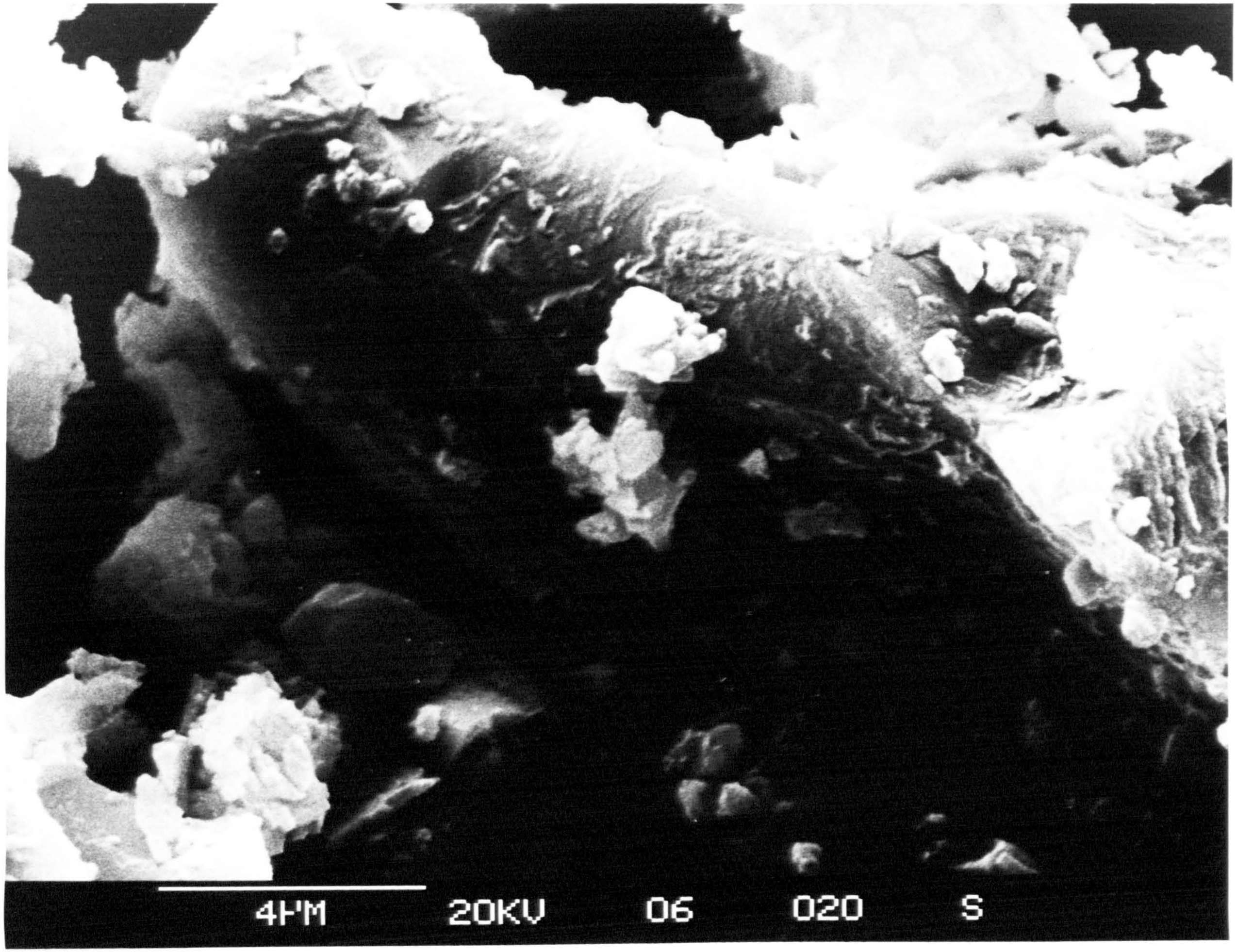

PLATE 5.2

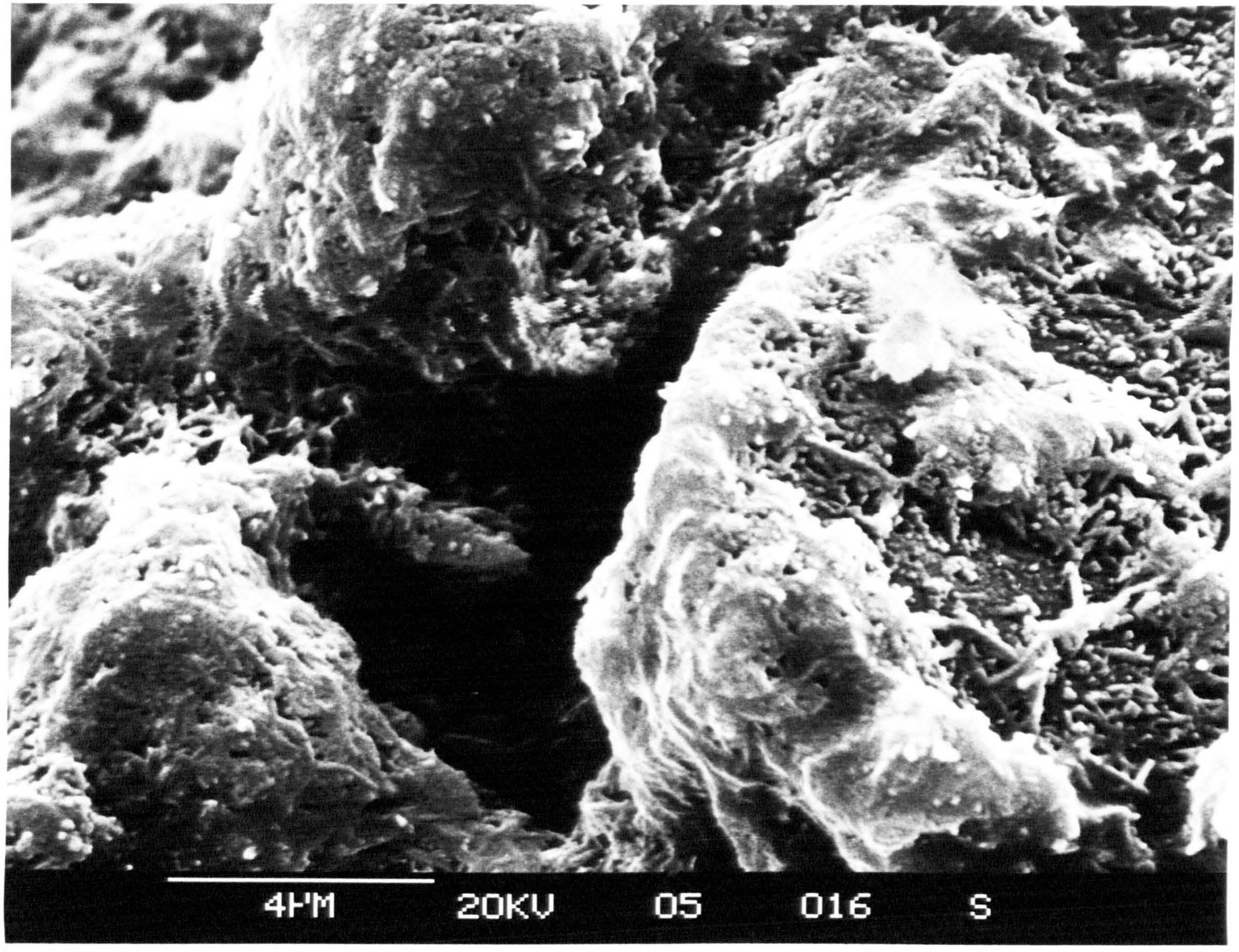

PLATE 5.3

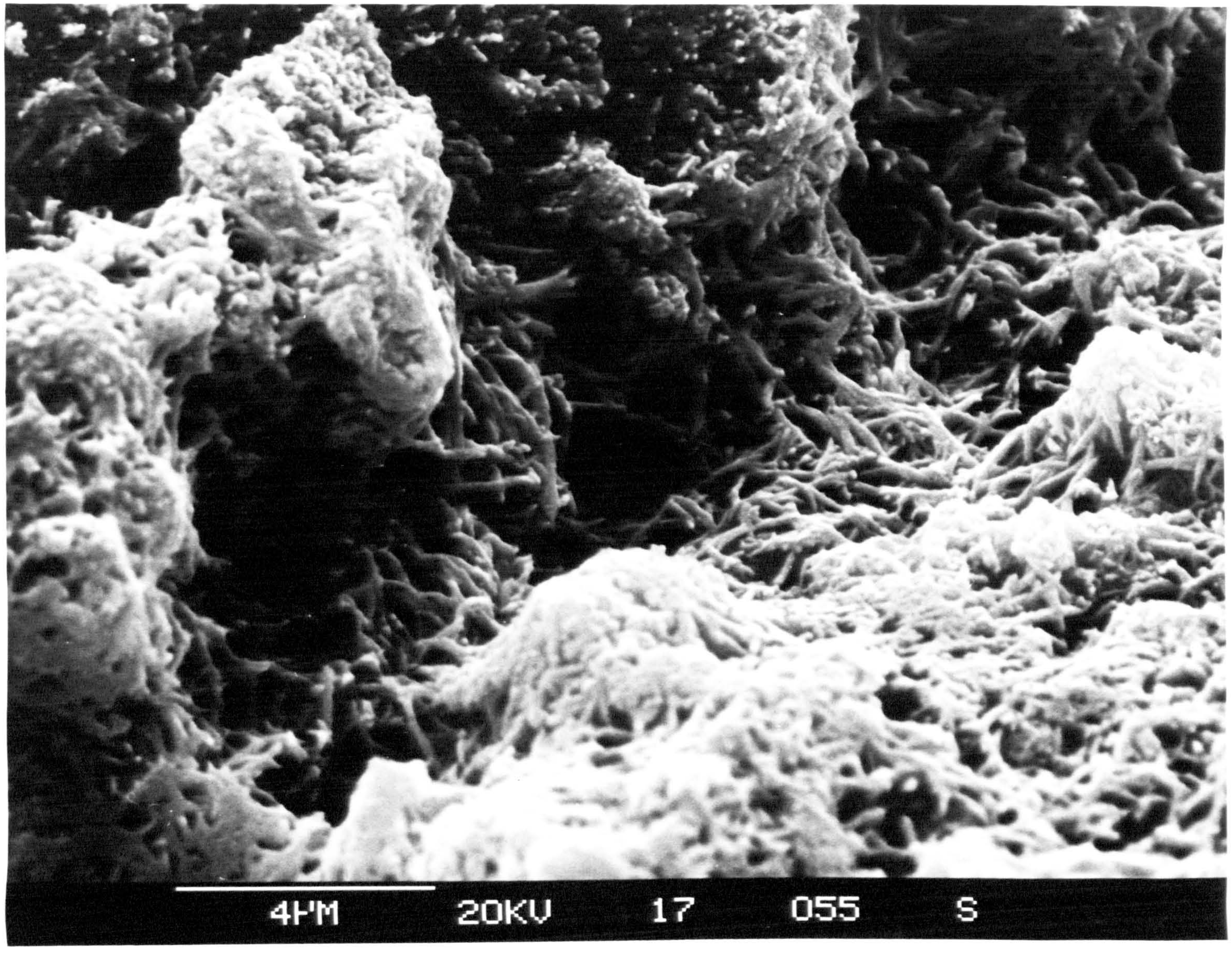

PLATE 5.4

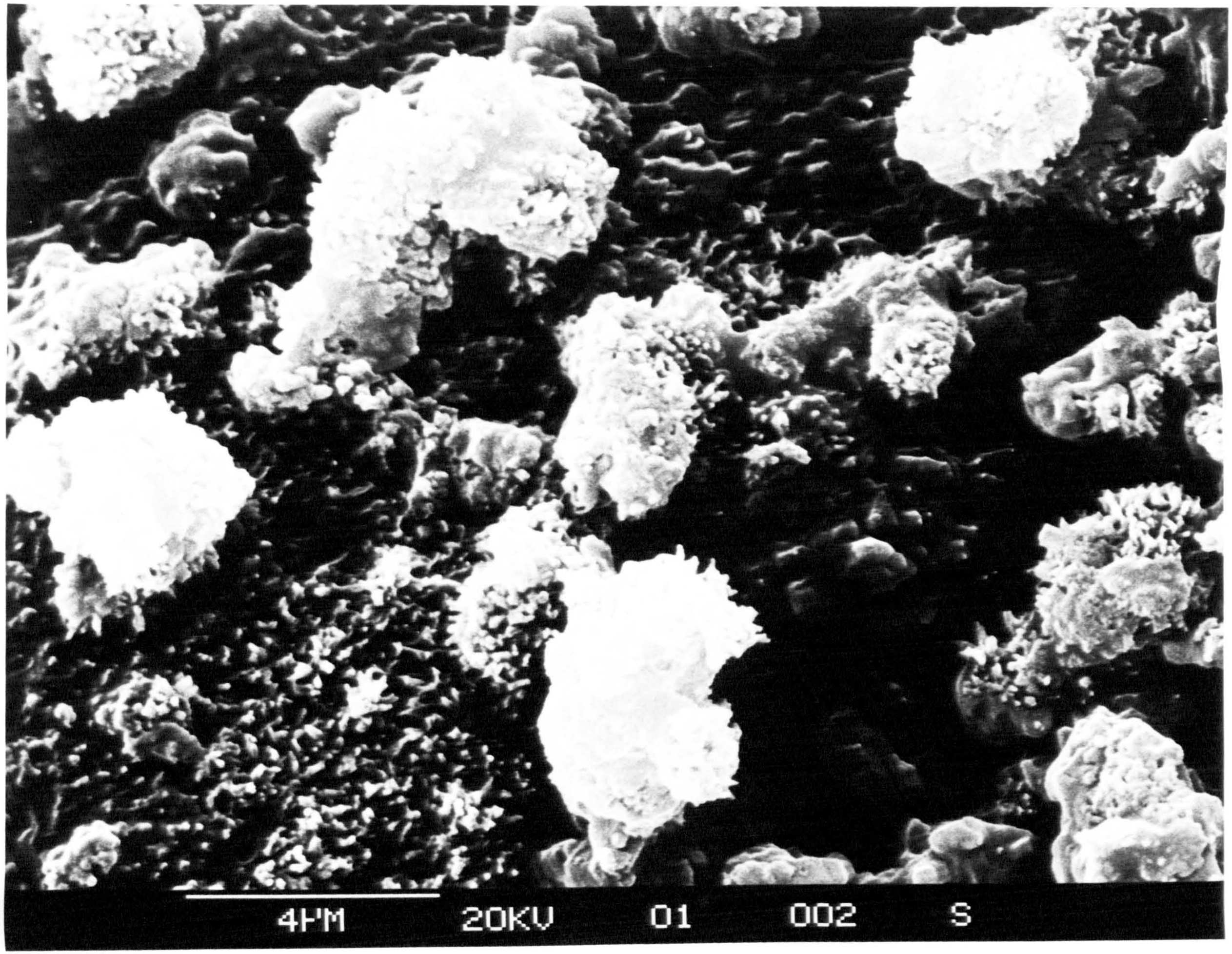

PLATE 5.5

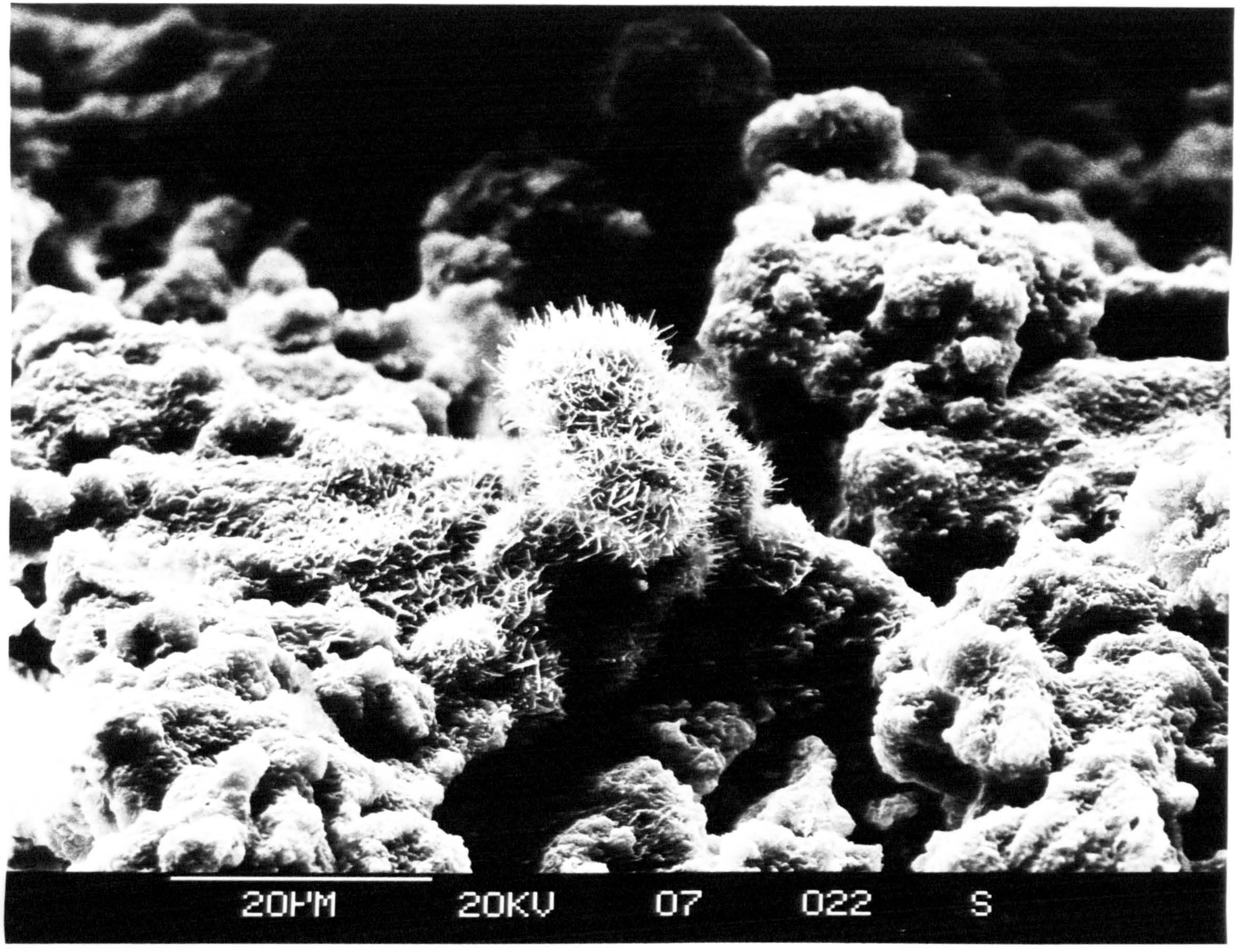

PLATE 5.6

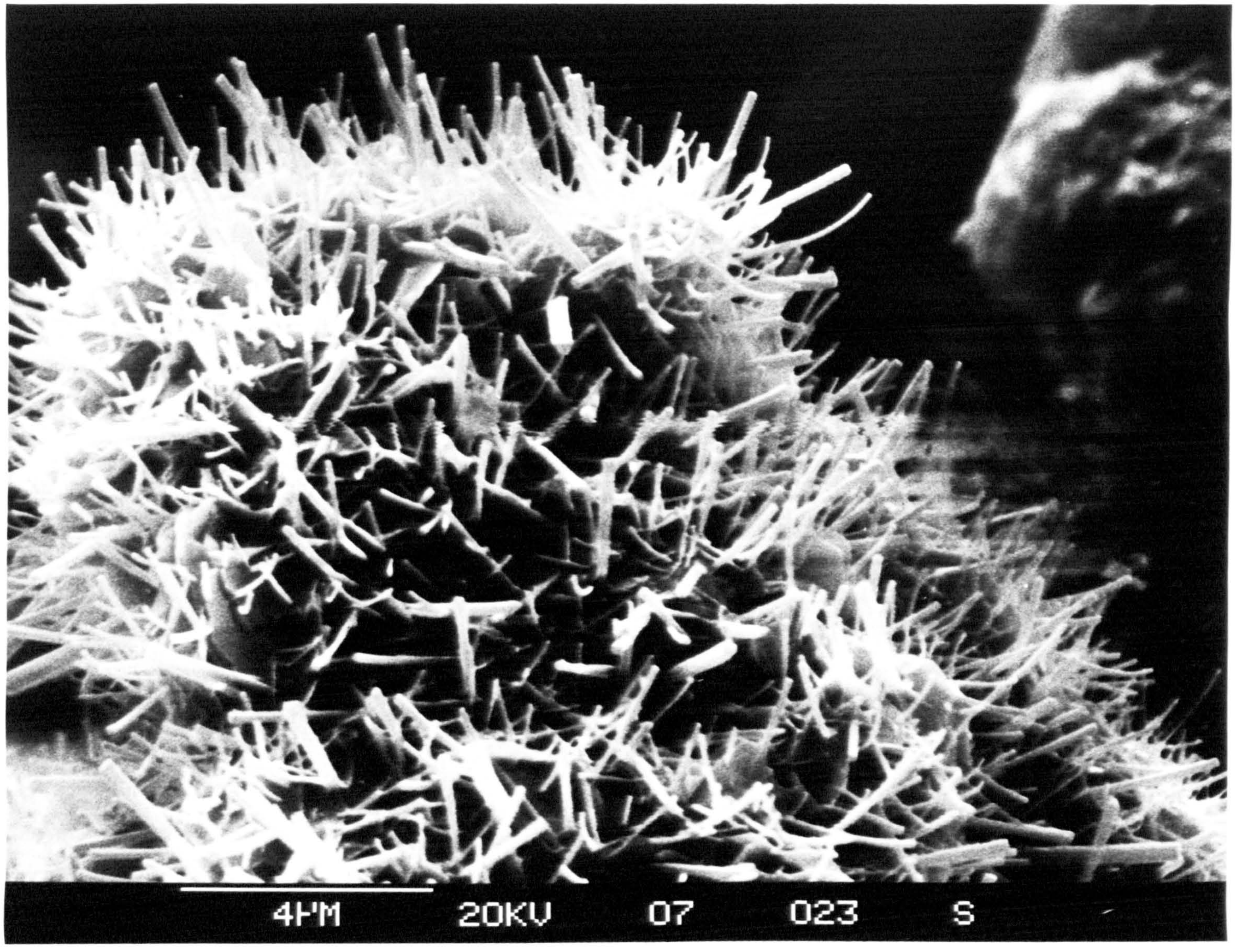

PLATE 5.7

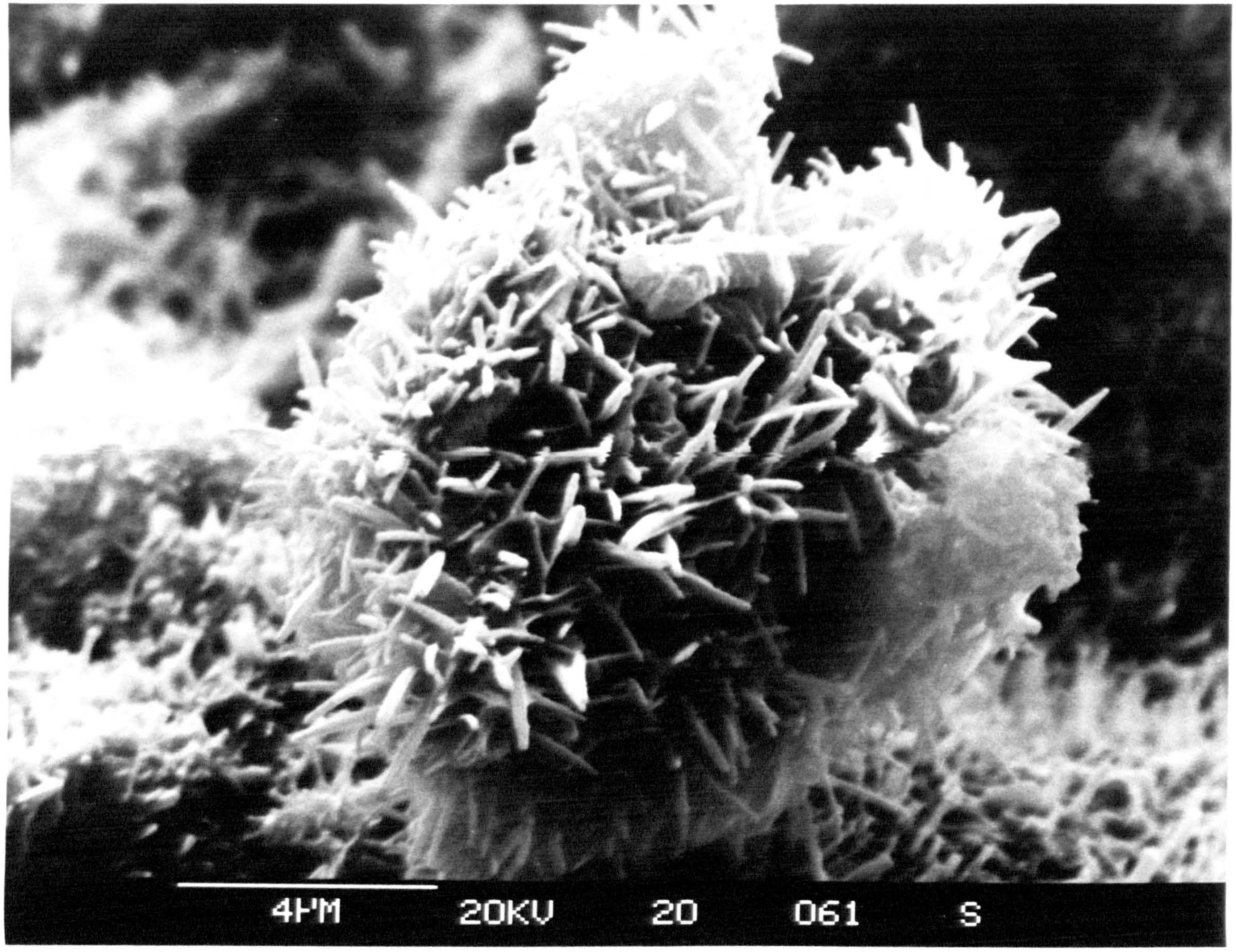

PLATE 5.8

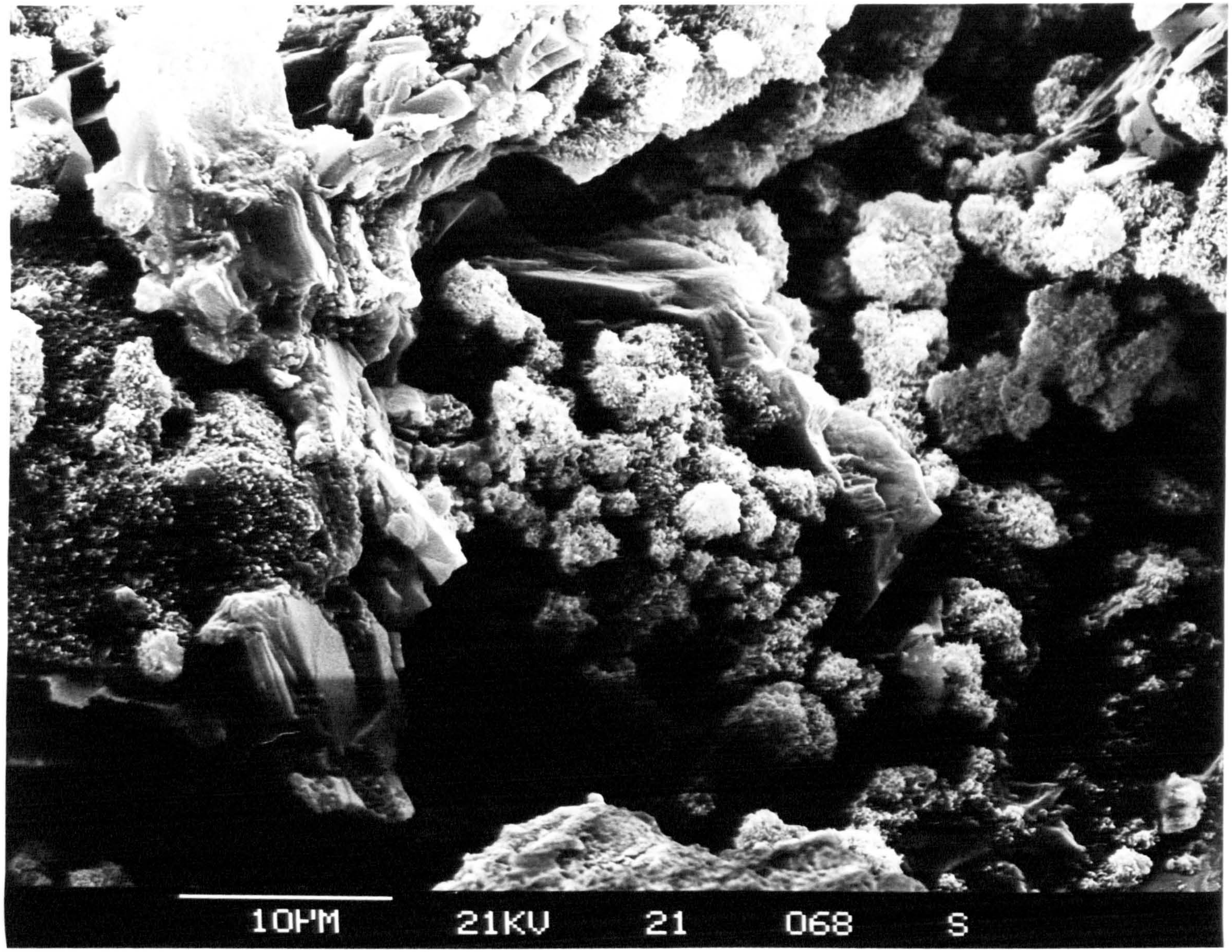

PLATE 5.9

PLATE 5.10

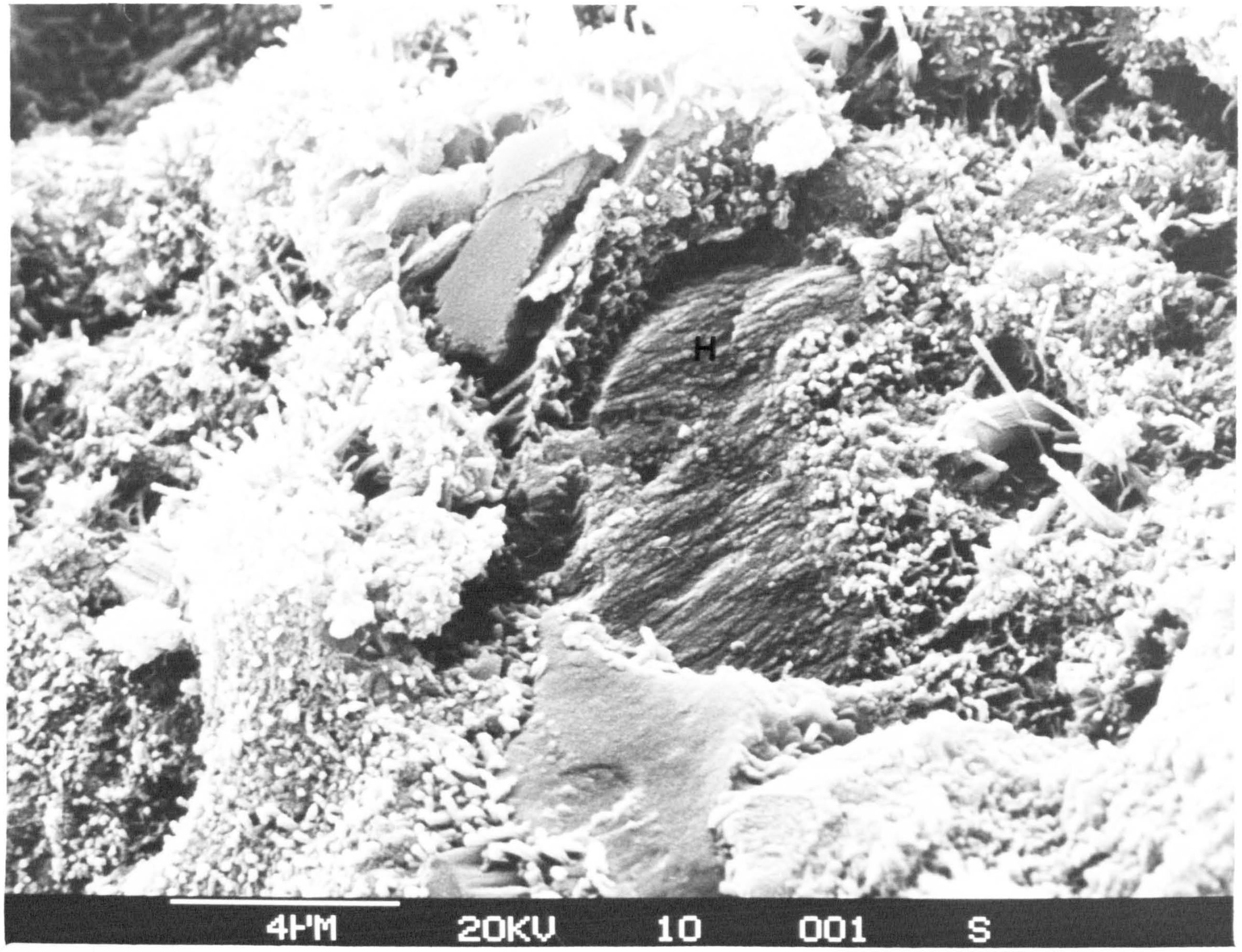

PLATE 5.11

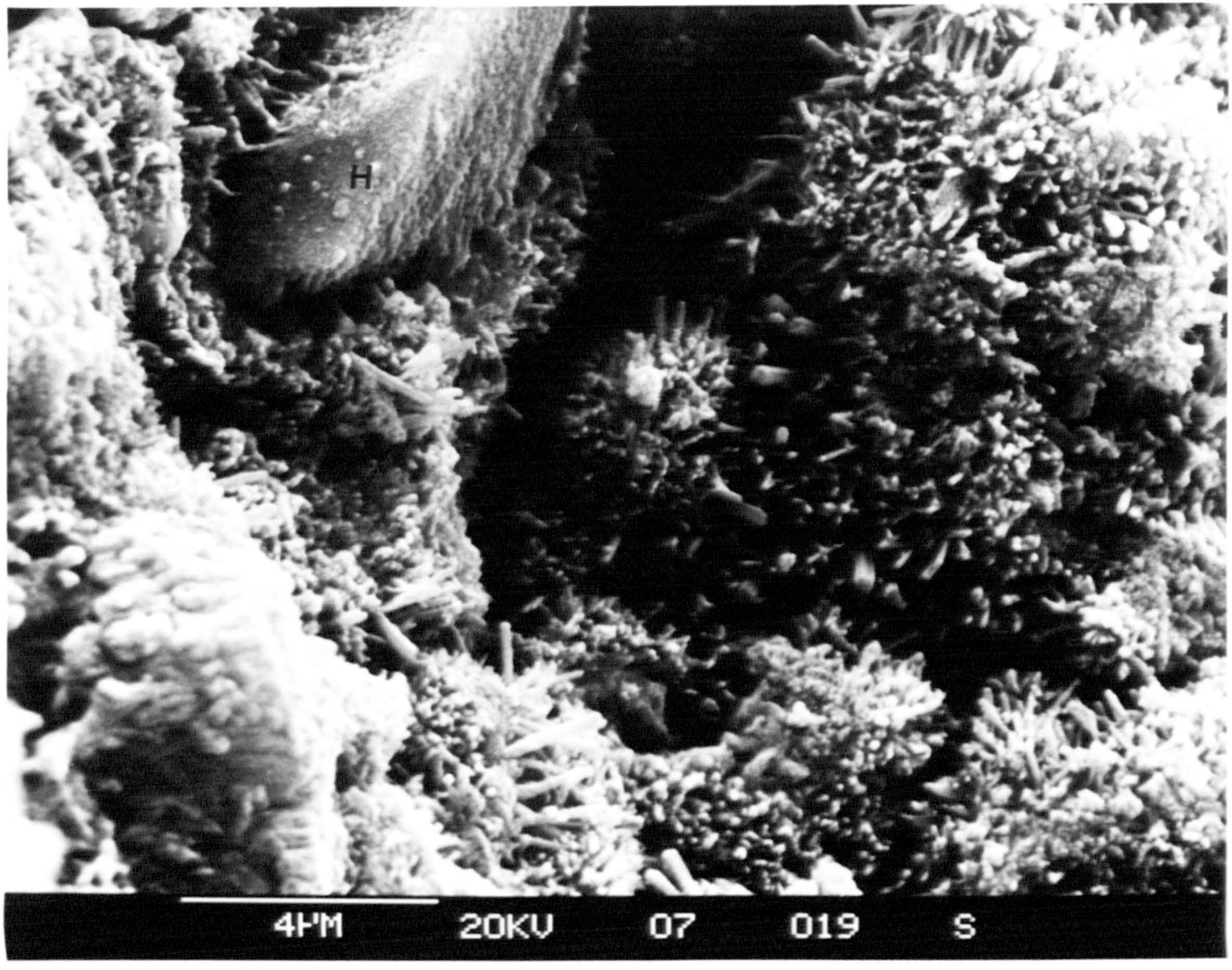

PLATE 5.12

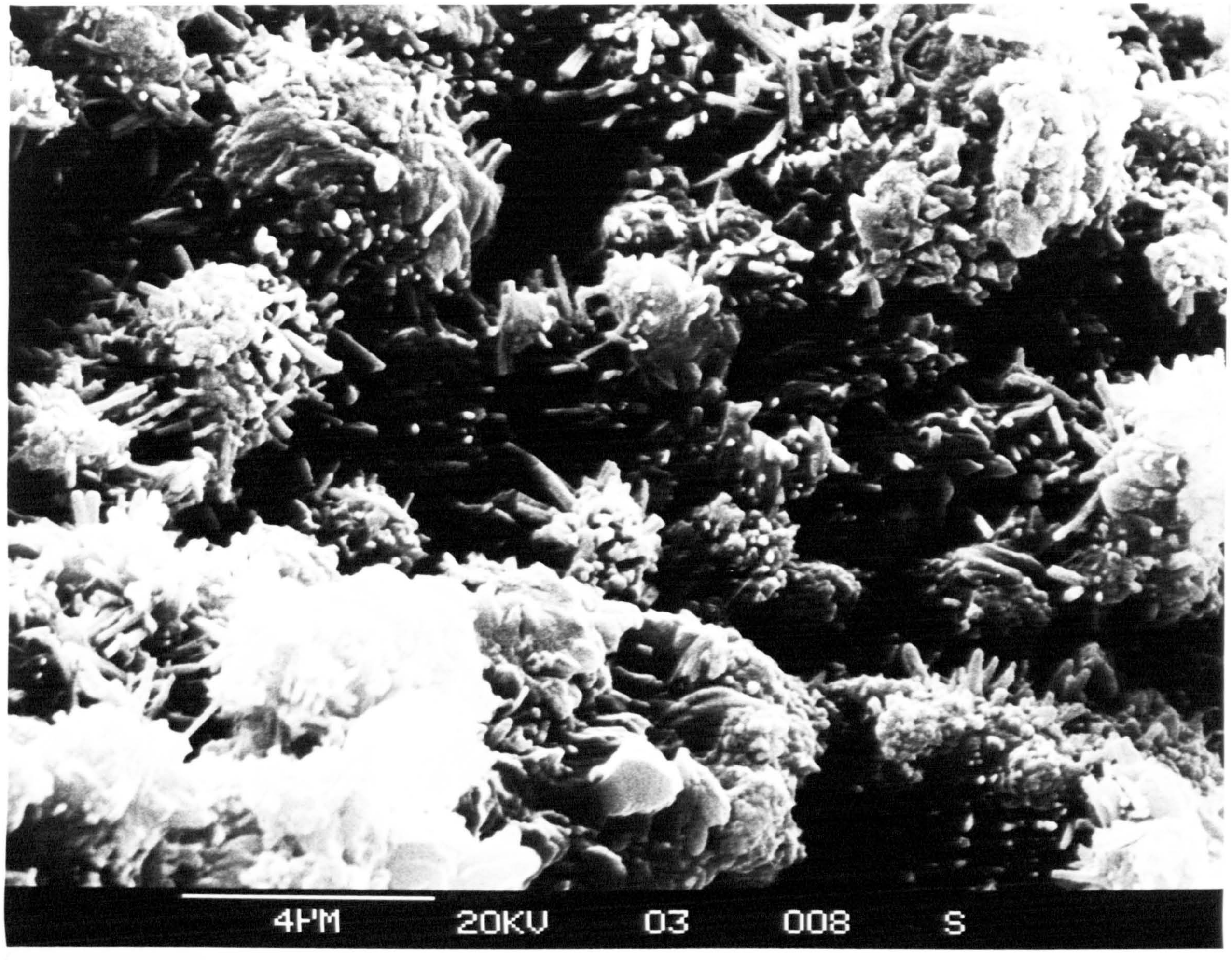

PLATE 5.13

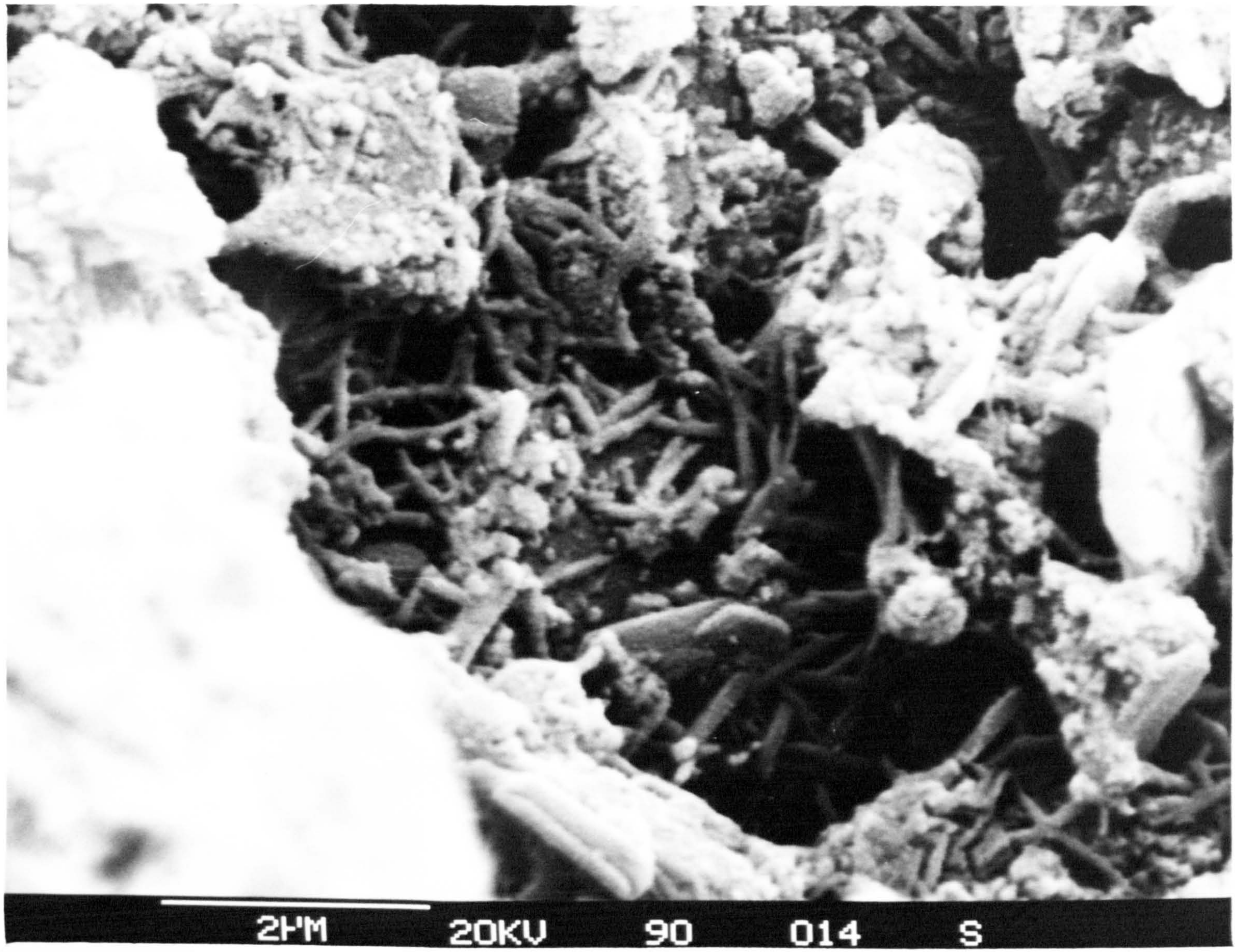

PLATE 5.14

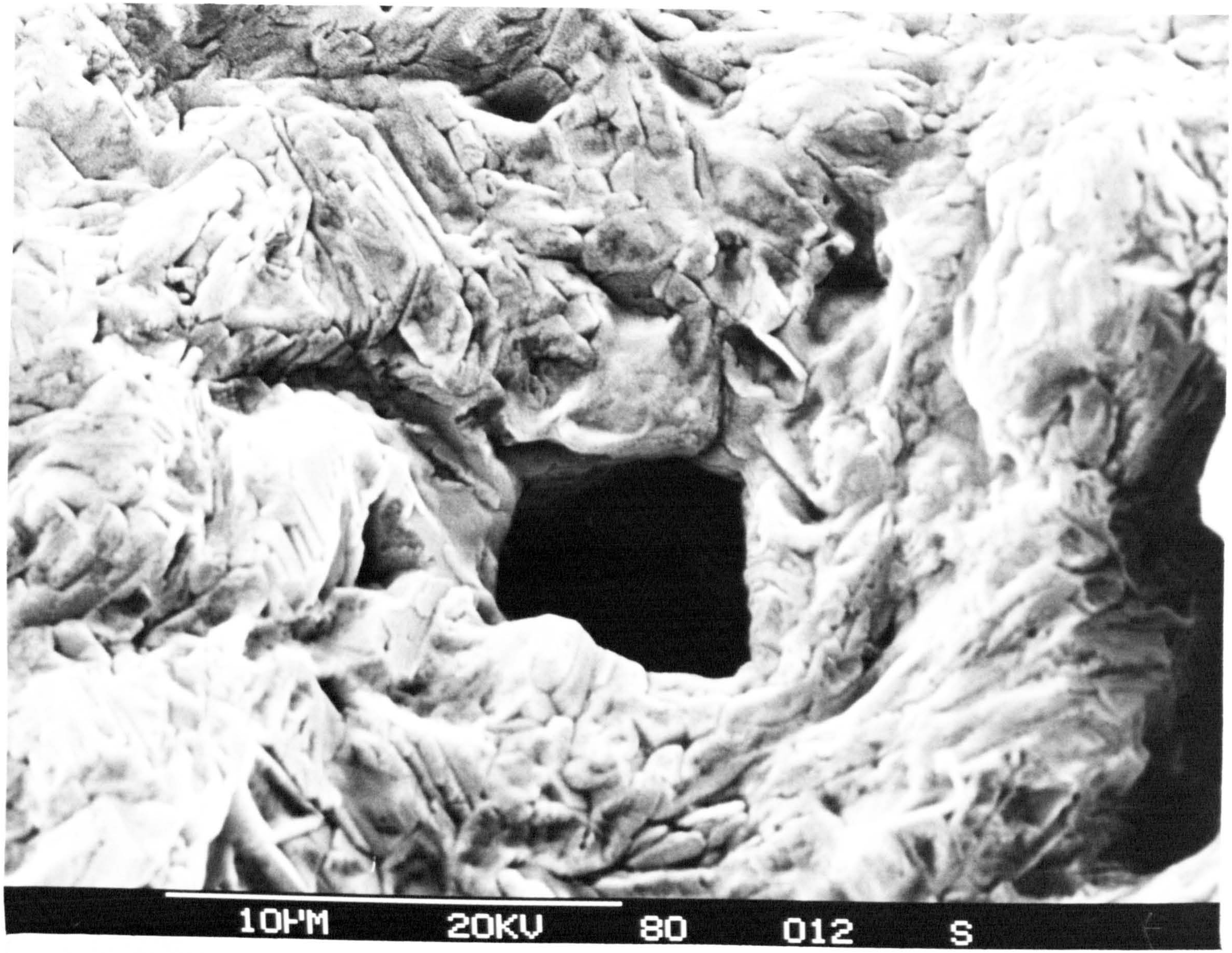

PLATE 5.15

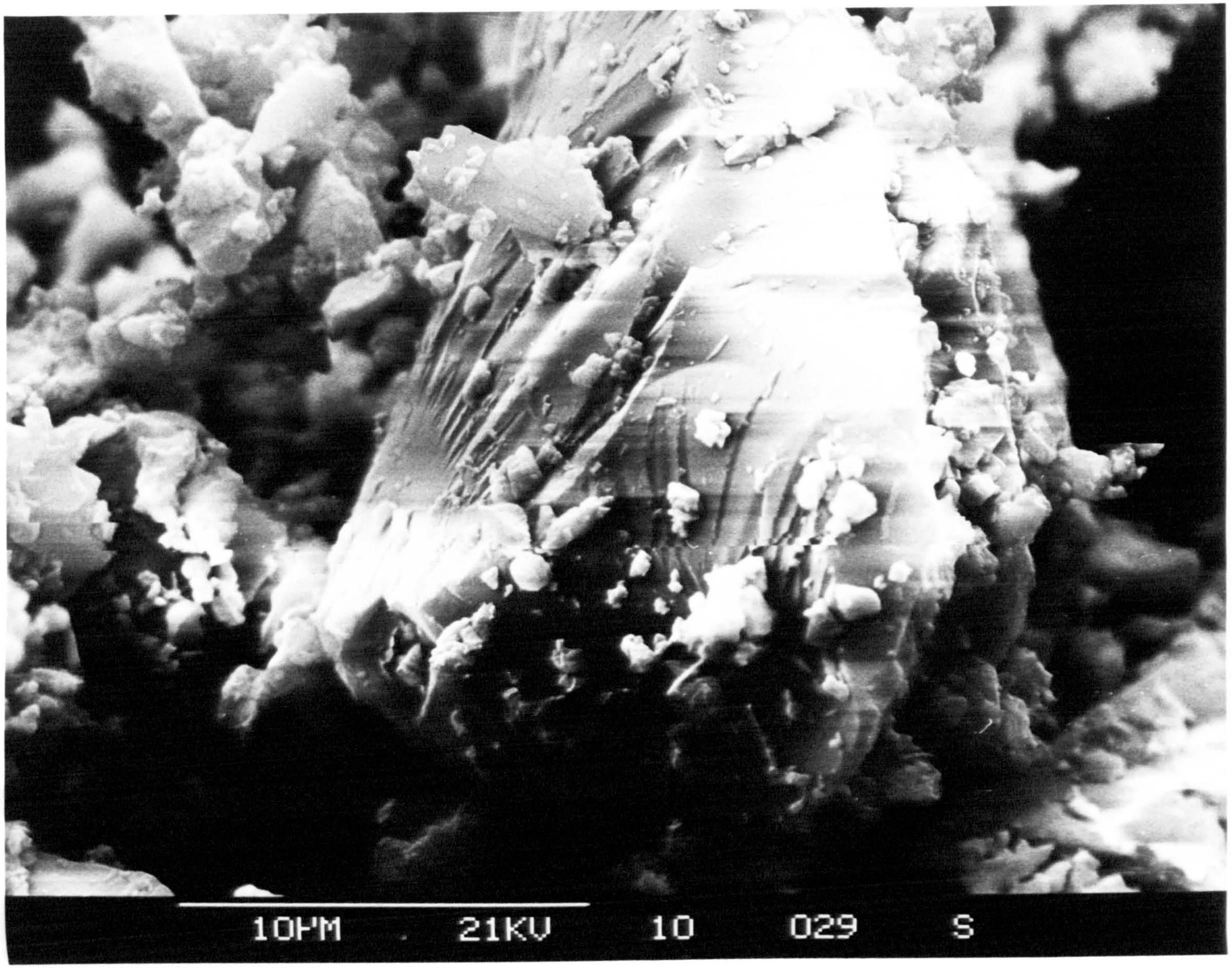

PLATE 5.16

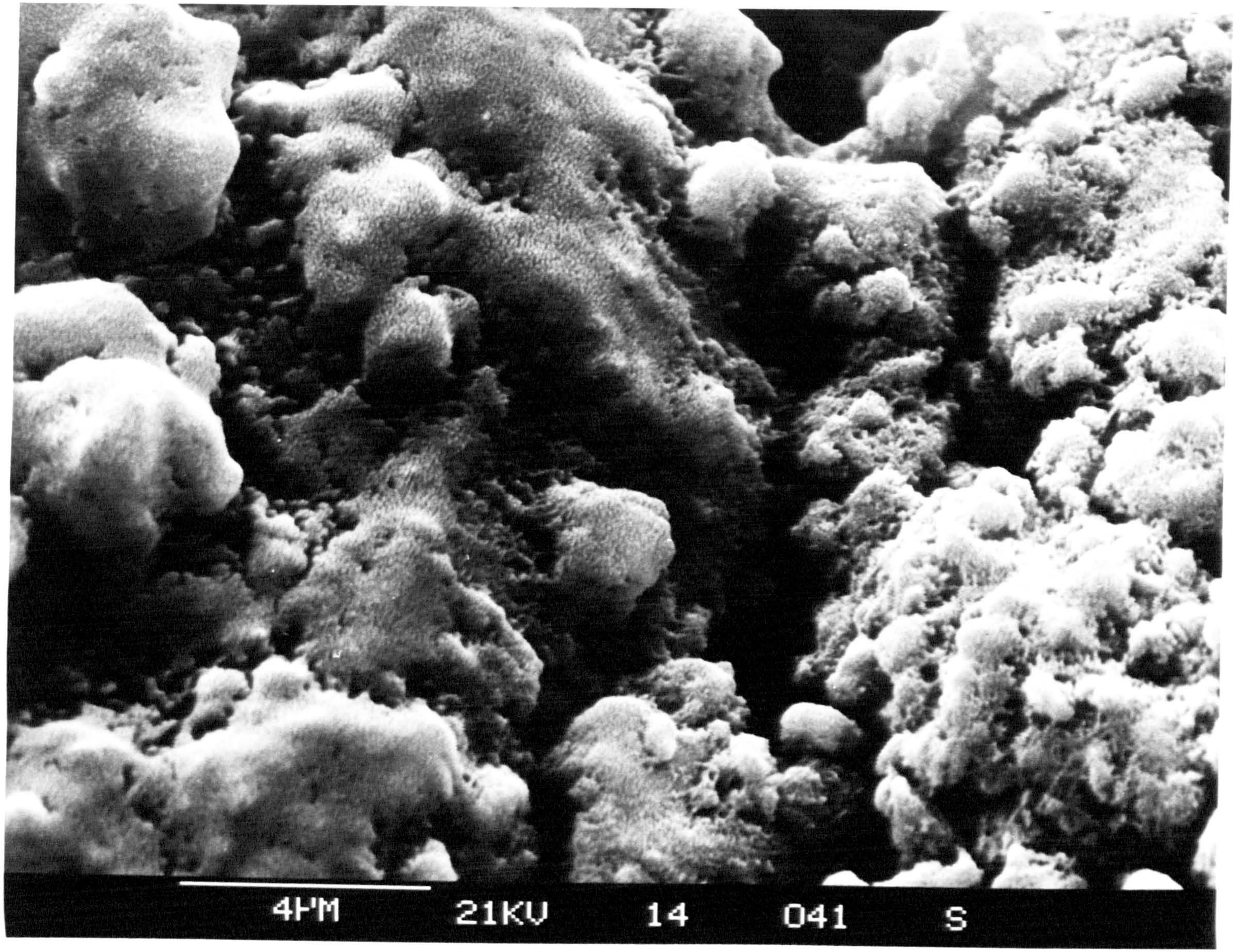

PLATE 5.17

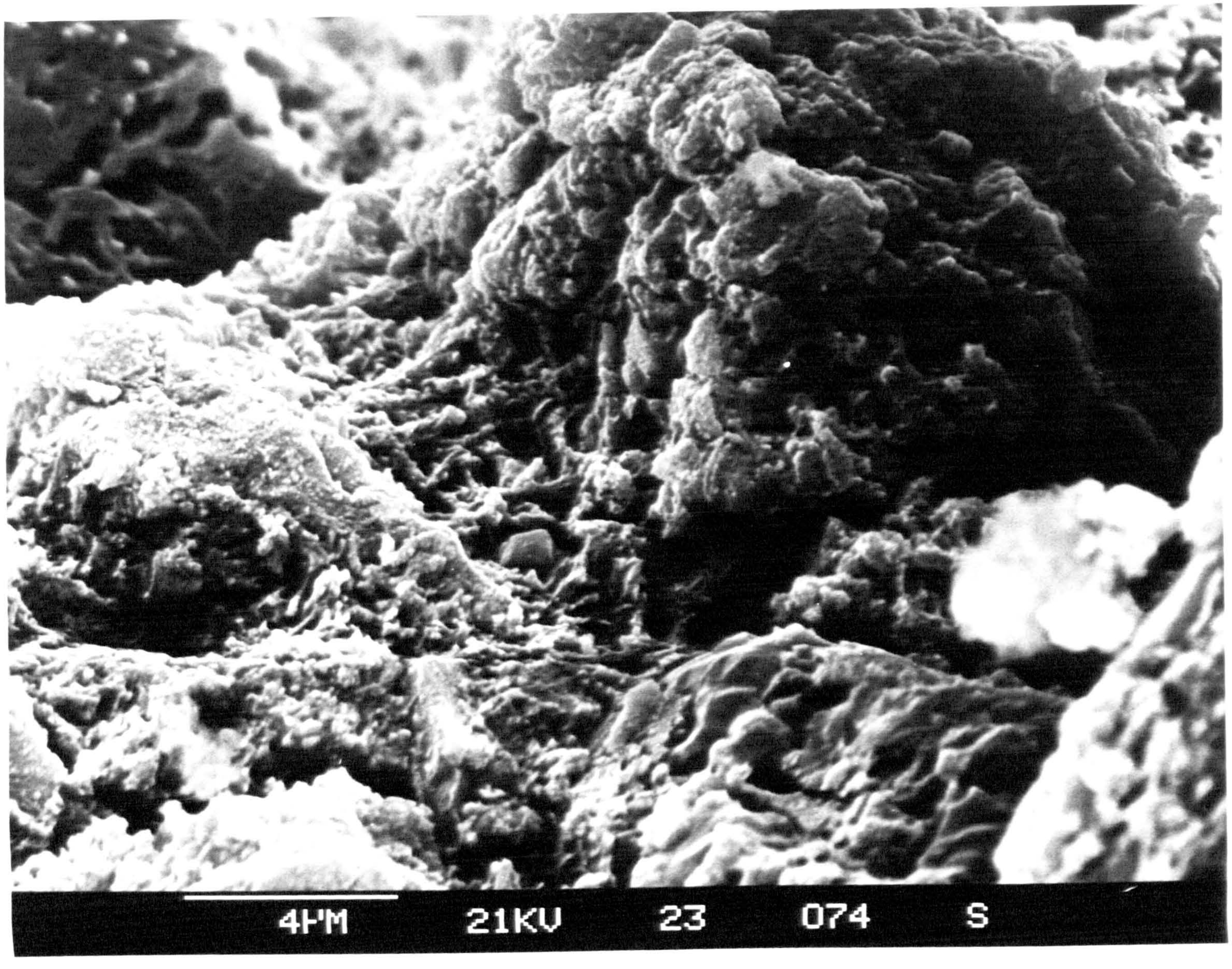

PLATE 5.18

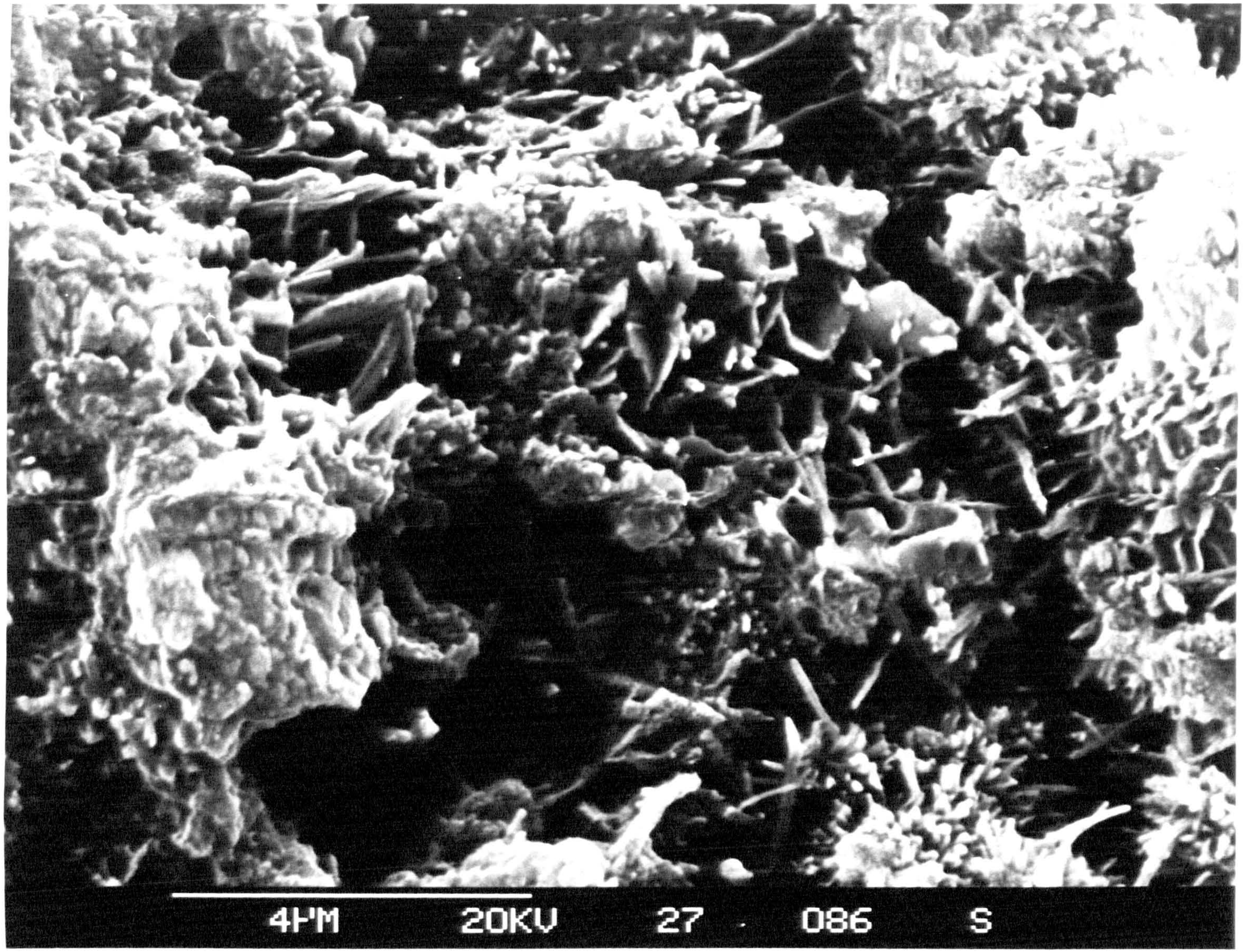

PLATE 5.19

CHAPTER 6

OVERVIEW AND RECOMMENDATIONS FOR FURTHER RESEARCH

The initial 24 hours of the hydration process of cement paste are perhaps the most important period, as it is during this time that the paste changes from a fluid to a solid state. The long-term structure and strength development is largely indicated by the processes occurring over this period.

The most important physical characteristics of cement paste during hydration is its increase in strength which is initiated by the setting process. Setting time has been traditionally measured using the Vicat Needle apparatus. The Vicat Needle Test gives an indication as to the physical state of the paste, however, setting is the direct consequence of chemical reactions occurring during hydration. Monitoring these chemical reactions would give a better indication as to the rate of hardening and the setting time of cement. Furthermore, a precise chemico-physical test that will;

a) monitor hydration characteristics, thereby ensuring correct setting and hardening of the cement without disturbing the fabric structure of the matrix; and
b) enable an accurate quantification of the influence of admixtures, and variation in chemical composition on hydration,

would be an advancment on earlier techniques, and yield more information for the cement technologist.

The technique developed in this research has shown that electrical response methods can be used to ensure the correct

setting and hardening characteristics, it has also been demonstrated that admixtures; chemical composition; the age of cement, and addition of aggregate have a definite influence on the electrical response, hence hydration characteristics, and their effect can be quantified.

The following conclusions can be drawn from this study:

a) An alternative method for testing cement has been investigated in which the system variables have been analysed in detail and measuring procedures formulated.

b) An automated microcomputer data logging system has been developed which allows the flow of instruction and data between a number of peripherals and a central contoller.

c) Customised software was developed for the microcomputer to control -

   i) the overall running of the experiment,

   ii) the action taken by the individual devices, and

   iii) the flow of data within the system.

d) Although both hardware and software in this system have been designed to cater for the specific requirements of the research programme outlined in this thesis, there is no reason why the system could not be adapted and the software modified to match the need of other users. Such a system, as opposed to manual logging systems, allows greater flexibility not only in the duration of the experiment but

also in the time interval between reading cycles.

e) The system requires minimum input, minimises the data acquisition time, minimises the delay time between experiments, and maximises the freedom of manipulating the data to reach a conclusion.

f) The system described provides data throughout the duration of the experiment. If required, this data could be used to give feedback to the controller which could then be programmed to make operational decisions as to the progress of the experiment.

g) Using the system described, the electrical response of setting cement paste can be logged, not only as a function of time, but also as a function of frequency with an accuracy that has hitherto not been achieved, and can be used to monitor the hydrolysis and hydration characteristics.

h) The electrical method developed has certain advantages over present structure determining techniques,

i) the fabric structure of the paste is not destroyed,

ii) the sample size is sufficiently large to evaluate macroscale behaviour; indeed, the sample size conforms to BS 1881 (standard 100mm cube).

iii) the electrical method offers an additional means for continuous monitoring of hydration processes over the initial 24-hours after gauging with water.

i) Four stages occurring during the early hydration of cement paste have been both identified and verified using an electrical response technique. The rate of change of these electrical parameters are indicative of the rate at which hydration is progressing.

j) Further new evidence on the early hydration of OPC has been given. It has been demonstrated that the electrical response of cement paste is sensitive to physical and chemical changes within the paste and the dielectric constant and electrical resistivity can be used as a diagnostic of the setting and hardening processes. The work presented could also help in elucidating such theories as the membrane theory presented by Birchall et al[43] and Double et al[40-42].

k) The continuous monitoring of the chemical processes in other types of cement (HAC, RHPC, SRPC) has shown that a change in chemical composition of the cement influences the electrical response. Indeed, the response characteristics of HAC indicate four identifiable stages in its hydration over the initial 24-hours. (Also of interest is the high internal temperature occurring within the HAC paste caused by secondary CA hydration. Some conversion must result from such a high temperature).

l) The influence of admixtures on the hydrolysis and hydration processes can be quantified. As this method is measuring the chemical processes within the paste, the arbitrary terms

'initial' and 'final' set could have more meaning if redefined in terms of their electrical parameters. A general time 'point of set' was introduced.

m) A relationship has been established and graphs are presented for two commonly used admixtures which enable the required percentage of additive to be calculated to achieve a required setting time.

n) It has been shown that the rate at which the paste gains strength is greatest over the period of intense chemical activity, i.e. when the electrical properties of the paste are undergoing significant changes (200-600 minutes).

o) From the SEM work, tentative predictions as to hydrate morphology have been linked to electrical response. The electrical response methods could offer an additional technique for monitoring the structure building processes and microstructure development in cement paste. Electrical response curves could be used as a 'fingerprint' to ensure correct setting and hardening of cement.

p) The electrical properties of cement have been found to be not only a function of time, but also of frequency.

q) The dielectric constant decreases with increase in frequency, this indicates a region of dielectric dispersion and thus can be related to double layer and interfacial effects, hence the polarizability of the paste.

r) Over the frequency range considered (20Hz - 300 kHz) the resistivity also decreases with increase in frequency, a feature not considered in previous research. The magnitude of the decrease is a function of water-cement ratio and degree of hydration. A PFE term was introduced to quantify this effect.

s) The resistivity of paste can be related to the rate of removal of evaporable water from the bulk aqueous phase, pore continuity and constriction.

With further development, electrical techniques would have wide practical applications in the civil engineering industry, in particular:

i) to assess the hydration characteristics of new cement blends, for example in the development of cementitious grouts, where rapid strength build-up may be required.

ii) It has been shown that water-cement ratio, type of cement, aggregate content and admixtures have a definite influence on the electrical response of cement paste, such techniques could be developed for the quality control of concrete and aid to mix-design.

iii) as a method for assessing setting time to allow for early striking of formwork so that maximum use could be made of formwork, and,

iv) to help in assessing the influence of admixtures on setting, hydration and microstructural development.

Further research can thus develop along two lines, further fundamental work and practical application. The following are worthy of further investigation:

a) Development of the technique for determining gel-structure, pore structure development, and crystal morphology. This should include the effect of a wider frequency range on the electrical response (resistivity and dielectric constant). The method should be extended to study the long-term microstructural development, in particular when admixtures[156] are used and when subjected to aggressive environments. The aim should be to assess durability.

b) It has been shown that the addition of aggregate, admixture, the curing condition, and chemical composition of cement have a definite influence on the electrical response. The development of the apparatus and introduction of a portable system for on-site investigation and control of the properties of fresh concrete (e.g. water-cement ratio, aggregate content and projected strength) could be a further practical application.

REFERENCES

1. Hirsch H
"Introductory remarks". Technology in the 1990's. Development in hydraulic cements.
Proc of a Royal Society discussion meeting 16-17 Feb, 1983. Published by the Royal Society.

2. Bechy A W and Hawes F L
"Action and reaction in concrete design 1935-1985"
Cement and Concrete Assoc, 1985.

3. Sudjic D, Jacobs A and Imerson M
"Hospital falls victim to the scourge of cancer"
The Sunday Times, 7 July 1985.

4. Connett D
"The faults that build up into disasters"
The Sunday Times, 7 July 1985.

5. Taylor M A and Arulanandan K
"Relationships between electrical and physical properties of cement pastes"
Cement & Concrete Research, Vol 4, 1974, Pergamon Press Inc, pp 881-897.

6. Mindness S and Young J F
"Concrete", 1981, Prentice-Hall, Eaglewood Cliffs, p 670.

7. Lea F M
"The chemistry of cement and concrete", Edward Arnold, London, 1970, p 727.

8. Neville A M
"Properties of concrete", Pitman 3rd Edition, London, 1981, p 779

9. Proc of the Symposium on the Chemistry of Cements, Stockholm,1938. Ingeniorsvetensakademie, Stockholm (1939).

10. Proc of the 3rd Int Symposium on the Chemistry of Cement, London, 1952. Cement & Concrete Assoc, London, 1954.

11. Proc of the 4th Int Symposium on the Chemistry of Cement, Washington, 1960. National Bureau of Standards Monograph 43, US Dept of Commerce (1962).

12. Proc of the 5th Int Symposium on the Chemistry of Cement, 1968, The Cement Assoc of Japan.

13. Proc of the 7th Int Symposium on the Chemistry of Cement, Paris, 1980.

14. Flint E P and Wells L S
"Study of the system $CaOSiO_2$-H_2O at 30° and the reaction of water on the anhydrous calcium silicates"
Int Res Nat But Stand 12 (1934), 751.

15. Parkinson I
"HAC: Panic over - lessons learned"
NCE, 10 Feb 1977, pp 24-25.

16. Parkinson I
"Stone's check-list will save HAC tests"
NCE, 14 Aug 1975, p 10.

17. Kurdowski W and Sorrentino F
"Structure and performance of cement"
Applied Science Publishers, P Barns (Ed), 1983,
pp 471-554.

18. Pollitt H W W
"The chemistry of cement"
Academic Press, London, H F W Taylor (Ed), 1964,
Chapter 1.

19. Kerton C P and Murray R J
"Structure and performance of cement"
Applied Science Publishers, B Barns (Ed), 1983,
pp 205-236.

20. Bucchi R
"Influence of the nature and preparation of raw materials on the reactivity of raw mix"
7th Int Congress on the Chemistry of Cement, Vol 1, Paris,
1980, 1-1/3 - 1-1/43.

21. Taylor H F W
"The chemistry of cements"
Academic Press, London & New York, Vol 1, 1964, p 459.

22. Griffith A A
"The phenomena of rupture and flow in solids"
Phil Trans Royal Society, London, 1920, 221, pp 16-98.

23. Kato A and Hirose K
"Factors in cement grinding process affecting strength of cement"
CAJ Review of the 23rd General Meeting (Techn Session),
Tokyo, 1969, pp 109-112.

24. Meric J P
"Influence of grinding and storage conditions of clinker"
7th Int Congress on the Chemistry of Cement, Vol 1, Paris,
1980, I-4/1 - I-4/16.

25. Sprung S
"Effect of the burning process on the formation of clinker"
7th Int Congress on the Chemistry of Cement, Vol 1, Paris,
1980, I-2/1 - I-2/17.

26. Dowell Schlumberger
"Cement in technology"
Chapter 3, Chemistry of Cement, New York, 1980

27. Carlson R W
"The significance of early heat liberation of cement paste"
Proc, Highway Research Board, 1937, Vol 17, pp 360-367.

28. Monfore G E and Ost B
"An isothermal conduction calorimeter for study of the early hydration reactions of Portland Cement"
Jnl of the PCA Research & Development Labs, 1966, Vol 8, Pt 2, pp 13-20.

29. Forester J A
"A conduction calorimeter for the study of cement hydration"
Cement Technology, 1970, May/June, pp 95-99.

30. Adams L D
"The measurement of very early hydration reaction of Portland Cement clinker by a thermoelectric conduction calorimeter"
Cement and Concrete Research, 1976, Vol 6, pp 293-307.

31. Kondo R and Veda S
"Kinetics and mechanisms of the hydration of cement"
Proc of 5th Int Symposium on the Chemistry of Cement, Tokyo, 1968, 2, 1969, p 203.

32. Skalny J S and Young J F
"Mechanisms of Portland Cement hydration"
7th Int Congress on the Chemistry of Cement, Vol 1, Paris, 1980, II-1/3 - II-1/45.

33. Jawad I, Skalny J S and Young J F
"Hydration of Portland Cement"
Structure and Performance of Cement, Applied Science Publications, Barns (Ed), 1983, pp 237-317.

34. Skalny J S, Jawad I and Taylor H F W
"Studies on hydration of cement - recent developments"
World Cement Technology, Sept 1978, pp 183-195.

35. Stein H N and Stevels J
"Influence of silica on the hydration of $3CaOsiO_2$"
Jnl Appl Chem, 14, 1964, p 338.

36. De Jong J G M, Stein H N and Stevels J M
"Hydration of tricalcium silicate"
Jnl Appl Chem, 17, 1967, p 246.

37. Stein H N
"The initial stages of the hydration of cement"
Cemento, 74, 1977, p 3.

38. Magnan R, Cottin B and Gardet J J
"Initial hydration of calcium binders"
Proc 6th Int Congress on the Chemistry of Cement, Moscow, 2(2), 1974, p 82.

39. Fujii K and Kondo W
"Kinetics of the hydration of tricalcium silicate"
Jnl Amer Ceram Soc, 57, 1974, p 473.

40. Double D D and Hellawell A
"The hydration of Portland Cement"
Nature, 261, London, 1976, pp 486-488.

41. Double D D and Hellawell A
"The solidification of cement"
Sci Amer, 237(7), 1977.

42. Double D D, Hellawell A and Perry S
"The hydration of Portland Cement"
Proc Royal Society, London, A359, 1978, p 435

43. Birchall J D, Howard A J and Bailly J E
"On hydration of Portland Cement"
Proc Royal Society, London, A360, 1978, p 445.

44. Powers T C
"Some physical aspects of the hydration of Portland Cement"
Jnl PCA Research & Development Labs, Jan 1961.

45. Young J F
"A review of the mechanisms of set-retardation in Portland Cement pastes containing organic admixtures"
Cement and Concrete Research, 2, No 4, 1972, pp 415-433.

46. Young J F, Tong H S and Berger R L
"Composition of solutions in contact with hydrating tricalcium silicate pastes"
Jnl Amer Ceram Soc, 1977, 60, p 193.

47. Slager P A and Rouxhel P G
"The hydration of tricalcium silicate calcium concentration and portlandite formation"
Cement and Concrete Research, Vol 7, No 1, 1977, pp 31-38.

48. Berger R L and Macgregor J D
"Effect of temperature and water-solid ratio on growth of $Ca(OH)_2$ crystal formed during hydration of Ca_3SiO_5"
Jnl Amer Ceram Soc, 56, 73.

49. Tadros M, Skalny J and Kalyoncu M
"Early hydration of C_3S"
Jnl Amer Ceram Soc, 1976, 59, p 344.

50. Glasser L, Lachowski E, Mohan K and Taylor H F W
"A multi-method study of C_3S hydration"
Cement Conc Res, 8, 2978, p 733.

51. Taylor H F W
"Cement hydration reaction: The silicate phase in cement production and use"
Proc Eng Found Conf. In press.

52. Menetrier D, McNamara D, Jawad I and Skalny J
"Effect of gypsum on C_3S hydration"
Jnl Cem Concr Res, 10, 1980, pp 697-701.

53. Breval E
"Gas phase and liquid phase hydration of C_3A"
Cem and Conc Res, 7, 1977, p 297.

54. Tadros M E, Jackson W Y and Skalny J
"Study of the dissolution and electrokinetic behaviour of tricalcium aluminate"
in Colloid and Interface Science, M Kerker (Ed), IV, 1976, p 211.

55. Skalny J and Tadros M E
"Retardation of tricalcium aluminate hydrate by sulphates"
Jnl Amer Ceram Soc, 60, 1977, p 174.

56. BS 4550: Part 3: Section 3.5: 1978
"Methods of testing cements"

57. Davies R E
"Admixtures come of age"
Concrete, Vol 18, No 12, Dec 1984, pp 13-15.

58. Young J F, Berger R L and Lawrence R V
"Studies on the early hydration of tricalcium silicate pastes. Influence of admixtures on hydration and strength development"
Cem & Concr Research, 3, No 6, Nov 1973, pp 689-700.

59. BS 5075: Part 1, 2 and 3: 1982
"Concrete admixtures"

60. Ashworth R
"Some investigations into the use of sugar as an admixture to concrete"
Proc Instn Civil Engrs, 31, London, June 1965, pp 129-145.

61. Bloem D L
"Preliminary tests of effect of sugar on strength of mortar"
Nat Ready-Mixed Concrete Assoc Public, Washington DC, Aug 1959.

62. Shideler J J
"Calcium chloride in concrete"
Jnl Amer Conc Inst, 48, Mar 1952, pp 537-559.

63. Prior M E and Adams A B
"Introduction to producers. Papers on water-reducing admixtures and set-retarding admixtures for concrete"
ASTM, SP Tech Publicn No 266, 1960, pp 170-179.

64. Vollick C A
"Effect of water-reducing admixtures and set-retarding admixtures on the properties of plastic concrete"
Ibid, pp 180-200.

65. Foster B
"Summary: Symposium on effect of water-reducing admixtures and set-retarding admixtures on properties of concrete"
Ibid, pp 240-246.

66. Brooks J J, Wainwright P J and Neville A M
"Time-dependent properties of concrete containing a superplasticizing admixture, superlasticizers in concrete"
Amer Conc Instn, SP Publicn No 62, 1979, pp 293-314.

67. Grudemo A
Proc 4th Int Symp Chem Cement, Washinton DC, 1960, NBC monograph 1962, 43, Vol II, pp 615-648.

68. Copeland L E and Schultz E G
Proc 4th Int Symp Chem Cement, Washinton DC, 1960, NBC monograph 1962, 43, Vol II, pp 648-655.

69. Copeland L E and Schultz E G
"Electron optical investigation of hydration products of calcium silicates and Portland Cement"
Jnl Portland Cem Assoc Res & Dev Labs, 4(1), Jan 1962, pp 2-12.

70. Kurczyk H G and Schwiete H A
Proc 4th Int Symp Chem Cement, Washinton DC, 1960, NBC monograph 1962, 43, Vol I, pp 349-358.

71. Chatterji S and Jeffery J W
"Three-dimensional arrangement of hydration products in set cement paste"
Nature, London, 209, 1966, pp 1233-1234.

72. Chatterji S and Jeffery J W
"Studies of early stages of paste hydration of different types of Portland Cement"
Jnl Amer Ceram Soc, 46(4), 1963, pp 187-191.

73. Richartz W
"Electron microscopic invesigation about the relation between structure and strength of hardened cement"
Proc 5th Int Symp Chem Cement, Tokyo, 1968, Vol III, pp 119-128.

74. Ciach T D and Swenson E G
"Morphology and microstructure of hydrating Portland Cement and its constitutents"
Cem and Conc Res, Vol 1, No 3, May 1971, pp 257-272.

75. Daimon M, Veda S and Kondo R
"Morphological study on hydration of tricalcium silicate"
Cem and Conc Res, 1, 1971, pp 391-401.

76. Diamond S
"Identification of hydrate of cement constituents using a scanning electron microscope/energy dispersive X-ray spectometer combination"
Cem and Conc Res, 2, 1972, pp 617-632.

77. Diamond S
"Cement paste microstructure - an overview at several levels"
Proc Conf Hydraulic Cement Pastes - their Structure and Properties, Cem Conc Assoc, Sheffield, 1976, pp 2-30.

78. Diamond S, Young J F and Lawrence F V
"Scanning electron microscopy - energy dispersive X-ray analysis of cement constituents - some cautions"
Jnl Conc Res, Vol 4, 6 Nov 1974, pp 899-914.

79. McCarter W J and Afshar A B
"A study of the early hydration of Portland Cement"
Proc Instn Civil Engrs, Pt 2, 79, Sept, 1985, pp 585-604.

80. Verbeck G
"Cement hydration reactions at early ages"
Jnl of PCA Res & Dev Labs, Vol 7, No 3, Sept 1965, pp 57-63.

81. Kantro D L and Copeland C H
"Quantitative determination of the major phases in Portland Cements by X-ray diffraction methods"
Jnl of the PCA Res & Dev Labs, 6, No 1, Jan 1964, pp 20-40.

82. Tian A
"Use of the dynamic chemical calorimetric method"
Bulletin Societe Chimique de France, Vol 33, No 4, 1923, pp 427-429.

83. Carlson R W
"The Vane Calorimeter"
Proc Amer Soc for Testing Materials, 34, Pt II, 1934 pp 322-328.

84. Thompson R A, Killah D C and Forrester J A
"Crystal chemistry and reactivity of MgO - stabilized alites"
Jnl of Amer Conc Soc, 1975, Vol 58, pp 54-57.

85. Karmazrin E and Murat M
"Study of Solid + Liquid → Solid reaction (hydration of calcium sulphate hemihydrate) by simultaneous isothermal calorimetry and electrical resistivity measurement"
Cem and Conc Res, Vol 8, 1978, pp 553-558.

86. Rao P P, Sutton D L et al
"An ultrasonic device for non-destructive testing of oilwell cements at elevated temperatures and pressures"
JPT, Nov 1982, pp 2611-2616.

87. Waters E H
(Discussion of a paper by Calleja J)
"New techniques in the study of setting and hardening of hydraulic materials"
Jnl Amer Conc Inst, Vol 24, 1952, pp 536-1-10.

88. Monfore G E
"The electrical restivity of concrete"'
Jnl of PCA Res & Dev Labs, May 1968, pp 35-48.

89. Woelfl G A and Lauer K
"The electrical resistivity of concrete with emphasis on the use of electrical resistance for measuring moisture content"
Cement, Concrete & Aggregate, Vol 1, No 2, 1979, pp 64-67.

90. Sriravindrarajah R and Swamy R N
"Development of a conductivity probe to monitor setting time and moisture movement in concrete"
Cement, Concrete and Aggregate, Vol 4, No 2, Winter 1982, pp 73-80.

91. McCarter W J, Forde M C and Whittington H W
"Resistivity characteristics of concrete"
Proc Instn of Civil Engrs, Pt 2, Res & Theory, Vol 71, March 1981, pp 107-117.

92. McCarter W J, Forde M C, Whittington H W and Simmons T
"Electrical resistivity characteristics of air-entrained concrete"
Proc Instn of Civil Engrs, Pt 2, Res & Theory, Vol 75, March 1983, pp 123-127.

93. Whittington H W, McCarter W J and Forde M C
"The conduction of electricity through concrete"
Mag of Conc Res, Vol 33, No 114, March 1981, pp 48-60.

94. McCarter W J
"Resistivity testing of piled foundations"
Thesis submitted Univ of Edinburgh, PhD, 1981, pp 96-153.

95. Archie G E
"The electrical resistivity log as an aid to determining some reservoir characteristics"
Trans Amer Soc Mining, Vol 146, 1942, pp 54-62.

96. Pirson S J
"Factors which affect true formation resistivity"
Oil and Gas Jnl, Vol 46, 1947, pp 76-81.

97. Wyllie M R J and Gregory A R
"Formation factors of unconsolidated porous media: Influence of particle shape and effect of cementation"
Petroleum Transaction, AIME, Vol 198, 1953, pp 103-110.

98. Wyllie M R J and Gregory A R
"The generalisation Kozeny-Carman equation, its application to problems of multi-phase flow in porous media"
World Oil, Production Section, Apr 1958, pp 210-228.

99. Lambe T W
"The structure of compacted clay"
Proc ASCE, Jnl of Soil Mech & Foundation Div, Vol 84, Pt SM2, 1958, pp 1654-1-33.

100. Mitchell J K and Arulanandan K
"Electrical dispersion in relation to soil structure"
Proc ASCE, Jnl of Soil Mech & Foundation Div, Vol 94, Pt SM2, Mar 1968, pp 447-471.

101. Hancox N L
"An electrical measurement of the effective cross-sectional area for conduction or flow processes in cement paste"
Mag of Conc Res, Vol 20, No 64, Sept 1968.

102. Petin N, Higeronitsch M and Gagrinovitsch E A
"A study of the setting process of cement paste by an electrical conductivity method"
Jnl of General Chemistry of USSR, Vol 2, 1932, pp 614-629.

103. Kind V A and Zhuraler V F
"Electrical conductivity of hardened Portland Cements"
Trement, Vol 5, No 9, 1937, pp 21-26.

104. Dorsch K E
"The hardening and corrosion of cement"
Cement & Cement Manf, Vol 6, No 4, Apr 1933, pp 21-26.

105. Langton N H
"The dielectric constant of zinc oxide over a range of frequencies"
British Jnl of Appl Physics, Vol 9, Nov 1958, pp 453-456.

106. Barr J P, Camps J P and Debuigne J
"Example and application of a method for measuring electrical impedance evolution of electrical conductivity"
Materials & Structures; Research & Testing, Vol 15, Pt 85, Jan 1982, pp 33-37.

107(a) Buenfield N R and Newman J B
"The permeability of concrete in a marine environment"
Mag of Concrete Research, Vol 36, No 127, June 1984.

107(b) Buenfield N R and Newman J B
"The resistivity of mortars immersed in sea-water"
Cem and Conc Res, Vol 16, 1986, pp 511-524.

108. Hill R M and Pickup C
"Barrier effects in dispersive media"
Jnl of Mat Sci, 20, 1985, pp 4431-4444.

109. McCarter W J and Curran P N
"The electrical response characteristics of setting cement paste"
Mag of Conc Res, Vol 36, No 126, March 1984, pp 42-49.

110. Cotton H
"Applied Electricity"
MacMillan & Co Ltd, Hume Press Ltd, London, 1966.

111. Lovell M C, Avery A J and Vernon M W
"Physical properties of materials"
Van Norstrand Reinhold Co, New York. Printed at the University Press, Cambridge, 1981.

112. McCarter W J and Curran P
"The electrical response characteristics of setting cement paste"
Closure to discussion.
Mag of Conc Res, Vol 37, No 130, March 1985, pp 52-53.

113. McCarter W J and Afshar A B
"Some aspects of the electrical properties of cement paste"
Jnl of Matl Sci and Letters 3(2984), pp 1083-1086.

114. McCarter W J and Afshar A B
"Further studies on the early hydration of Portland Cement paste"
Jnl of Matl Sci and Letters 4(1985), pp 405-408.

115. Afshar A B and McCarter W J
"Early hydration characteristics of aluminous cement"
Jnl of Matl Sci and Letters 4(1985), pp 851-854.

116. Hughes B P, Soleit A K O and Brierly R W
"New techniques for determining the electrical resistivity of concrete"
Mag Conc Res, Vol 37, No 133, Dec 1985, pp 243-248.

117. McCarter W J and Afshar A B
"Diagnostic monitoring of the physio-chemical processes in hydrating cement paste"
Cement, Concrete & Aggregate, CCAGDP, Vol 7, No 2, Winter 1985, pp 57-68.

118. Debye P
"Polar molecules"
Dover Publications Inc, New York, 1929, pp 43-56.

119. O'Dwyer J J and Harting E
"Theories of dielectric loss"
Progress in Dielectrics, Vol 7, (Ed: J B Birks), Heywood Books, London, 1967, pp 3-44.

120. Van Beck L K H
"Dielectric behaviour of heterogeneous systems"
Progress in Dielectrics, Vol 7, (Ed: J B Birks), Heywood Books, London, 1967, pp 71-94.

121. Maxwell J C
"A treatise on electricity and magnetism"
Oxford Univ Press, Vol 1, 1973, p 464.

122. Wagner K W
"Archimum elektrotechniki"
Warrow, 1914, Vol 2, p 371.

123. Schwan H P, Schwarz G, Maczuk J and Pauly H
"On the low-frequency dielectric dispersion of colloidal particles in electrolytic solutions"
Jnl of Physics & Chem, Vol 66, Dec 1962, p 2626.

124. Schwarz G
"A theory of the low-frequency dielectric disperson of colloidal particles in electrolyte solution"
Jnl of Physics & Chem, Vol 66, Dec 1962, p 2636.

125. Hasted J B
"Aqueous Dielectrics"
Chapman & Hall, London

126. Hartington J R
"An advanced treatise on physical chemistry"
Longmans, Green & Co, London, Vol V, 1954, pp 365-390.

127. Nikkannen P
"On electrical properties of concrete and their application"
Valtion Teknillinen Tulkimurlaitos, Tiedotus, Serja III, Rakennus 60. 1962 (In Finnish with English summary).

128. Hammond E and Robson T D
"Comparison of electrical properties of various cements and concrete"
The Engineer, Vol 199, 21 Jan 1975, pp 78-80.

129. Wayne Kerr Multi Bridge 6425 Operational Manual.

130. Hewlett Packard HP 3456A Digital Voltmeter Operating Manual No 03456-90005.

131. Hewlett Packard HP9000, Series 200/300 Instruction Manuals.

132. Hewlett Packard HP-IB Bus, Interface Owner's Manual, No 82937-90017.

133. Wayne Kerr Automatic Precision Bridge B905 Operating and Maintenance Manual, TP 202.

134. Hewlett packard HP-9915 Modular Computer System Development Manual No 09915-90010.

135. Calcomp, Model 84 Manual, 1983, California Computer Products Inc, USA.

136. BS 4550: Part 3: Section 3.5: 1978, "Methods of testing cement".

137. Private communication with Dr R S Dhariwal, Dept of Electrical & Electronic Eng, Heriot-Watt Univ, Edinburgh.

138. Mindness S
"Mechanical performance of cementitious systems"
Structure and Performance of Cement, Barns (Ed), Applied Science Publications, 1983, pp 319-363.

139. Shah S and Chandra S
"Fracture of concrete subjected to cyclic and sustained loading"
Jnl Amer Conc Inst, 67(10), 1970, p 816.

140. Oberholster R E, Van Hardt J H P and Brandt M P
"Durability of cementitious systems"
Structure and Performance of Cement, Barns P (Ed), Applied Science Publications, London, 1983, pp 365-413.

141. Davies R E
"Admixtures"
Concrete, Vol 18, No 12, Dec 1984, pp 13-15.

142. McCormack S
"Cement report seeks longer lasting concrete"
NCE, 20 Sept 1984, pp 4-5.

143. Pratt P L and Ghose A
"Electron microscope studies of Portland Cement microstructure during setting and hardening"
Phil Trans Roy Soc, London, A 310, 1983, pp 93-103.

144. Double D D
"New development in understanding the chemistry of cement hydration"
Phil Trans Roy Soc, London, A 310, 1983, pp 53-66.

145. Taylor H R W
Private communication, Univ of Aberdeen, May 1985.

146. Dalgleish B J amd Pratt P L
"Fractographic studies of microstructural development in hydrating Portland Cement"
Jnl Matl Sci, 17, 1982, pp 2199-2207.

147. Hadley D N
PhD thesis, School of Engineering, Purdue Univ, USA, 1972.

148. Tomas F D
"Electrical conductivity of cement paste"
Cement & Conc Res, Vol 12, No 1, 1982, pp 115-120.

149. Feldman R F and Sereda P J
"A model for hydrating Portland Cement paste as deduced from sorption-length change and mechanical properties"
Material and Structures, No 6, Nov-Dec 1968, Paris, pp 509-519.

150. Morelli R
"Resistivity testing of concrete"
Thesis submitted Univ of Edinburgh, PhD, 1985, p 220.

151. McCarter W J and Afshar A B
"A study of early hydration of Portland Cement"
Closure to discussion.
Proc Instn Civil Engrs, Pt 2, 81, June 1986, pp 305-308.

152. McCarter W J and Afshar A B
"A method for quantifying the effect of admixtures on the setting of cement"
Proc Instn Civil Engrs, (In print, Winter 1986).

153. McCarter W J and Afshar A B
"Monitoring chemico-physical changes and microstructure development in OPC during early hydration"
Presented at 8th Int Congress on the Chemistry of Cement, Sept 22-27, 1986, Rio-de-Janeiro, Vol 3, p 198.

154. Afshar A B and McCarter W J
"Monitoring the influence of admixtures and composition on the early hydration of cement paste using electrical response techniques"
Presented at 8th Int Congress on the Chemistry of Cement, Sept 22-27, 1986, Rio-de-Janeiro, Vol 3, p 193.

155. McCarter W J and Afshar A B
"A microcomputer controlled data acquisition system for monitoring cement hydration"
ASCE, (Technical Council on Computer Practices). In print.

156. McCurrich L H
"Reduction in permeability and chloride diffusion with superplasticisers"
Concrete, Vol 20, No 8, Aug 1986, pp 4-7.

APPENDIX 1

SAMPLE OF PROGRAMMES

THE CONTROL PROGRAMME

```
10    ! *CONTROL*
20    ! ************************************************************************
30    !
40    !                  THIS PROGRAMME WILL CONTROL THE OPERATION OF
50    !                   ALL THE INSTRUMENTS USED IN THE SYSTEM AND
60    !                  PLOT THE DISPERSION CURVES/DIELECTRIC CONSTANT,
70    !                   RESISTIVITY AND TEMPERATURE V TIME CURVES
80    ! ************************************************************************
90    BEEP
100   OUTPUT KBD;"K";
110   MASS STORAGE IS ":INTERNAL"
120   PRINTER IS 703
130   PRINT CHR$(27)&"&k2S"
140   CREATE BDAT "9TT037",260,16
150   CREATE BDAT "9CT037",260,224
160   CREATE BDAT "9RT037",260,224
170   ASSIGN @Path1 TO "9TT037"
180   ASSIGN @Path2 TO "9CT037"
190   ASSIGN @Path3 TO "9RT037"
200   OPTION BASE 1
210   DIM T(2)
220   DIM C(28)
230   DIM R(28)
240   REMOTE 722
250   REMOTE 706
260   REMOTE 703
300   LOCAL LOCKOUT 7
310   PRINTER IS 1
320   BEEP
330   PRINT "                              LABELING  DETAILS"
340   PRINT ""
350   PRINT ""
360   PRINT "Date eg:10,9,85"
370   INPUT A,D,E
380   IMAGE "DATE:",DD,"/",DD,"/",DD
390   OUTPUT 703 USING 380;A,D,E
400   BEEP
410   PRINT "Water:Cement ratio "
420   INPUT A
430   IMAGE  2/,"WATER:CEMENT RATIO =",D.DD
440   OUTPUT 703 USING 430;A
450   BEEP
460   PRINT "Mix Proportions:type PASTE if only cement & water."
470   PRINT "If mortar or concrete give mix ratio ie.Cement:Fine:Coarse"
480   INPUT D$
490   IMAGE 2/,"MIX PROPORTIONS:",15A
500   OUTPUT 703 USING 490;D$
510   BEEP
520   PRINT "If any admixtures have been added give type and % by weight.If no "
530   PRINT "admixtures have been added type NONE."
540   INPUT T$
550   IMAGE 2/,"ADMIXTURE :",15A
560   OUTPUT 703 USING 550;T$
570   BEEP
580   PRINT "Data File number:"
```

```
590   INPUT A$
600   IMAGE 2/,"DATA FILE NUMBER:",15A
610   OUTPUT 703 USING 600;A$
620   BEEP
630   PRINT "Starting Time"
640   INPUT G$
650   IMAGE 2/,"STARTING TIME:",15A
660   OUTPUT 703 USING 650;G$
670   BEEP
680   PRINT "Preparation time (in minutes)"
690   INPUT A
700   IMAGE 2/,"PREPARATION TIME=",2D,"minutes"
710   OUTPUT 703 USING 700;A
720   IMAGE 5/,"TIME",6X,"TEMP.",40X,"DIELECTRIC  CONSTANT & RESISTIVITY"
730   OUTPUT 703 USING 720
740   IMAGE "-----------------------------------------------------------
------------------------------------------------------"
750   OUTPUT 703 USING 740
760   IMAGE X,"Min.",6X,"C",6X,"20Hz",6X,"60Hz",6X,"100Hz",7X,"600Hz",7X,"1KHz",
7X,"6KHz",6X,"10KHz",6X,"60KHz",6X,"100KHz",5X,"300KHz"
770   OUTPUT 703 USING 760
780   T(1)=0
790   C(1)=0
800   R(1)=0
810   OUTPUT KBD;"K";
820   BEEP
830   PRINT "                AXES  SCALING  DETAILS"
840   PRINT ""
850   PRINT ""
860   PRINT "TIME AXIS        :maximum,minimum,scale increment"
870   INPUT Tmax,Tmin,Tinc
880   BEEP
890   PRINT "TIME AXIS        :major tic mark every ? divisions"
900   INPUT Ttic
910   BEEP
920   PRINT "DIELECTRIC AXIS :maximum,minimum,scale increment,exponent"
930   INPUT Dmax,Dmin,Dinc,Dexp
940   BEEP
950   PRINT "DIELECTRIC AXIS :Major tic mark every ? divisions"
960   INPUT Dtic
970   BEEP
980   PRINT "RESISTIVITY AXIS:Maximum,minimum,scale increment"
990   INPUT Rmax,Rmin,Rinc
1000  BEEP
1010  PRINT "RESISTIVITY AXIS:major tic mark every ? divisions"
1020  INPUT Rtic
1030  BEEP
1040  PRINT "TEMP. AXIS       :maximum,minimum,scale increment"
1050  INPUT Cmax,Cmin,Cinc
1060  BEEP
1070  PRINT "TEMP. AXIS       :major tic mark every ? divisions"
1080  INPUT Ctic
1090  BEEP
1100  PRINT ""
1110  PRINT ""
1120  PRINT "                  PRESS ANY NUMBER TO  START."
1130  INPUT A
1140  OUTPUT KBD;"K";
1150  GINIT
1160  GRAPHICS ON
1170  PLOTTER IS 3,"INTERNAL"
1180  VIEWPORT 0,133,0,100
1190  FRAME
1200  MOVE 0,50
1210  DRAW 133,50
1220  MOVE 69,0
1230  DRAW 69,100
1240  CSIZE 4,.5
1250  DEG
1260  LDIR 0
```

```
1270  MOVE 35,45
1280  LORG 6
1290  LABEL "DIEL./RES.V TIME"
1300  MOVE 100,45
1310  LABEL "TEMP. V TIME"
1320  MOVE 35,93
1330  LORG 6
1340  LABEL "DIEL.V FREQ."
1350  MOVE 105,93
1360  LORG 6
1370  LABEL "LOSS ANG. V FREQ"
1380  !-----------------------------
1390  !DIELECTRIC & RESISTIVITY AXIS
1400  !-----------------------------
1410  CSIZE 3,.5
1420  VIEWPORT 10,60,10,45
1430  WINDOW Tmin,Tmax,Dmin,Dmax
1440  AXES Tinc,Dinc,Tmin,Dmin,Ttic,Dtic,3
1450  CLIP OFF
1460  FOR Time=Tmin TO Tmax STEP Tinc*Ttic
1470  LORG 6
1480  MOVE Time,Dmin-Dinc/5
1490  LABEL USING "#,K";Time
1500  NEXT Time
1510  FOR Diel=Dmin TO Dmax STEP Dinc*Dtic
1520  MOVE -Tinc/4,Diel
1530  LORG 8
1540  LABEL USING "#,K";Diel/10^Dexp
1550  NEXT Diel
1560  LORG 4
1570  LDIR 90
1580  MOVE -Tinc,(Dmax-Dmin)/2
1590  LABEL USING 1600;Dexp
1600  IMAGE "Diel. Const.(x10^",K,")"
1610  LDIR 0
1620  LORG 6
1630  MOVE (Tmax-Tmin)/2,Dmin-Dinc/2
1640  LABEL "Time(mins.)"
1650  CLIP ON
1660  VIEWPORT 10,60,10,45
1670  WINDOW Tmin,Tmax,Rmin,Rmax
1680  AXES Tinc,Rinc,Tmax,Rmin,Ttic,Rtic,3
1690  CLIP OFF
1700  FOR Resty=Rmin TO Rmax STEP Rinc*Rtic
1710  LDIR 0
1720  LORG 2
1730  MOVE Tmax+Tinc/4,Resty
1740  LABEL USING "#,K";Resty
1750  NEXT Resty
1760  LDIR 90
1770  LORG 4
1780  MOVE Tmax-Tinc/2,(Rmax-Rmin)/2
1790  LABEL "Resistivity"
1800  !--------------------
1810  !TEMPERATURE AXIS
1820  !--------------------
1830  VIEWPORT 75,125,10,45
1840  WINDOW Tmin,Tmax,Cmin,Cmax
1850  AXES Tinc,Cinc,Tmin,Cmin,Ttic,Ctic,3
1860  CLIP OFF
1870  FOR Time=Tmin TO Tmax STEP Tinc*Ttic
1880  LDIR 0
1890  LORG 6
1900  MOVE Time,Cmin-Cinc/4
1910  LABEL USING "#,K";Time
1920  NEXT Time
1930  MOVE (Tmax-Tmin)/2,Cmin-Cinc
1940  LABEL "Time(mins.)"
1950  LORG 8
1960  FOR Temp=Cmin TO Cmax STEP Cinc*Ctic
```

```
1970  MOVE -Tinc/4,Temp
1980  LABEL USING "#,K";Temp
1990  NEXT Temp
2000  MOVE Tinc,(Cmax+Cmin)/2
2010  LORG 6
2020  LDIR 90
2030  LABEL "Temp."
2040  !--------------------
2050  !DISPERSION CURVE
2060  !--------------------
2070  VIEWPORT 10,60,58,93
2080  WINDOW 1,6,1,9
2090  AXES 1,1,1,1,1,2,2
2100  CLIP OFF
2110  LDIR 0
2120  FOR F=1 TO 6
2130  MOVE F,.5
2140  LORG 9
2150  LABEL "10"
2160  NEXT F
2170  FOR F=1 TO 6
2180  MOVE F,.25
2190  LORG 1
2200  LABEL USING "#,K";F
2210  NEXT F
2220  MOVE .25,5
2230  LORG 5
2240  LDIR 90
2250  LABEL "Diel.Const"
2260  FOR D=1 TO 9 STEP 2
2270  MOVE .75,D
2280  LDIR 0
2290  LORG 8
2300  LABEL "10"
2310  NEXT D
2320  FOR D=1 TO 9 STEP 2
2330  MOVE .75,D
2340  LORG 1
2350  LABEL USING "#,K";D
2360  NEXT D
2370  !-----------------
2380  !LOSS ANGLE CURVE
2390  !-----------------
2400  VIEWPORT 79,129,58,93
2410  WINDOW 1,6,0,200
2420  AXES 1,50,1,0,1,2,2
2430  CLIP OFF
2440  FOR F=1 TO 6
2450  MOVE F,-15
2460  LORG 9
2470  LABEL "10"
2480  NEXT F
2490  FOR F=1 TO 6
2500  MOVE F,-22
2510  LORG 1
2520  LABEL USING "#,K";F
2530  NEXT F
2540  FOR I=0 TO 200 STEP 50
2550  MOVE .75,I
2560  LORG 8
2570  LABEL USING "#,K";I
2580  NEXT I
2590  FOR I=1 TO 260
2600  OUTPUT 722;"M6T1R1F4"
2610  TRIGGER 722
2620  ENTER 722;T(2)
2630  OUTPUT 706;"PAR;AUT;C;R;SLO;SIN"
2640  FOR M=20 TO 120 STEP 20
2650  IMAGE "FREQ",K,";TRG"
2660  OUTPUT 706 USING 2650;M
```

```
2670  ENTER 706;A
2680  ENTER 706;W
2690  ENTER 706;Q
2700  ENTER 706;S
2701  IF W<0 THEN 2660
2702  IF Q<0 THEN 2660
2710  G=1+M/20
2720  C(G)=1.564E+12*W
2730  R(G)=Q*.1
2740  NEXT M
2750  FOR J=200 TO 1200 STEP 200
2760  IMAGE "FREQ",K,";TRG"
2770  OUTPUT 706 USING 2760;J
2780  ENTER 706;A
2790  ENTER 706;W
2800  ENTER 706;Q
2810  ENTER 706;S
2811  IF W<0 THEN 2770
2812  IF Q<0 THEN 2770
2820  G=7+J/200
2830  C(G)=1.564E+12*W
2840  R(G)=Q*.1
2850  NEXT J
2860  FOR J=2000 TO 12000 STEP 2000
2870  IMAGE "FREQ",K,";TRG"
2880  OUTPUT 706 USING 2870;J
2890  ENTER 706;A
2900  ENTER 706;W
2910  ENTER 706;Q
2920  ENTER 706;S
2921  IF W<0 THEN 2880
2922  IF Q<0 THEN 2880
2930  G=13+J/2000
2940  C(G)=1.564E+12*W
2950  R(G)=Q*.1
2960  NEXT J
2970  FOR H=20000 TO 120000 STEP 20000
2980  G=19+H/20000
2990  IF H=80000 THEN H=H-5000
3000  IMAGE "FREQ",K,";TRG"
3010  OUTPUT 706 USING 3000;H
3020  ENTER 706;A
3030  ENTER 706;W
3040  ENTER 706;Q
3050  ENTER 706;S
3051  IF W<0 THEN 3010
3052  IF Q<0 THEN 3010
3060  C(G)=1.564E+12*W
3070  R(G)=Q*.1
3080  IF H=75000 THEN H=H+5000
3090  NEXT H
3100  OUTPUT 706;"FREQ150E3;TRG"
3110  ENTER 706;A
3120  ENTER 706;W
3130  ENTER 706;Q
3140  ENTER 706;S
3141  IF W<0 THEN 3100
3142  IF Q<0 THEN 3100
3150  C(26)=1.564E+12*W
3160  R(26)=Q*.1
3170  OUTPUT 706;"FREQ200E3;TRG"
3180  ENTER 706;A
3190  ENTER 706;W
3200  ENTER 706;Q
3210  ENTER 706;S
3211  IF W<0 THEN 3170
3212  IF Q<0 THEN 3170
3220  C(27)=1.564E+12*W
3230  R(27)=Q*.1
3240  OUTPUT 706;"FREQ300E3;TRG"
```

```
3250  ENTER 706;A
3260  ENTER 706;W
3270  ENTER 706;Q
3280  ENTER 706;S
3281  IF W<0 THEN 3240
3282  IF Q<0 THEN 3240
3290  C(28)=1.564E+12*W
3300  R(28)=Q*.1
3310  OUTPUT @Path1,I;T(*)
3320  OUTPUT @Path2,I;C(*)
3330  OUTPUT @Path3,I;R(*)
3340  IMAGE DDDD,2X,MDDD.DD,2X,DD.DDE,2X,DD.DDE,2X,DD.DDE,2X,DD.DDE,2X,DD.DDE,2X
,DD.DDE,2X,DD.DDE,2X,DD.DDE,2X,DD.DDE,2X,DD.DDE,2X,DD.DDE
3350  OUTPUT 703 USING 3340;T(1),T(2),C(2),C(4),C(6),C(10),C(12),C(16),C(18),C(2
2),C(24),C(28)
3360  IMAGE 15X,DD.DDE,2X,DD.DDE,2X,DD.DDE,2X,DD.DDE,2X,DD.DDE,2X,DD.DDE,2X,DD.D
DE,2X,DD.DDE,2X,DD.DDE,2X,DD.DDE
3370  OUTPUT 703 USING 3360;R(2),R(4),R(6),R(10),R(12),R(16),R(18),R(22),R(24),R
(28)
3380  IMAGE "-----------------------------------------------------------------
--------------------------------------------------"
3390  OUTPUT 703 USING 3380
3400  !-------------------------------------------------
3410  !Lines 1490  to 1610 plot results every reading cycle
3420  !Dielectric and Resistivity curves given for 1000Hz.
3430  !-------------------------------------------------
3440  VIEWPORT 10,60,10,45
3450  WINDOW Tmin,Tmax,Dmin,Dmax
3460  MOVE C(1),C(12)
3470  PLOT C(1),C(12)
3480  VIEWPORT 10,60,10,45
3490  WINDOW Tmin,Tmax,Rmin,Rmax
3500  MOVE R(1),R(12)
3510  PLOT R(1),R(12)
3520  VIEWPORT 75,125,10,45
3530  WINDOW Tmin,Tmax,Cmin,Cmax
3540  MOVE T(1),T(2)
3550  PLOT T(1),T(2)
3560  A=C(1)/200 !Plots Dispersion /Loss Curves every 200 mins.
3570  IF FRACT(A)=0 THEN 3590
3580  GOTO 4070
3590  !-------------------------------------
3600  !Dispersion / Loss plotting subroutine
3610  !-------------------------------------
3620  VIEWPORT 10,60,58,93
3630  WINDOW 1,6,1,9
3640  FOR J=2 TO 28 STEP 1
3650  IF J<=7 THEN F=20*J-20
3660  IF J>7 AND J<=13 THEN F=200*J-1400
3670  IF J>13 AND J<=19 THEN F=2000*J-26000
3680  IF J>19 AND J<=25 THEN F=20000*J-380000
3690  IF J=26 THEN F=1.50E+5
3700  IF J=27 THEN F=2.00E+5
3710  IF J=28 THEN F=3.00E+5
3720  IF F=80000 THEN F=F-5000
3730  H=LGT(C(J))
3740  F=LGT(F)
3750  IF J=2 THEN 3820
3760  IF FRACT(A/2)=0 THEN 3790 !Plots dashed line every 400,800...mins
3770  LINE TYPE 1  !Solid line every 200,600....mins
3780  GOTO 3800
3790  LINE TYPE 4
3800  DRAW F,H
3810  GOTO 3830
3820  MOVE F,H
3830  NEXT J
3840  VIEWPORT 79,129,58,93
3850  WINDOW 1,6,0,200
3860  FOR J=2 TO 28 STEP 1
3870  IF J<=7 THEN F=20*J-20
```

```
3880  IF J>7 AND J<=13 THEN F=200*J-1400
3890  IF J>13 AND J<=19 THEN F=2000*J-26000
3900  IF J>19 AND J<=25 THEN F=20000*J-380000
3910  IF J=26 THEN F=1.50E+5
3920  IF J=27 THEN F=2.00E+5
3930  IF J=28 THEN F=3.00E+5
3940  IF F=80000 THEN F=F-5000
3950  H=1/(2*PI*F*R(J)*C(J)*8.84E-12)
3960  F=LGT(F)
3970  IF J=2 THEN 4040
3980  IF FRACT(A/2)=0 THEN 4010 !Plots dashed line every 400,800...mins
3990  LINE TYPE 1 !Solid line every 200,600...mins
4000  GOTO 4020
4010  LINE TYPE 4
4020  DRAW F,H
4030  GOTO 4050
4040  MOVE F,H
4050  NEXT J
4060  !-------------------------
4070  WAIT 250
4080  T(1)=T(1)+5
4090  C(1)=C(1)+5
4100  R(1)=R(1)+5
4110  NEXT I
4120  ASSIGN @Path1 TO *
4130  ASSIGN @Path2 TO *-   -
4140  ASSIGN @Path3 TO *
4150  !--------------
4160  !Graphics Dump
4170  !--------------
4180  INTEGER Device_selector
4190  Device_selector=703
4200  OUTPUT 703 USING 4210
4210  IMAGE 5/
4220  CALL Graphics_dump(Device_selector)
4230  PRINT "The dump is complete.That is the test over"
4240  PRINTER IS 1
4250  END
4260 SUB Graphics_dump(INTEGER Device_selector)
4270!  82905DUMP  Dumps Graphics to HP82905B printer SECURED CODE
4280*
4290*
4300*
4310*
4320*
4330*
4340*
4350*
4360*
4370*
4380*
4390*
4400*
4410*
4420*
4430*
4440*
4450*
4460*
4470*
4480*
4490*
4500*
4510*
4520*
4530*
4540*
4550*
4560*
4570*
```

TYPICAL PLOTTING PROGRAMME

```
10    !PLOTTER
20    PRINTER IS 1
30    BEEP
40    PRINT "                                LABELING  DETAILS "
50    PRINT ""
60    PRINT ""
70    PRINT "Graph Number"
80    INPUT G
90    BEEP
91    PRINT ""
100   PRINT "Water/Cement Ratio"
110   INPUT Wc
120   BEEP
121   PRINT ""
130   PRINT "Type of cement eg.OPC,HAC."
140   INPUT T$
150   BEEP
151   PRINT ""
160   PRINT "Cement paste,Mortar or Concrete.If no aggregate type PASTE."
170   PRINT "If Mortar or Concrete give mix proportions ie.Cement:Fine:Coarse (b
y weight)"
180   INPUT M$
190   BEEP
191   PRINT ""
200   PRINT "If any admixture has been added give type & % (by weight)."
210   PRINT "If no admixture has been added type NONE "
220   INPUT A$
230   BEEP
231   PRINT ""
240   PRINT "Select Frequency you require plot (in Hz) eg. 20,1000 etc."
250   INPUT Fq
260   OUTPUT KBD;"K";
270   PRINT "                    AXIS SCALING DETAILS"
280   PRINT ""
290   PRINT ""
300   BEEP
310   PRINT "TIME AXIS        :maximum,minimum,scale increment"
320   INPUT Tmax,Tmin,Tinc
330   BEEP
331   PRINT ""
340   PRINT "DIELECTRIC AXIS :maximum,minimum,scale increment,exponent"
350   INPUT Dmax,Dmin,Dinc,Dexp
360   BEEP
361   PRINT ""
370   PRINT "RESISTIVITY AXIS:maximum,minimum,scale increment"
380   INPUT Rmax,Rmin,Rinc
390   BEEP
391   PRINT ""
400   PRINT "TEMP. AXIS       :maximum,minimum,scale increment"
410   INPUT Cmax.Cmin.Cinc
```

```
420   BEEP
421   PRINT ""
430   PRINT "TIME AXIS        :major TIC mark every ? divisions"
440   INPUT Ttic
450   BEEP
451   PRINT ""
460   PRINT "DIELECTRIC AXIS :major TIC mark every ? divisions"
470   INPUT Dtic
471   PRINT ""
480   PRINT "RESISTIVITY AXIS:major TIC mark every ? divisions"
490   BEEP
500   INPUT Rtic
510   BEEP
511   PRINT ""
520   PRINT "TEMP. AXIS       :major TIC mark every ? divisions"
530   INPUT Ctic
531   PRINT ""
532   PRINT ""
540   BEEP
550   PRINT "                  Enter preperation time."
560   INPUT Pt
570   OUTPUT KBD;"K";
580   GINIT
590   PLOTTER IS 705,"HPGL"
600   GRAPHICS ON
610   OUTPUT 705;"VS10"
620   OUTPUT 705;"SP1"
630   VIEWPORT 0,140,0,100
640   FRAME
650   MOVE 11,7
660   LORG 2
670   CSIZE 4,.5
680   LABEL "FIG.";G
690   MOVE 28,7
700   LABEL "Variation of electrical parameters and internal"
710   MOVE 28,4
720   LABEL "     temperature over initial 24-hours."
730   MOVE 5,97
740   CSIZE 3,.5
750   LABEL "W/C Ratio:0";Wc
760   MOVE 5,94
770   LABEL "Cement    :";T$
780   MOVE 5,91
790   LABEL "Admixture:";A$
800   MOVE 5,88
810   LABEL "Mix       :";M$
820   MOVE 100,97
830   LABEL "Frequency=";Fq;"Hz"
840   VIEWPORT 15,115,15,80
850   WINDOW Tmin,Tmax,Dmin,Dmax
860   AXES Tinc,Dinc,Tmin,Dmin,Ttic,Dtic,3
870   MOVE -1.3*Tinc,(Dmax-Dmin)/2
880   DEG
890   LDIR 90
900   LORG 6
910   CLIP OFF
920   LABEL USING 930;Dexp
930   IMAGE "DIELECTRIC CONSTANT(x10^",K,")"
940   LDIR 0
950   MOVE (Tmax-Tmin)/2,(Dmin-.1*Dinc)
960   LORG 6
970   LABEL "TIME(mins.)"
980   CLIP ON
990   WINDOW Tmin,Tmax,Rmin,Rmax
1000  AXES Tmax,Rinc,Tmax,Rmin,Ttic,Rtic,3
1010  MOVE (Tmax-1.3*Tinc),(Rmax-Rmin)/2
1020  LORG 4
1030  CLIP OFF
1040  LDIR 90
1050  LABEL "RESISTIVITY(Ohm-m)"
```

```
1060  VIEWPORT 15,120,15,80
1070  WINDOW Tmin,Tmax,Cmin,Cmax
1080  CLIP ON
1090  AXES Tmax,Cinc,Tmax,Cmin,Ttic,Ctic,3
1100  VIEWPORT 15,115,15,80
1110  CLIP OFF
1120  LDIR 0
1130  FOR Time=Tmin TO Tmax STEP Tinc*Ttic
1140  WINDOW Tmin,Tmax,Dmin,Dmax
1150  LORG 6
1160  MOVE Time,-Dinc/5
1170  LABEL USING "#,K";Time
1180  NEXT Time
1190  FOR Diel=Dmin TO Dmax STEP Dinc*Dtic
1200  WINDOW Tmin,Tmax,Dmin,Dmax
1210  CLIP OFF
1220  MOVE -Tinc/4,Diel
1230  LORG 8
1240  LABEL USING "#,K";Diel/10^Dexp
1250  NEXT Diel
1251  MOVE 0,0
1260  FOR Resty=(Rmin+Rinc)*Rtic TO Rmax STEP Rinc*Rtic
1261  VIEWPORT 15,115,15,80
1270  WINDOW Tmin,Tmax,Rmin,Rmax
1271  CLIP OFF
1280  MOVE 1450,Resty
1290  LORG 8
1300  LABEL USING "#,K";Resty
1310  NEXT Resty
1320  FOR Temp=Cmin TO Cmax STEP Cinc*Ctic
1330  VIEWPORT 15,120,15,80
1340  WINDOW Tmin,Tmax,Cmin,Cmax
1350  CLIP OFF
1360  MOVE 1520,Temp
1370  LORG 2
1380  LABEL USING "#,K";Temp
1390  NEXT Temp
1400  MOVE (Tmax+1.3*Tinc),(Cmax+Cmin)/2
1410  LDIR 90
1420  LORG 4
1430  LABEL "TEMPERATURE (Deg C)"
1440  OPTION BASE 1
1450  DIM T(2)
1460  DIM C(28)
1470  DIM R(28)
1480  !-------------------------------------------------------
1490  !Dielectric Constant,Resistivity & Temperature Vs. Time.
1500  !-------------------------------------------------------
1510  GOSUB 2170
1520  IF Fq=75000 THEN Fq=Fq+5000
1530  IF Fq<=120 THEN M=1+Fq/20
1540  IF Fq>120 AND Fq<=1200 THEN M=7+Fq/200
1550  IF Fq>1200 AND Fq<=12000 THEN M=13+Fq/2000
1560  IF Fq>12000 AND Fq<=120000 THEN M=19+Fq/20000
1570  IF Fq=1.50E+5 THEN M=26
1580  IF Fq=2.00E+5 THEN M=27
1590  IF Fq=3.00E+5 THEN M=28
1600  !------------------------
1610  VIEWPORT 15,115,15,80
1620  WINDOW Tmin,Tmax,Dmin,Dmax
1630  MOVE Tmin,Dmin
1640  OUTPUT 705;"SP2"
1650  FOR I=1 TO 255 STEP 1
1660  ENTER @Path2,I;C(*)
1670  IF I=1 THEN 1710
1680  LINE TYPE 1
1690  DRAW (C(1)+Pt),C(M)
1700  GOTO 1720
1710  MOVE (C(1)+Pt),C(M)
1720  NEXT I
```

```
1730  ASSIGN @Path2 TO *
1740  !-------------------------
1750  VIEWPORT 15,115,15,80
1760  WINDOW Tmin,Tmax,Rmin,Rmax
1770  MOVE Tmin,Rmin
1780  OUTPUT 705;"SP3"
1790  FOR I=1 TO 255 STEP 1
1800  ENTER @Path3,I;R(*)
1810  IF I=1 THEN 1850
1820  LINE TYPE 1
1830  DRAW (R(1)+Pt),R(M)
1840  GOTO 1860
1850  MOVE (R(1)+Pt),R(M)
1860  NEXT I
1870  ASSIGN @Path3 TO *
1880  !-------------------------
1890  VIEWPORT 15,115,15,80
1900  WINDOW Tmin,Tmax,Cmin,Cmax
1910  MOVE Tmin,Cmin
1920  OUTPUT 705;"SP4"
1930  FOR I=1 TO 255 STEP 1
1940  ENTER @Path1,I;T(*)
1950  PLOT (T(1)+Pt),T(2)
1960  NEXT I
1970  ASSIGN @Path1 TO *
1980  !-------------------------
1990  LDIR 0
2000  LORG 2
2010  VIEWPORT 0,140,0,100
2020  WINDOW 0,140,0,100
2030  OUTPUT 705;"SP2"
2040  MOVE 50,95
2050  DRAW 65,95
2060  LABEL " Dielectric Constant"
2070  OUTPUT 705;"SP3"
2080  MOVE 50,90
2090  DRAW 65,90
2100  LABEL " Resistivity"
2110  OUTPUT 705;"SP4"
2120  MOVE 50,85
2130  DRAW 65,85
2140  LABEL " Temperature"
2150  MOVE 0,0
2160  GOTO 2240
2170  !-----------------------------------
2180  !Open Data Files
2190  ASSIGN @Path2 TO "9CT034"
2200  ASSIGN @Path3 TO "9RT034"
2210  ASSIGN @Path1 TO "9TT034"
2220  RETURN
2230  !-----------------------------------
2240  END
```

TYPICAL SET OF RESULTS WITH GRAPHICAL OUTPUT

DATE:20/ 5/86

WATER:CEMENT RATIO = .27

MIX PROPORTIONS:O.P.C./PASTE

ADMIXTURE :NONE

DATA FILE NUMBER:9WK061

STARTING TIME:10.40AM

PREPARATION TIME=10minutes

TIME	TEMP.	DIELECTRIC CONSTANT & RESISTIVITY									
Min.	C	20Hz	60Hz	100Hz	600Hz	1KHz	6KHz	10KHz	60KHz	100KHz	300KHz
0	27.02	88.60E+07	27.04E+07	13.18E+07	62.14E+05	24.37E+05	84.30E+03	35.42E+03	10.01E+03	95.40E+02	86.02E+02
		98.90E-02	66.44E-02	59.10E-02	51.00E-02	50.52E-02	50.02E-02	50.02E-02	50.04E-02	50.04E-02	50.40E-02
5	27.46	92.35E+07	27.93E+07	13.53E+07	63.08E+05	24.71E+05	85.08E+03	35.42E+03	10.32E+03	97.75E+02	89.15E+02
		99.63E-02	65.28E-02	57.90E-02	49.98E-02	49.52E-02	49.05E-02	49.04E-02	49.06E-02	49.08E-02	49.50E-02
10	27.54	94.58E+07	28.59E+07	13.82E+07	64.05E+05	25.06E+05	86.02E+03	35.82E+03	10.48E+03	10.01E+03	90.71E+02
		10.04E-01	64.64E-02	57.20E-02	49.33E-02	48.89E-02	48.43E-02	48.43E-02	48.46E-02	48.50E-02	48.90E-02
15	27.50	94.37E+07	28.21E+07	13.56E+07	62.18E+05	24.31E+05	83.36E+03	34.25E+03	10.32E+03	97.75E+02	89.15E+02
		10.14E-01	65.01E-02	57.61E-02	49.88E-02	49.45E-02	49.03E-02	49.04E-02	49.10E-02	49.14E-02	49.60E-02
20	27.48	94.13E+07	27.84E+07	13.32E+07	60.78E+05	23.76E+05	81.48E+03	34.72E+03	10.17E+03	96.97E+02	87.58E+02
		10.16E-01	65.25E-02	57.92E-02	50.29E-02	49.87E-02	49.44E-02	49.44E-02	49.50E-02	49.52E-02	49.90E-02
25	27.46	94.20E+07	27.75E+07	13.26E+07	60.17E+05	23.51E+05	81.17E+03	33.86E+03	10.17E+03	96.19E+02	87.58E+02
		10.26E-01	65.46E-02	58.11E-02	50.49E-02	50.07E-02	49.65E-02	49.65E-02	49.70E-02	49.72E-02	50.10E-02
30	27.46	94.22E+07	27.63E+07	13.17E+07	59.54E+05	23.26E+05	80.39E+03	33.63E+03	10.17E+03	96.19E+02	87.58E+02
		10.30E-01	65.59E-02	58.25E-02	50.69E-02	50.27E-02	49.84E-02	49.85E-02	49.90E-02	49.92E-02	50.30E-02
35	27.47	94.15E+07	27.51E+07	13.09E+07	58.93E+05	23.02E+05	79.45E+03	33.31E+03	10.01E+03	95.40E+02	86.02E+02
		10.35E-01	65.77E-02	58.42E-02	50.89E-02	50.47E-02	50.05E-02	50.05E-02	50.10E-02	50.12E-02	50.50E-02
40	27.49	94.04E+07	27.31E+07	12.97E+07	58.23E+05	22.73E+05	78.67E+03	33.00E+03	10.01E+03	94.62E+02	86.02E+02
		10.33E-01	65.88E-02	58.58E-02	51.11E-02	50.69E-02	50.27E-02	50.28E-02	50.32E-02	50.34E-02	50.70E-02
45	27.54	93.85E+07	27.19E+07	12.89E+07	57.66E+05	22.54E+05	77.89E+03	32.77E+03	98.53E+02	93.84E+02	86.02E+02
		10.41E-01	66.12E-02	58.80E-02	51.34E-02	50.93E-02	50.51E-02	50.51E-02	50.56E-02	50.58E-02	51.00E-02
50	27.60	93.60E+07	26.99E+07	12.77E+07	57.01E+05	22.27E+05	77.11E+03	32.45E+03	98.53E+02	93.84E+02	84.46E+02
		10.42E-01	66.30E-02	59.01E-02	51.59E-02	51.18E-02	50.77E-02	50.77E-02	50.82E-02	50.84E-02	51.20E-02
55	27.68	93.28E+07	26.86E+07	12.69E+07	56.48E+05	22.05E+05	76.32E+03	32.22E+03	98.53E+02	93.06E+02	84.46E+02
		10.54E-01	66.62E-02	59.29E-02	51.87E-02	51.46E-02	51.05E-02	51.05E-02	51.10E-02	51.12E-02	51.50E-02
60	27.78	92.94E+07	26.64E+07	12.57E+07	55.77E+05	21.77E+05	75.38E+03	31.75E+03	96.97E+02	92.28E+02	84.46E+02
		10.55E-01	66.86E-02	59.55E-02	52.17E-02	51.76E-02	51.35E-02	51.35E-02	51.40E-02	51.42E-02	51.80E-02

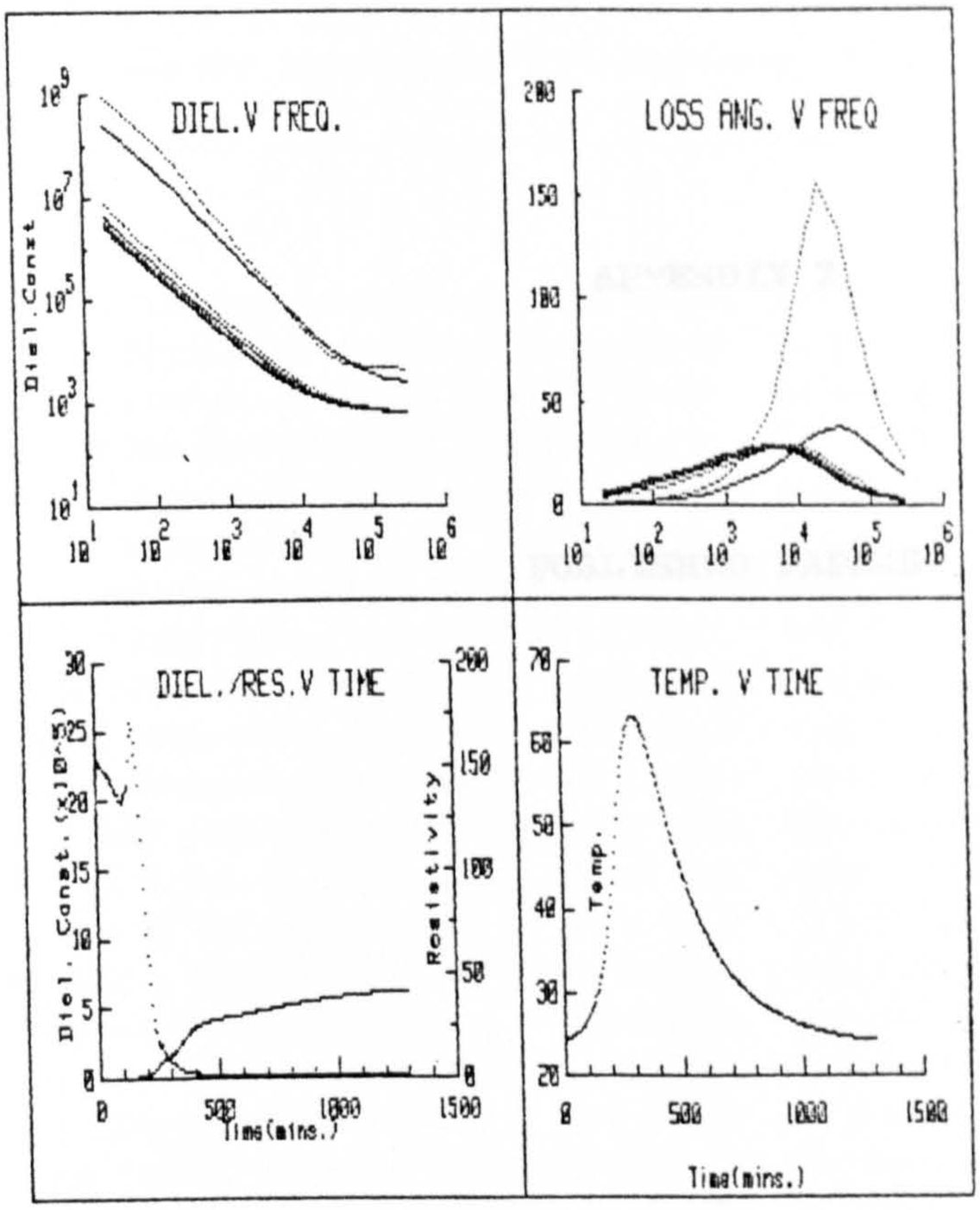

The dump is complete.That is the test over

APPENDIX 2

PUBLISHED PAPERS

JOURNAL OF MATERIALS SCIENCE LETTERS 3 (1984) 1083–1086

Some aspects of the electrical properties of cement paste

W. J. McCARTER, A. B. AFSHAR
Heriot-Watt University, Department of Civil Engineering, Riccarton Campus, Edinburgh, UK

Over the last few years attention has been drawn to the use of electrical properties of cement paste as a technique for measuring the degree of hydration, and hence hardening and strength characteristics of the paste [1–3]. This previous work, however, has concentrated on measuring the change in electrical resistivity of cement pastes, mortars and concretes up to periods of 250 days, with little attention given to the initial 24 h after mixing with water. This letter describes a preliminary investigation into the electrical properties of cement pastes during the first 24 h after gauging with water. It is during this period that the viscosity of the cement paste increases as it changes from a fluid to rigid state. Attention has been directed towards monitoring the change in dielectric constant, electrical resistivity and loss angle over this period to establish if there is any correlation between changes in the physical and chemical state of the paste and changes in the measured electrical parameters.

The raw materials used in the manufacture of cement consist mainly of lime, silica, alumina and iron oxide. Four compounds are usually regarded [4–6] as the major constituents of cement and in a typical ordinary Portland cement (OPC) are, by percentage weight, 60% C_3S (tricalcium silicate, $3CaOSiO_3$); 15% C_2S (diacalcium silicate, $2CaOSiO_2$); 10% C_3A (tricalcium aluminate, $3CaOAl_2O_3$); 9% C_4AF (tetracalcium-aluminoferrite, $4CaOAl_2O_3Fe_2O_3$). The remaining percentage consists of minor compounds, e.g. MgO, TiO_2, Mn_2O_3, K_2O and Na_2O. The two calcium silicates are the main cementitious compounds in cement and the physical behaviour of cement is largely dictated by these compounds [7].

When OPC is mixed with water a series of complicated chemical reactions begin to take place. The reaction of cement clinker and water proceeds at different rates for the various mineral phases and involves both hydrolysis and hydration processes. The main events that take place during the setting process of a normal paste are visualised as proceeding through four stages [8–10] – an inital supersaturation of the gauging water with Ca^{2+} and OH^- ions and other minor ions leached out of the cement grains, primarily, SO_4^{2-}, Na^+, K^+ and an initial coating of hydration products (gel) on the cement grains; a period of little activity as the gel builds up on the grains and retards the reaction; a period of renewed chemical activity as the hydration products on the C_3S phase rupture and expose unhydrated cement grain surfaces; this is followed by the fourth stage or period of hardening.

The instrumentation used in the experimental programme comprises a Wayne–Kerr automatic precision bridge (B905) which was used to measure both the in-phase and quadrature components of the impedance. The B905 can operate at three standard frequencies: 100 Hz, 1 kHz and 10 kHz. In addition, a Hewlett Packard HP3456A digital voltmeter, with compatible thermistor, was used to record the internal temperature changes of the specimens. These and other peripherals which comprise the data logging system were controlled by a HP9915A modular computer. The software initiated a reading cycle under clock control and processed and stored the incoming data. The tests were continuous over a 24 h period, with a reading cycle being initiated every minute over the first hour and every five minutes during the remaining 23 h.

All specimens were made with OPC and the experiments were carried out at constant ambient air temperature of 20° C (± 1° C). The cement paste was contained between the plates of a dielectric cell.

Typical results are given in Figs. 1 and 2, in this instance, for a paste with a water/cement ratio (W/C) of 0.30 (by weight). Fig. 1 shows the change in dielectric constant, resistivity and internal temperature of the cement paste over the 24 h test period for the three frequencies (a)

0261–8028/84 $03.00 + .12

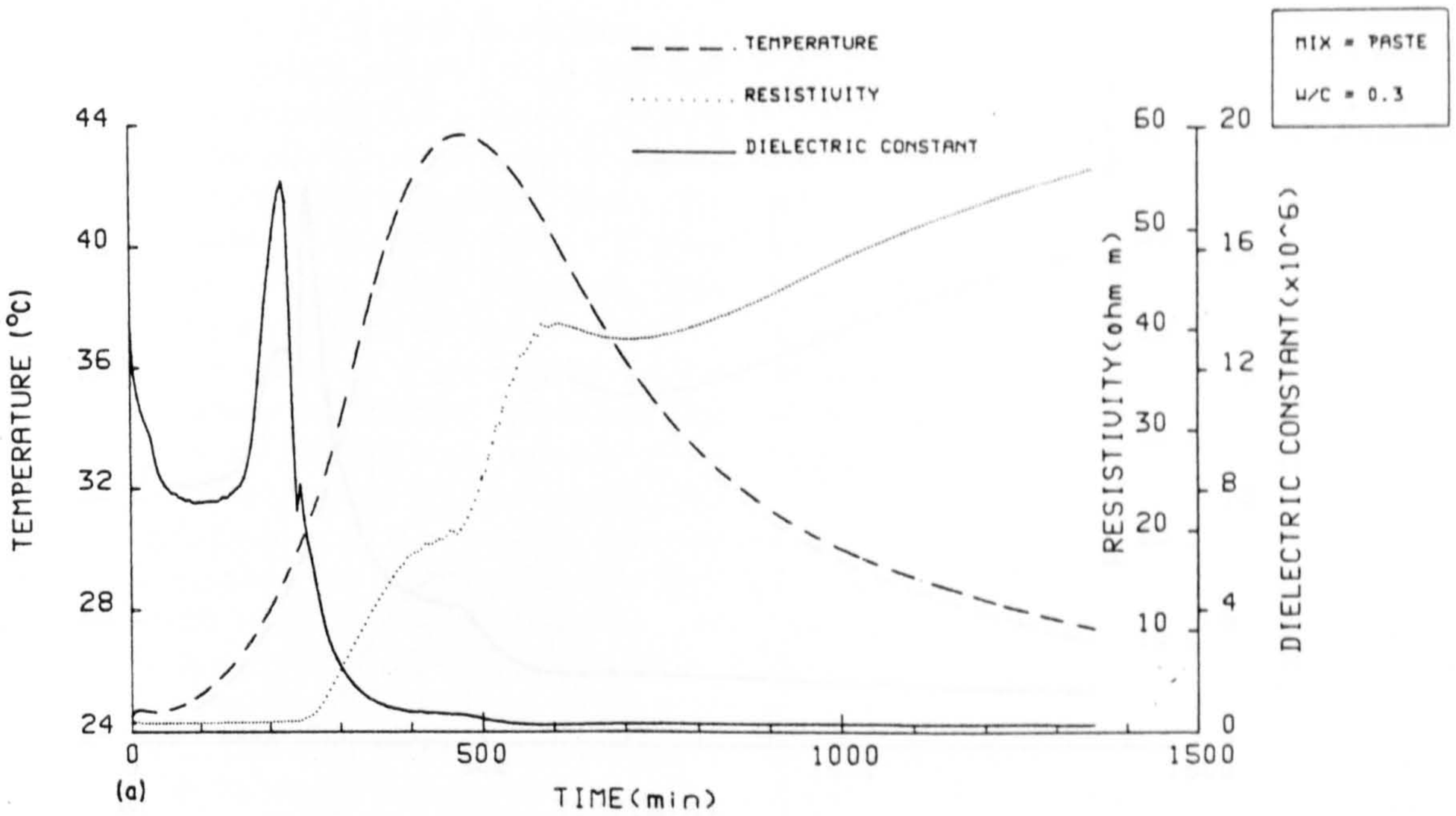

Figure 1 Variation of temperature, resistivity and dielectric constant during the first 24 h after gauging with water. (a) Frequency = 100 Hz. (b) Frequency = 1 kHz. (c) Frequency = 10 kHz.

100 Hz, (b) 1 kHz, and (c) 10 kHz. Fig. 2 shows the change in loss angle for this paste over the same period.

One of the striking features of Fig. 1 is the initially high dielectric constant and relatively low electrical resistivity of the paste (relative to that of ceramic materials), also, over the two decades of frequency considered (100 Hz to 10 kHz) the dielectric constant drops by almost three orders of magnitude, whilst the resistivity drops by less than 5%. The high polarizability and low resistance of the paste are attributable to, and indicative of, the high ionic concentrations and ease of mobility of charges at these early stages. Over the initial 240 min the resistivity remains constant at a particular frequency. At

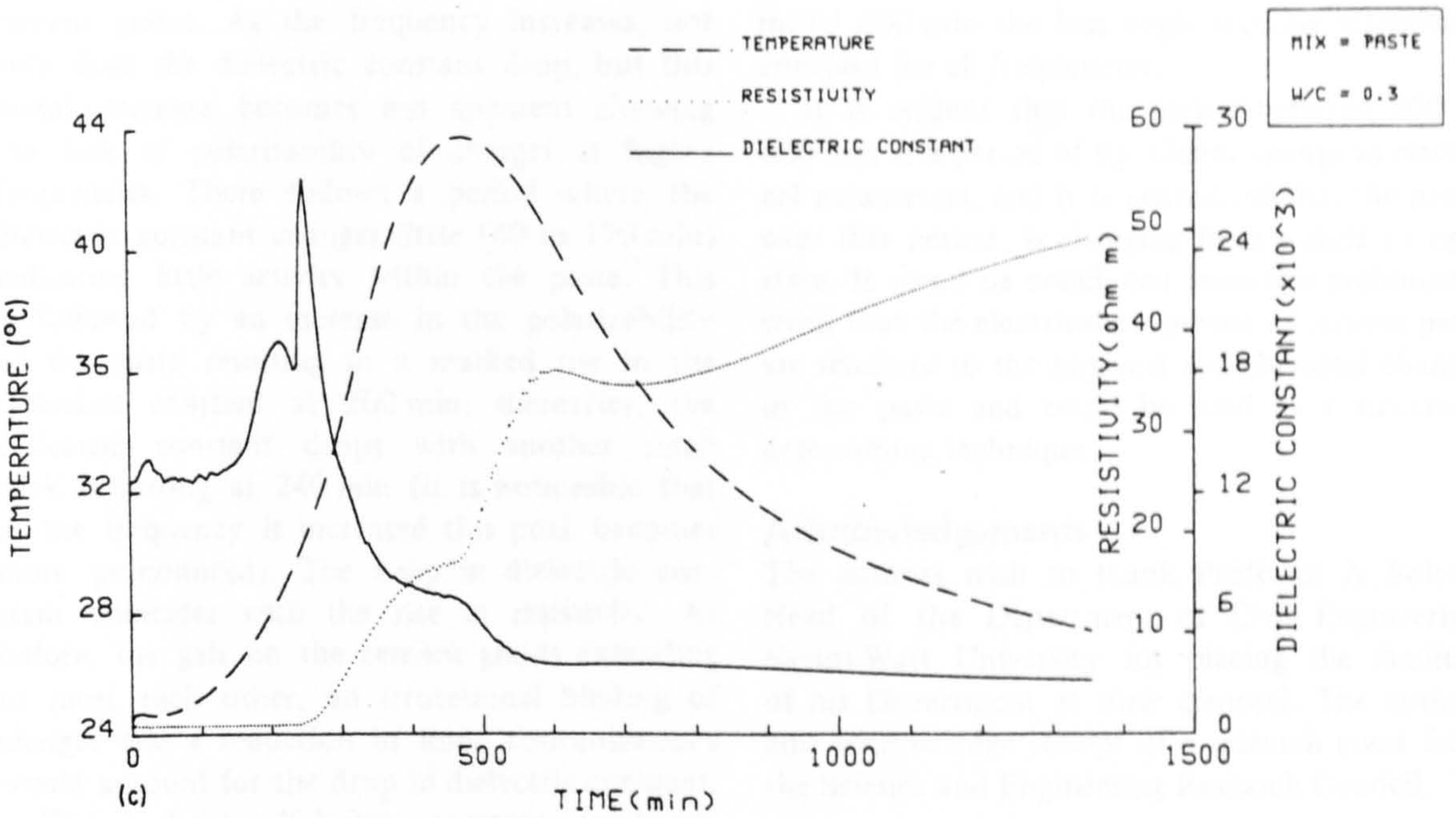

Figure 1 Continued.

240 min, the resistivity (irrespective of frequency) increases quite rapidly and could signify that ionic conduction paths through the paste are becoming more tortuous as the gel on the cement grains extends to form a fibrous rigid structure. The plateau region (450 min) coincides with the temperature maximum at this time. Since cement paste exhibits a negative temperature coefficient of resistivity [1], it would account for the slight reduction in the rate of change of resistivity at this time. At 600 min, the rate of change of resistivity decreases indicating, perhaps, that the paste has attained a rigid structure and the period of hardening has started.

The dielectric constant shows equally significant changes over the initial 600 min. The dielectric constant drops sharply over the first 40 min as the initial hydration products build up on the

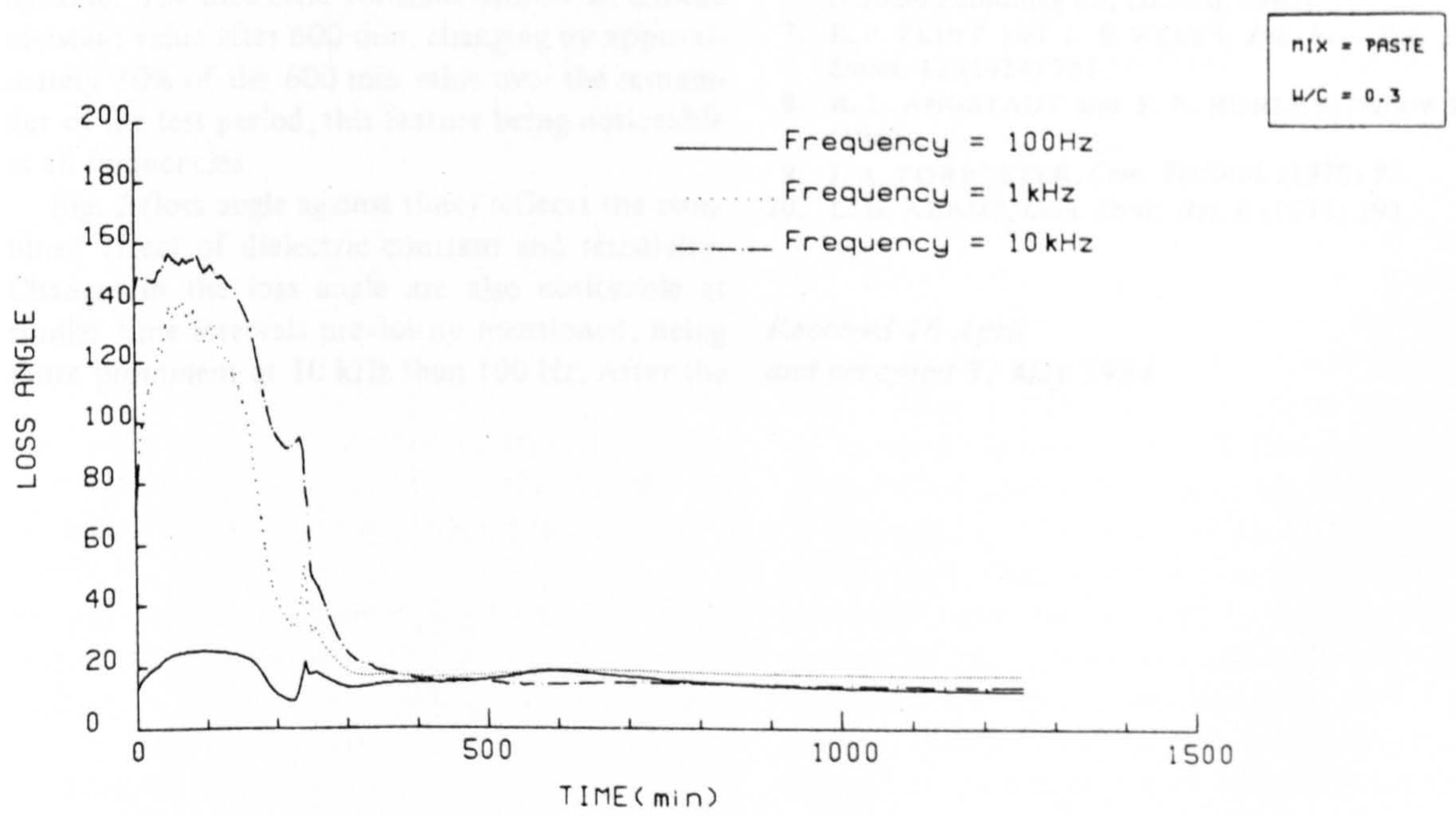

Figure 2 Variation of loss angle over test-period.

cement grains. As the frequency increases, not only does the dielectric constant drop, but this initial decrease becomes less apparent showing the lack of polarizability of charges at higher frequencies. There follows a period where the dielectric constant changes little (40 to 170 min) indicating little activity within the paste. This is followed by an increase in the polarizability of the paste resulting in a marked rise in the dielectric constant at 200 min; thereafter, the dielectric constant drops with another small peak occurring at 240 min (it is noticeable that as the frequency is increased this peak becomes more pronounced). The drop in dielectric constant coincides with the rise in resistivity. As before, the gels on the cement grains extending to meet each other, an irrotational binding of charges and a reduction in ionic concentrations would account for the drop in dielectric constant.

The peaks in dielectric constant previously described (i.e. at 200 min) would signify renewed chemical activity within the paste. The primary products formed on the cement grains at this early stage have a large excess of lime in their structure and are unstable. This lime could be released, resulting in compounds of lower basicity and an increase in the polarizability of the paste at this time. The magnitude of this peak could be considered as a measure of the escaping tendency of this lime and also a measure of the excess free energy (or degree of instability) of the unstable hydrate. The dielectric constant attains an almost constant value after 600 min, changing by approximately 10% of the 600 min value over the remainder of the test period, this feature being noticeable at all frequencies.

Fig. 2 (loss angle against time) reflects the combined effect of dielectric constant and resistivity. Changes in the loss angle are also noticeable at similar time intervals previously mentioned, being more prominent at 10 kHz than 100 Hz. After the initial 600 min the loss angle remains reasonably constant for all frequencies.

It is evident that the period between 200 to 600 min is a period of significant change in electrical parameters, and it is postulated that the paste, over this period, is changing from a fluid to rigid state. It could be concluded from this preliminary work that the electrical properties of cement paste are sensitive to the physical and chemical changes in the paste and could be used as a structure-determining technique.

Acknowledgements

The authors wish to thank Professor A. Bolton, Head of the Department of Civil Engineering, Heriot-Watt University for placing the facilities of his Department at their disposal. The authors also acknowledge receipt of a research grant from the Science and Engineering Research Council.

References

1. W. J. McCARTER, M. C. FORDE and H. W. WHITTINGTON, *Proc. Inst. Civ. Eng. Part 2* (1981) 107.
2. *Idem, Mag. Conc. Res.* 33 (1981) 48.
3. W. J. McCARTER, M. C. FORDE, H. W. WHITTINGTON and T. SIMONS, *Proc. Inst. Civ. Eng. Part 2* (1983) 123.
4. F. M. LEA, "The Chemistry of Cement and Concrete" (Edward Arnold (Publishers) Ltd, London, 1970).
5. R. H. BROGUE, "Chemistry of Portland Cement" (Reinhold, New York, 1955).
6. A. M. NEVILLE, "Properties of Concrete" 3rd edn. (Pitman Publishing Co, London, 1983).
7. E. P. FLINT and L. S. WELLS, *Jnl. Res. Nat. Bur. Stand.* 12 (1934) 751.
8. R. L. ANGSTADT and F. R. HURLEY, *Nature* 197 (1963).
9. J. A. FORRESTER, *Cem. Technol.* (1970) 95.
10. L. D. ADAMS, *Cem. Conc. Res.* 6 (1976) 293.

Received 16 April
and accepted 31 May 1984

JOURNAL OF MATERIALS SCIENCE LETTERS 4 (1985) 405–408

Further studies on the early hydration of Portland cement paste

W. J. McCARTER, A. B. AFSHAR
Department of Civil Engineering, Heriot Watt University, Edinburgh, UK

Previous work by the authors [1] monitored the variation in the electrical response characteristics of ordinary Portland cement (OPC) paste during the initial 24 h after gauging with water*. The electrical parameters measured were dielectric constant, electrical resistivity and loss-angle and, from these parameters, it was shown that four stages in the early hydration of cement could be identified – an initial stage of supersaturation of the gauging water with Ca^{2+} and OH^- ions and a build-up of hydration products (gel) on the cement grains; this is followed by a dormant period of little chemical activity; the dormant period is then followed by a period of renewed chemical activity as the gel on the cement grains ruptures and exposes unhydrated cement grain surfaces. The authors postulate that it is this stage which leads to an increase in rigidity of the cement paste (referred to as setting). The final stage which can be identified is the period of hardening.

This letter extends this work by investigating the influence of admixtures on the setting and hardening of cement paste. The influence of admixtures on cement paste is of importance to the cement technologist as setting and hardening can be adversely affected by additives. Furthermore, setting and hardening can be intentionally accelerated or delayed depending on the type and amount of admixture incorporated in the paste and, at present, it is difficult to assess the amount of admixture that need be added to the cement. The work presented provides an accurate method for monitoring and quantifying the influence of admixtures on the setting characteristics of cement paste.

Two common admixtures used in cement are sugar and calcium chloride which, respectively, delay and accelerate the setting of cement paste. These admixtures were used in the present programme and dissolved in the gauging water before addition to the cement. The amount added was fixed percentage, by weight, of cement. A microcomputer-controlled data acquisition system was employed to monitor the change in dielectric constant and electrical resistivity over the initial 24 h. In addition, the internal temperature of the specimens was monitored. Further details on instrumentation and experimental procedure have already been given [1].

Typical results are given in Figs. 1 to 3. The water/cement (w/c) ratio was kept constant (at 0.27), and the frequency of the applied electric field was 1000 Hz. Fig. 1 shows the change in the measured parameters over the 24 h test period for OPC paste without additives (taken as the control). Fig. 2 shows the influence of the addition of (a) 0.05% and (b) 0.1% sugar to the cement paste, and Fig. 3 shows the influence of the addition of (a) 1.0% and (b) 1.5% calcium chloride to the cement paste.

The results of Fig. 1 confirm previous findings. The authors ascribe the peak in dielectric constant at 200 min to renewed chemical activity within the paste as the gel on the C_3S phase ruptures, releasing ions and increasing the polarizability of the paste. This activity is short-lived and quickly leads to a decrease in viscosity of the paste as the dielectric constant drops and electrical resistivity rises – a reduction and irrotational binding of charges as the gel on the cement grains extend to form a fibrous rigid structure would accout for the curves at this stage. A reduction in the rate of change of resistivity at 600 min signifies the onset of hardening and hydration of the C_2S phase. It is evident from Figs. 2a and b that the addition of a retarding agent has the effect of delaying the reaction of the C_3S phase associated with stage 3 and increasing the dormant period of stage 2. The peak in dielectric constant is progressively more delayed as the proportion of retarder is increased,

*OPC comprises four main constituents which are written in shorthand form as: $C_3S = 3CaO \cdot SiO_2$, $C_2S = 2CaO \cdot SiO_2$, $C_3A = 3CaO \cdot Al_2O_3$, $C_4AF = 4CaO \cdot Al_2O_3 \cdot Fe_2O_3$.

0261–8028/85 $03.00 + .12

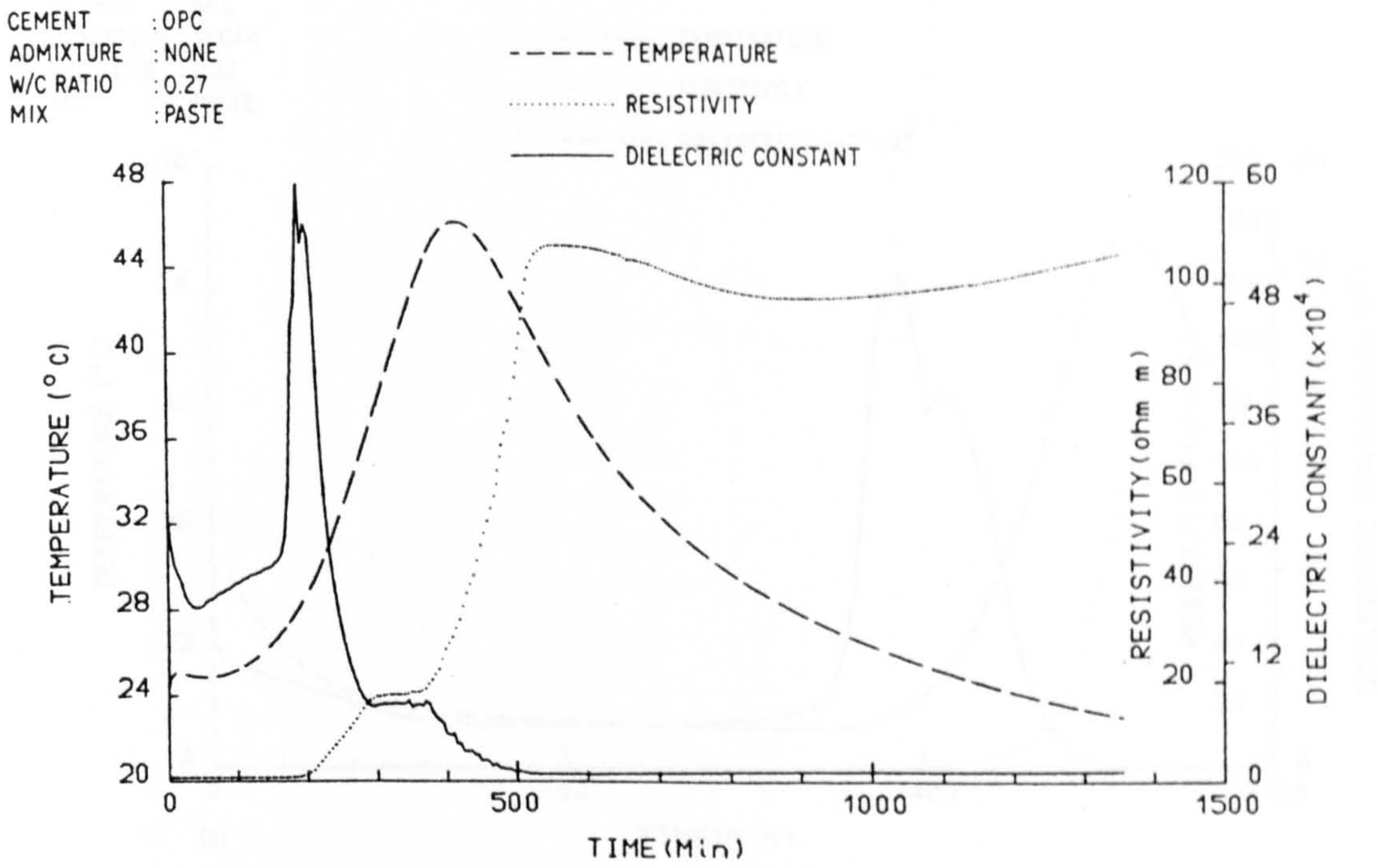

Figure 1 Variation of temperature, resistivity and dielectric constant during 24 h after gauging with water.

the amount of delay is proportional to the quantity of sugar added. As intimated earlier, as the reaction on the C_3S phase leads to setting then, from the data given, 0.05% sugar delays setting by 450 min; 0.1% delays setting by 1250 min (in this instance the test programme was extended over 36 h. Thus, the time during which the paste remains in a plastic state (i.e. workable) can be controlled by the amount of retarder added to the mix. It is noticeable from this figure that the temperature and resistivity curves are also displaced. The work has also shown that the

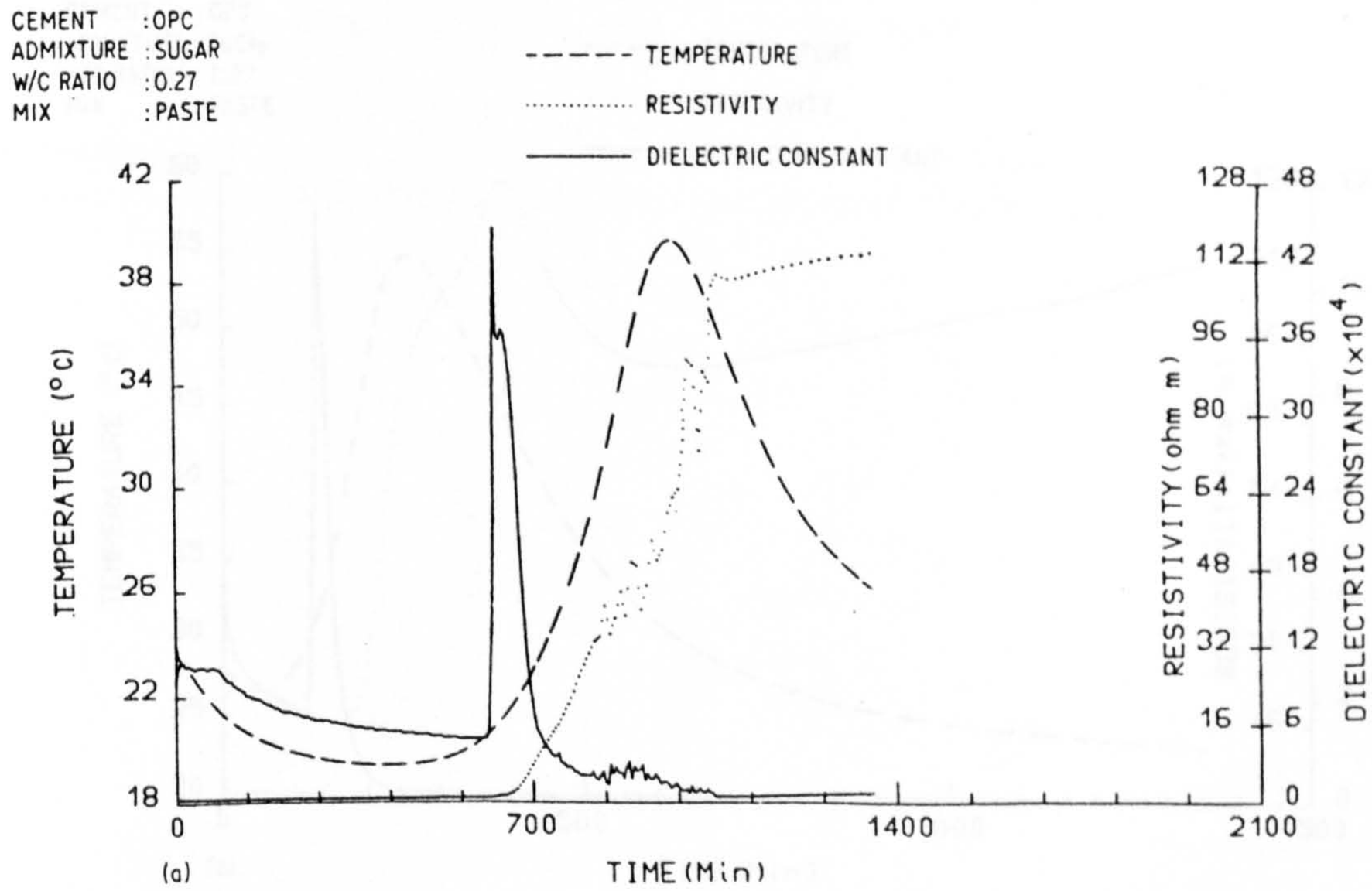

Figure 2 Influence of retarder on measured parameters: (a) 0.05% retarder; (b) 0.1% retarder.

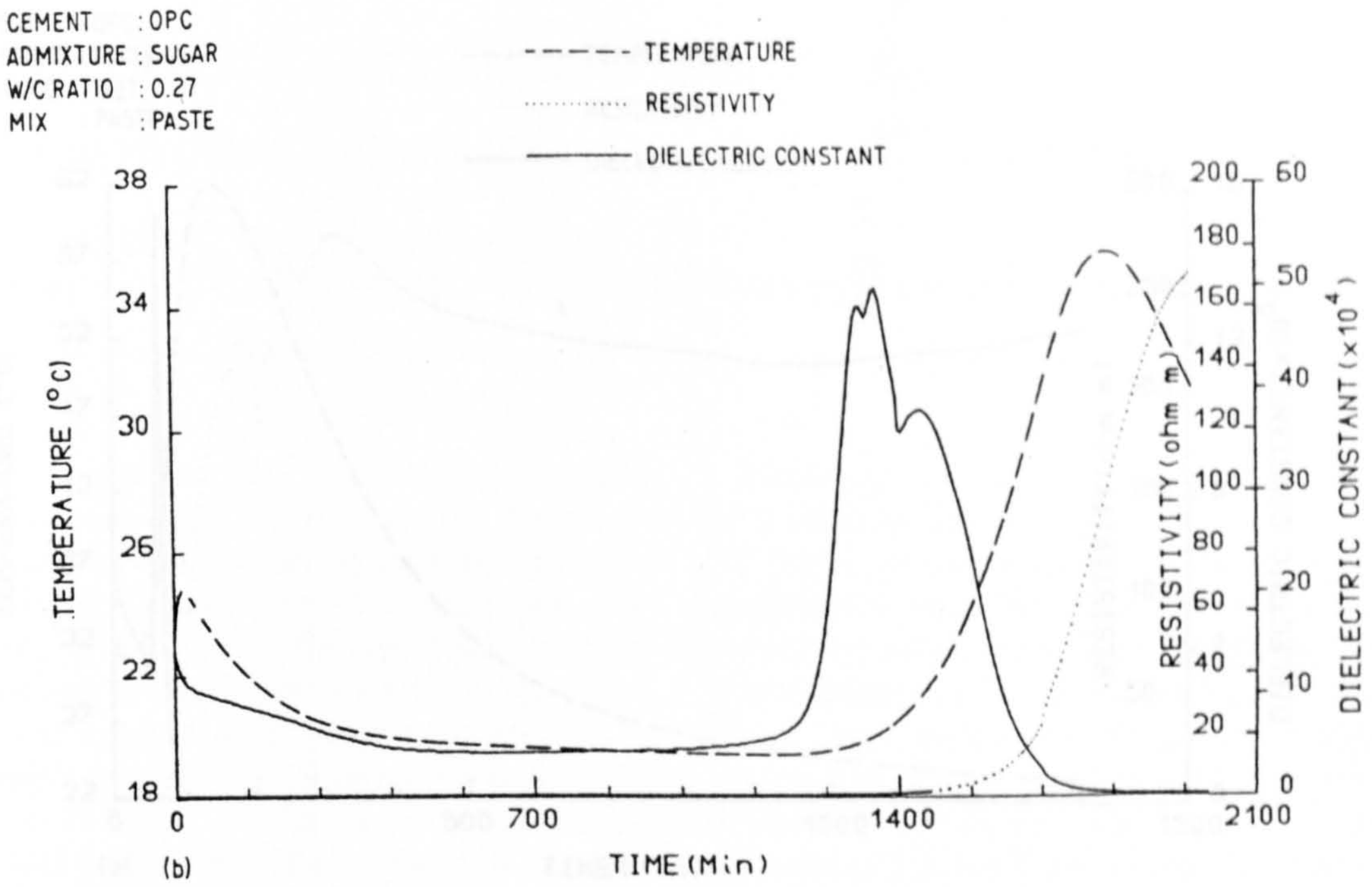

Figure 2 Continued.

addition of more than about 0.2% sugar could "kill" setting completely.

When an accelerator is added to the paste (Fig. 3a and b) the dormant period is reduced and the C_3S hydration peak associated with the dielectric constant curve occurs earlier. Since it is this peak which leads to stiffening of the paste then the time the paste remains in a plastic state is reduced. The addition of 1.0% and 1.5% of $CaCl_2$ to the paste advanced setting to 130 and 70 min, respectively, after gauging. The temperature and resistivity curves are also "compressed" compared to that of the control.

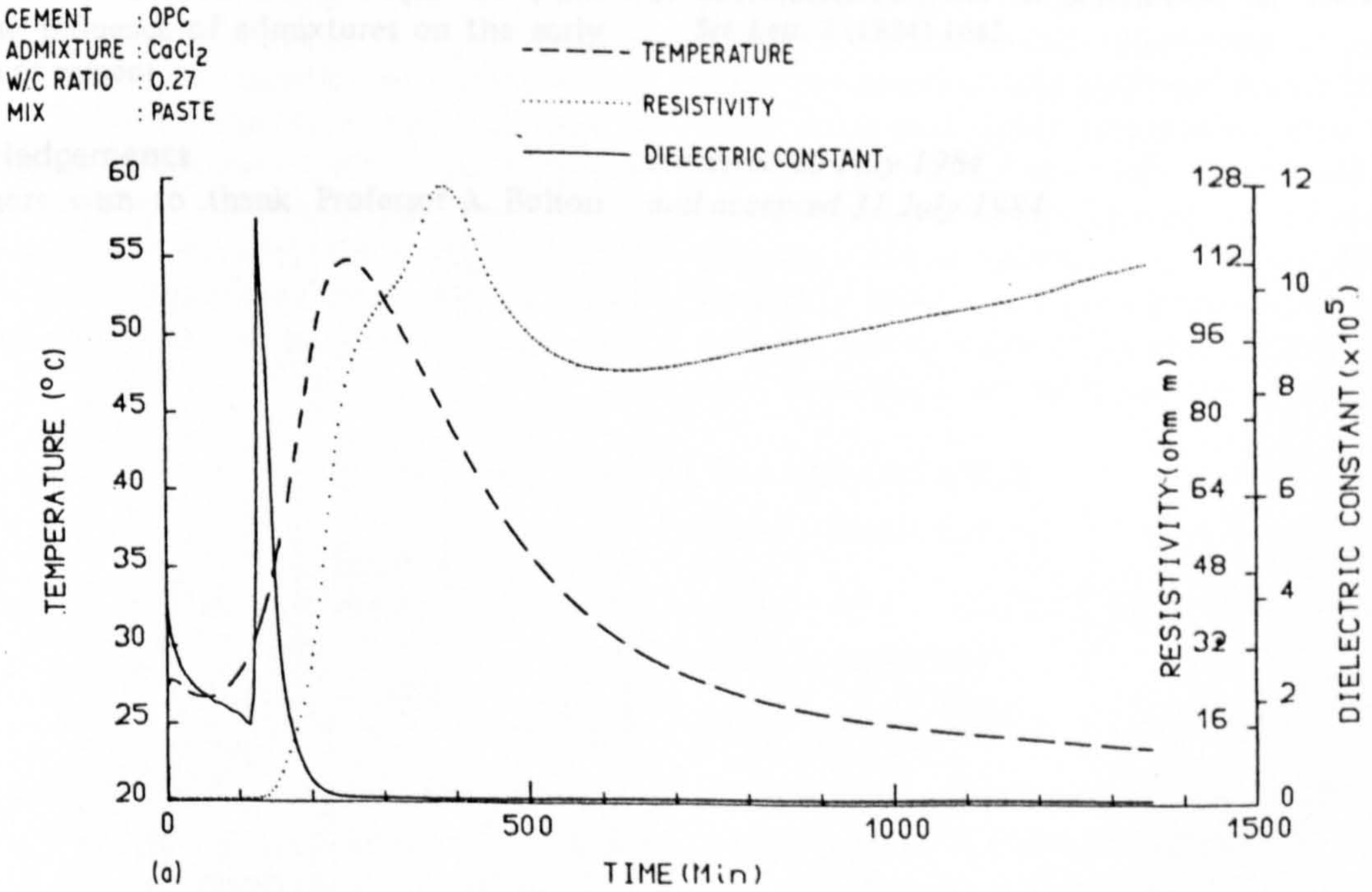

Figure 3 Influence of accelerator on measured parameters: (a) 1.0% accelerator; (b) 1.5% accelerator.

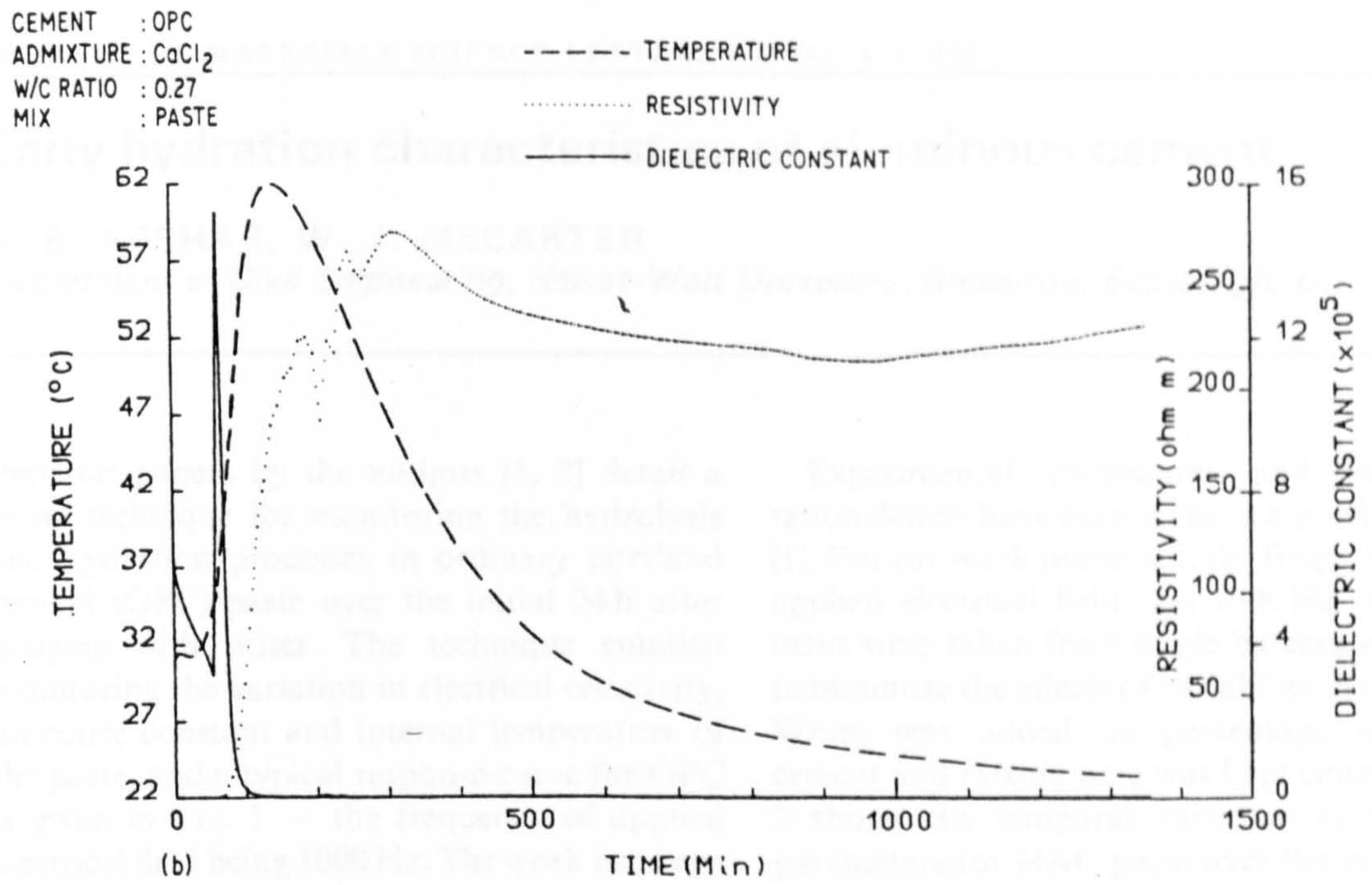

Figure 3 Continued.

The work presented in this letter has given further evidence of the mechanisms of cement hydration and structure building processes. Insight into the mode of action of retarders and accelerators on the setting and hardening of cement paste has been given and the method described offers an accurate technique for quantifying the influence of admixtures on the early hydration of cement.

Acknowledgements

The authors wish to thank Professor A. Bolton for placing the facilities of his Department at their disposal. The receipt of a research grant from the Science and Engineering Research Council is gratefully acknowledged.

References

1. W. J. McCARTER, and A. B. AFSHAR, *J. Mater. Sci. Lett.* **3** (1984) 1083.

Received 25 July 1984
and accepted 31 July 1984

JOURNAL OF MATERIALS SCIENCE LETTERS 4 (1985) 851-854

Early hydration characteristics of aluminous cement

A. B. AFSHAR, W. J. McCARTER
Department of Civil Engineering, Heriot-Watt University, Riccarton, Edinburgh, UK

Previous papers by the authors [1, 2] detail a novel technique for monitoring the hydrolysis and hydration processes in ordinary portland cement (OPC) paste over the initial 24 h after gauging with water. The technique entailed monitoring the variation in electrical resistivity, dielectric constant and internal temperature of the paste, and a typical response curve for OPC is given in Fig. 1 – the frequency of applied electrical field being 1000 Hz. The work has been extended to investigate the effect on electrical response of cements of different chemical composition.

This letter reports a preliminary investigation into high-alumina cement (HAC) and HAC/OPC mixtures. HAC is characterized by its rapid hardening properties and consequent high strength development within 24 h. Although HAC has a setting time comparable to that of OPC cement, its early strength gain over the first 24 h is comparable to that of OPC over the first 7 days. The principal cementitious phase of high alumina cement (Ciment Fondu Lafarge) is monocalcium aluminate, $CaO \cdot Al_2O_3$ (approximately 78% by weight). Minor constituents comprise iron oxides (FeO and Fe_2O_3) and silica (SiO_2). The hydration of monocalcium aluminate ($CaO \cdot Al_2O_3$) is temperature dependent [3–5].

Experimental procedures and instrumentation details have been given in a previous work [1]. For the work presented, the frequency of the applied electrical field was 1000 Hz. All specimens were taken from single batches of cement to minimize the effects of variability in materials. Water was added by percentage weight of cement and mixing time was kept constant. Fig. 2 shows the temporal variation in measured parameters for HAC paste over the initial 24 h. Fig. 3 shows the variation in loss angle over the test period for HAC. Fig. 4 shows the change in the measured parameters for an OPC/HAC mixture and Fig. 5 shows the variation in loss angle over the test period for this mixture.

The response curves for HAC cement paste (Fig. 2) show certain similarities to those of OPC (Fig. 1) and the work given, shows some important points which may throw light on the early hydration of HAC.

With reference to data presented (Fig. 2), the dielectric constant and electrical resistivity are much lower and higher, respectively, than those of OPC paste at the same age. This would indicate an overall reduction in ionic concentrations. The initial rise in dielectric constant and drop in resistivity (this is not noticeable on the graph owing to scale) is due to the gradual leaching of ions from the grain surfaces into solution and

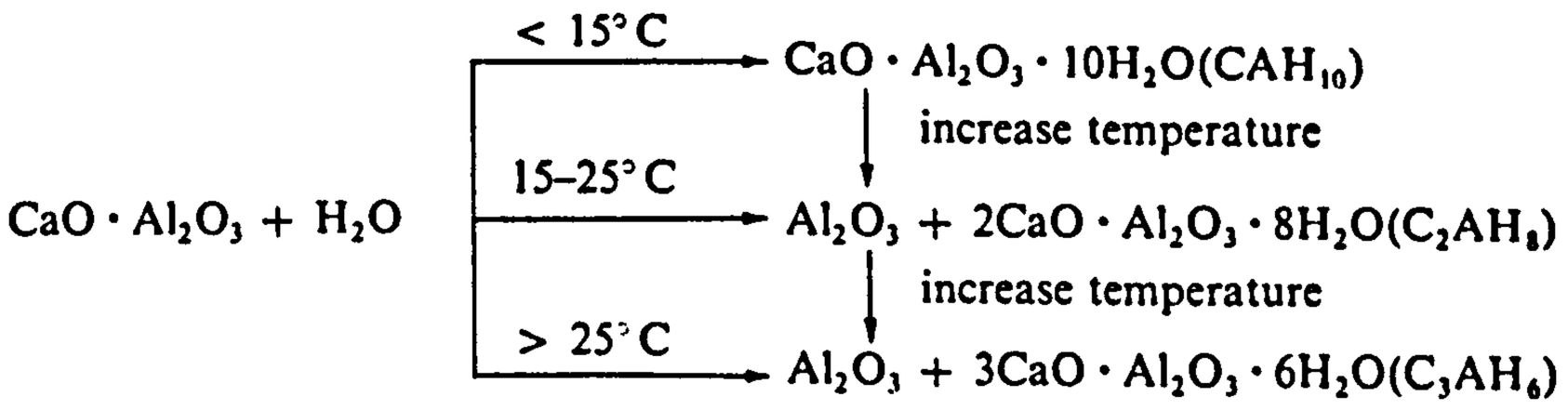

At normal ambient temperatures, CAH_{10} and C_2AH_8 would be normal products of hydration. However, if the temperature rises above 25° C conversion takes place as CAH_{10} and C_2AH_8 are transformed to C_3AH_6.

double layer polarization effects on the grain surfaces. In OPC paste, reactions set in rapidly; i.e. while mixing, and, consequently, this initial rise in dielectric constant and drop in resistivity go undetected. From Fig. 2 the peak in dielectric

0261-8028/85 $03.00 + .12

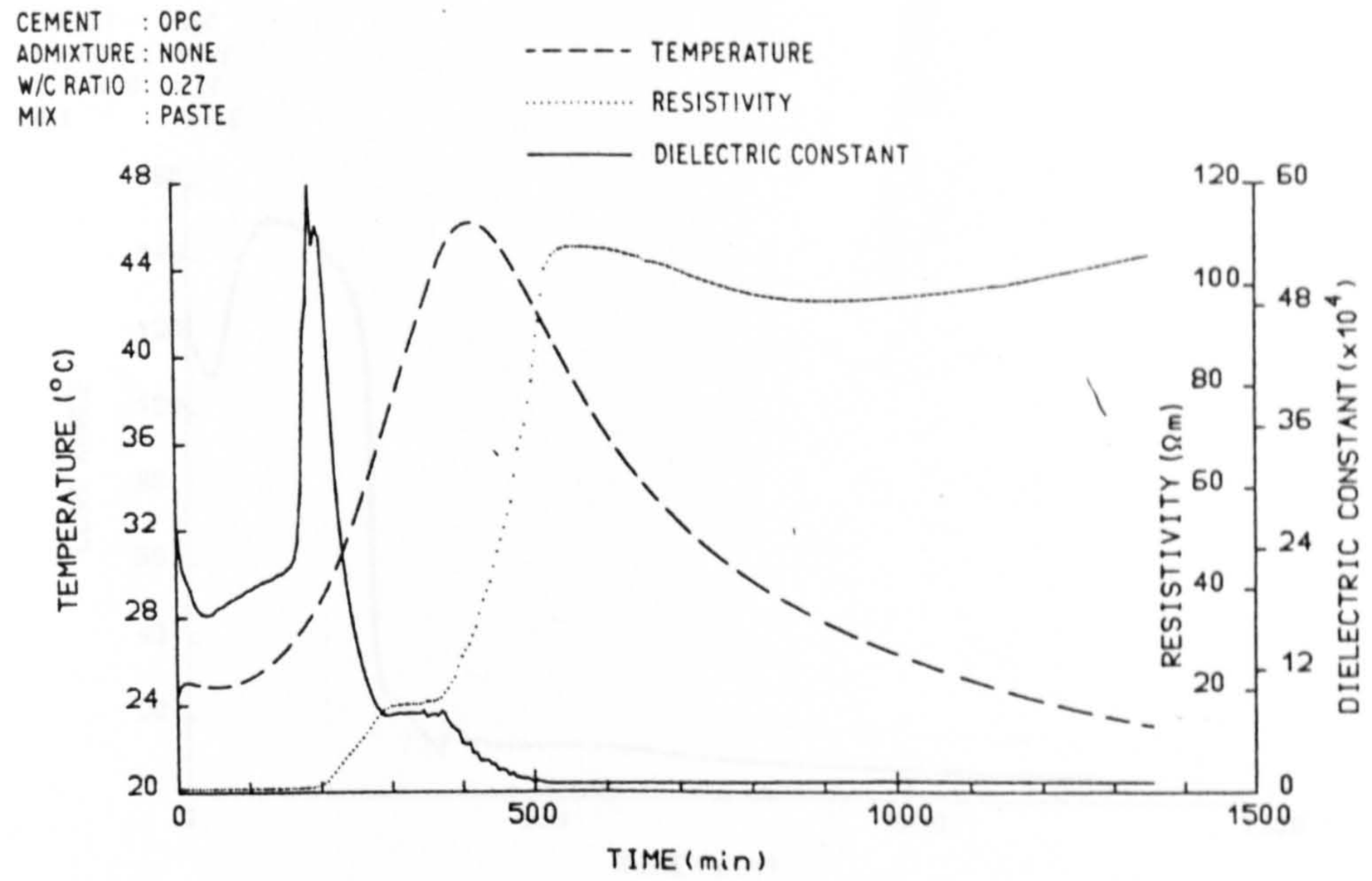

Figure 1 Variation of temperature, resistivity and dielectric constant during 24 h after gauging with water.

constant at 40 min is followed by a gradual drop; the formation of a weak aluminous gel and amorphous calcium aluminate hydrates on the grain surfaces, reducing charge mobility, could be responsible for this reduction in dielectric constant. The resistivity reaches a minimum at this time (40 min) and is taken to mean that the gauging water has achieved a supersaturated state. At 100 min and up to 200 min, the dielectric constant remains constant and the resistivity shows only a very gradual rise. This signifies an overall reduction in reaction rate and a period of little chemical activity as the weak coating formed on the grains temporarily prevents further hydration, that is, a dormant period. There is a similar dormant period in OPC hydration. At approximately 200 min, rupturing of the weak coating initiates renewed hydration of $CaO \cdot Al_2O_3$ resulting in an increase in the polarizability of the paste and subsequent rise in

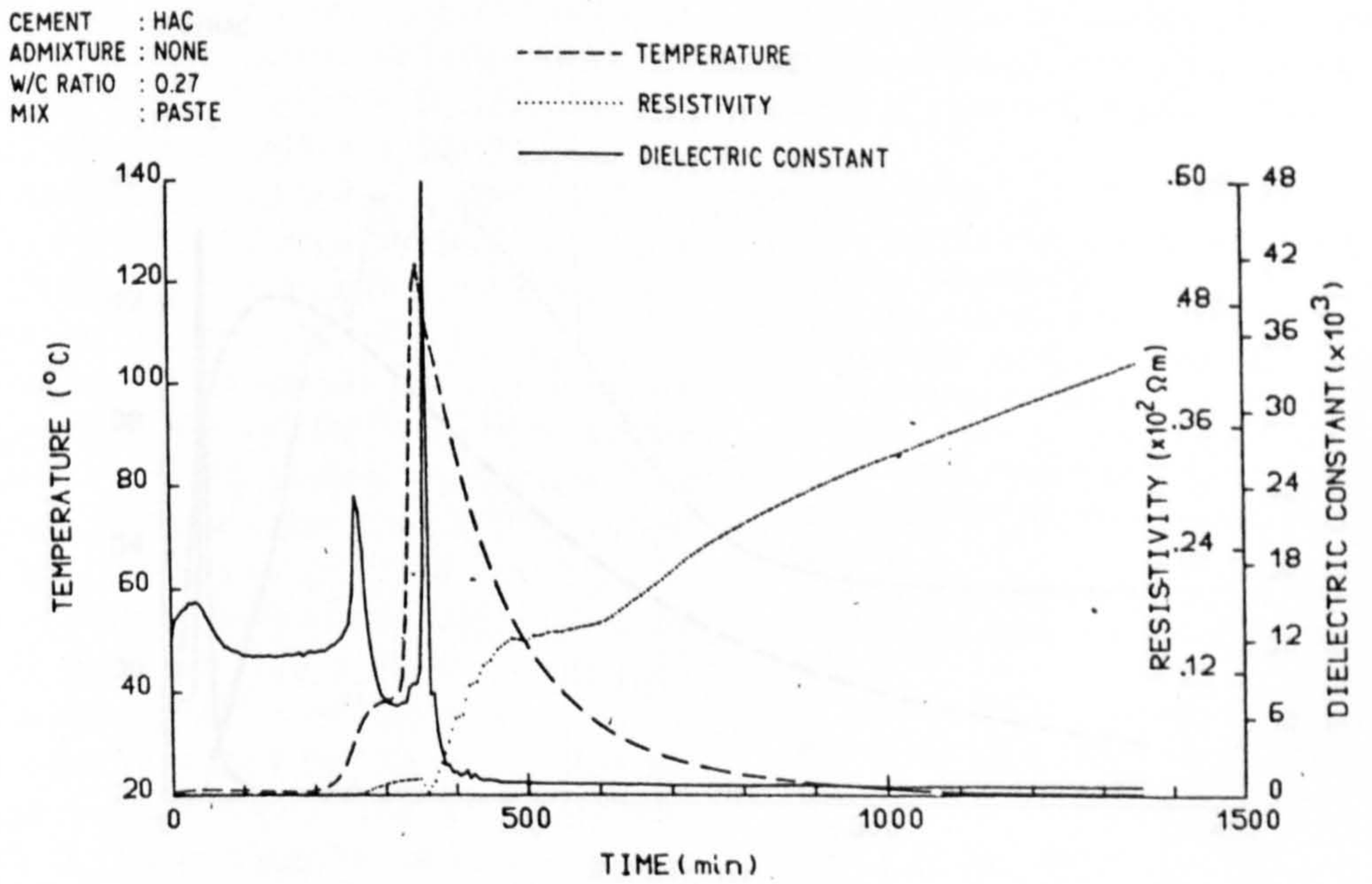

Figure 2 Variation of measured parameters for HAC.

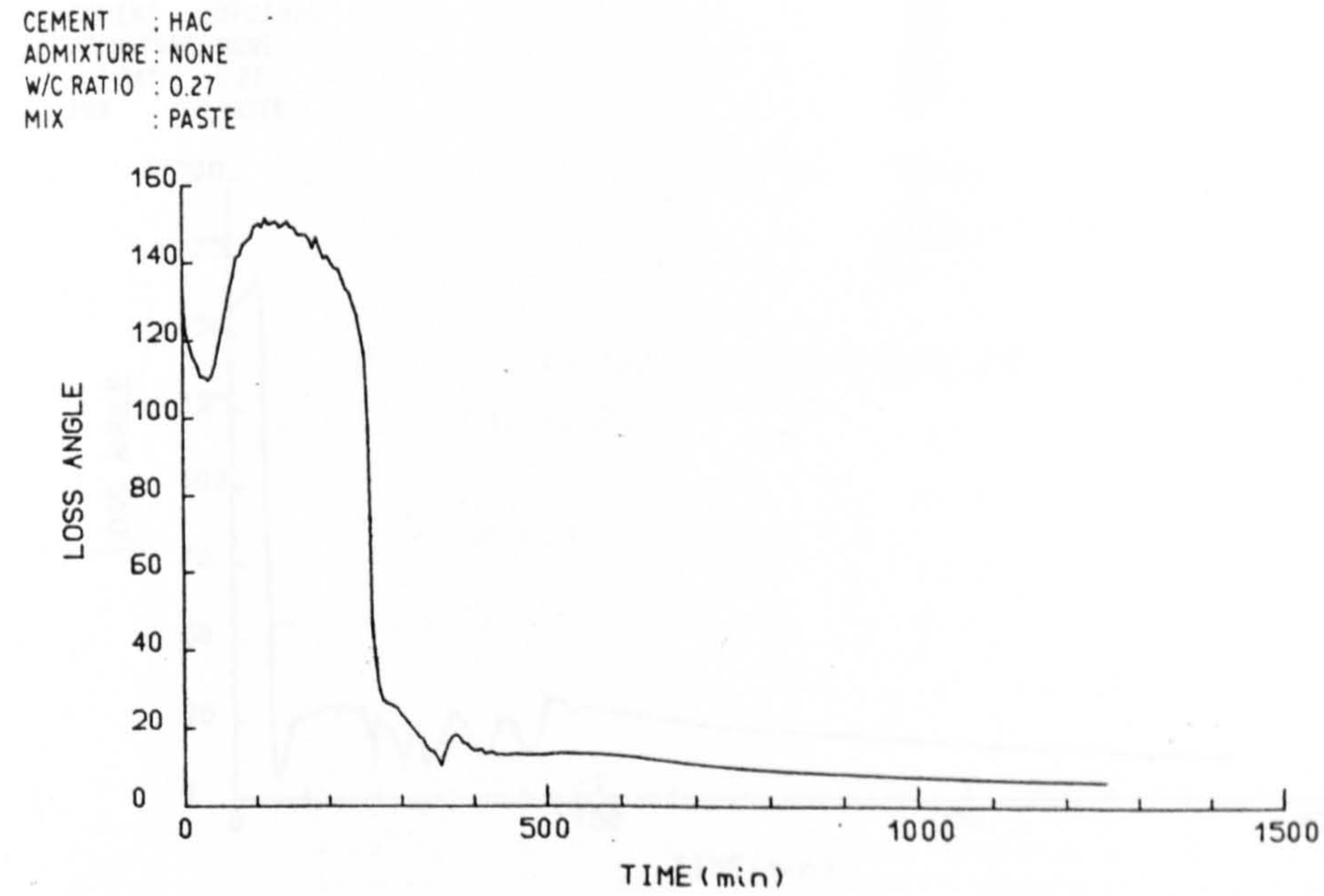

Figure 3 Variation of loss angle over test period.

dielectric constant. It is evident that the renewed hydration results in a release of charges which are associated with the grain surfaces and not with the bulk aqueous phase, as no reduction in resistivity is detected at this time. The peak in dielectric constant at 260 min coincides with a rise in resistivity (signifying the start of setting, cf. OPC paste at 200 min) and an increase in the internal temperature of the paste (which is conducive to the formation of $2CaO \cdot Al_2O_3 \cdot 8H_2O$). At this point in time, the paste is increasing in rigidity. However, because of the exothermic nature of monocalcium aluminate hydration, the temperature of the mix rises considerably ($\sim 120^\circ C$) and conversion of the hydrates to $3CaO \cdot Al_2O_3 \cdot 6H_2O$ must result.

The authors attribute the peak in dielectric constant and the drop in resistivity noticeable at peak temperature (350 min) to a combination of $3CaO \cdot Al_2O_3 \cdot 6H_2O$ formation and the rise in

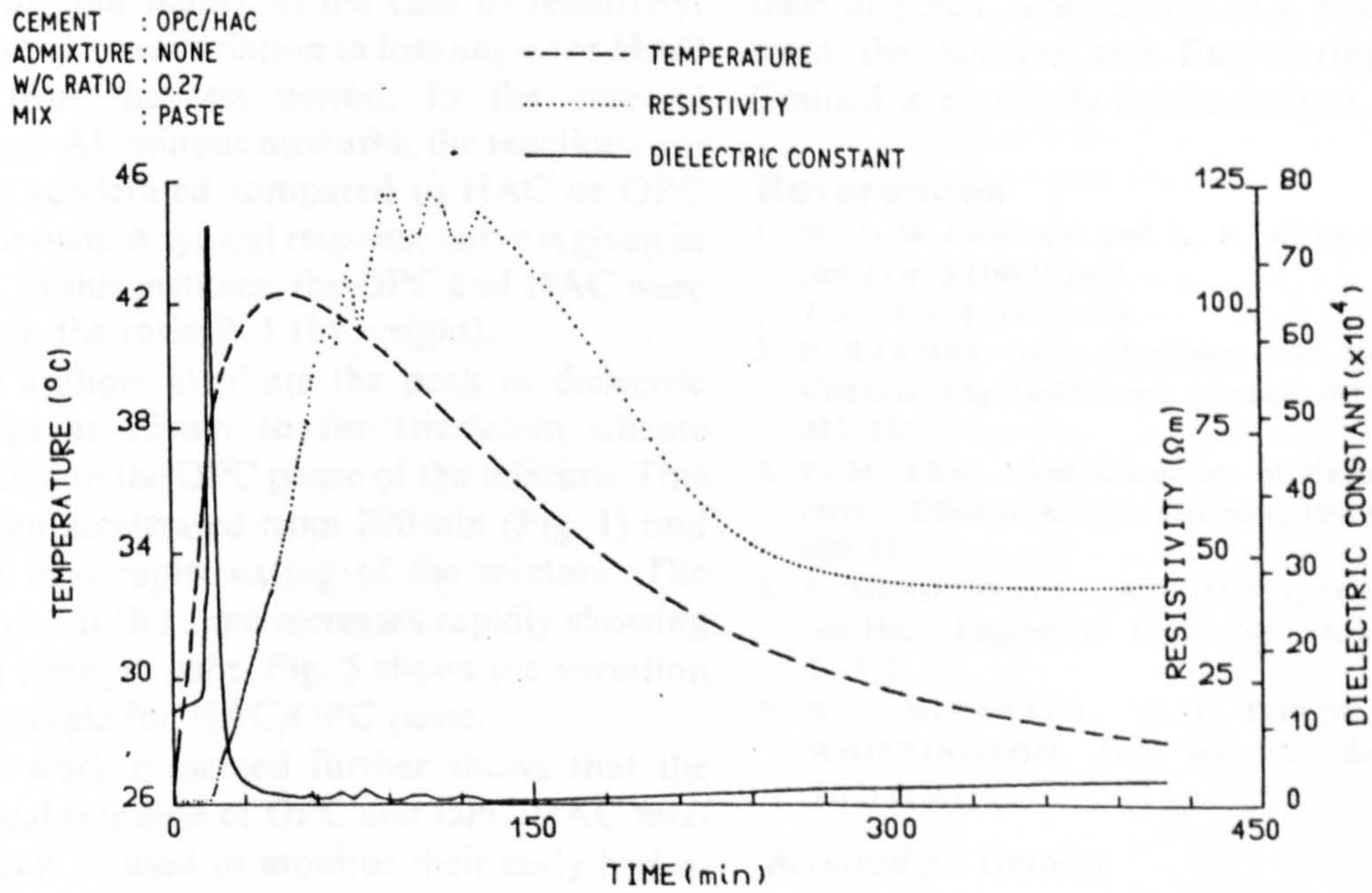

Figure 4 Variation of measured parameters for OPC/HAC.

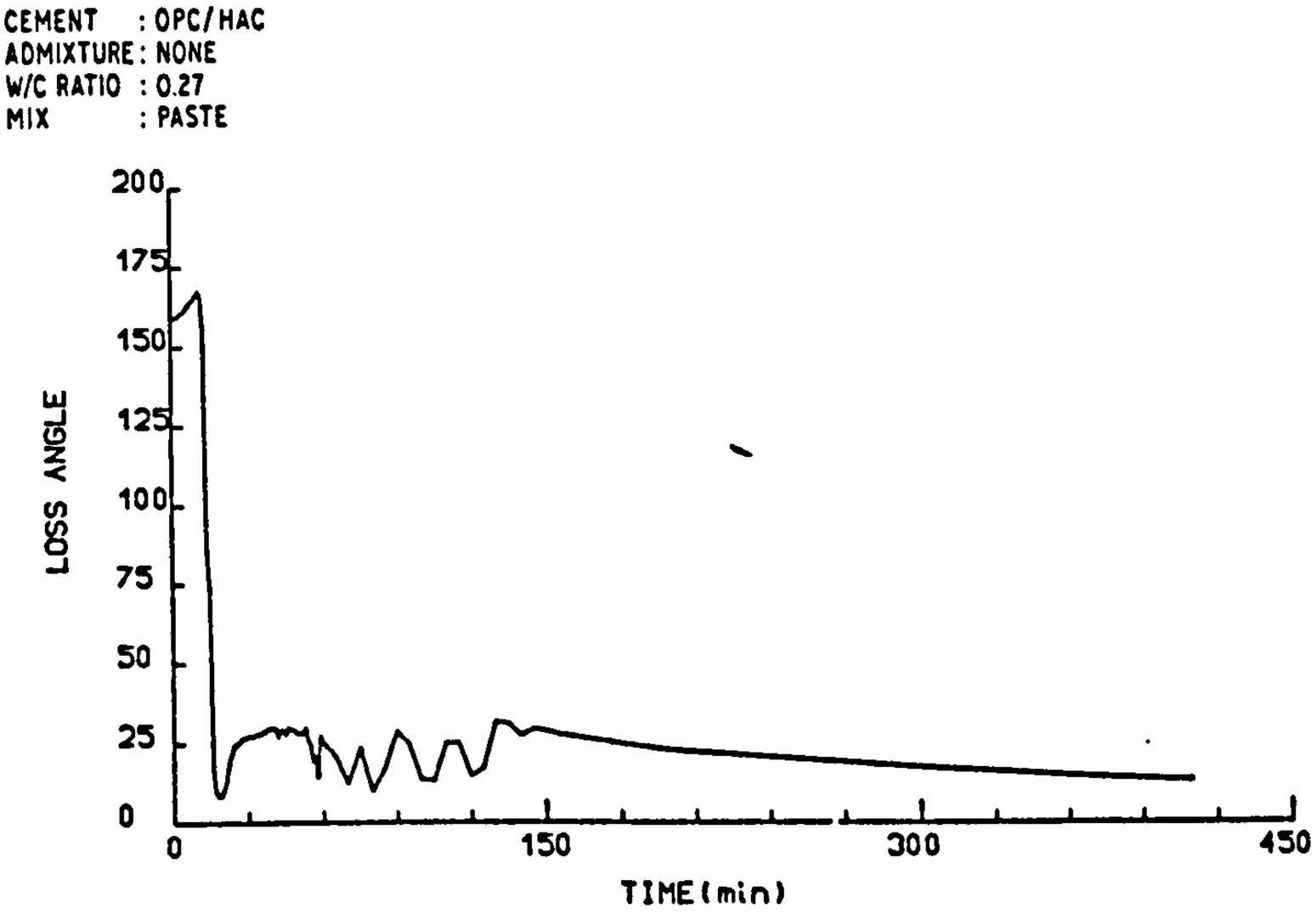

Figure 5 Variation of loss angle over test period.

internal temperature of the paste (the dielectric constant and resistivity [6] being temperature dependent). A certain amount of internal desiccation must result from this rise in temperature. The peak and drop in dielectric constant and resistivity is short-lived as the paste rapidly gains rigidity, and the period of hardening commences. Thereafter, the curves follow the same trend as OPC paste, although the magnitudes of the measured electrical parameters are an order of magnitude lower, in the case of dielectric constant, and higher in the case of resistivity. Fig. 3 shows the variation in loss angle for HAC paste over the test period. In the case of Portland–Aluminous mixtures, the reactions are greatly accelerated compared to HAC or OPC on their own. A typical response curve is given in Fig. 4. In this instance, the OPC and HAC were mixed in the ratio 9:1 (by weight).

The authors attribute the peak in dielectric constant at 15 min to the tricalcium silicate hydration in the OPC phase of the mixture. This has been accelerated from 200 min (Fig. 1) and results in a rapid setting of the mixture. The resistivity at this time increases rapidly showing a high strength gain. Fig. 5 shows the variation in loss angle for HAC/OPC paste.

The work presented further shows that the electrical response of OPC and OPC/HAC mixtures can be used to monitor their early hydration characteristics, and the rate of change of these parameters (dielectric constant and resistivity) gives an indication of the rate at which reactions are progressing.

The technique outlined offers a practical method for determining mixture proportions to obviate hyper-fast-setting of the Portland–Aluminous cement mixtures.

Acknowledgements

The authors wish to thank Professor A. Bolton for placing the facilities of his department at their disposal. The receipt of a research grant from the Science and Engineering Research Council is gratefully acknowledged.

References

1. W. J. McCARTER and A. B. AFSHAR, *J. Mater. Sci. Lett.* **3** (1984) 1083.
2. *Idem, ibid.* **4** (1985) 405.
3. P. BARNES (ed.), "Structure and Performance of Cements" (Applied Science, London, 1983) pp. 237–353, 415, 554.
4. F. M. LEA, "The Chemistry of Cement and Concrete" (Edward Arnold, Glasgow, 1970) pp. 177–250, 490–557.
5. S. MINDESS and J. R. YOUNG, "Concrete" (Prentice-Hall, Englewood Cliffs, New Jersey, 1981) pp. 76–112.
6. W. J. McCARTER, M. C. FORDE and H. W. WHITTINGTON, *Proc. Inst. Civ. Engng. (London)* **71**(2) (1981) 123.

Received 31 October
and accepted 11 December 1984

Proc. Instn Civ. Engrs, Part 2, 1985, 79, Sept., 585–604
PAPER 8954 STRUCTURAL ENGINEERING GROUP

A study of the early hydration of Portland cement

W. J. McCARTER, BSc, PhD*

A. B. AFSHAR, BSc, MSc

A novel electrical response technique for monitoring cement hydration is presented. The response data can be used to monitor the chemical and structure-building processes associated with hydration and also in assessing the influence of, for example, additives, cement composition and environment on these processes. Scanning electron microscopy is used to corroborate predictions about the state of the paste inferred from the electrical response. Practical applications of the method are discussed.

Introduction

Techniques in examining the structure of hydrating cement paste have advanced quite considerably with the development of the scanning electron microscope (SEM) and transmission electron microscope, and nuclear magnetic resonance and X-ray diffraction methods.[1–5] The hydration of silicate material is of central interest in the study of ordinary Portland cement (OPC), yet, in spite of the amount of research carried out using these techniques, much about the very early structure and nature of the hydration products remains obscure. Inferences about the products of hydration in cement have been made from more or less pure silicate compounds;[6–8] however, in cement paste, the various anhydrous compounds will not react independently but cross-reaction and synergistic effects will occur.

2. Such sophisticated techniques have certain disadvantages: instrumentation is not readily available; they require skilled interpretation; samples for testing require special preparation techniques and the fabric structure can be disrupted when samples are evacuated under low pressures. In addition, only a very small area of the sample is examined, as little as a few microns, and care must be taken in evaluating macroscale performance for microscale examination.

3. This Paper has, as its purposes,

(*a*) description of the alternating current (a.c.) response characteristics of cement paste during the early stages of setting and hardening;
(*b*) interpretation of this response in terms of chemical and structure-building processes;
(*c*) illustration of the influences of admixtures and changes in composition on the electrical response of cement paste; and
(*d*) the presentation of a new method for the study of hydrating cement paste.

Written discussion closes 15 November 1985; for further details see p. ii.
* Department of Civil Engineering, Heriot-Watt University.

4. It is essential for the cement technologist to have a full understanding of the hydration characteristics of special cements and the effects of admixtures and varying chemical composition[9–11] to ensure correct setting and hardening of the cement. This Paper presents a simple practical method in gaining this understanding, by using the electrical response as a 'fingerprint' for cement hydration.

A.C. Response characteristics of cement paste

5. Much work has been undertaken in measuring the change in the electrical resistance of cement paste, mortars and concretes throughout the setting and hardening processes,[12–14] and attempts have been made, with varying degrees of success, to correlate changes in the physical state of the paste[15–18] with changes in electrical resistance. Little attempt has been made to relate changes in electrical resistance with the chemical processes associated with setting and hardening or the rates at which reactions are progressing; furthermore, differing specimen sizes, electrode configurations, measuring techniques and test conditions together with a general lack of data points over the initial 24 h period make results vary within wide limits.

6. The electrical model used by previous workers in representing the early stages of hydrating cement paste has been a purely resistive one; however, the application of an alternating electrical field to a colloidal dispersion such as cement paste produces a response which can be measured not only in terms of a resistance, R, but also as a capacitance, C. Cement paste, reduced to its equivalent electrical circuit, can be represented by a series combination of resistance and capacitance, a parallel combination of resistance and capacitance or a combination of both. Such models have been successively used in representing relatively mature specimens of cement;[19,20] this study uses a parallel electrical model[21,22] to represent cement paste during the initial 24 h of the hydration process—even this model is perhaps an oversimplification of the actual physical situation.

7. The measured values of capacitance and resistance can be converted into dielectric constant ε which is defined as

$$\varepsilon = C/C_0 \tag{1}$$

in which C_0 is the capacitance of the system when a vacuum occupies the space between the pair of electrodes, and resistivity ρ which is defined as

$$\rho = RA/L\ \Omega\text{m} \tag{2}$$

where L is the length of the specimen (metres) and A is the cross-sectional area of the specimen (metres squared), assumed uniform.

Conduction and polarization mechanisms

8. When an electric field is applied to a colloidal dispersion such as cement paste, some charges, in the form of ions in solution, are free to drift through the solution and discharge at the electrodes. This produces a conduction effect which is reflected by the resistance R and hence the resistivity ρ. Charges, which are bound to grain surfaces, are not able to contribute to the conduction effect but are able to oscillate about their equilibrium position in the presence of an alternating electrical field. Oscillation of charges, without conduction, is called polarization and the main polarization mechanisms operative within a cement paste are

(*a*) double-layer or colloidal layer polarization, in which charges adjacent to grain surfaces can be displaced[23–25] thereby inducing a large effective dipole moment (Fig. 1(a))

(*b*) interfacial polarization or Maxwell–Wagner effect, which results in an accumulation or build-up of charges at crystal boundary interfaces[26,27] (Fig. 1(b)).

The total of the polarization mechanisms is reflected by the capacitance C and hence the dielectric constant ε. As the frequency of the applied electrical field is increased then the contribution of each mechanism diminishes.

Setting and hardening processes in cement paste

9. The reaction between cement clinker and water is a complicated chemical process and takes place in a number of stages.[28–30] There are four stages in the hydration of cement paste which can be summarized as follows

(1) an initial period of rapid chemical activity and saturation of the gauging water with Ca^{2+} and OH^- ions, and other minor ions leached from the surfaces of the cement grains, primarily Na^+, K^+ and SO_4^{2-}. Tricalcium silicate (C_3S) and tricalcium aluminate (C_3A) hydration are prominent during this stage

(2) an induction, or dormant, period of little chemical activity and slower reaction rates as the gel, which forms on the grain surface, retards the action

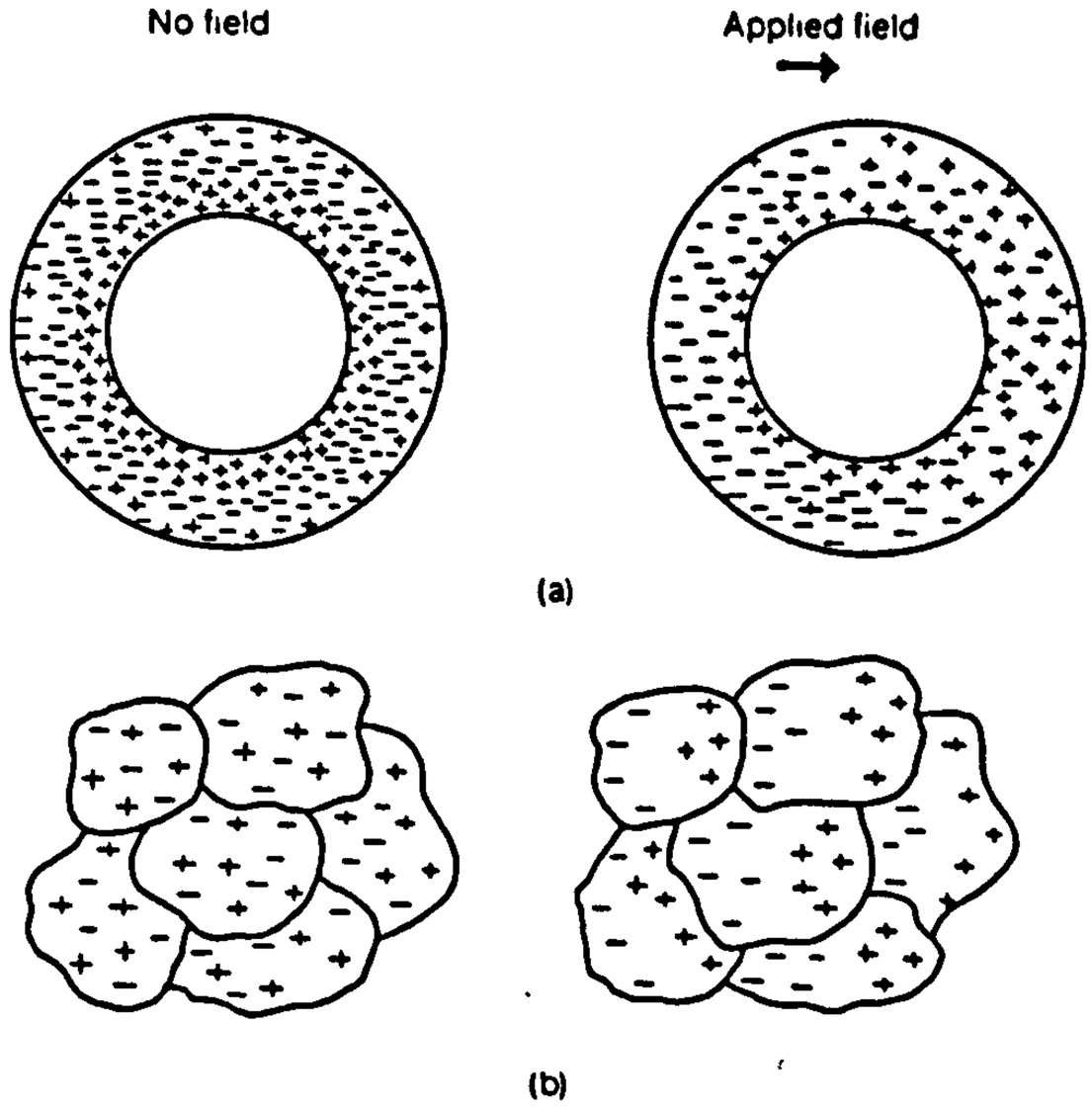

Fig. 1. Polarization mechanisms in cement paste: (*a*) *double-layer polarization;* (*b*) *interfacial polarization*

(3) a period of renewed chemical activity on the cement grains as the relatively weak gel coating ruptures, thereby exposing unhydrated cement grain surfaces: the gel extends to form a fibrous rigid structure and this stage is characterized by an increase in the rate of heat evolution (this secondary reaction occurs on the C_3S phase)
(4) after this renewed chemical activity the period of hardening begins and is characterized by much slower reaction rates: hydration of C_2S becomes prominent and, depending on the Ca^{2+} and SO_4^{2-} ion concentration, renewed activity on the C_3A phase.

It is during stage 3 that the paste changes from a fluid to a rigid state and over this transition period the terms 'initial set' and 'final set' are used to define arbitrary degrees of firmness of the paste. Traditionally, the Vicat Needle[31] has been used to quantify these terms.

10. It is evident that during the four stages of hydration, definite chemical and structural changes occur which

(*a*) change the physical state of water;
(*b*) increase or reduce ionic concentrations within the gauging water;
(*c*) increase the viscosity of the paste; and
(*d*) absorb and irrotationally bind charges.

Since the electrical parameters, resistivity and dielectric constant, depend on the ease with which charges can conduct or be polarized, then they should reflect the chemical processes associated with cement hydration.

Experimental programme

11. The experimental programme was developed on two fronts: quantitative information about the progress of hydration reactions was obtained from electrical response techniques and qualitative information about the morphology of hydrate development and surface topography of the grain surfaces was obtained by scanning electron microscopy.

Scanning electron microscopy

12. Freshly prepared fracture surfaces of cement paste samples (approximately 5 mm diameter and 5 mm thick) were examined in a Cambridge Stereoscan electron microscope (model 250 Mk2). The specimens were dried under a low pressure and the surface sputtered by vacuum deposition with a thin layer of gold to render them electrically conducting to prevent build-up of charge on the surface.

13. It should be emphasized that at such early stages some disruption of the microstructure through rapid dehydration is inevitable, but the basic skeletal morphology will remain substantially unchanged.

Electrical method

14. The in-phase (resistance) and quadrature (capacitance) components of the impedance were measured using a Wayne Kerr B905 Component Bridge at three frequencies—100 Hz, 1 kHz and 10 kHz. In addition, the internal temperature of the specimens was monitored using an HP3465A digital voltmeter with compatible thermistor. The instruments were controlled using an HP9915 modular microcomputer and a schematic diagram of the system architecture is shown in

Fig. 2. A reading cycle was initiated, under clock control, at 300 s intervals over the 24 h test period and data were processed and then stored on a floppy disc storage medium. The address sequence of the peripherals is given in Fig. 3.

15. The samples were contained in a dielectric cell (Fig. 4) which had been calibrated to eliminate errors due to field fringing effects and capacitance associated with cell material. Electrodes were placed at opposite faces of the cell and the sample size was 100 mm × 100 mm × 100 mm. Lead inductance, which introduces errors into the results at higher frequencies, was also calibrated from the incoming data.

16. OPC (ASTM type 1) was used for all tests and water (dielectric constant, approximately 80; resistivity, approximately 100 Ωm) was added by weight of cement. Specimens were made from single batches of cement to minimize the effects of variability of materials and mixed using a Hobart planetary motion rotary mixer. The mixing time was kept constant and specimens were vibration compacted. All experiments were carried out under constant environmental conditions (temperature and humidity). A water-to-cement ratio of 0·27 was used for the data presented, this water-to-cement ratio producing a paste of standard consistency.[31]

Results

17. Results from the experimental programme have been presented

(*a*) to demonstrate the use of the electrical response of cement paste as a means of monitoring early hydration
(*b*) to throw light on the morphology of hydrates on grain surfaces using SEM micrographs and correlation of electrical response with crystal growth and formation
(*c*) to demonstrate the influence of admixtures and chemical composition on electrical response curves.

The electrical response graphs are typical results taken from over 100 tests. Although the electrical response was obtained at three frequencies of applied field—100 Hz, 1 kHz and 10 kHz—data have only been given for 1 kHz.

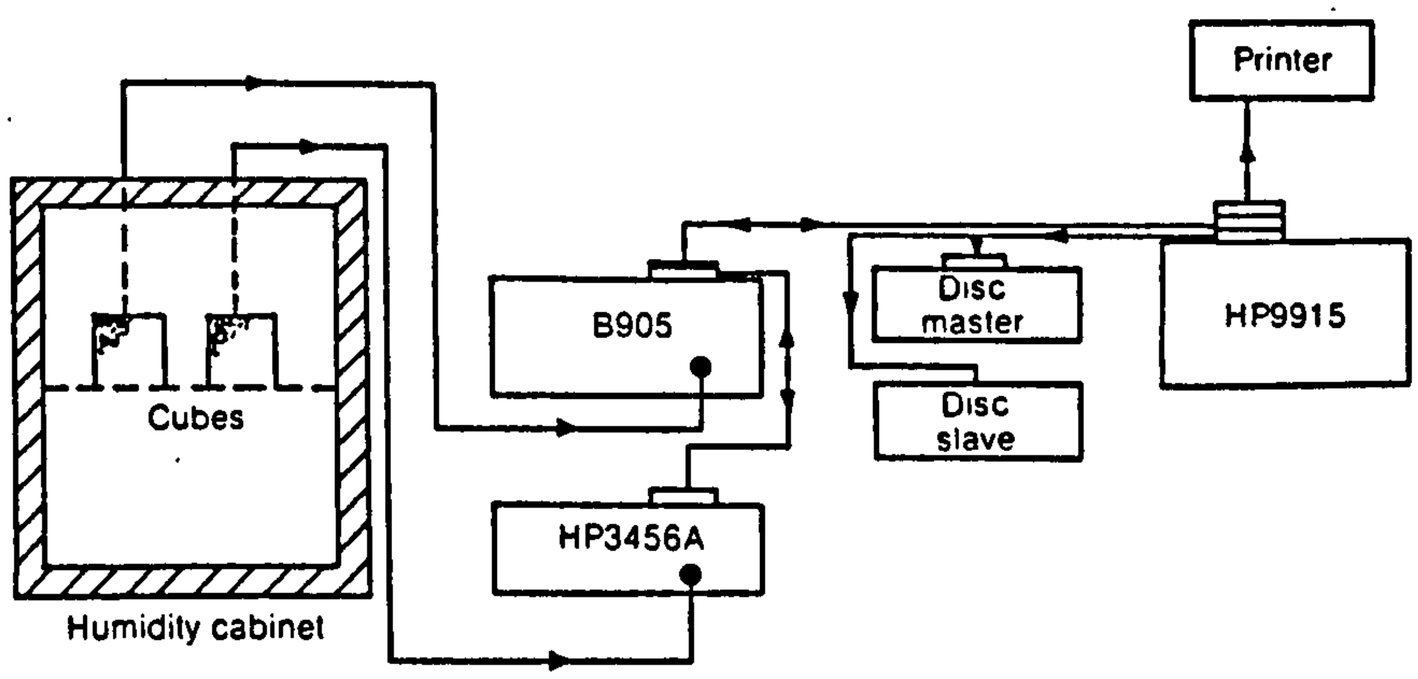

Fig. 2. Schematic diagram of system architecture

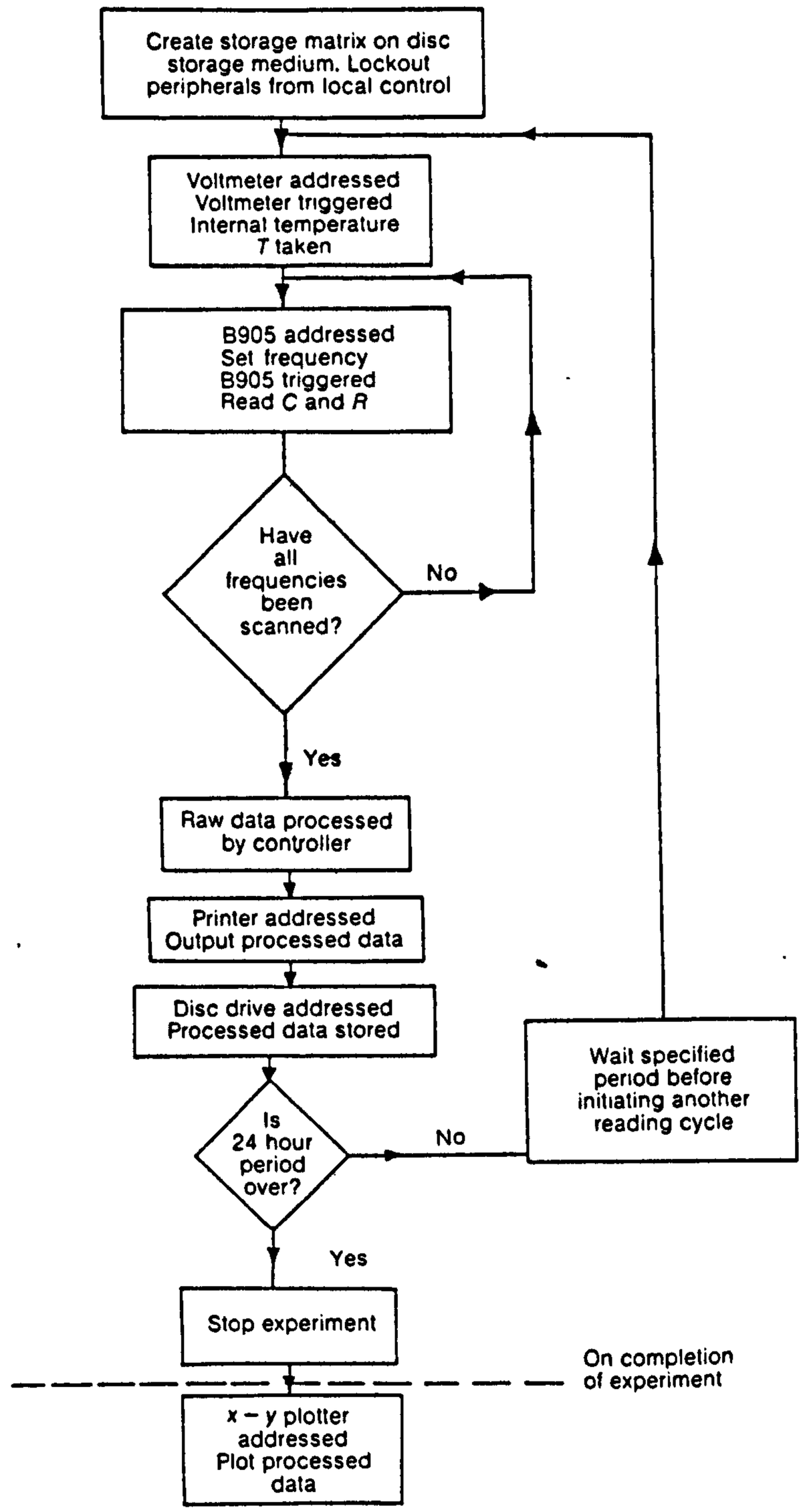

Fig. 3. Address sequence of peripherals

Discussion of results

Electrical response of ordinary Portland cement

18. Figure 5 shows the changes in dielectric constant, electrical resistivity and internal temperature of cement paste over the initial 24 h period. The electrical response of the paste varies quite markedly; chemical reactions occurring within the paste can be identified with changes in electrical response and, in addition, the rate of change of the electrical parameters are indicative of the rate at which reactions are occurring.

19. Immediately on gauging cement and water, the bulk aqueous phase becomes saturated with calcium and hydroxyl ions, while the cement grains will be surrounded by a weak, highly amorphous C–S–H layer and stabilized by an electrical double layer comprising, primarily, Ca^{2+} and OH^- ions. Ions in the aqueous phase will result in a low electrical resistivity at these early stages (compared with that of the original mixing water); charges, associated with the grain surface, while not available for the conduction process, can be polarized by the alternating electric field and result in high induced dipole moments. As a consequence, high dielectric constants at low frequencies of applied field are

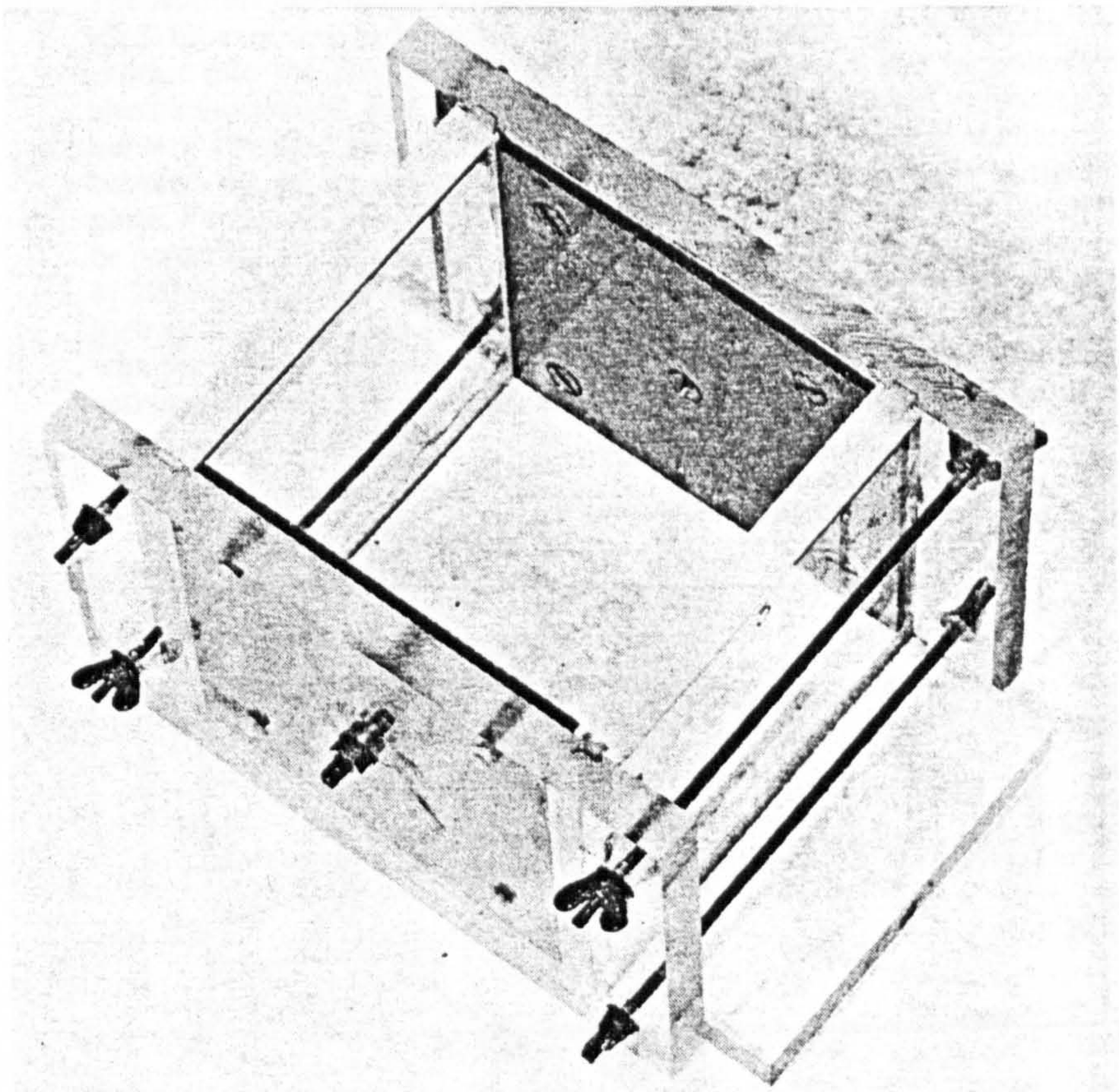

Fig. 4. Dielectric cell

expected as the charges, associated with grain surfaces, can follow the alternations of the electric field. The dielectric constant over the initial 40 min decreases quite rapidly and could be accounted for by a build-up of the gelatinous (gel) coating on the grains reducing charge mobility. The build-up of the semipermeable membrane surrounding the grain will hinder diffusion of ions into solution and result in an overall reduction in reaction rate. It is evident that from 40 min, and up to 180 min, the rate of change of dielectric constant is considerably reduced and would signify little activity within the paste. The initial burst of activity up to 40 min could be identified as stage 1 of the hydration process while the period 40–180 min would give credence to the dormant, or induction, period of little chemical activity associated with stage 2. The resistivity, however, shows little change over the initial 180 min rising by approximately 8% of its initial value. The gauging water at this early stage will be electrolytically saturated and even though ions are moving out of solution little effect on the resistivity would be noticed.

20. At approximately 180 min there is a marked rise in the dielectric constant peaking at approximately 200 min followed by an equally significant drop. The sudden rise indicates a spontaneous burst of chemical activity within the paste. The Authors attribute this peak to a rupturing of the relatively weak gel coating (C–S–H) exposing unhydrated cement grain surfaces and subsequent release of charges into the double layer around the grain which can be polarized by the alternating electric field. The peak at 200 min is short lived indicating a sudden burst of chemical activity leading to an irrotational binding of charges, contact between the gel on the grain surfaces and an overall increase in rigidity of the paste. Formation of a more stable C–S–H and crystallization of $Ca(OH)_2$ would be occurring over the period of the peak (180–600 min). The magnitude of the peak at 200 min gives an indication of the degree of instability of the relatively weak hydrate formed on the grain surface. The rise in resistivity at 200 min coincides with the drop in dielectric constant, and it is postulated that the renewed chemical activity is associated with grain surfaces and not the bulk aqueous phase. If

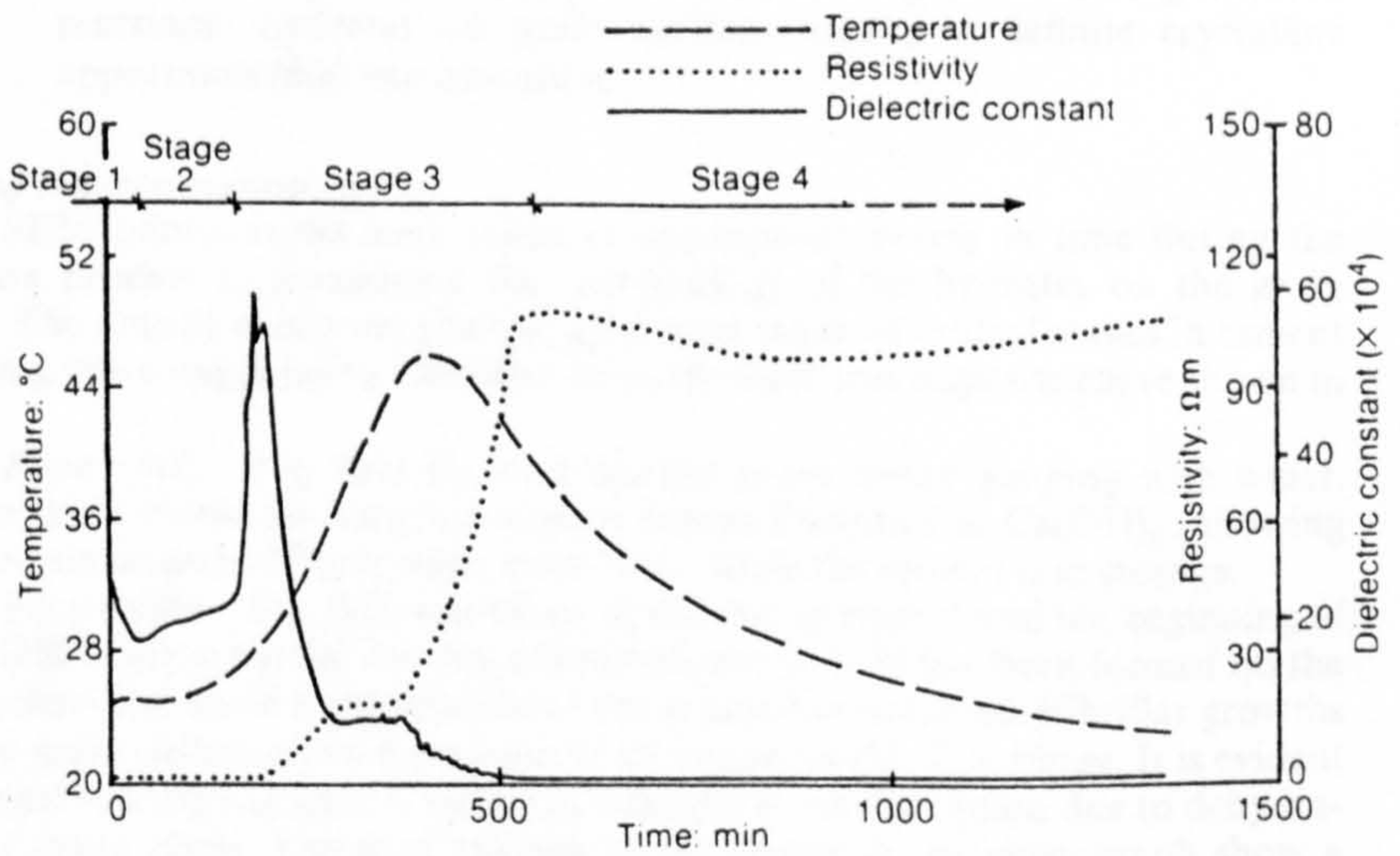

Fig. 5. Variation in dielectric constant, resistivity and temperature of cement paste during 24 h after gauging with water (water-to-cement ratio, 0·27)

charges are released into the capillary water then a drop in resistivity should be detected; however, this is not evident.

21. Over the period 200–600 min the resistivity rises quite sharply indicating that conduction paths through the continuous capillary pores in the paste are becoming more tortuous as the grains segment and ionic concentrations decrease. At 600 min the electrical parameters undergo yet another change and this is taken to signify the end of stage 3 and the beginning of stage 4 of the hydration process. The resistivity decreases and, coinciding with this, there is a rise in dielectric constant (although slightly obscured by scale). This is taken to indicate further activity within the paste; however, the reactions are at a much slower rate as indicated by the rate of change of these parameters. At this point in time (600 min) the paste has considerable strength and the grains have segmented. This renewed activity must release charges into the continuous capillary pores—thereby reducing the electrical resistivity—and into blocked capillary and gel pores—thereby increasing the dielectric constant by interfacial polarization. The period after 600 min is regarded as the beginning of the hardening process, the changes in resistivity and dielectric constant indicating activity on the C_2S phase and renewed activity on the C_3A phases. The magnitude of the decrease in resistivity indicates that, perhaps, the C_2S phase predominates as this is present in a greater percentage by weight. The initial set and the final set, as defined by the Vicat Needle, were at 110 min and 210 min respectively for this consistency of paste.

22. From the electrical response curve, four stages in the early hydration of Portland cement have been identified and corroborate previous theories on the chemistry of cement hydration, these stages being

(1) initial build-up of amorphous hydrates on the grain surface (0–40 min)
(2) a dormant period of little chemical activity (40–180 min)
(3) a period of renewed chemical activity and a gain in rigidity of the paste (180–600 min)
(4) a reduction in the rate of chemical activity and a general slowing-down of reactions: hydrates on grain surfaces assume a definite crystalline appearance (600 min onwards).

Scanning electron microscopy

23. SEM photographs were taken at appropriate points in time during the hydration process to investigate the morphology of the hydrates on the grain surface. The time at which the photographs were taken at critical stages in cement hydration, these stages being identified from the electrical response curve shown in Fig. 5.

24. *Figure 6(a).* Fig. 6(a) shows a cement grain before gauging with water. White crystals visible on the grain surface can be identified as $Ca(OH)_2$, showing that a certain amount of hydration must occur while the cement is in storage.

25. *Figure 6(b).* Fig. 6(b) was taken at the end of stage 2 and the beginning of stage 3 (180 min): a partial coating of amorphous C–S–H has been formed on the grain surface and some segmentation of the grains has occurred. Fibrillar growths from the grain surface show formation of ettringite on the C_3A phase. It is evident that the gel coating has gained sufficient strength as no disruption due to dehydration has taken place. The dark regions in the centre of the photograph show a capillary pore which has been evacuated of water.

26. *Figure 6(c).* Fig. 6(c) was taken midway through stage 3 (330 min): the

grains now show a complete coating of amorphous C–S–H resembling fish scales. There is little evidence, at this stage, to suggest that the hydrates on the grain surface have any definite crystalline structure.

27. *Figure 6(d)*. Fig. 6(d) was taken at the end of stage 3 and the beginning of stage 4 (approximately 600 min). The hydrates on the grain surface have now taken on a definite morphology. The stumpy surface protruberances are identified as C–S–H, while the large white crystals attached to the fibrillar growths are portlandite ($Ca(OH)_2$).

28. *Figure 6(e)*. Fig. 6(e) was taken at 700 min after gauging: the grain surface shows the development of long slender needles, believed to be ettringite growing from the C_3A phase. The structure of the cement paste has taken on a crystalline appearance.

29. *Figure 6(f)*. Fig. 6(f) was taken at 900 min and the surface of the cement grains shows a definite crystalline morphology. The grain shows C–S–H crystals, which appears as a burr on the grain surface, together with large portlandite crystals (centre left of photograph).

30. *Figure 6(g)*. Fig. 6(g) was taken 1000 min after gauging: long slender ettringite crystals are evident. Closer examination shows plate-like foils growing through the ettringite believed to be monosulphoaluminate crystals, caused by secondary reaction on the C_3A phase associated with stage 4.

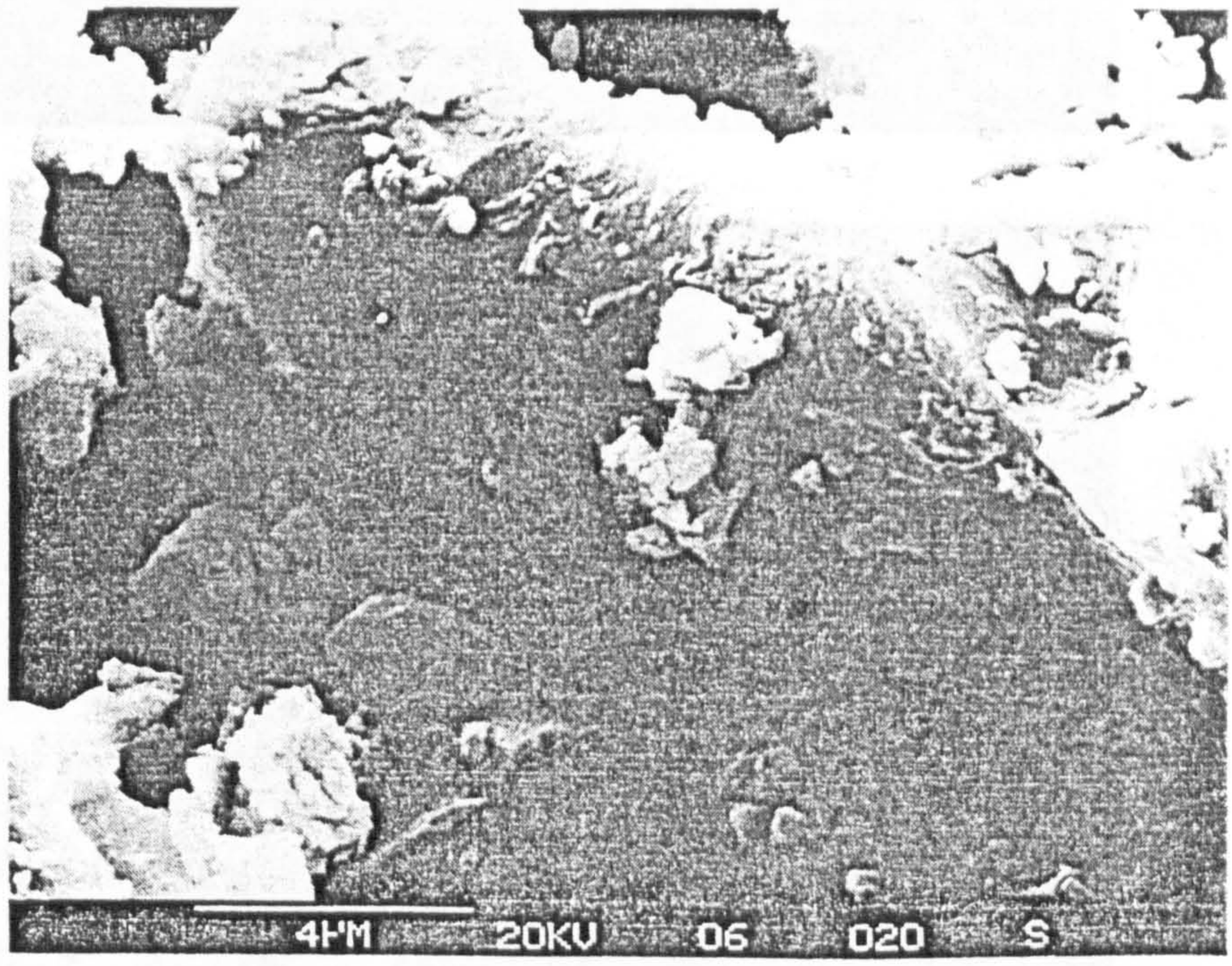

(*a*)

Fig. 6. (Above, facing and overleaf) *SEM micrographs taken during the initial 24 h*: (*a*) *cement grains before gauging* (× 2940); (*b*) 180 *min* (× *2940*); (*c*) *330 min* (× *588*); (*d*) *600 min* (× *2940*); (*e*) 700 *min* (× *588*); (*f*) 900 *min* (× 2940); (*g*) 1000 *min* (× *2940*)

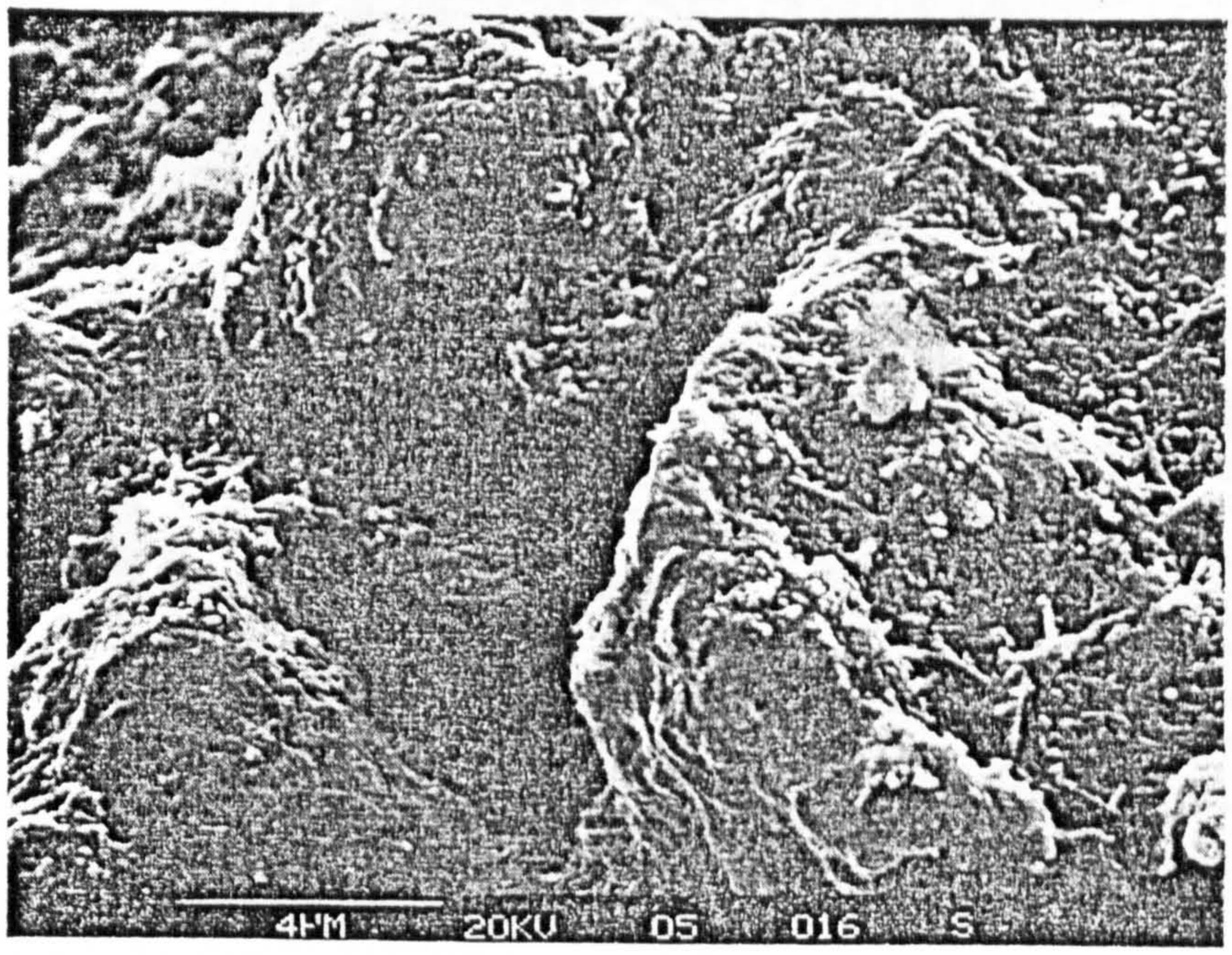

(*b*)

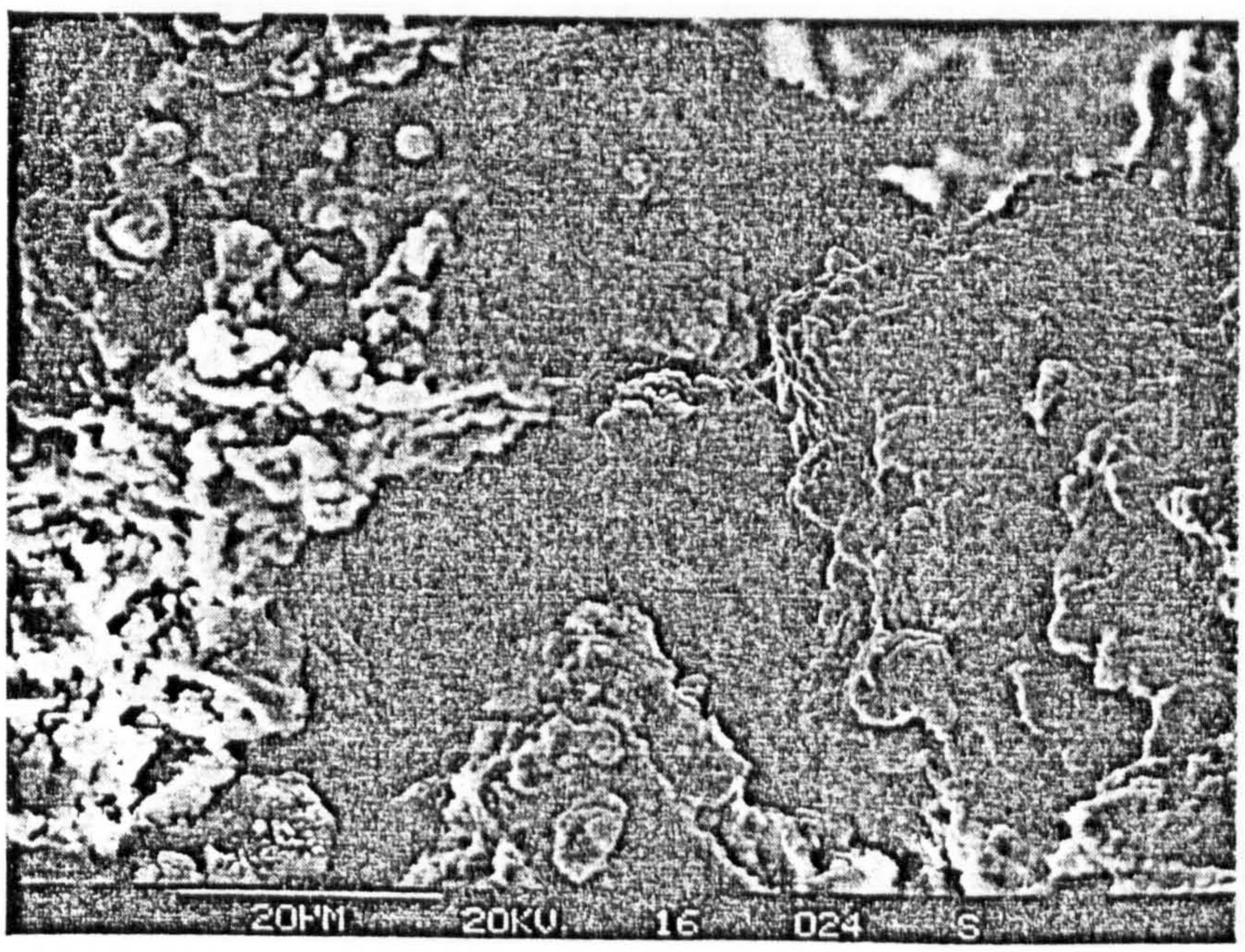

(*c*)

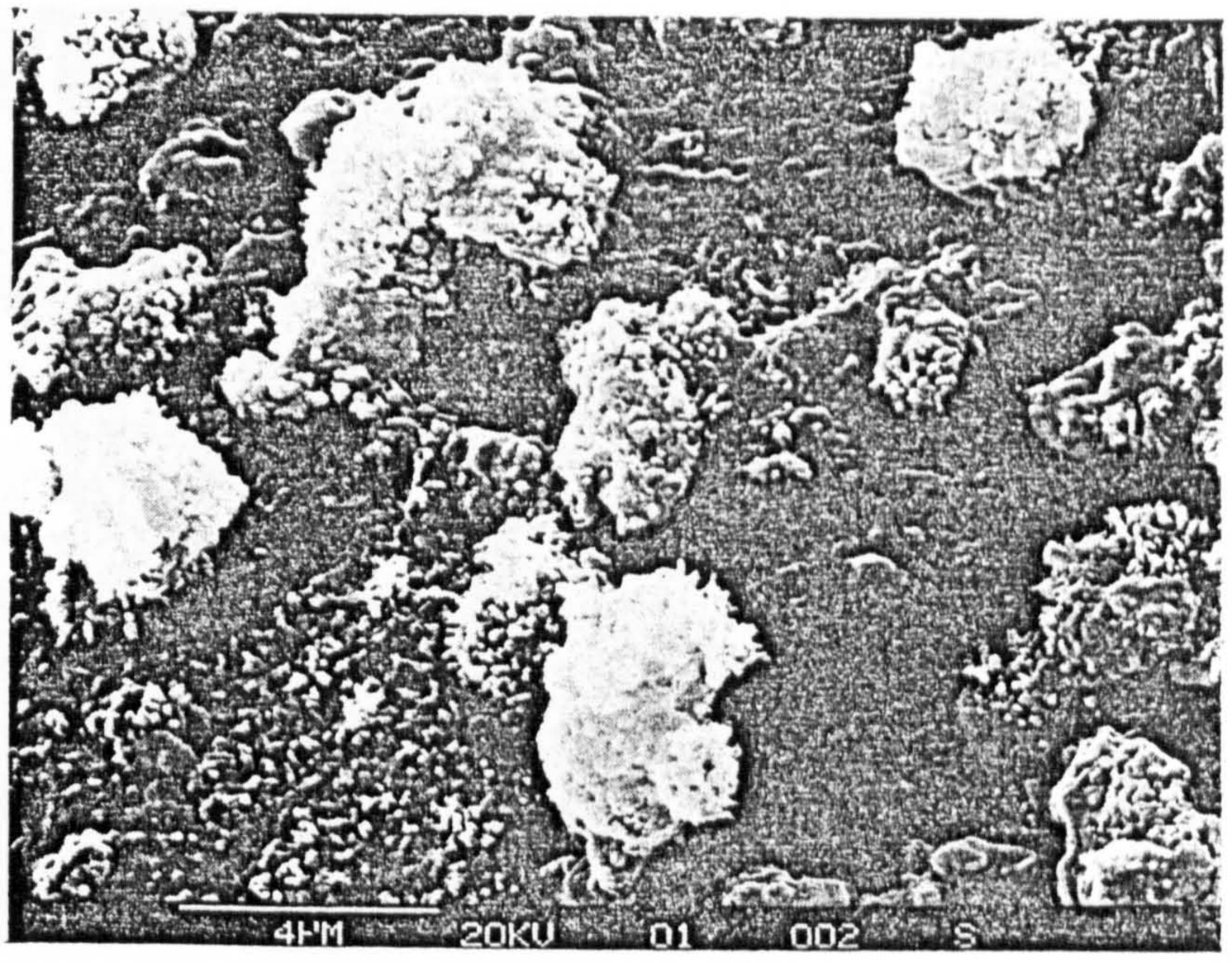

(*d*)

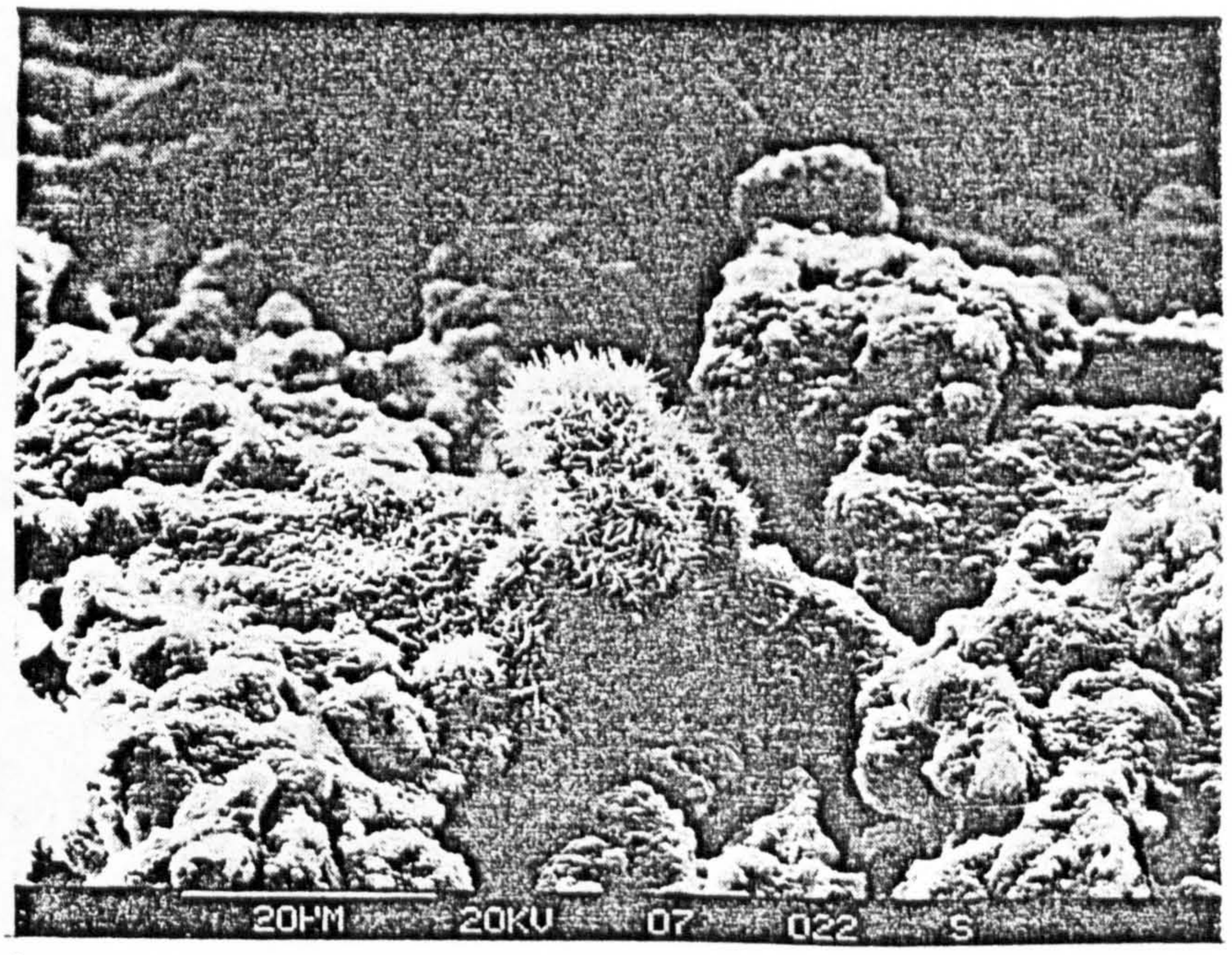

(*e*)

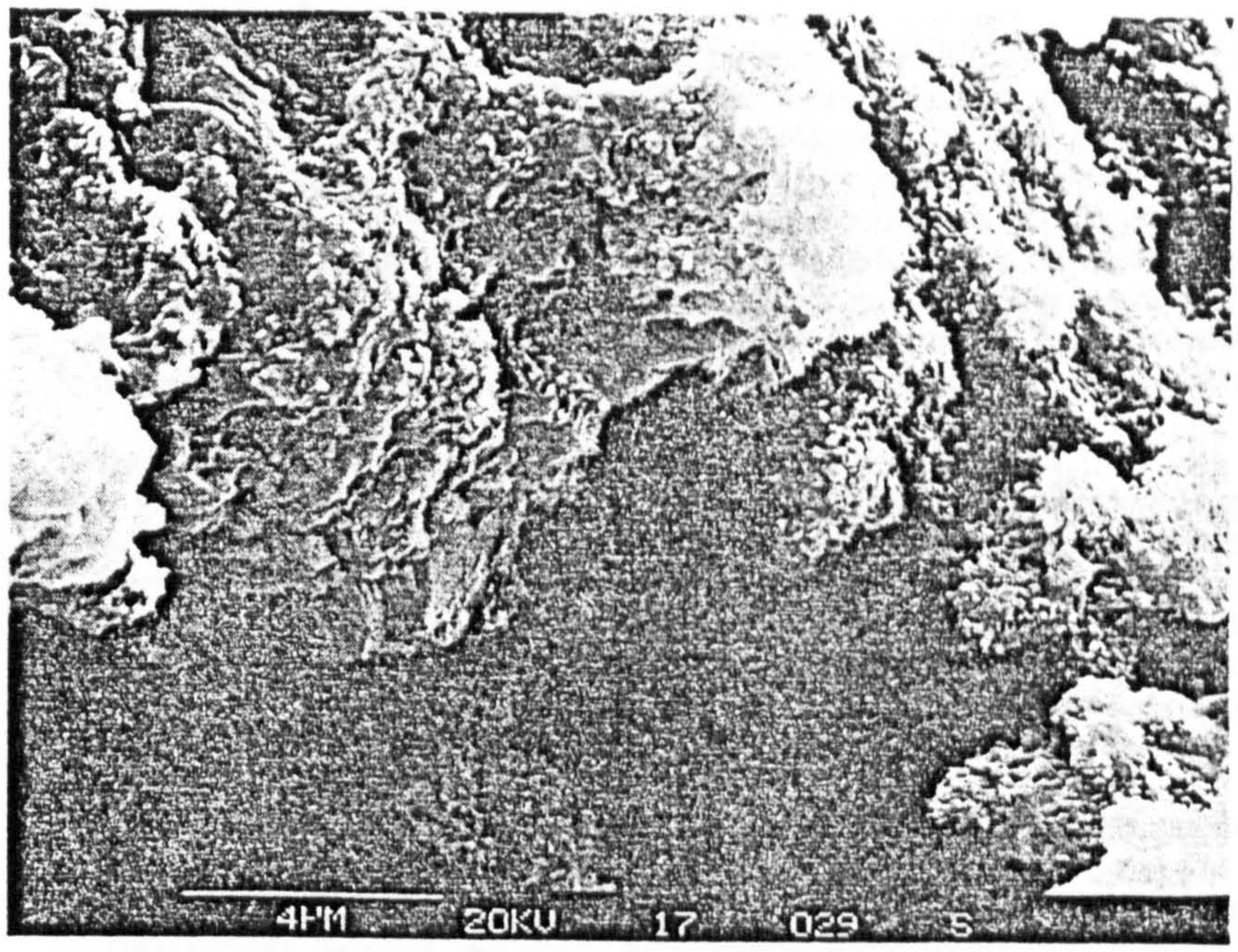

(*f*)

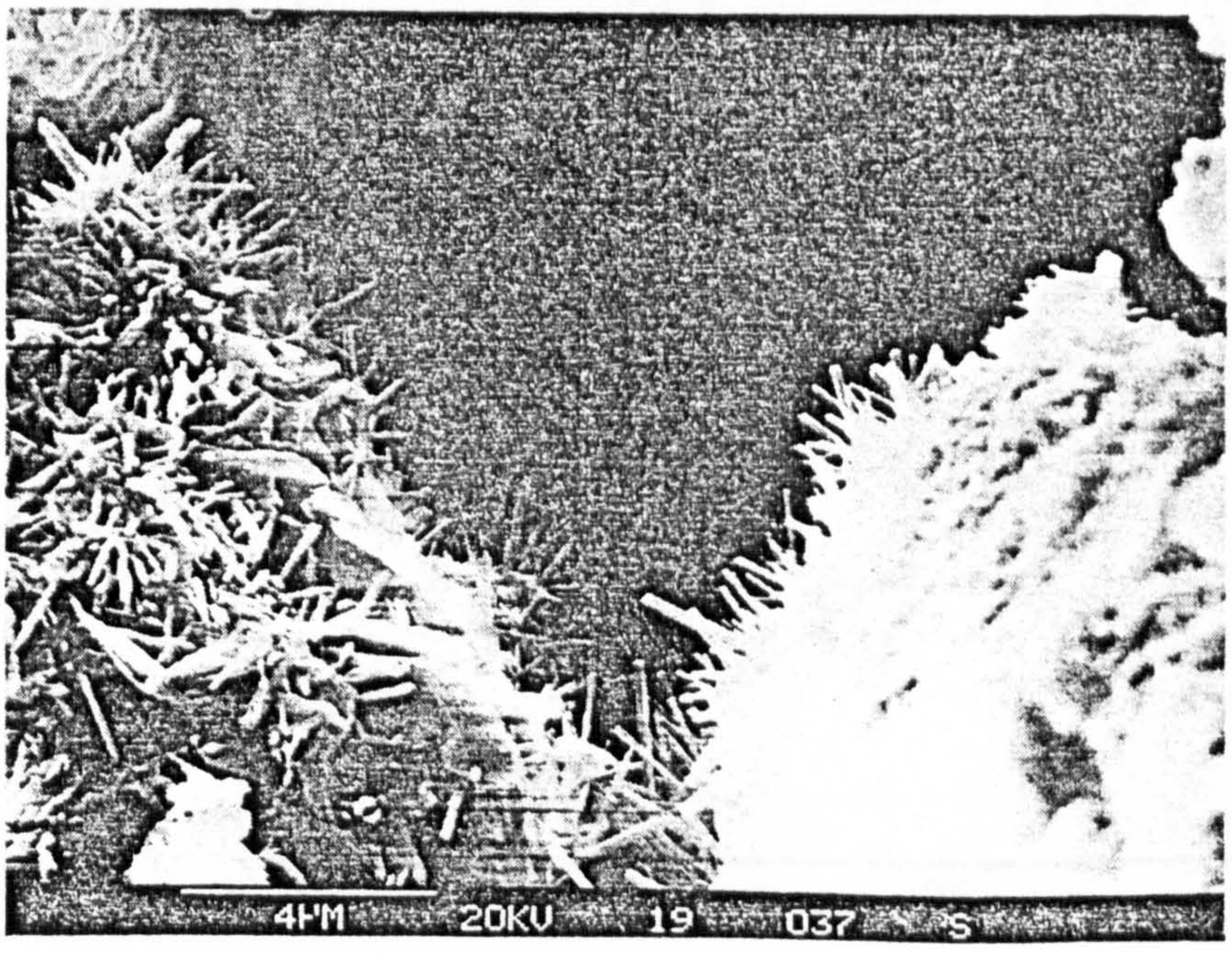

(*g*)

Strength development of paste

31. A series of tests was carried out to investigate the development of strength of the paste over the initial 24 h. 50 mm cubes of cement paste were tested at discrete points in time and the strength development curve is given in Fig. 7. By 200 min the paste has gained sufficient strength to be demoulded, failure of the cube being akin to that of a heavily consolidated clay, i.e. plastic. At 250 min the failure pattern resembles that of a 'classic' cube failure, indicating that the paste is taking on the behaviour of the solid. Over the next 400 min the rate of gain of strength increases, coinciding with the period where the electrical parameters are undergoing rapid changes and the structure-building processes are occurring.

Influence of retarders and accelerators on electrical response

32. Tests were carried out to investigate the effect of retarders (sugar) and accelerators (calcium chloride) on the hydration process and their influence on the electrical response. The additives were added by percentage weight of cement and the response curves are given in Fig. 8. From Fig. 8(a) (retarder) and 8(b) (accelerator), it is evident that the critical points on the dielectric constant and electrical resistivity curves associated with hydration processes discussed previously have been reproduced at later and earlier stages for retarders and accelerators respectively.

33. For the retarder, the dormant period of stage 2 has been extended and renewed activity on the C_3S phase (which leads to setting) takes place at approximately 600 min. When an accelerator is added to the mix, the dormant period is considerably reduced and the C_3S hydration peak occurs over a much reduced time-scale. Reaction rates, inferred from the rate of change of electrical parameters, are considerably reduced for the retarder and increased for the accelerator, particularly over stage 3 of the hydration process. (In Fig. 8(b) the dielectric constant does not become zero at 100 min, as the scale of the graph masks the actual values at this stage.) For the data given, the addition of 0·05% sugar delays setting by 400 min (i.e. from 200 min to 600 min), while 1·5% calcium chloride accelerates setting by 120 min (i.e. from 200 min to 80 min).

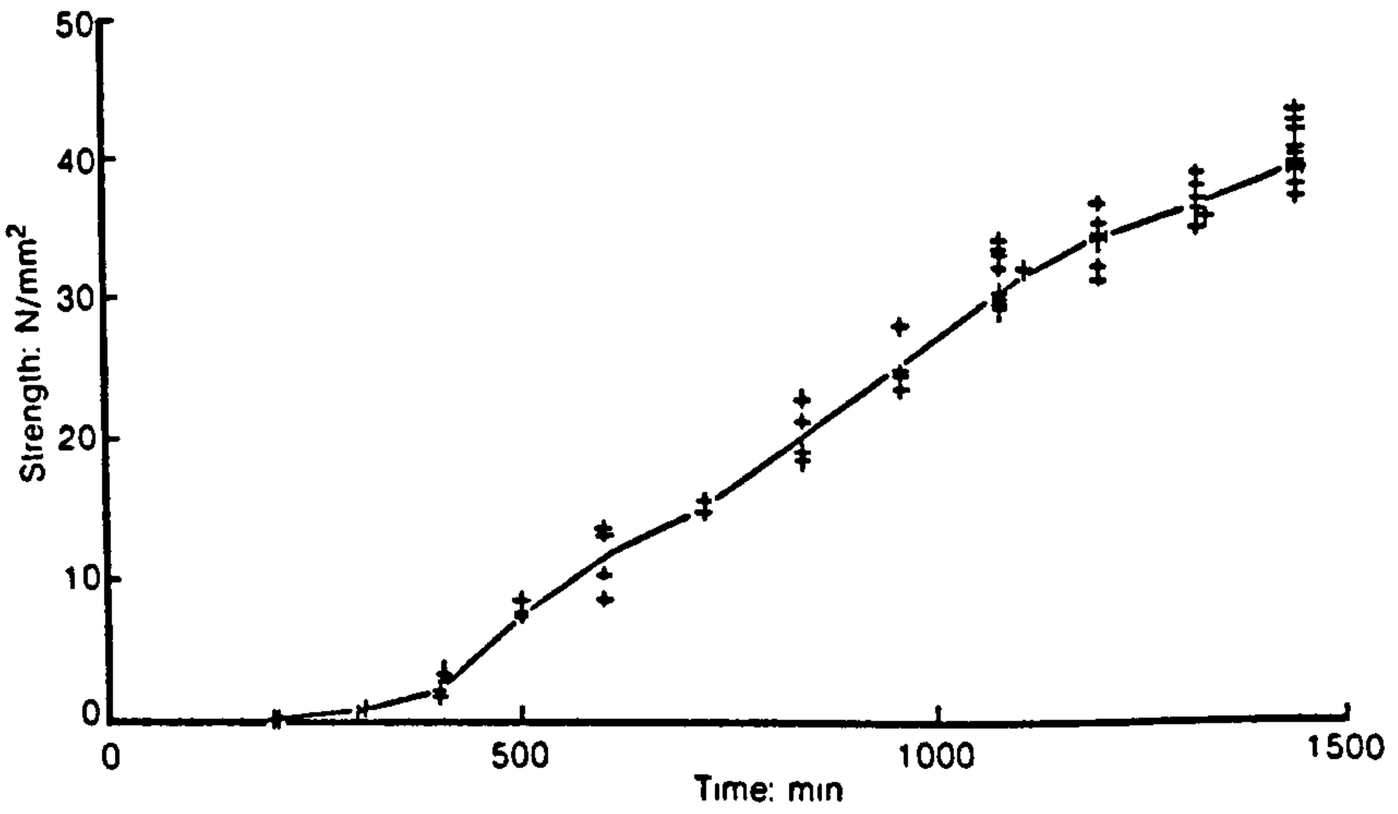

Fig. 7. Increase in strength of cement paste over initial 24 h

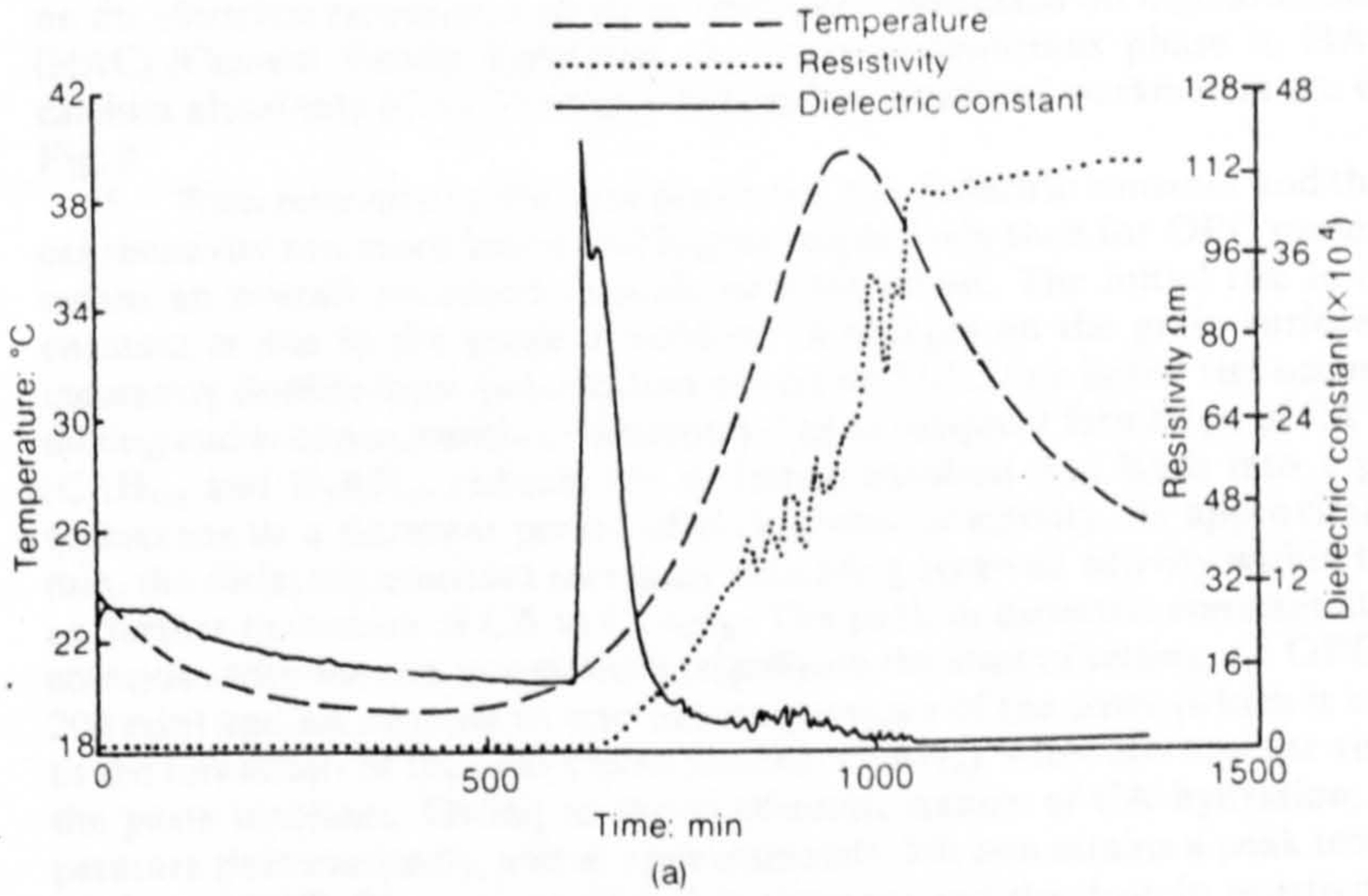

Fig. 8. Influence of admixtures on electrical response: (a) retarder (0·1% sugar); (b) accelerator (1·5% calcium chloride)

Influence of chemical composition on electrical response

34. To investigate the effect of varying the chemical constituents of the cement on the electrical response, a series of tests were conducted on high alumina cement (HAC) (Cement Fondu Lafargue), the main cementitious phase in HAC being calcium aluminate (CA). The variations in the measured parameters are shown in Fig. 9.

35. With reference to the data presented, the dielectric constant and the electrical resistivity are much lower and higher respectively than for OPC paste and this means an overall reduction in ionic concentrations. The initial rise in dielectric constant is due to the gradual build-up of charges on the grain surface thereby increasing double-layer polarization effects (in OPC this initial rise occurs during mixing and is consequently undetected). The subsequent formation of CA hydrates (CAH_{10} and C_2AH_8) reduces the dielectric constant and leads into a period of quiescence or a dormant period of little chemical activity. At approximately 200 min, the dielectric constant increases indicating renewed activity within the paste, i.e. further hydration of CA to C_2AH_8. The peak in dielectric constant at 260 min coincides with the rise in resistivity (signifying the start of setting, c.f. OPC paste at 200 min) and an increase in internal temperature of the paste (which is conducive to the formation of the conversion product C_3AH_6). After 260 min the viscosity of the paste increases. Owing to the exothermic nature of CA hydration, the temperature rises markedly, and at approximately 350 min attains a peak temperature of about 120°C. The peak in dielectric constant and the drop in resistivity noticeable at peak temperature are attributed to a combination of C_3AH_8 formation and an increase in internal temperature—the dielectric constant and resistivity being temperature dependent. Some internal desiccation must result from this rise in temperature. The peak in dielectric constant and the drop in resistivity are short lived as the paste rapidly gains rigidity and the period of hardening begins (at about 500 min). The values of dielectric constant and electrical resistivity are substantially lower and higher respectively than those of OPC paste at all stages throughout hydration.

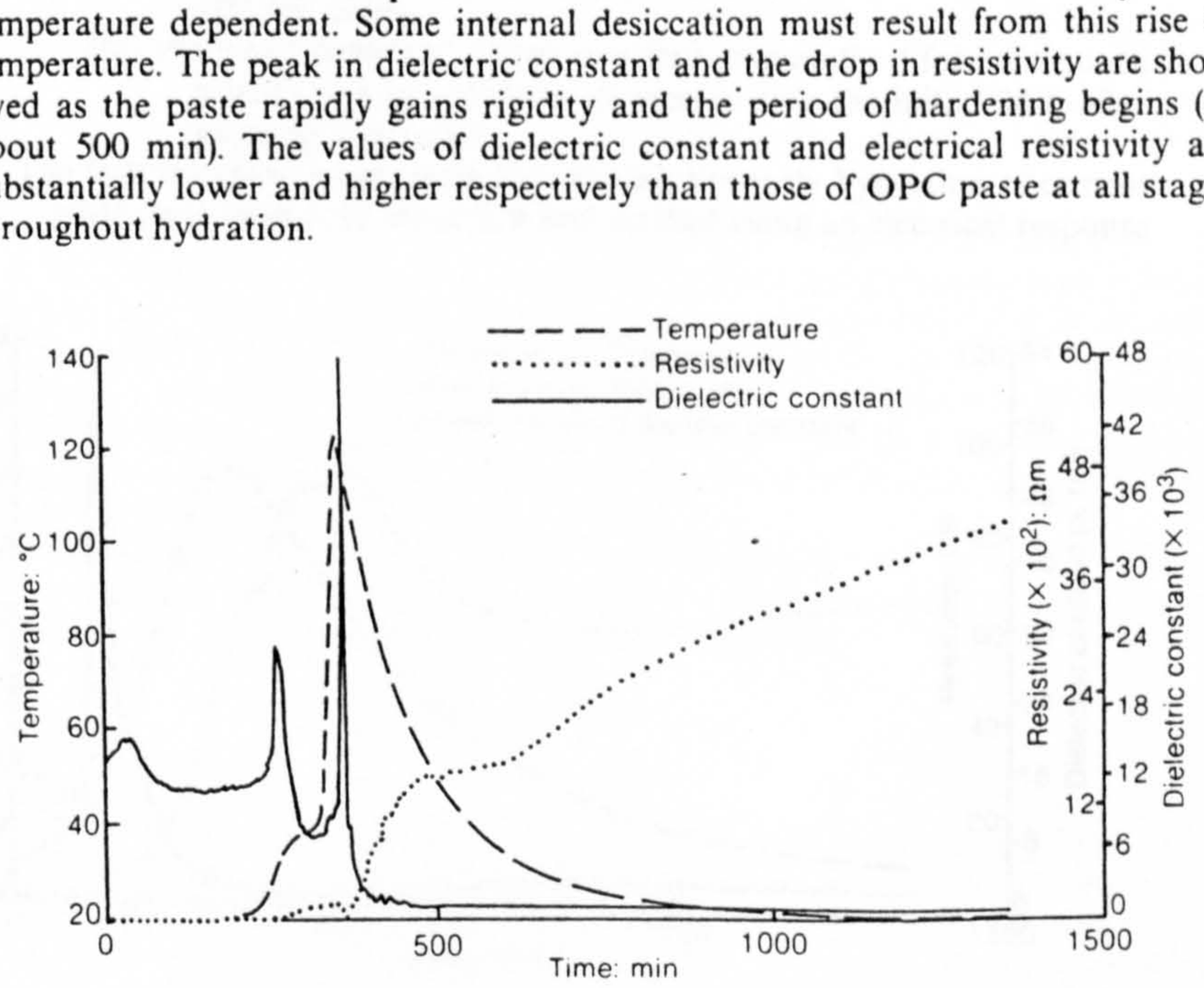

Fig. 9. Electrical response characteristics of HAC (water-to-cement ratio, 0·27)

Effect of age of cement on hydration characteristics

36. The results given are for OPC supplied from a builder's merchant and had been estimated to be lying in storage for about 4–6 weeks before delivery. Experiments were conducted on ex-works' cement which was approximately 1 week old and the response curve for this cement is given in Fig. 10. Certain similarities between 'old' and 'new' cement are noticeable, but, perhaps, the most significant differences are

(*a*) the reduction in length of the dormant period of stage 2 (20–100 min)
(*b*) a more significant drop in resistivity and a rise in dielectric constant associated with stage 4.

The implication of (*a*) and (*b*) is that the 'new' cement sets at an earlier stage (about 100 min) and will, consequently, be stronger than the 'old' cement at any stage in time over the 24 h test period. In addition, the cement lying in storage will have developed hydrates on the grain surface due to moisture absorption (Fig. 6(a)) and will result in an overall reduction in reaction rate.

Conclusions and concluding remarks

37. The following conclusions can be drawn from the present study.

(*a*) The method developed in this Paper has certain advantages over present structure determining techniques
  (i) the fabric structure of the paste is not destroyed
  (ii) the sample size is sufficiently large to evaluate macroscale behaviour; indeed, the sample size conforms to BS 1881 (standard 100 mm cube)
  (iii) the work presented offers an alternative method for continuous monitoring of hydration processes over the initial 24 h after gauging with water.
(*b*) The four accepted stages occurring during the early hydration of cement paste have been both identified and verified using an electrical response

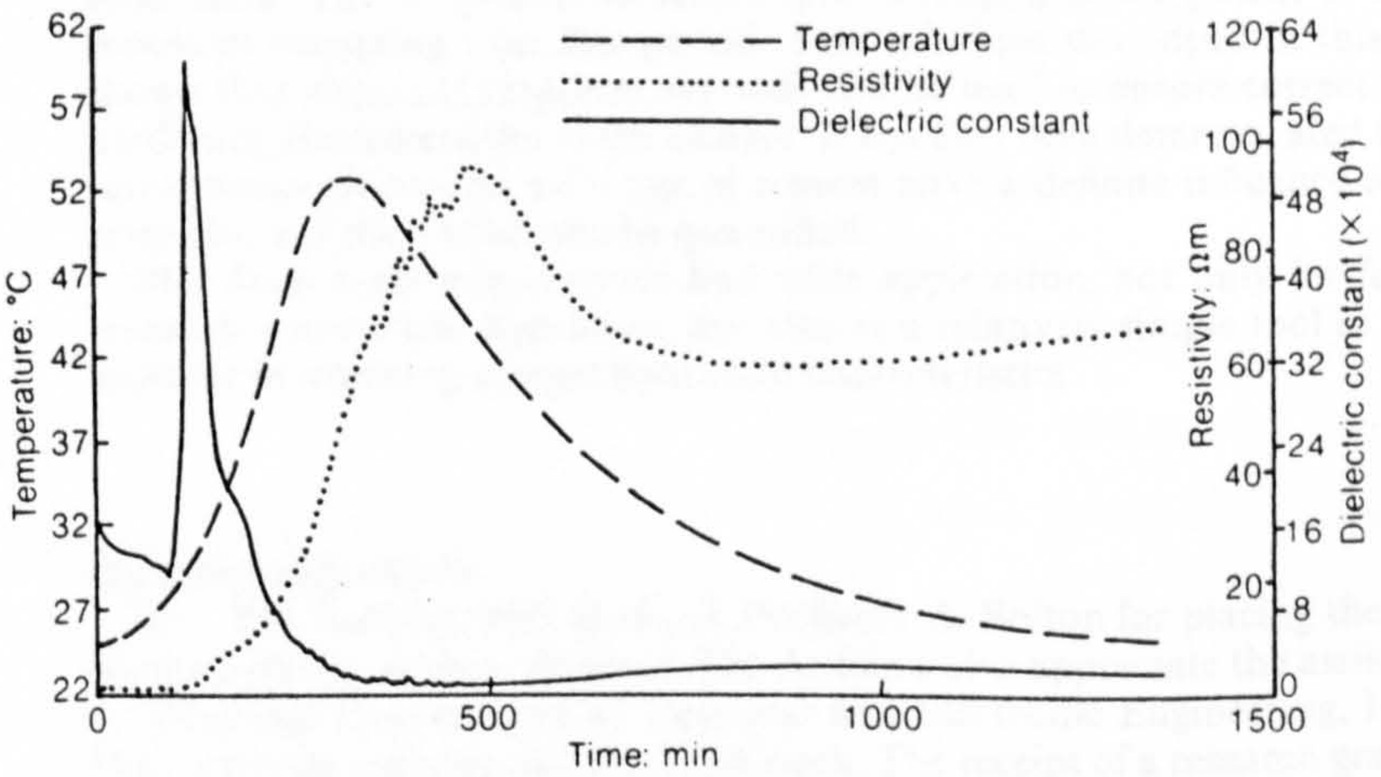

Fig. 10. Effect of storage on the electrical response of cement paste

technique. The rates of change of these electrical parameters indicate the rate at which hydration is progressing.

(*c*) Further new evidence on the early hydration of OPC has been given. It has been demonstrated that the electrical response of cement paste is sensitive to physical and chemical changes within the paste and the dielectric constant and electrical resistivity can be used as a diagnostic of the setting and hardening processes. The work presented could also help in elucidating such theories as the membrane theory postulated by Birchall *et al.*[1] and Double *et al.*[2].

(*d*) The influence of admixtures on the hydrolysis and hydration processes can be quantified with greater accuracy than has hitherto been achieved. As this method is measuring the chemical processes within the paste, the arbitrary terms initial and final set could have more meaning if redefined in terms of their electrical parameters.

(*e*) It has been shown that the rate at which the paste gains strength is greatest over the period of intense chemical activity, i.e. when the electrical properties of the paste are undergoing significant changes (200–600 min).

(*f*) The continuous monitoring of the chemical processes in, for example, HAC has shown that a change in chemical composition of the cement influences the electrical response. Indeed, the electrical response characteristics of HAC indicate four identifiable stages in its hydration over the initial 24 h. Also of interest is the high internal temperature occurring within the HAC paste caused by secondary CA hydration. Some conversion must result from such a temperature rise.

(*g*) from the SEM work undertaken, definite crystal formation during the initial 24 h has been identified and the electrical response data can be used to give indications about the morphology of the hydrates forming on the cement grain surfaces.

38. The first 24 h of the hydration process of cement paste are perhaps the most important as it is during this period that the paste changes from a fluid to a solid state. The long-term structure (and strength) development is dictated by processes occurring over this period. The technique developed in this Paper has shown that electrical response methods can be used to ensure correct setting and hardening characteristics of the cement. It has also been demonstrated that admixtures, composition and even age of cement have a definite influence on electrical response, and their effect can be quantified.

39. Such a technique could find wide application, not only for fundamental research into cement hydration, but also as a relatively simple tool in helping the engineer in assessing cement hydration characteristics.

Acknowledgements

40. The Authors wish to thank Professor A. Bolton for placing the facilities of his department at their disposal. The Authors also appreciate the assistance of Dr R. Dhariwal (Department of Electrical and Electronic Engineering, Heriot-Watt University) in carrying out the SEM work. The receipt of a research grant from the Science and Engineering Research Council is gratefully acknowledged.

References

1. BIRCHALL J. D. *et al.* On the hydration of Portland Cement. *Proc. R. Soc. A*, 1978, 360, 445–453.
2. DOUBLE D. D. *et al.* The hydration of Portland Cement. *Proc. R. Soc. A*, 1978, 359, 435–451.
3. TAYLOR H. F. W. *The chemistry of cements.* Academic Press, London, 1964.
4. VERBECK G. Cement hydration reactions at early ages. *J. Res. Dev. Labs Portld Cem. Ass.*, 1965, 7, Sept., No. 3, 57–63.
5. SELIGMANN P. Nuclear magnetic resonance studies of the water in hardened cement paste. *J. Res. Dev. Labs Portld Cem. Ass.*, 1968, 10, Jan., No. 1, 52–65.
6. BARNES P. and GHOSE A. *Structure and performance of cements.* Applied Science Publishers, London, 1983.
7. MINDESS S. and FRANCIS YOUNG J. *Concrete*, Prentice-Hall, Eaglewood Cliffs, 1981.
8. ANGSTADT R. L. and HURLEY F. R. Hydration of the alite phase in Portland Cement. *Nature*, 1963, 197, 16 Feb., 688.
9. NEW CIVIL ENGINEER. Strength gain is durability's loss. *New Civ. Engr*, 1984, 23 Oct., 4–5.
10. NEW CIVIL ENGINEER. Cement report seeks longer lasting concrete. *New Civ. Engr*, 1984, 23 Oct., 4.
11. NEW CIVIL ENGINEER. Blue Circle suspends PFA cement blend. *New Civ. Engr*, 1984, 4 Oct., 8.
12. MCCARTER W. J. *et al.* Resistivity characteristics of concrete. *Proc. Instn Civ. Engrs*, Part 2, 1981, 71, Mar., 107–117.
13. MCCARTER W. J. *et al.* Electrical resistivity characteristics of air-entrained concrete. *Proc. Instn Civ. Engrs*, Part 2, 1983, 75, Mar., 123–127.
14. MCCARTER W. J. *et al.* The conduction of electricity through concrete. *Mag. Concr. Res.*, 1981, 33, Mar., No. 114, 48–60.
15. DORSCHE K. E. The hardening and corrosion of cement—IV. *Cem. Concr. Mf.*, 1933, Apr., 131–142.
16. CALLEJA J. New techniques in the study of setting and hardening of hydraulic materials. *J. Am. Concr. Instn*, 1952, 23, 525–536.
17. SRIRAVINDRAJAH R. and SWAMY R. N. Development of a conductivity probe to monitor setting time and moisture movement in concrete. *Cem. Concr. Agg.*, 1983, 4, No. 2, 73–80.
18. BARS J. R. *et al.* Example and application of a method for measuring electrical impedance: evaluation of electrical conductivity of cement paste during its setting time. *Mater. Struct. Res. Test.*, 1982, 15, Part 85, Jan.–Feb., 33–37.
19. MICHAEL H. *et al.* Relationships between electrical and physical properties of cement paste. *Cem. Concr. Res.*, 1974, 4, July, 881–897.
20. DE LOOR G. P. The effect of moisture on the dielectric constant of hardened Portland Cement paste. *Appl. Sci. Res. B*, 1961, 9, May, 297–307.
21. MCCARTER W. J. and AFSHAR A. B. Some aspects of the electrical properties of cement paste. *J. Mater. Sci. Lett.*, 1984, 3, 1083–1086.
22. MCCARTER W. J. and CURRAN P. N. The electrical response characteristics of setting cement paste. *Mag. Concr. Res.*, 1984, 36, Mar., No. 126, 42–49.
23. SCHWAN H. P. *et al.* On the low-frequency dielectric dispersion of colloidal particles in electrolytic solutions. *J. Phys. Chem.*, 1962, 66, 2626.
24. SCHWARZ G. A theory of the low-frequency dielectric dispersion of colloidal particles in electrolyte solution. *J. Phys. Chem.*, 1962, 66, 2636.
25. HASTED J. B. *Aqueous dielectrics.* Chapman and Hall, London, 1973, 286.
26. MAXWELL J. C. *A treatise on electricity and magnetism.* Oxford University Press, London, 1873, 1, 464.
27. WAGNER K. W. *Arch. Elektrotech.*, 1914, 2, 371.
28. POWERS T. C. Some physical aspects of the hydration of Portland Cement. *J. Res. Dev. Labs Portld Cem. Ass.*, 1961, 3, Jan., No. 1, 47–56.

29. SKALNY J. *et al.* Studies on hydration of cement—recent developments. *Wld Cem. Technol.*, 1978, 9, Sept., No. 6, 183–195.
30. LEA F. M. *The chemistry of cement and concrete*. Arnold, London, 1970, 2nd edn.
31. BRITISH STANDARDS INSTITUTION. *Methods of testing cement*. BSI, London, 1978. BS 4550, Part 3, Section 3.5.

William J. McCarter[1] *and Ali B. Afshar*[1]

Diagnostic Monitoring of the Physio-Chemical Processes in Hydrating Cement Paste

REFERENCE: McCarter, W. J. and Afshar, A. B., "Diagnostic Monitoring of the Physio-Chemical Processes in Hydrating Cement Paste," *Cement, Concrete, and Aggregates*, CCAGDP, Vol. 7, No. 2, Winter 1985, pp. 57-68.

ABSTRACT: This paper details a novel electrical technique for monitoring the chemical and physical changes occurring within cement paste. The present study has concentrated on the initial 24 h after gaging with water and investigates the influence of retarders, accelerators, and cements of different type on electrical response. A microcomputer-controlled data acquisition system was developed to obtain results that can be used to obtain accurate electrical response/time curves. This is an advancement on earlier techniques. The work has correlated changes in electrical response with known chemical changes and structure building processes in cement paste. The method described also offers a technique for assessing the influence of chemical additives on the setting and hardening processes.

KEYWORDS: cement paste, hydrolysis, hydration, dielectric properties, resistivity, microcomputer, additives, materials tests

Studies on the changes in electrical resistance of cement paste in both the liquid and hardened state have been the subject of investigation by several workers [*1-4*], and attempts have been made, with varying degrees of success, in trying to determine the physical state of the paste in terms of this parameter. Little attempt has been made to relate changes in electrical resistance with the chemical process of setting and hardening; furthermore, differing specimen sizes, electrode configurations, measuring techniques and test conditions together with a general lack of data points make results vary within wide limits. More recently, attention has been drawn to the use of the electrical resistivity characteristics of cement paste as a technique for measuring the degree of hydration, and hence hardening and strength characteristics of the paste [5-7]. This work, however, has concentrated on measuring the electrical resistivity of prisms from one-day old to periods in excess of 250 days, that is, hardening specimens.

This study uses a modified electrical model for cement paste and monitors the changes in electrical characteristics over the initial 24 h after gaging with water with improved accuracy by means of a microcomputer-controlled data acquisition system. Attempts have also been made to correlate known chemical changes occurring in cement paste with changes in the measured electrical response.

[1]Lecturer and research associate, respectively, Department of Civil Engineering, Heriot-Watt University, Edinburgh EH14 4AS, Scotland, United Kingdom.

Electrical Model for Cement Paste

The work outlined above has used a resistive model for cement paste, mortar, and concrete with the aggregate and cement paste represented by a parallel combination of resistive elements. This model is more applicable to relatively mature specimens of cement paste, mortar, or concrete. The electrical model used in the present study to represent the macroscopic response of a colloidal dispersion, such as setting cement paste, has modified this previous model to include a capacitive element C in parallel with the resistive element R (Fig. 1) [*8*]. The capacitive element, as will be explained, is dependent upon polarization mechanisms that can develop within the paste and is sensitive to chemical and structural changes occurring within the paste.

The values of capacitance and resistance can be converted into the more meaningful electrical parameters, dielectric constant ϵ, and electrical resistivity ρ, by using the relationships

$$\epsilon = CL/\epsilon_0 A \tag{1}$$

$$\rho = (RA/L) \text{ ohm-m} \tag{2}$$

where

L = length of specimen, m,
A = cross-sectional area of specimen, m^2, (assumed uniform), and
ϵ_0 = absolute dielectric constant of a vacuum, 8.854×10^{-12} farads/m.

The dielectric constant ϵ can also be defined as

$$\epsilon = C/C_a \tag{3}$$

where C_a is the capacitance of the system when air occupies the space between the electrodes. It should be emphasized that capacitance and resistance depend upon the size and shape of the specimen, whereas dielectric constant and resistivity are constants for the particular material, that is, comparing resistance and capacitance of specimens can be erroneous, but dielectric constant and electrical resistivity can be compared no matter the size or shape of the specimen.

Another term used in measuring the combined effects of dielectric polarization and electrical conduction at a particular frequency f is the loss angle δ, and is defined numerically as

$$\tan\delta = 1/2\pi f\epsilon\epsilon_0\rho \tag{4}$$

0149-6123/85/0012-0057$02.50

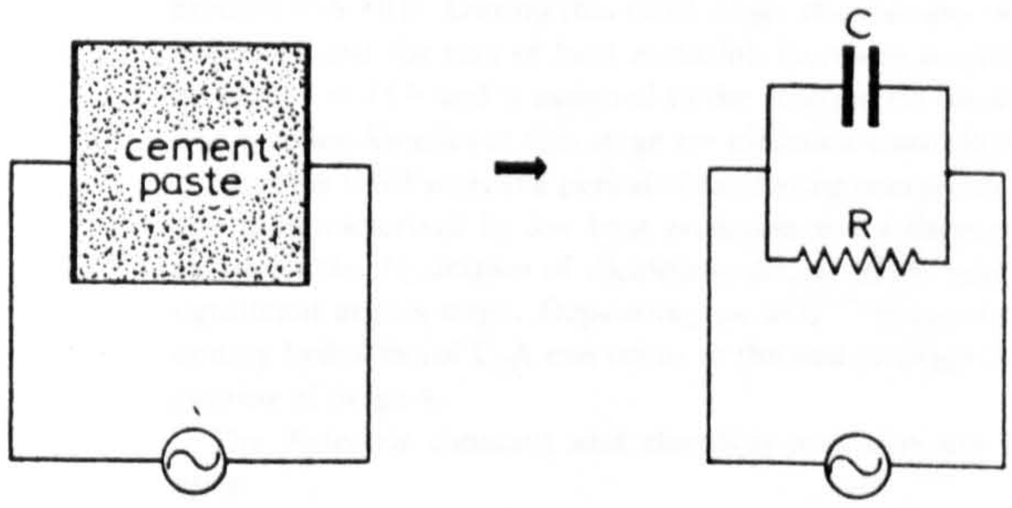

FIG. 1—*Electrical model for cement paste.*

and is the tangent of the ratio of the current flowing through the resistive element to the current flowing through the capacitive element.

Polarization and Conduction in Cement Paste

In a fine grained material, such as cement, there will be a concentration of electrical charges adjacent to the surface of the individual particles. The amount of charge and the strength by which it is held depends on such factors as particle surface texture, the number of unsatisfied surface bonding sites, and the net electrical charge on the particle itself. When an alternating electrical field is applied, the charges next to the particle surface tend to oscillate back and forth with a certain amplitude. The amplitude of oscillation will vary with such factors as the type of charge, the degree of association of the charge with the particle surface, particle orientation, and the temperature of the system as well as the strength and frequency of the electrical field. The oscillation, or movement, of charges in an electrical field is called polarization.

The polarization (on a microscopic scale) produced by an alternating electrical field in a cement which includes both ions and permanent dipoles can be classified under three main headings:

1. Particle alignment of permanent dipoles and polar molecules in the field direction [*9-11*] (Fig. 2*a*).
2. Accumulation or buildup of charges at crystal boundary interfaces [*12,13*] (Maxwell-Wagner effect) (Fig. 2*b*).
3. Induced polarization in the field direction because of

(i) displacement of ions from their zero field equilibrium positions [*14*] (Fig. 2*c*) and

(ii) displacement of double-layer charges adjacent to particle surfaces [*15,16*] (colloidal-layer polarization) (Fig. 2*d*).

The capacitance C and hence the dielectric constant ϵ are a measure of the amount of polarization that can develop within the paste when subjected to an alternating electric field and will be the sum total of all the polarization mechanisms mentioned above.

Some charges, usually in the form of ions in solution, which are not bound to particle surfaces, are free to drift through the solution and discharge at the electrodes. This produces a conduction effect that is reflected by the resistance R and hence, resistivity ρ.

The frequency of the applied alternating electric field has a significant influence on polarization (and hence dielectric constant) with certain polarization mechanisms operative only over a particular frequency range. Resistance, on the other hand, is not as sensitive to frequency changes. For this study, the frequency of the applied electrical field was varied over two decades, that is, from 100 Hz to 10 kHz.

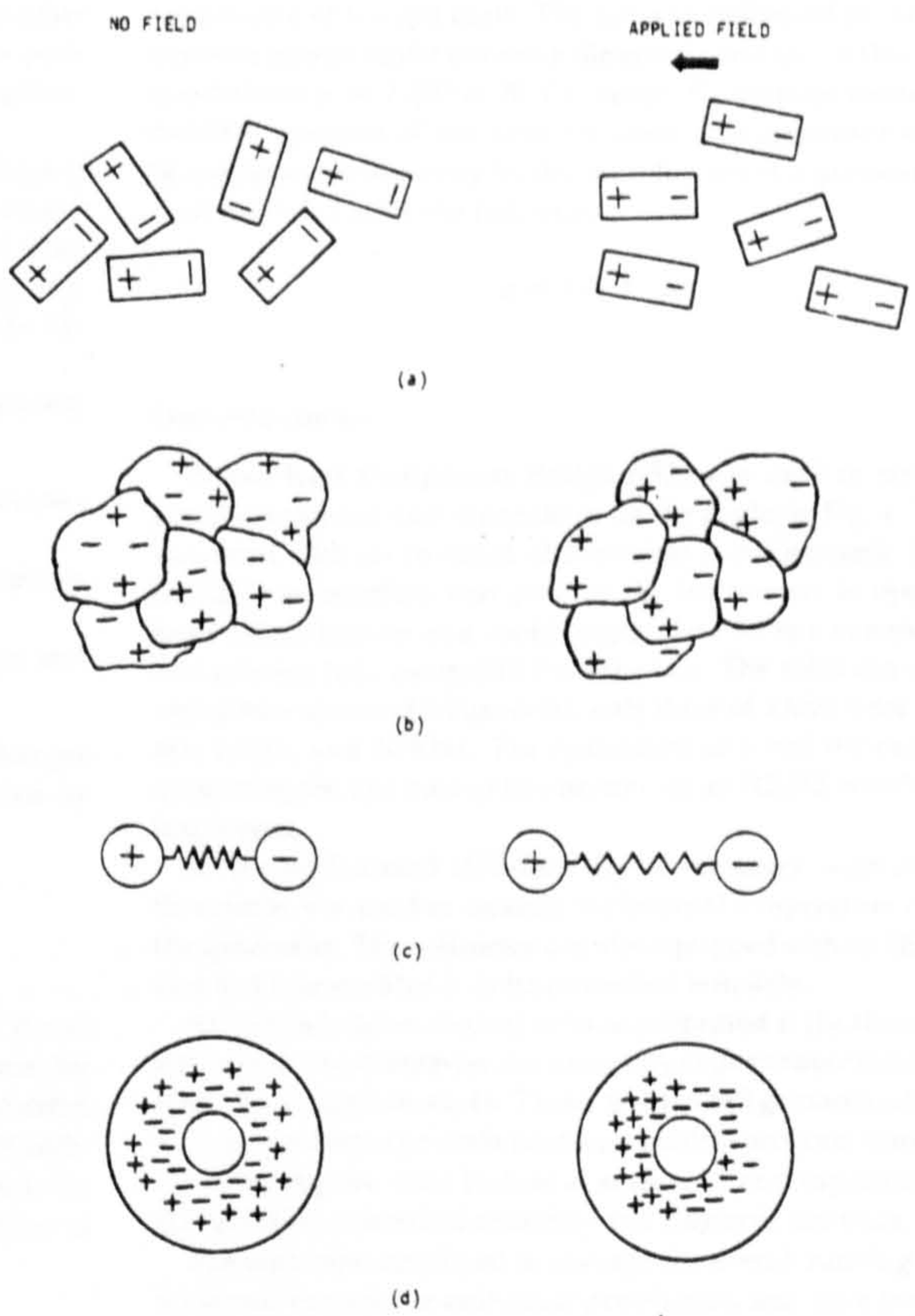

FIG. 2—*Polarization mechanisms.*

Physio-Chemical Processes in Setting Cement Paste

Hydration of portland cement is a sequence of overlapping chemical reactions that proceed at different rates for the various mineral phases. The main events that take place during the setting process of a normal cement paste are visualized as proceeding through four stages [*17-23*].

The first stage lasts for only a few minutes. Immediately upon contact of cement with water an exchange of ionic species initiates between the solids and the liquid phase. The high solubility of some of the clinker components leads to a rapid increase in concentration of the liquid phase with respect to Ca^{2+}, OH^-, SO_4^{2-}, K^+, Na^+, and $Al(OH)^-$. Hydration commences quickly on the tricalcium silicate (C_3S) and tricalciumaluminate (C_3A) phases as the first hydration products are formed (calcium-silicate-hydrate [C-S-H] and calcium-aluminate-hydrate [C-A-H], respectively), and a large amount of heat is evolved. The gel, which forms on the clinker particles, retards the reaction and results in a dormant period of little activity with the reaction kinetics nucleation controlled (Stage 2). The unstable primary hydration product (C-S-H) has a large excess of lime in its structure, and after several hours, dissolution, or splitting off, of the initial products results in renewed acceleration of alite dissolution (Stage 3). This leads to the formation of a second product of C-S-H(II) and is quickly followed by the formation of a third stable

product C-S-H(I). During this third stage, the viscosity of the paste decreases and the rate of heat evolution increases reaching a peak between 6 to 11 h and is assigned to the reaction on the alite phase. The reaction kinetics at this stage are diffusion controlled.

After the third stage the period of hardening commences (Stage 4) and is characterized by low heat evolution and a decreased overall reaction rate. Hydration of dicalcium silicate (C_2S) becomes more significant at this stage. Depending on SO_4^{--} concentration, secondary hydration of C_3A can occur at the end of Stage 3 or the beginning of Stage 4.

The dielectric constant and electrical resistivity are dependent upon

(1) changes in the physical state of water and ionic concentrations within the gaging water,

(2) the ease with which dipoles and polar molecules can be polarized within the paste, and

(3) the degree of association of charges with grain surfaces and temperature of the system.

As outlined above, since definite chemical and structural changes occur within the cement paste then these should be reflected by changes in the measured electrical parameters.

Experimental Program and Scope of Investigation

The variables that had to be measured were the resistance R and capacitance C of the cement paste over a 24-h test period. From this raw data the required constants, ϵ, ρ, and $\tan\delta$ could be determined at predetermined frequencies in the range 100 Hz to 10 kHz. In addition, the internal temperature of the specimens was monitored. All experiments were carried out in the confines of a humidity cabinet to maintain constant ambient air conditions.

Materials

Tests were carried out using ordinary portland cement (OPC) (ASTM Type I), and the water/cement ratio was kept within the region 0.27 to 0.35 (by weight)—this region producing a paste of standard consistence. Tests were also carried out on high alumina cement (Ciment Fondu).

The specimens were made from single batches of cement to minimize the effects of variability in materials. Tap water was used for all experiments (electrical resistivity = 100 $\Omega \cdot$ m; dielectric constant = 80). The cement was mixed using a Hobart planetary motion rotary mixer. Mixing time was kept constant at 2 min, and specimens were vibration compacted in approximately three equal layers.

Calcium chloride and table sugar were used in the present program as an accelerator and retarder, respectively.

Test Cell

The cell used to contain the cement paste comprised a 100- by 100- by 100-mm perspex mold fitted with 100- by 100- by 5-mm brass plate electrodes, the electrodes being attached to two opposite faces of the mold.

For conversion of the measured capacitance value to dielectric constant the cell had to be calibrated to take account of errors introduced because of field fringing effects around the electrodes and capacitance of the cell itself. The cell was calibrated at the test frequencies using a liquid of known dielectric constant, in this instance, cyclohexane (ϵ = 2.025 at 20°C); hence, C_a could be found and the dielectric constant of the paste obtained. The resistance values can be converted to resistivity by the introduction of a geometrical constant $G(=A/L)$, for the cell, thus

$$\rho = RG\ \Omega \cdot \mathrm{m} \tag{5}$$

Data Acquisition

Wayne-Kerr Component Bridge B905 was used to measure the parallel resistance and capacitance for the model in Fig. 1. The B905 was fitted with an Institute of Electrical and Electronic Engineers (IEEE) bus interface that permits the instrument to operate as a basic talker/listener and could output data on to a common bus as well as being fully controlled from the bus. The B905 can operate at any of four standard frequencies, only three of which were used: 100 Hz, 1 kHz, and 10 kHz. The instrument also had the capability of outputting the raw data onto a printer via an RS232 interface on the instrument.

A Hewlett Packard HP3456A digital voltmeter, with compatible thermistor, was used to measure the internal temperature changes of the specimens. The voltmeter was also equipped with an IEEE interface bus that enabled it to be controlled remotely.

As outlined above, the test cell was calibrated at the three frequencies in order to determine the necessary capacitance/dielectric constant conversion constants. These, and the cell gemoetrical constant, were entered into the main hardware control program thus enabling the incoming raw data (values of resistance and capacitance) to be converted into electrical resistivity and dielectric constant.

The controller employed to manage the overall running of the experiment, control the individual peripherals, and store the data was a HP9915 modular computer. Four other peripherals completed the system: a disk storage unit, two printers, and a Calcomp 84 X-Y eight pen plotter. An HP-IB interface bus was used to interface the B905, HP3456A, disk-storage unit and one of the printers to the controller, this printer giving a hardcopy of the processed data. The other printer, as mentioned above, was interfaced via a RS232 serial interface direct to the B905 bridge. The plotter was serially interfaced to a HP85 microcomputer, enabling the data analysis to be carried out independently of data acquisition.

The microcomputer controlled data acquisition system described could

(1) monitor the experiment and control the various peripherals that comprise the system over the 24-h test period,

(2) initiate a reading cycle (under clock control), and log, process and store eight pieces of data at each reading cycle, viz. initiating time; internal cube temperature; capacitance (at three frequencies) and resistance (at three frequencies), and

(3) store the data on a floppy disk storage medium, which could then be easily accessed for analysis.

The experiment was continuous over a 24-h period, and with the interval between reading cycles of 1 min during the first hour, and 5 min over the remaining 23-h, approximately 340 reading cycles were triggered and over 2500 individual pieces of data recorded.

A schematic diagram of the system architecture and peripheral address sequence is shown in Figs. 3 and 4, respectively, with arrows showing the flow of information.

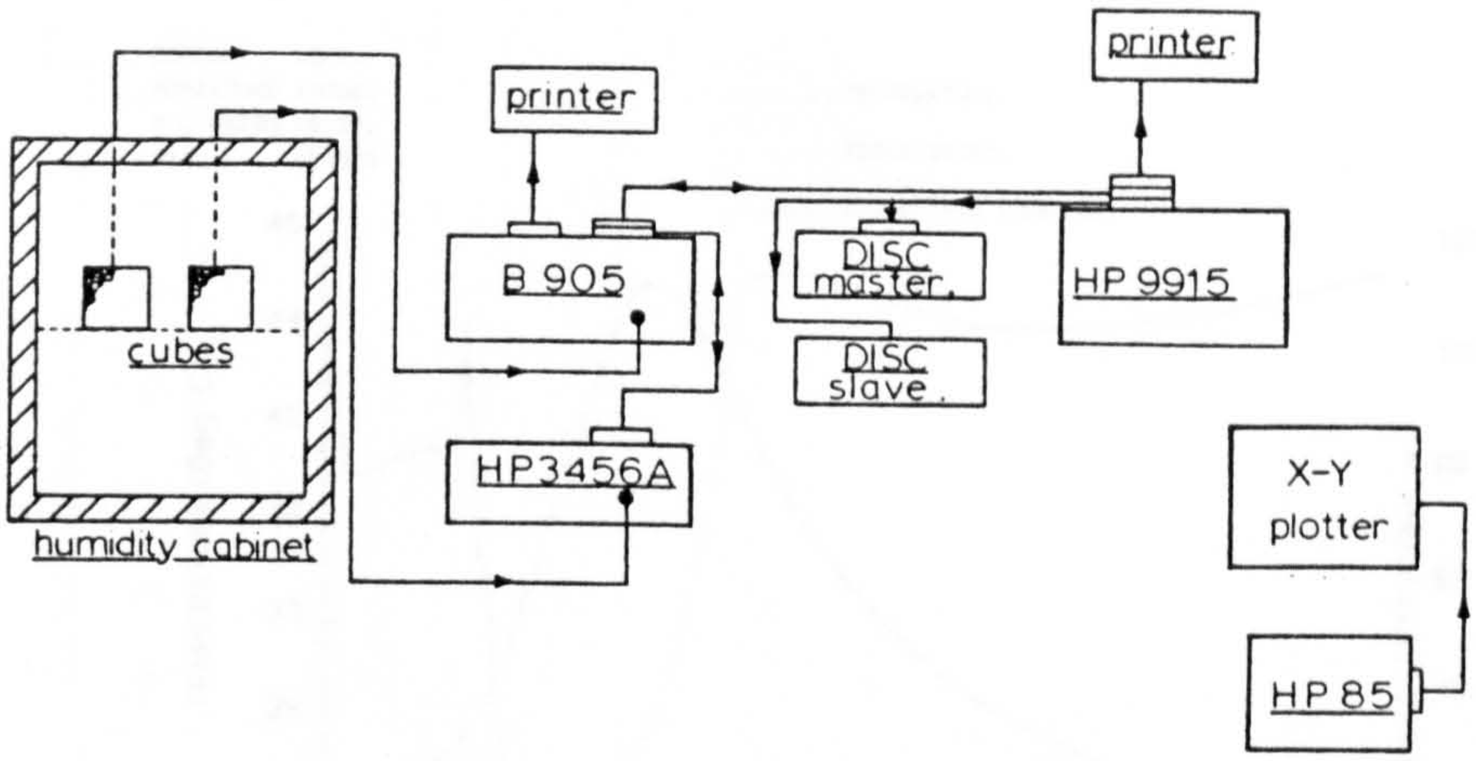

FIG. 3—*Schematic diagram of system architecture.*

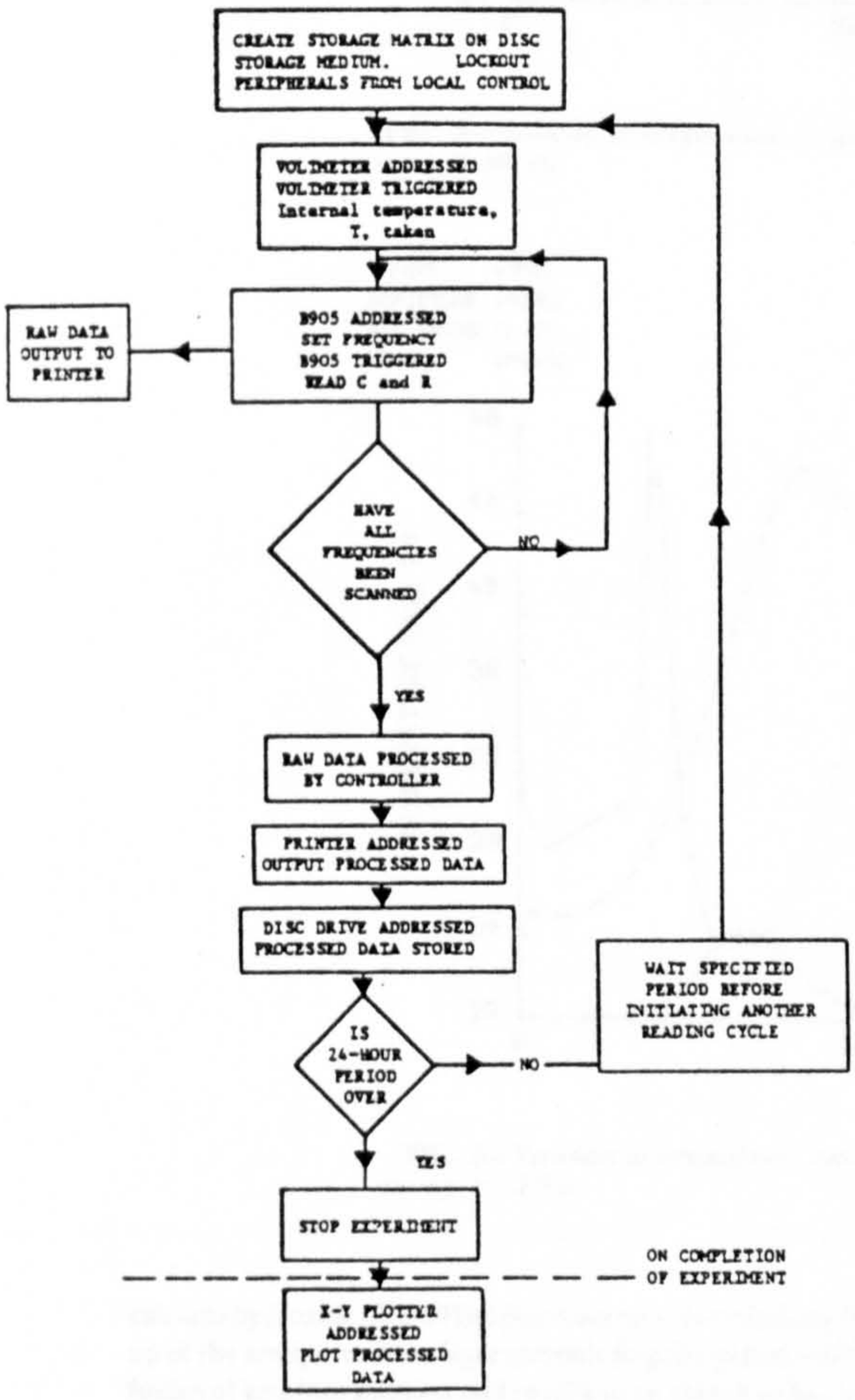

FIG. 4—*Address sequence of peripherals.*

Results

The results from the test program have been given in graphical form, and typical results are given in Figs. 5 to 16, that is, dielectric constant, resistivity and tan δ as a function of time and frequency. The change in internal temperature with time for the cement paste has also been included on all graphs for comparative purposes. For each figure given, up to ten tests were carried out to ensure repeatability of results.

Discussion of Results

Figures 5 through 8

Immediately after portland cement is contacted with water, calcium and hydroxyl ions are rapidly leached from the clinker, resulting in high ionic concentrations in the bulk aqueous solution. The low electrical resistivity (in comparison to that of the original mixing water) at the initial stages of hydration are indicative of, and attributable to, the ease of mobility and availability of charges for the conduction process. On mixing, hydration products quickly build up on the C_3S and C_3A phases in the cement grain forming a membranous precipitate of surface hydrates consisting of amorphous C-S-H and C-A-H.

Associated with this partial surface coating, the coating will be surrounded and stabilized by an electrical double layer comprising Ca^{++} and OH^- ions. Ions within this double layer, while not available for the electrical conduction process, can be polarized by the alternating electric field and will result in high induced dipole moments (Fig. 2*d*); this will result in very high dielectric constants at low frequencies as the charges can follow the alterations of the electric field. In addition, a contribution from Maxwell-Wagner polarization must result, albeit a relatively small contribution as crystal boundaries are not defined at this stage. The sum total of these mechanisms will result in producing a high dielectric constant (compared to that of the original gaging water). Considering Figs. 5 through 7 only, the dielectric constant over the initial 40 min decreases quite rapidly—a buildup of hydration products on the cement grains reducing charge mobility and some crystallization of

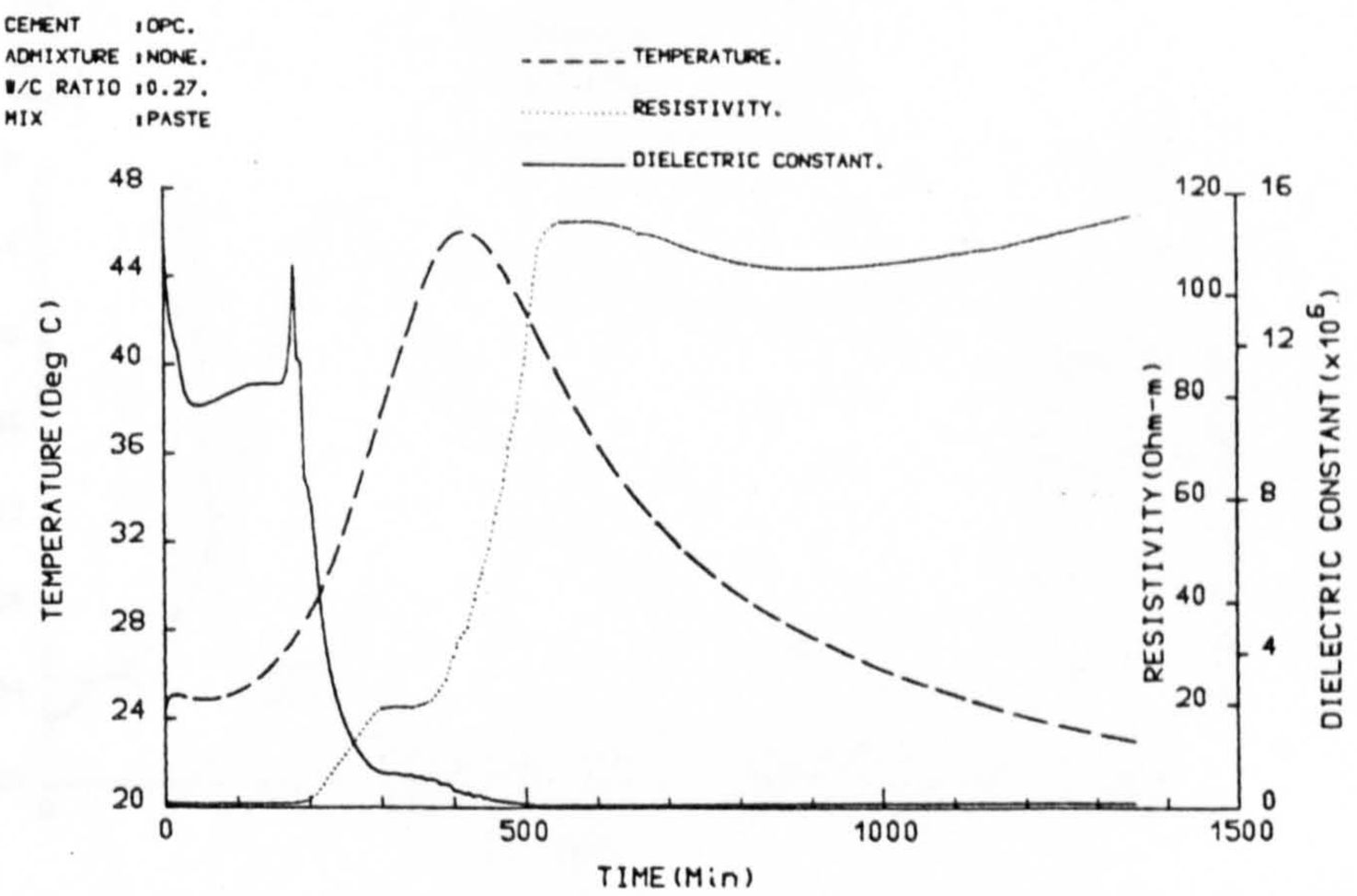

FIG. 5—*Variation of temperature, resistivity, and dielectric constant during 24 h after guging with water frequency = 100 Hz.*

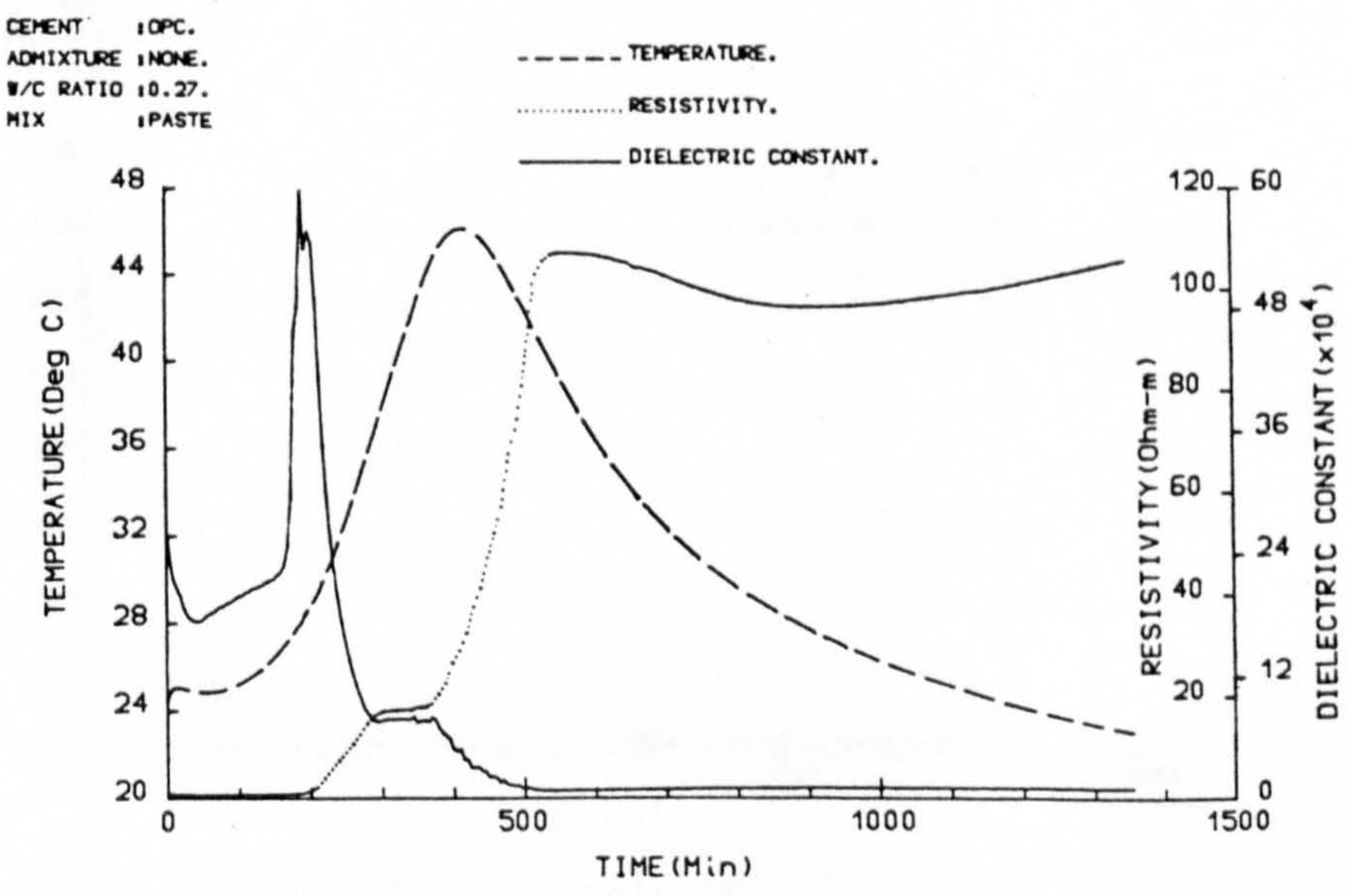

FIG. 6—*Variation of temperature, resistivity, and dielectric constant during 24 h after guging with water (frequency = 1 kHz).*

calcium hydroxide ($Ca(OH)_2$) could account for this drop. The build-up of the semipermeable layer surrounding the grains will hinder diffusion of ions into solution and results in an overall reduction in reaction rate. It is noticeable that after 40 min and up to 180 min, the rate of change of the dielectric constant is considerably reduced and would signify little activity within the paste giving credence to the dormant or induction period of Stage 2.

Although obscured by the scale of the graph, the resistivity, at all frequencies, falls to a minimum at 40 min. This is taken to mean that the paste has achieved supersaturation; thereafter, and up to 180

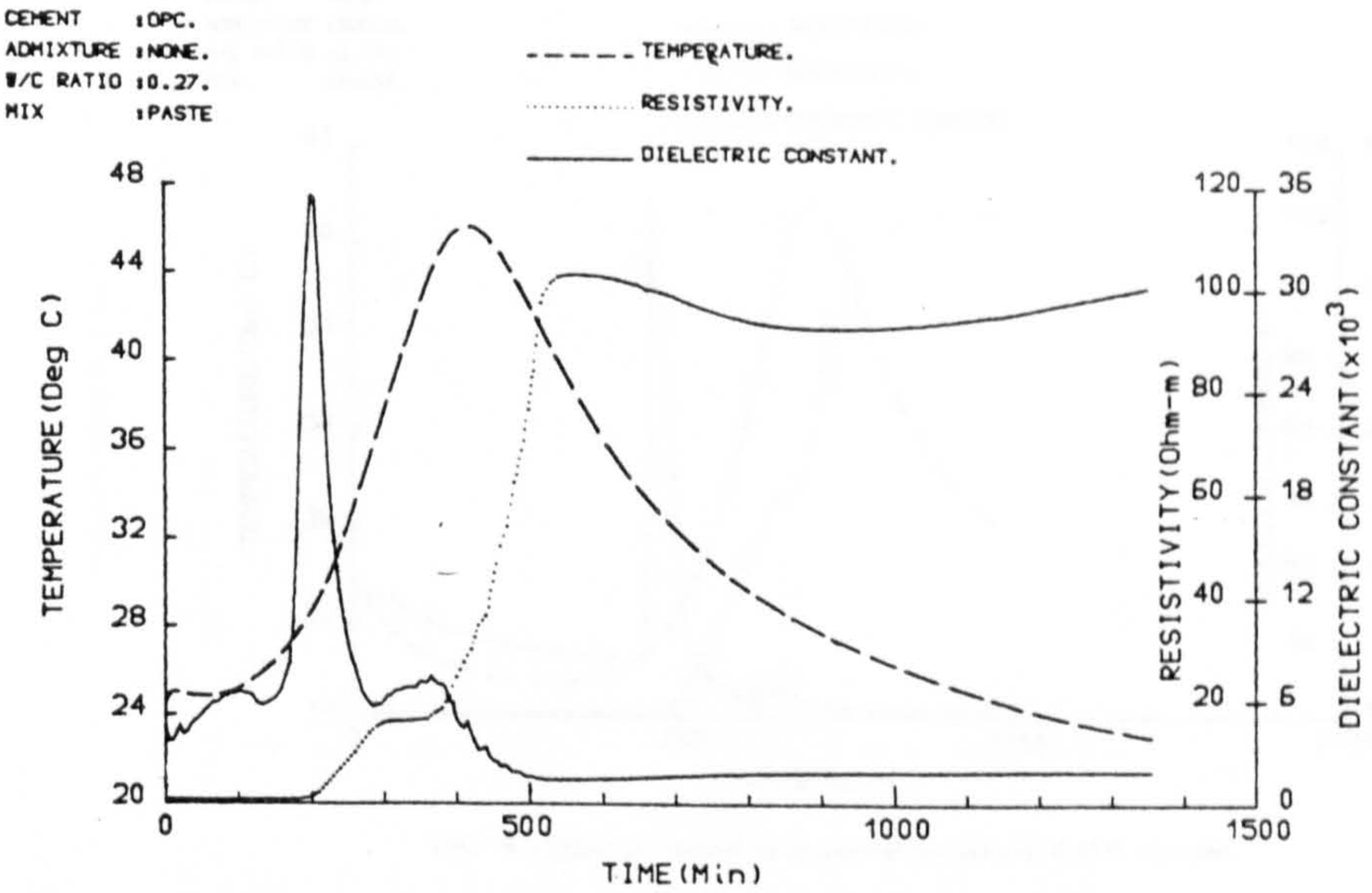

FIG. 7—*Variation of temperature, resistivity, and dielectric constant during 24 h after gaging with water (frequency = 10 kHz).*

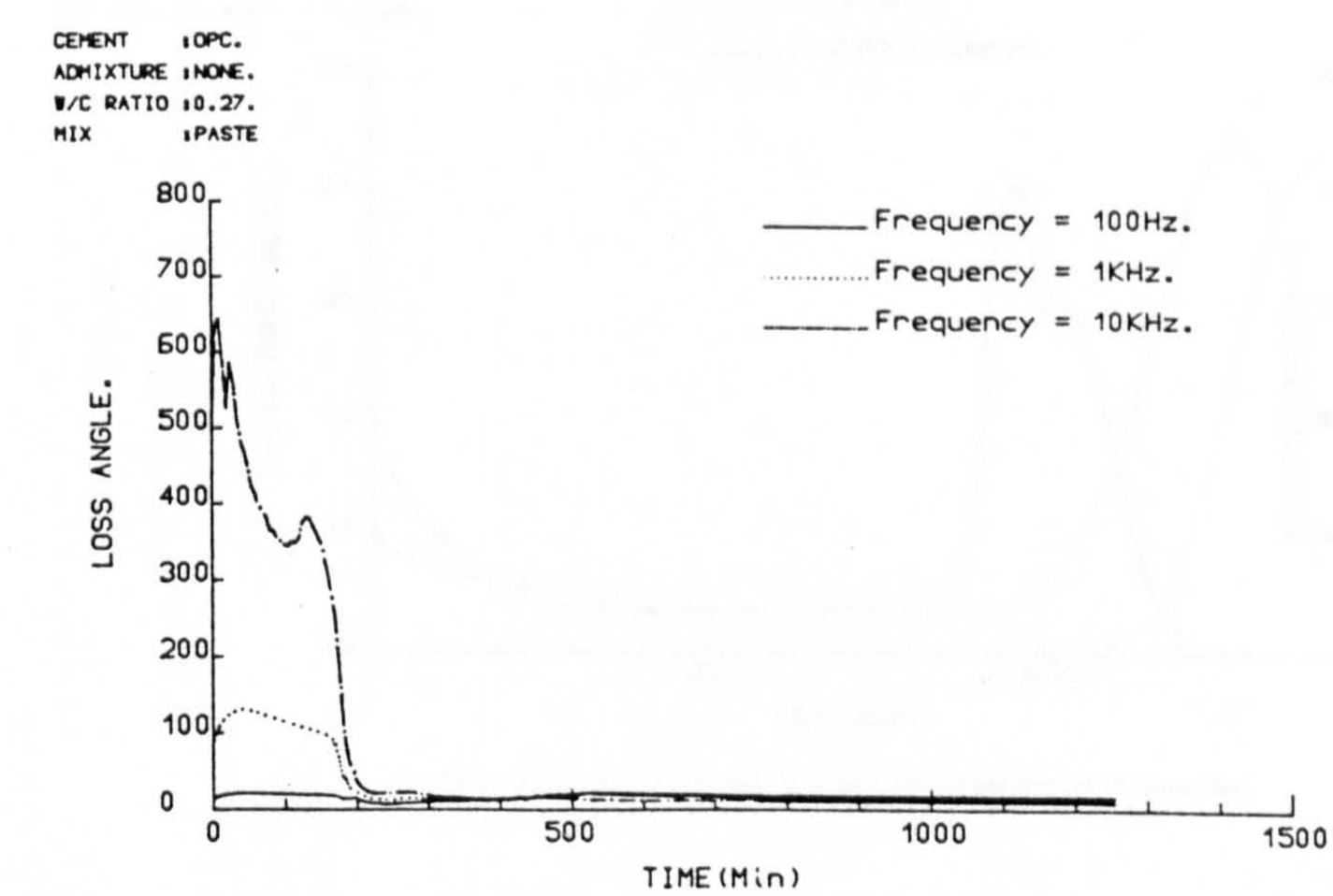

FIG. 8—*Variation of loss angle over test period.*

min, the resistivity increases only very gradually, further emphasizing the lack of activity within the paste associated with Stage 2.

At approximately 180 min the dielectric constant undergoes rapid changes, peaking at approximately 200 min before dropping. The authors believe that this peak is taken to mean renewed chemical activity on the C_3S phase within the paste, with subsequent release of charges that can be polarized by the electrical field. The peak at 200 min is short-lived, showing a sudden burst of activity, which leads to an increase in rigidity of the paste. Contact between grains and formation of more stable C-S-H and further crystallization of $Ca(OH)_2$ results in an irrotational binding of charges and consequent drop in dielectric constant. It is also postulated that the renewed activity of the coating releases charges that are not available for the conduction process but are associated with grain surfaces as there is no reduction

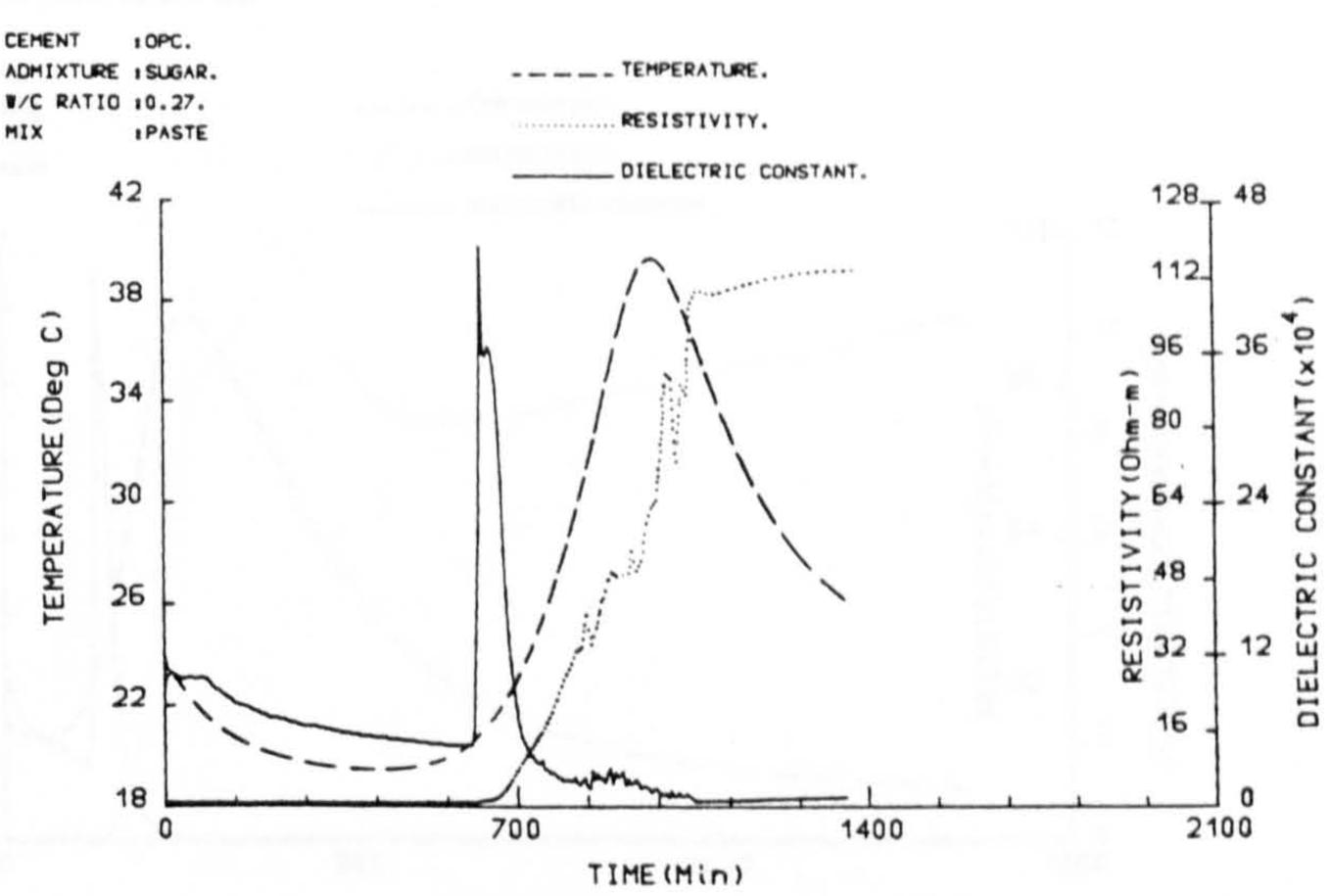

FIG. 9—*Effect of retarder on measured parameters: 0.05% retarder.*

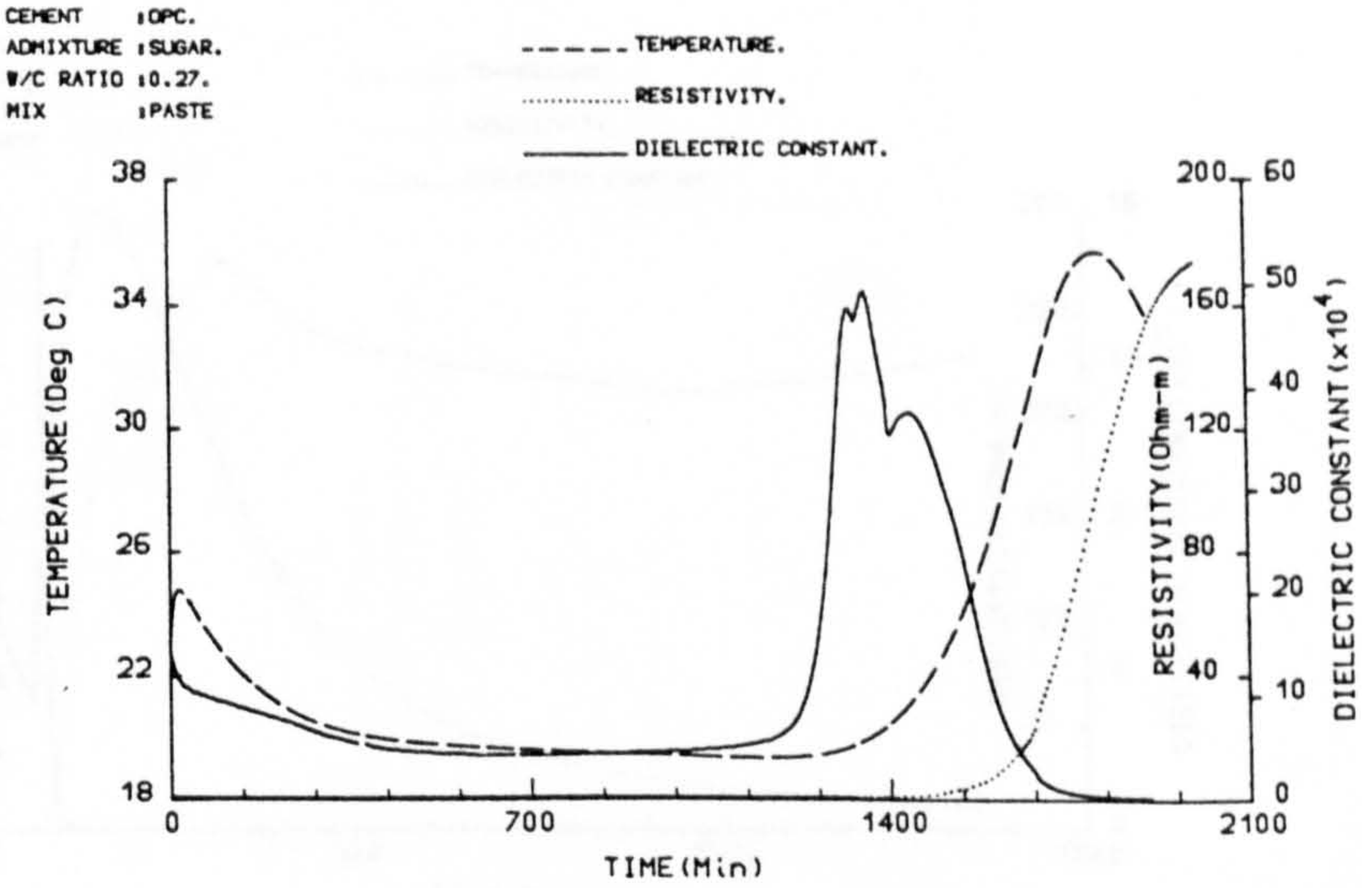

FIG. 10—*Effect of retarder on measured parameters: 0.1% retarder.*

in resistivity at this time, that is, 200 min. The magnitude of the peak in the dielectric constant could be a measure of the excess free energy or degree of instability of the unstable C-S-H hydrate on the grain surface. As the frequency is increased, the peak becomes more pronounced. At 200 min the resistivity rises rapidly coinciding with the drop in dielectric constant. This would indicate that ionic concentrations are decreasing and ionic conduction paths through the continuous capillary pores in the cement paste are becoming more tortuous as the paste gains rigidity. (Also at this point in time the internal temperature of the paste increases).

At 300 min there is a reduction in the rate of change of electrical parameters resulting in a plateau region on both curves. As both electrical parameters are temperature dependent [5], then this region is to be expected at peak temperature. More importantly, however, over the period 200 to 500 min the overall drop in the dielectric constant and rise in resistivity signifies crystallization of $Ca(OH)_2$, grain segmentation, and general reduction in ionic concentrations in the gaging water. Reduction in SO_4^{--} concentration will stimulate renewed chemical activity on the C_3A phase [*19, 20*] as ettringite is converted to monosulpho-aluminate, and results in a further change in

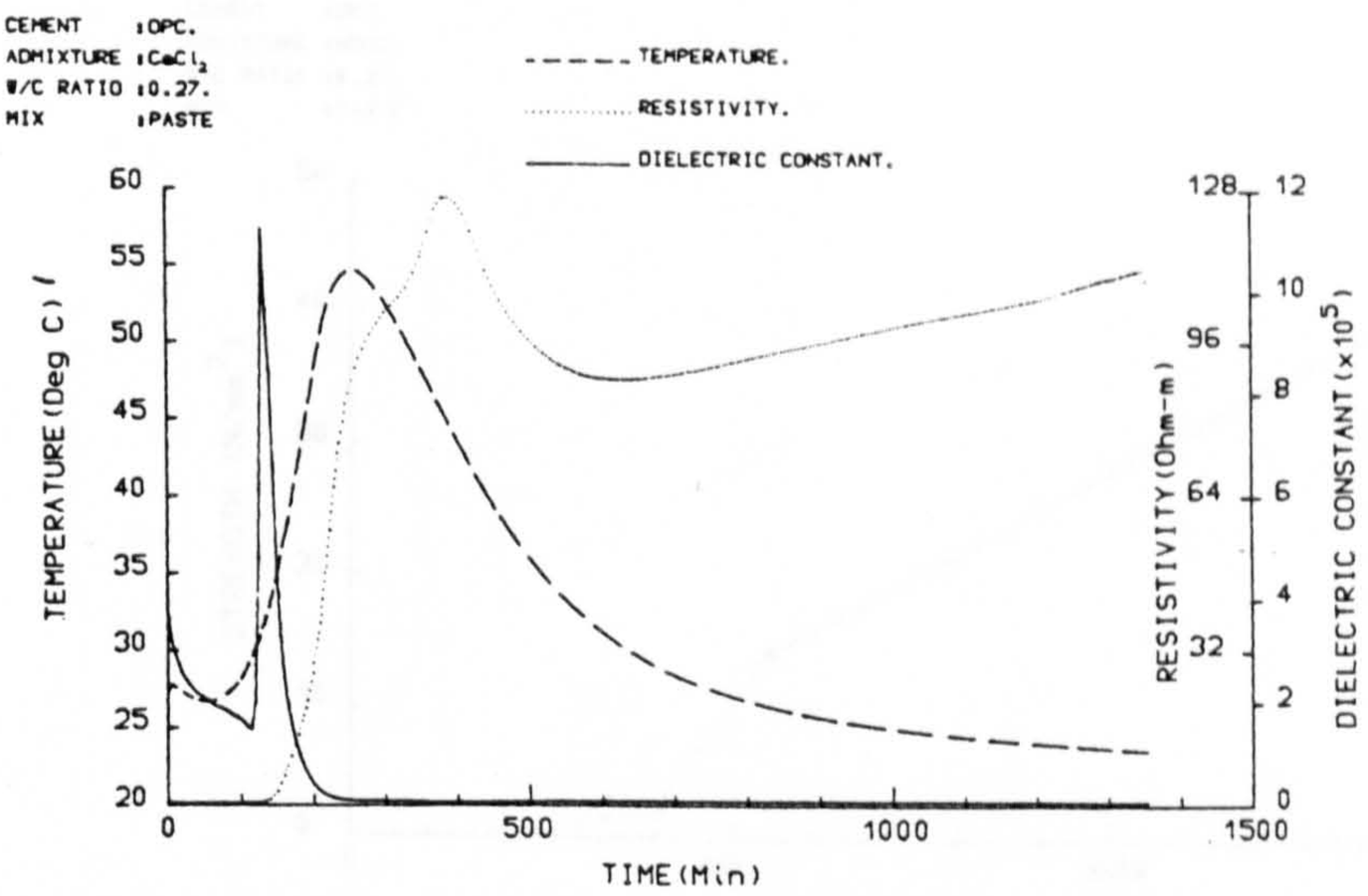

FIG. 11—*Effect of accelerator on measured parameters: 1% accelerator.*

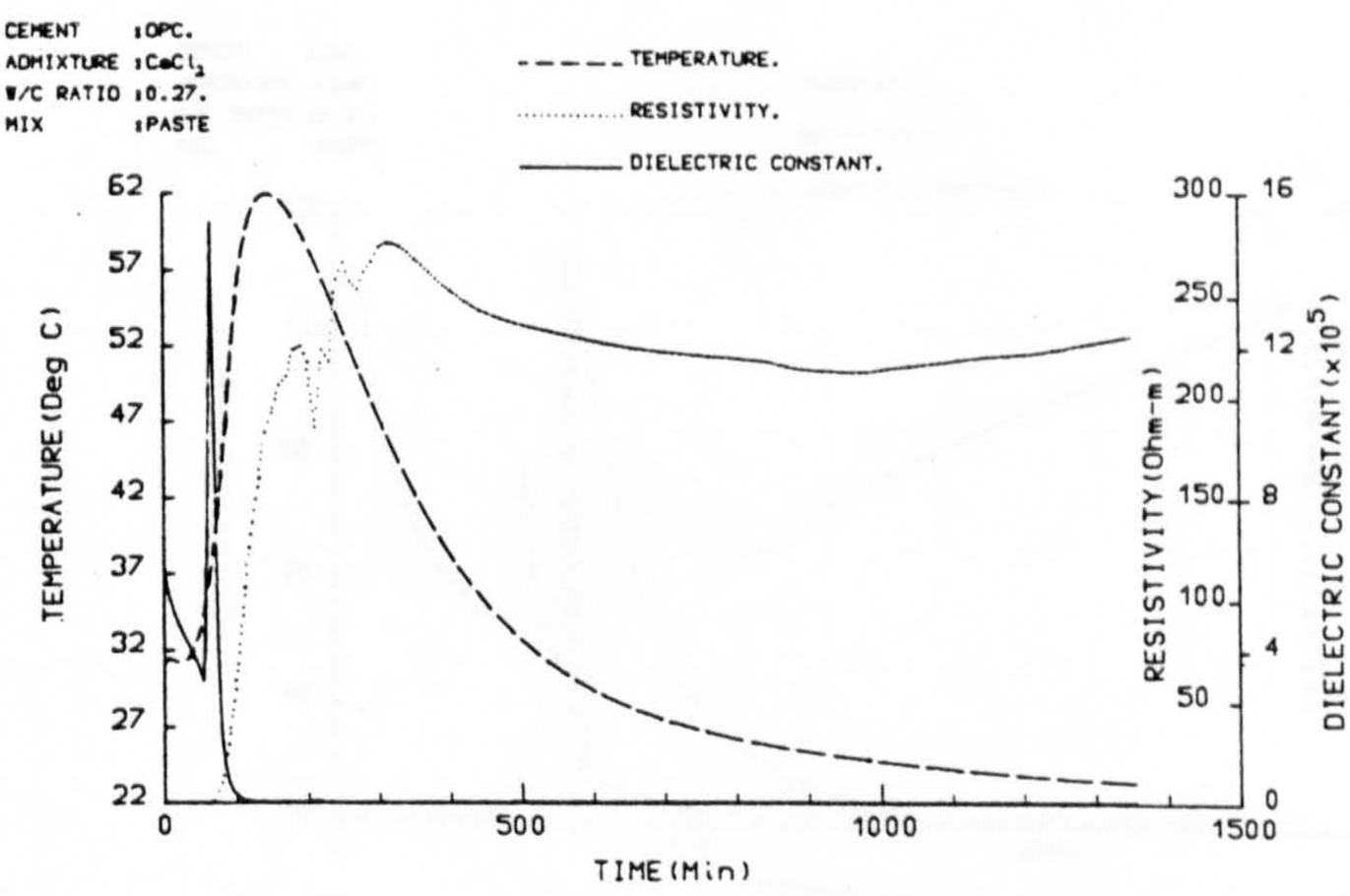

FIG. 12—*Effect of accelerator on measured parameters: 1.5% accelerator.*

electrical parameters after 500 min—the resistivity decreasing and dielectric constant increasing, the latter being more noticeable at higher frequencies. The paste, at this stage, has gained considerable strength, and the cement grains segmented. Maxwell-Wagner polarization would predominate at this stage. The rate of change of electrical parameters after 500 min is considerably reduced indicating much slower reaction rates, indeed, changes in resistivity and dielectric constant after 500 min must not only be attributable to secondary C_3A hydration, but there must also be a contribution from initial C_2S hydration. Charges must be released into the continuous capillary pores thereby reducing resistivity, and into the blocked capillary and gel pores thereby increasing the dielectric constant by Maxwell-Wagner effects. The authors have assigned the period 180 to 500 min to Stage 3 of the hydration process, and the period after 500 min as the beginning of hardening or Stage 4.

Figures 5 through 7 also display the frequency dependence of the dielectric constant, which varies by almost three orders of magnitude over the two decades of frequency (100 Hz to 10 kHz) indicating a region of dielectric dispersion. The two principal polarization mechanisms operative within cement paste will be double-layer and Maxwell-Wagner effects, with the dielectric constant reflecting a proportion of each mechanism at any frequency; at low frequencies

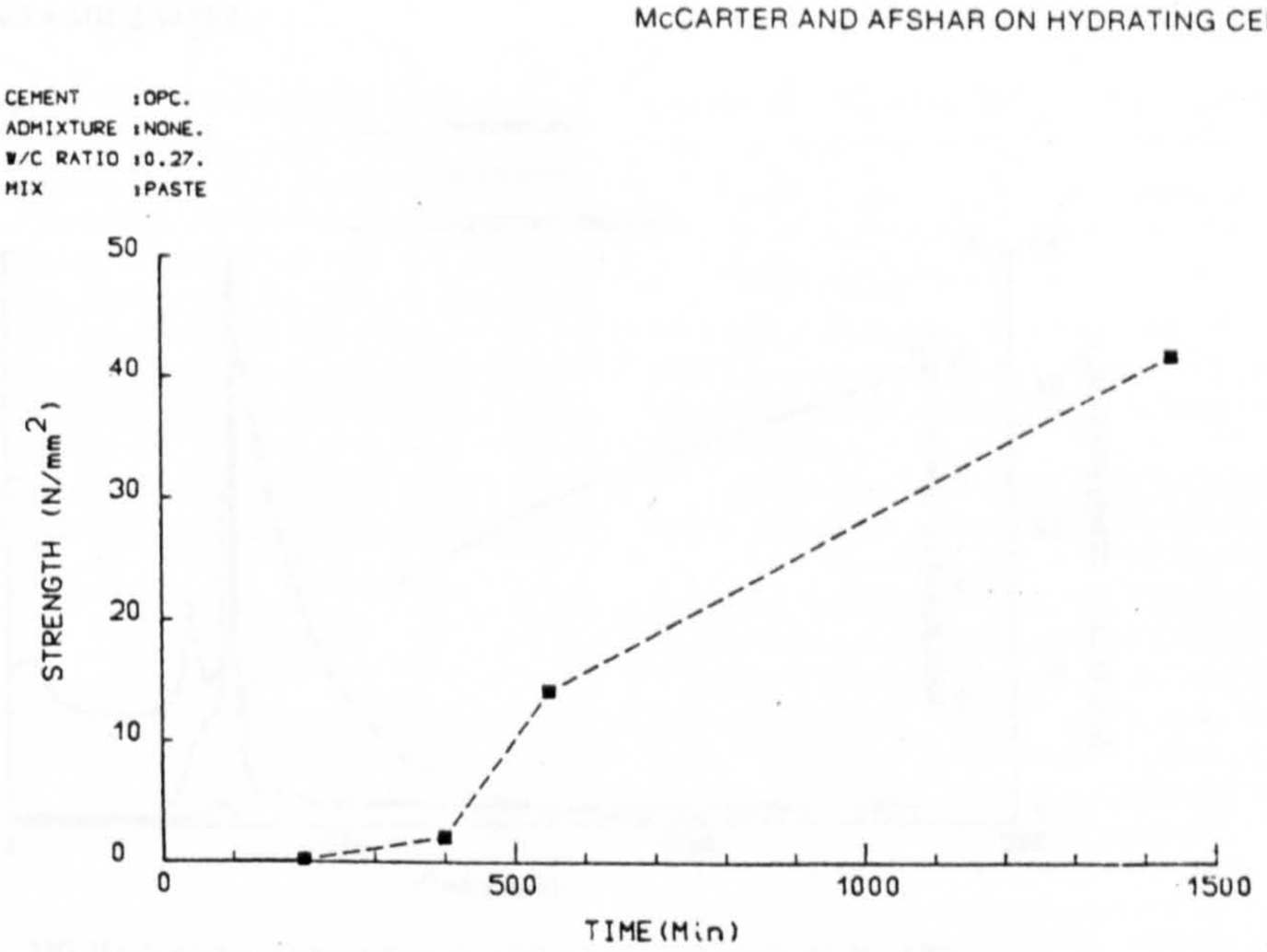

FIG. 13—*Increase in strength over initial 24 h.*

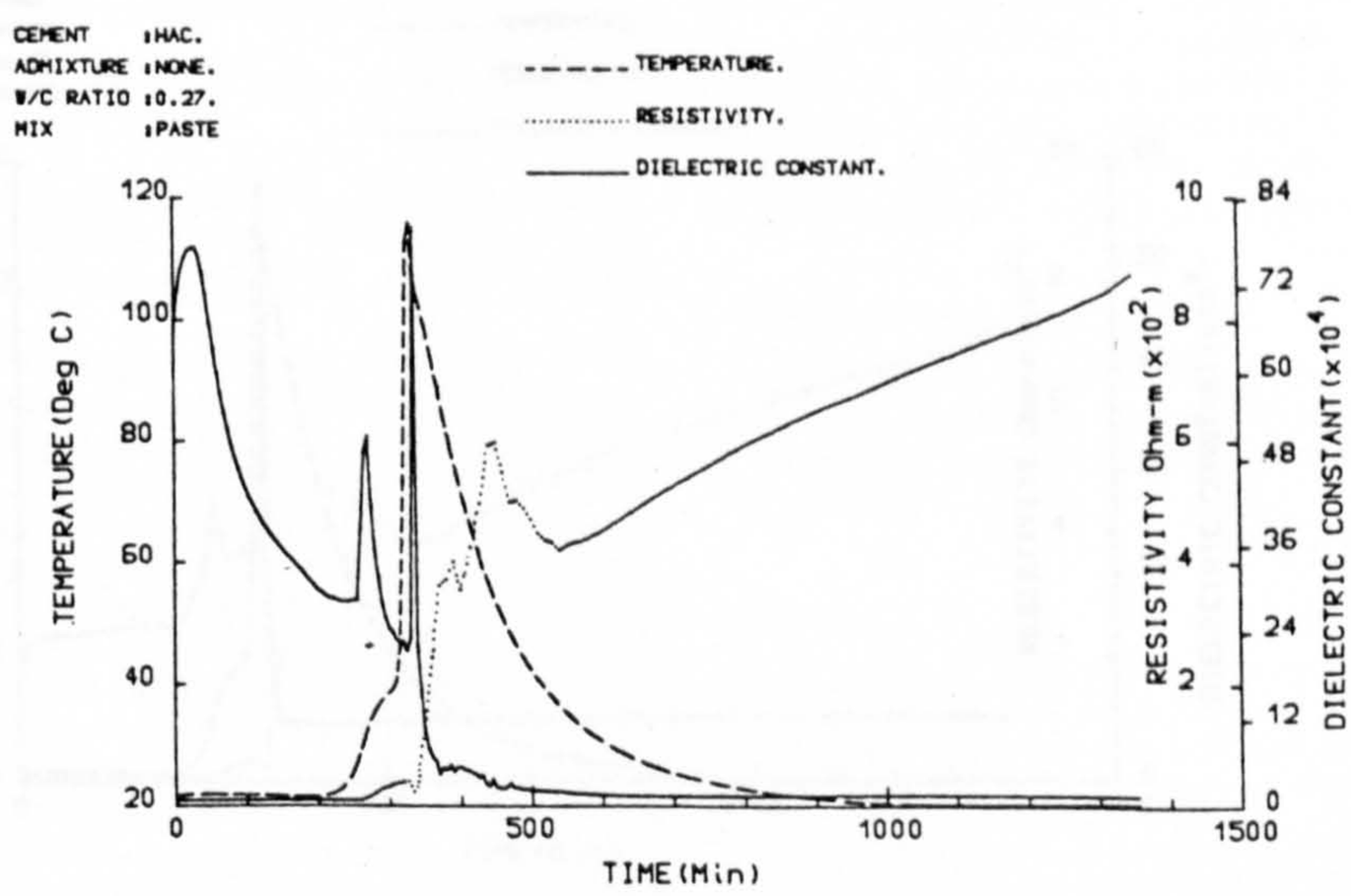

FIG. 14—*Variation of temperature, resistivity and electrical response during 24 h after gaging with water (frequency = 100 Hz).*

double-layer and Maxwell-Wagner effects are both operative, however, as the frequency increases, Maxwell-Wagner polarization will begin to predominate over double-layer polarization. When cement paste is in the liquid state, double-layer polarization effects will form a large proportion of the dielectric constant as charges can follow the alternation of the electrical field; as the paste sets and hardens, charges become irrotationally bound, and Maxwell-Wagner effects will predominate (that is, polarization of charges in gel pores and blocked capillary pores).

Figure 8 reflects the combined effect of dielectric constant and resistivity, and changes in loss angle are also noticeable at similar time intervals previously mentioned, being more prominant at 10 kHz than 100 Hz. After the initial 600 min, the loss angle attains an almost constant value for all frequencies.

Although not given, similar results were obtained for all water/cement ratios in the range tested (0.27 to 0.35). As the water/cement ratio is increased; however, the dormant period is increased and the C_3S hydration peak delayed.

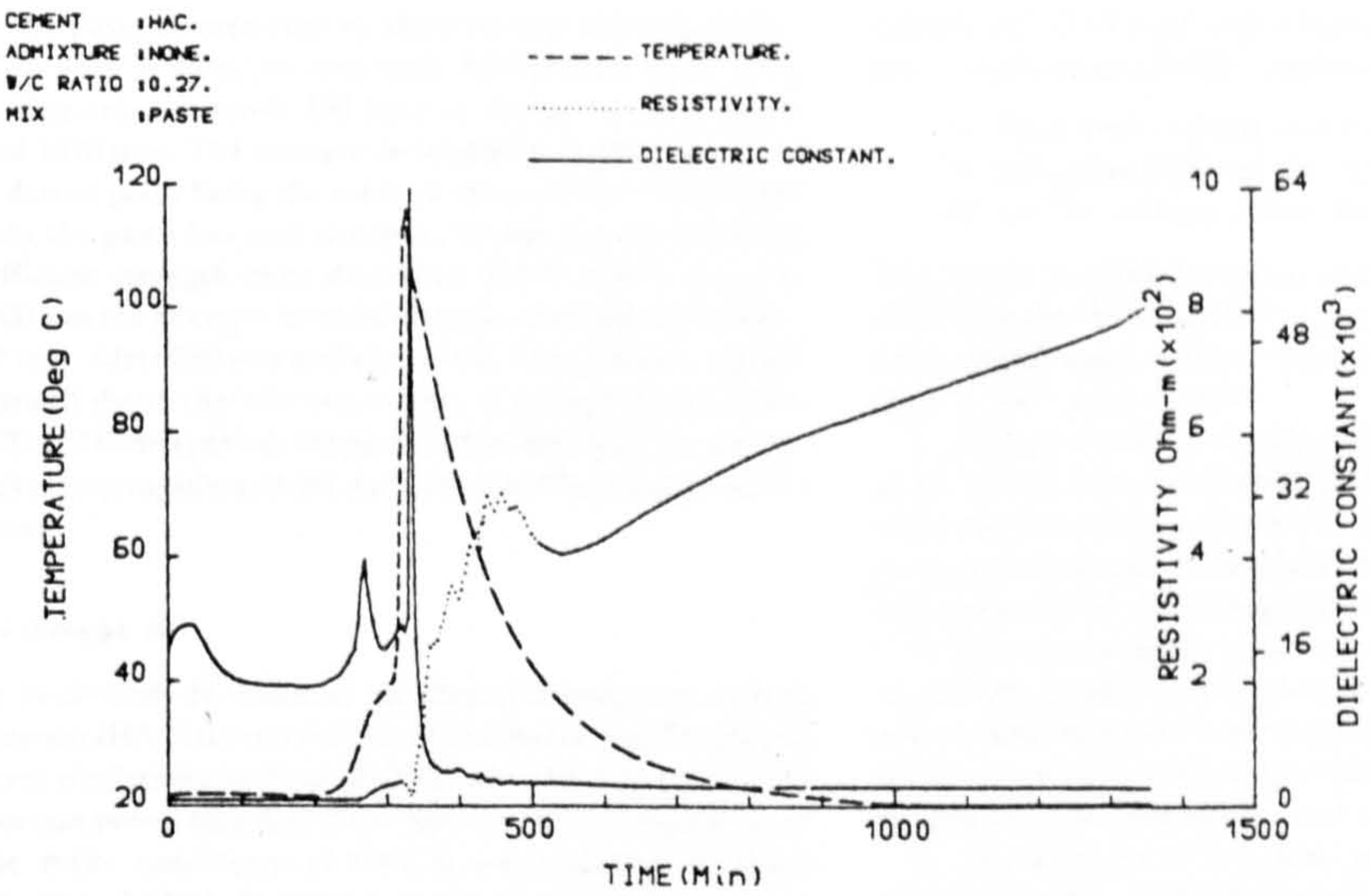

FIG. 15—*Variation of temperature and electrical response (frequency = 1 kHz).*

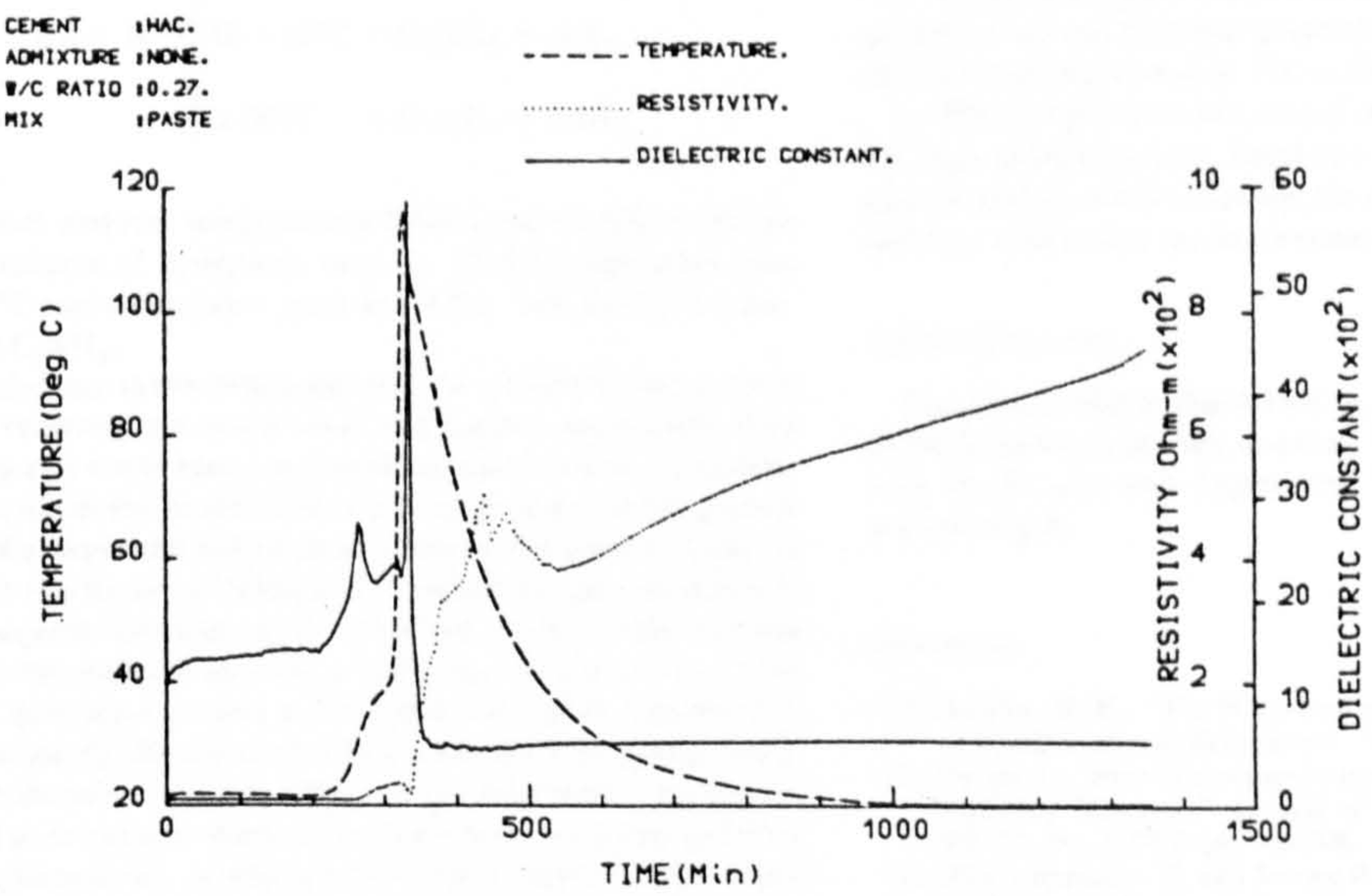

FIG. 16—*Variation of temperature and electrical response during 24 h after gaging with water (frequency = 10 kHz).*

Figures 9 through 12

The influence of the addition of retarder on the electrical response (and internal temperature) is shown in Figs. 9 and 10, and that for an accelerator is shown in Figs. 11 and 12. Results are given for a frequency of 1000 Hz. Both admixtures were added by percentage weight of cement and dissolved in the gaging water before mixing.

Considering Figs. 9 through 12, it is apparent that the critical points on the dielectric constant and electrical resistivity responses curves discussed in the previous section for Figs. 5 through 7 have all been reproduced but at later or earlier stages in the case of retarders or accelerators, respectively. The work shows that the addition of retarders or accelerators has the effect of altering the position of the C_3S hydration peak on the time axis and increasing/decreasing the dormant period of Stage 2. This further shows that the peak in dielectric constant at 200 min in Figs. 5 through 7 (C_3S hydration) together with the sudden increase in resistivity indicates the beginning of the gain of rigidity of the paste (that is, setting).

Figure 13

Strength tests were carried out of 100-mm cubes of cement paste at predetermined times over the 24-h period. The time at which the cubes were crushed were where critical chemical reactions were oc-

curring in the paste as predicted by the electrical response curves, namely, 200 (peak in dielectric constant), 400 (plateau region resistivity and dielectric constant), 550 (rate of change of resistivity reduces), and 1440 min. The strength development is given in Fig. 13 with each datum point being the mean of three cubes, it is assumed that initially the paste has zero strength. By 200 min the paste has gained sufficient strength to be demolded (0.1 N/mm^2), and over the next 400 min the strength increases rapidly, particularly between 400 to 550 min. After 550 min and up to 24-h, strength gain is gradual. The graph shows that the rate of gain of strength is maximum over the 200 to 500-min period; the period where the electrical parameters are changing rapidly and the main structure building processes are occurring.

Figures 14 through 16

Figures 14 through 16 illustrate the electrical properties of high alumina cement (HAC) during the first 24-h of hydration. The graphs show certain similarities to those of OPC, and the data given show some important points that may throw light on the early hydration of HAC. The major constituent of HAC is monocalcium aluminate (CA), hydration of which depends on temperature [*20,21*]

$$\mathrm{CA} + \mathrm{H} \rightarrow \begin{cases} <10^\circ\mathrm{C} & \rightarrow \mathrm{CAH_{10}} \\ 10-30^\circ\mathrm{C} & \rightarrow \mathrm{C_2AH_8} + \mathrm{AH_3} \\ >30^\circ\mathrm{C} & \rightarrow \mathrm{C_3AH_6} + 2\mathrm{AH_3} \end{cases}$$

At normal ambient temperatures CAH_{10} and C_2AH_8 would be normal products of hydration; however, if the temperature rises above 30°C conversion takes place as CAH_{10}, and C_2AH_8 is transformed to C_3AH_6.

With reference to the data presented, the dielectric constant and electrical resistivity are much lower and higher, respectively, then OPC paste and would mean an overall reduction in ionic concentrations. The initial rise in the dielectric constant is due to the gradual buildup of charges and hydration products on the grain surfaces. In OPC paste this happens rapidly and the initial rise goes undetected. The subsequent formation of C-A-H (CAH_{10} and C_2AH_8) reduces the dielectric constant showing a reduction in reaction rate (this period of quiescence is more noticeable at the higher frequencies). At approximately 200 min further hydration of CA to C_2AH_8 results in a rise in dielectric constant. The peak coincides with a rise in resistivity and an increase in temperature of the paste (which is conducive to C_2AH_8 formation). At this point the mix is beginning to increase in rigidity; however, because of CA hydration the temperature of the paste rises dramatically. The temperature rise is so considerable that the formation of C_3AH_6 must result. A third peak in the dielectric constant curve at peak temperature, and a drop in resistivity is also noticeable (350 min). The authors attribute the peak in dielectric constant and drop in resistivity to the formation of C_3AH_6 and rise in temperature. This peak is short-lived as the paste increases in rigidity. The rise in resistivity at this time would also signify stiffening of the paste. Thereafter the curves follow the same trend as for OPC.

Conclusions

The following conclusions can be drawn from the present study:

1. An automated microcomputer data logging system has been developed, which allows the flow of instruction and data between a number of peripherals and a central controller. Customized software was developed for the microcomputer to control:

   (a) the overall running of the experiment,
   (b) the action taken by the individual devices, and
   (c) the flow of data within the system.

The system developed requires minimum input from the operator, minimizes the data acquisition time, minimizes the delay time between experiments, and maximizes the freedom of manipulating the data to reach a conclusion.

2. Further evidence on the early hydration of OPC has been given. It has been demonstrated that the electrical response of cement paste is sensitive to physical and chemical changes within the paste, and the dielectric constant and electrical resistivity can be used as a diagnostic of the setting and hardening processes.

3. The four accepted stages occurring during setting and hardening of cement paste can be identified using electrical response techniques, and the methods developed by the authors offer an additional technique to such methods as scanning electron microscopy, transmission electron microscopy, and conduction calorimetry.

4. The influence of retarders, accelerators, and, indeed, admixtures in general, on the hydrolysis and hydration processes can be quantified, and the rate of change of electrical parameters indicates the rate at which hydration is progressing.

5. It has been shown that the rate of gain of strength of the paste is greatest when the electrical properties of the paste are undergoing significant changes (that is, 200 to 600 min).

6. The continuous monitoring of chemical processes in, for example, high alumina cement, has shown that a change in chemical composition of the cement influences the electrical response. The method could be used to test special cements in general.

Acknowledgments

The authors wish to thank Prof. A. Bolton for placing the facilities of his department at their disposal. The receipt of a research grant from the Science and Engineering Research Council is gratefully acknowledged.

References

[1] Dorsche, K. E., "The Hardening and Corrosion of Cement—IV," *Cement and Concrete Manufacture*, Vol. 6, April 1933, pp. 131-142.
[2] Calleja, J., "New Techniques in the Study of Setting and Hardening of Hydraulic Materials," *Journal of the American Concrete Institute*, Vol. 23, No. 7, 1952, pp. 525-536.
[3] Sriravindrarajah, R. and Swamy R. N., "Development of a Conductivity Probe to Monitor Setting Time and Moisture Movement in Concrete," *Cement, Concrete, and Aggregates*, Vol. 4, No. 2, Winter 1982, pp. 73-80.
[4] Bars, J. P., Camps, J. P., and Debuigne, J., "Example and Application of a Method for Measuring Electrical Impedance: Evolution of Electrical Conductivity of Cement Paste During Its Setting Time," *Materials and Structures: Research and Testing*, Vol. 15, No. 85, Jan./Feb. 1982, pp. 33-37.
[5] McCarter, W. J., Forde, M. C., Whittington, H. W., "Resistivity Characteristics of Concrete," *Proceedings of the Institution of Civil Engineers (London)*, Part 2, No. 71, March 1981, pp. 107-117.
[6] McCarter, W. J., Forde, M. C., Whittington, H. W., and Simons, T., "Electrical Resistivity Characteristics of Air-Entrained Concrete," *Proceedings of the Institution of Civil Engineers*, Part 2, No. 75, March 1983, pp. 123-127.
[7] McCarter, W. J., Forde, M. C., and Whittington, H. W., "The Conduction of Electricity Through Concrete," *Magazine of Concrete Research*, Vol. 33, No. 114, March 1981, pp. 48-60.
[8] McCarter, W. J. and Curran, P. N., "Electrical Response of Setting

Cement Paste." *Magazine of Concrete Research*. Vol. 36. No. 126. March 1984. pp. 42-49.

[9] Debye. P., "Polar Molecules." Dover Publications Inc., New York. 1929.

[10] O'Dwyer. J. J. and Harting. E., "Theories of Dielectric Loss." *Progress in Dielectrics*. Vol. 7. J. B. Birks. Ed., Heywood Books. London. 1967. pp. 3-44.

[11] Van Beek. L. K. H., "Dielectric Behaviour of Heterogeneous Systems," *Progress in Dielectrics*. Vol. 7. Heywood Books. London. pp. 69-114.

[12] Maxwell. J. C., "A Treatise on Electricity and Magnetism," Vol. 1. Oxford University Press. 1873. p. 464.

[13] Wagner. K. W., *Archiwum Elektrotechniki*. Poland. Vol. 2. Warsaw. 1914. p. 371.

[14] Schwan. H. P., Schwarz. G., Maczuk. J., and Pauly. H., "On the Low-Frequency Dielectric Dispersion of Colloidal Particles in Electrolytic Solutions." *Journal of Physics and Chemistry*. Vol. 66. Dec. 1962. p. 2626.

[15] Schwarz. G., "A Theory of the Low-Frequency Dielectric Dispersion of Colloidal Particles in Electrolyte Solution." *Journal of Physics and Chemistry*. Vol. 66. Dec. 1962. p. 2636.

[16] Hasted. J. B., *Aqueous Dielectrics*. Chapman and Hall. London. 1973. p. 286.

[17] Powers. T. C., "Some Physical Aspects of the Hydration of Portland Cement." *Journal of the Portland Cement Association Research and Development Labs*. Vol. 3. No. 1. Jan. 1961. pp. 47-56.

[18] Angstadt. R. L. and Hurley. F. R., "Hydration of the Alite Phase in Portland Cement." *Nature*. Vol. 197. 16 Feb. 1963. p. 688.

[19] Lea. F. M., *The Chemistry of Cement and Concrete*. Edward Arnold (Publishers) Ltd. London. 1970. pp. 177-249.

[20] Barnes. P., Ed., *Structure and Performance of Cements*. Applied Science Publishers. London. 1983. pp. 237-317.

[21] Mindess. S. and Young. J. E., *Concrete*. Prentice-Hall Inc. Englewood Cliffs. NJ. 1981. pp. 51-54.

[22] Birchall. J. D., Howard. A. J., and Bailey. J. E., "On the Hydration of Portland Cement." *Proceedings of the Royal Society London*. Vol. A 360. Series A. 1978. pp. 445-453.

[23] Double. D. D., Hellawell. A., and Perry. S. J., "The Hydration of Portland Cement." *Proceedings of the Royal Society London*. Vol. A 359. Series A. 1978. pp. 435-451.

Proc. Instn Civ. Engrs, Part 2, 1986, 81, June, 305–308
DISCUSSION ON PAPER 8954 STRUCTURAL ENGINEERING GROUP

A study of the early hydration of Portland cement

W. J. McCarter and A. B. Afshar

Professor B. P. Hughes, Mr A. K. O. Soleit and Mr R. W. Brierley, *University of Birmingham*

The Authors are to be congratulated on their demonstration of how well the hydration of Portland cement can be monitored by an electrical technique. Some recent work carried out at Birmingham has investigated the possibilities of using the electrical resistance as a non-destructive testing technique for concrete.

42. The first requisite for such a study was the development of compact inexpensive equipment which would be simple to use; the ohmeter was the result.[32] Difficulties arising from the effects of polarization and capacitance reactance have been virtually eliminated. The voltage output of the electrolytic ohmeter can be connected directly to automatic data loggers or chart recorders, so eliminating the need to balance a traditional bridge type circuit. When results for resistivity of 7 and 28 day old concretes were compared with more conventional methods, the AC resistivity using parallel variable capacitance and variable resistance bridge balancing techniques was typically 5% lower, and the DC resistivity was typically 10% higher, than that given by the ohmeter. Because the polarization effect for DC measurements could increase the measured resistivity, while capacitance reactance could decrease the measured resistivity, the ohmeter appeared to give both quick and accurate results.[32]

43. Figure 5 in the Paper shows results for 0·27 water–cement ratio. Did the Authors carry out tests on OPC and HAC pastes at higher water–cement ratios, and if so could they show results for, say, a 0·30 or 0·35 water–cement ratio?

Mr A. D. Buck, Mr S. Wong and Mr P. Burkes, *Concrete Technology Division, Department of the Army, Waterways Experiment Station, Corps of Engineers, Vicksburg, Mississippi*

Our interest is mainly with the scanning electron microscope (SEM) data presented in the Paper, and we would like to comment as follows.

45. Paragraphs 28 and 30 refer to crystals which the Authors believe to be ettringite (Fig. 6(e)), and both ettringite and monosulphoaluminate (Fig. 6(g)). While we agree that these identifications may be correct, we believe the validity of them would be much improved by partial chemical analysis using either an energy-dispersive technique, a phase identification using X-ray diffraction, a higher SEM magnification, or some combination of these methods. I believe that all seven of the Fig. 6 micrographs were at about 3000X.

46. The second comment is that in view of the fact that many of those working with SEM and cement hydration phases tend to use the C-S-H I, II, III and IV morphological designations of Diamond,[33] the Authors might also wish to do this in the future and to include his paper in the list of references.

Paper published: *Proc. Instn Civ. Engrs*, Part 2, 1985, 79, Sept., 585–604.

DISCUSSION

Dr McCarter and Mr Afshar

We wish to thank *Professor Hughes*, *Mr Soleit* and *Mr Brierley* for their comments on our work and, indeed, welcome the opportunity to discuss work of mutual interest. We have been working for a number of years on electrical methods for testing cement, mortar and concrete, and would wish to reiterate the comments made by Professor Hughes *et al.* that electrical methods could certainly be developed for non-destructive testing and on-line condition monitoring of concrete; needless to say, much more work is required to identify what is actually being measured when an electrical reading is taken on concrete, and the main variables which influence the electrical response of the material. In our Paper, we have gone a little way towards clarifying these latter points.

48. We have been using AC bridge techniques for fundamental research into the mechanisms of cement hydration but, as stated in our Paper, there could be many 'spin-off' developments which could be taken-up by industry; for example, the influence of admixtures on hydration characteristics. Because of the fundamental nature of our work, we are logging large amounts of data and our system, as it stands, does not lend itself to portability! However, as Professor Hughes and his team have shown, compact instrumentation can be developed—certainly as far as resistivity measurements are concerned. Portable equipment for non-destructive testing is essential for site use; the ideal solution would be a 'black-box' which could be taken on to site, take a reading/series of readings on concrete, and could, subsequently, analyse the results on site. To this end, we are exploring the possibility of developing an impedance measuring system (resistivity and dielectric constant) for site use.

49. Professor Hughes and his team have quite rightly pointed out that electrode polarization using DC and periodically reversed DC is always a problem in electrical measurements, giving, in effect, a capacitance term in series with the bulk resistance of the material (caused by the formation of a gas layer at the electrodes). This effect can be eliminated by means of AC techniques[34] or 4-terminal measuring methods. What we have shown in our Paper is that measurement of dielectric polarization could be used to give an insight into cement hydration.

50. In connection with electrical measurements, it is worth mentioning the following points.

(*a*) Bulk resistivity is itself, in general, frequency dependent, decreasing with increasing frequency. We have conducted tests over a wide frequency band on hardened specimens and have found the electrical resistivity to follow such a relationship. Professor Hughes *et al.* do not mention the frequency at which their AC measurements were taken (~1000 Hz?) using bridge balancing techniques; however, if resistance readings were taken at much higher frequencies, the variation between the ohmeter results and that of the bridge would certainly be greater than 5%.

(*b*) In resistivity measurements, air and aggregate are electrically similar,[14] and resistivity measurements alone may not be able to distinguish between these two components of concrete. An increase in resistivity of concrete (compared to datum mix) could result from an increase in the amount of aggregate in the mix or an increase in the air content of the mix.[13]

51. We have carried out an extensive series of electrical tests on the following: cement pastes of varying consistency; cements of different composition; and the

influence of the addition of aggregates to the paste. Fig. 11 shows the variation in measured parameters for OPC for water–cement ratios of 0·30 and 0·35. It is evident that although similar trends can be observed, absolute values change.

52. We are pleased to hear about the work Professor Hughes and his team are undertaking, and hope that our work and comments are of interest. Electrical measurements on concrete can certainly be developed as a testing technique; however, a full appreciation of all the variables is essential to ensure correct interpretation of results.

53. The contribution by *Mr Buck*, *Mr Wong* and *Mr Burkes* is appreciated, and our comments on the points they raise are as follows.

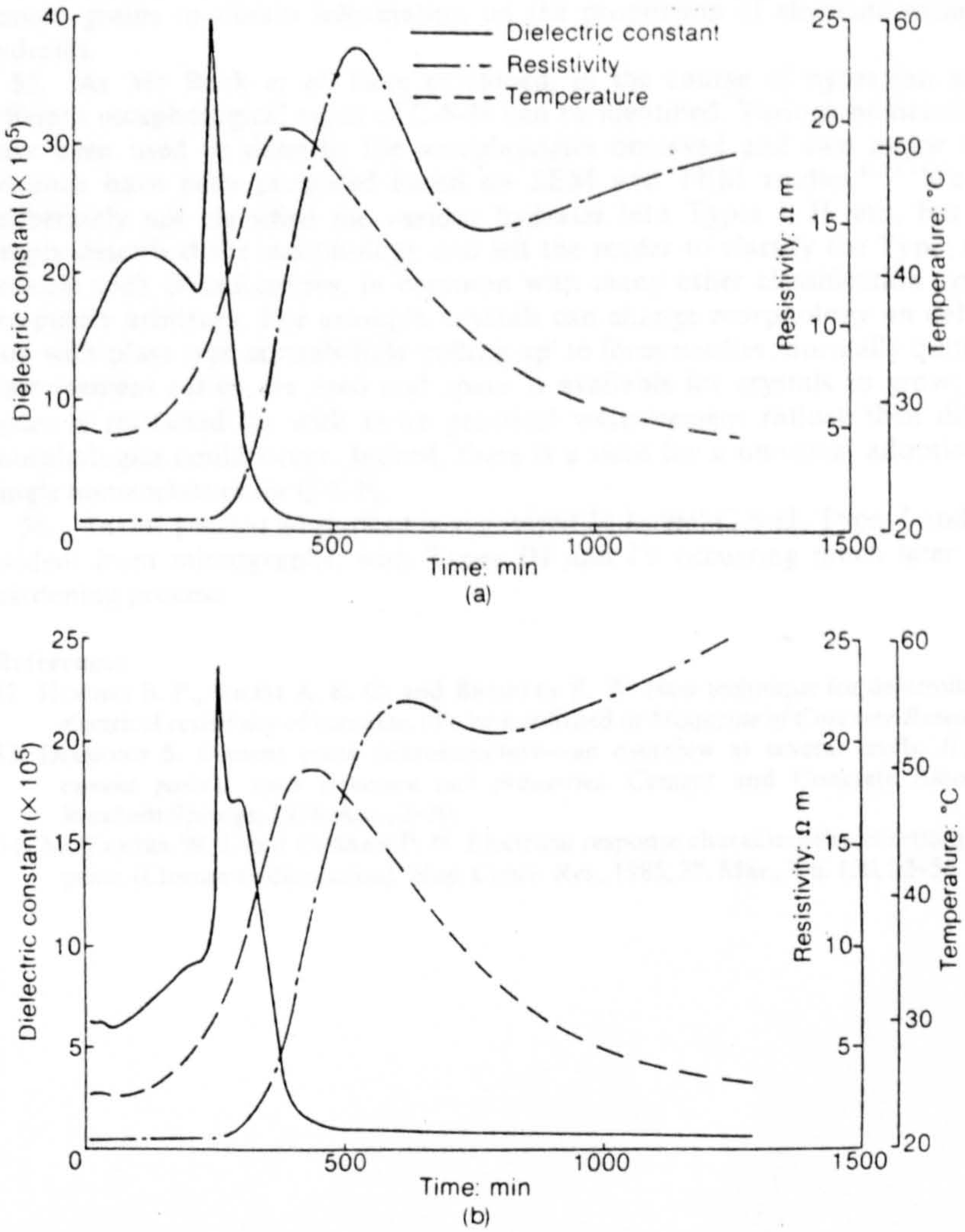

Fig. 11. Variation in measured parameters for OPC (frequency = 1000 Hz): (a) water–cement ratio = 0·30; (b) water–cement ratio = 0·35

DISCUSSION

54. The initial aim of our research programme was to link the mechanisms of cement hydration with the variations in electrical response of the paste, with particular interest over the initial 24-hour period after gauging. We have tried to substantiate our claims with traditional methods which are familiar to researchers in the field and are accepted as 'tools of the trade', namely SEM, strength development, internal temperature changes and Vicat Needle. We have shown that tentative links can be made with electrical response and crystal morphology. However, it is outside the scope of our present Paper to present all the techniques currently available for microstructure examination. Indeed, exhaustive and well-documented studies have been carried out by many workers using SEM, TEM and X-ray diffraction. Although not presented in our original Paper, we have undertaken electron-probe microanalysis on selected surfaces of the hydrating cement grains to obtain information on the proportion of elements within the hydrates.

55. As Mr Buck *et al.* have explained, in the course of hydration several different morphological types of C-S-H can be identified. Various nomenclatures have been used to describe the morphologies observed and two major classifications have been proposed based on SEM and TEM studies.[6,33] We have deliberately not classified the various hydrates into Types I, II, etc., but have simply described the morphology and left the reader to classify the Type; this is because such classifications, in common with many other classification systems, are purely arbitrary. For example, crystals can change morphology on dehydration with plate type crystals/foils 'rolling up' to form needles; normally quite high water/cement ratios are used and space is available for crystals to grow; if the space is restricted (as with more practical water/cement ratios), then different morphologies could occur. Indeed, there is a need for a universal adoption of a single nomenclature for C-S-H.

56. In our present work (that is, the initial 24-hours) C-S-H- Types I and II are evident from micrographs, with Types III and IV occurring much later in the hardening process.

References

32. HUGHES B. P., SOLEIT A. K. O. and BRIERLEY R. W. New technique for determining the electrical resistivity of concrete. (To be published in *Magazine of Concrete Research*).
33. DIAMOND S. Cement paste microstructure—an overview at several levels. *Hydraulic cement pastes: their structure and properties.* Cement and Concrete Association, Wexham Springs, 1976, Apr., 2–30.
34. MCCARTER W. J. and CURRAN P. N. Electrical response characteristics of setting cement paste. (Closure to discussion). *Mag. Concr. Res.*, 1985, 37, Mar., No. 130, 52–56.